TARGET RECOGNITION BY CALMODULIN

Submitted in fulfillment of the requirements for the Degree of Doctor of Philosophy in the Faculty of Biochemistry of the University of London.

Murray Alexander Skinner

National Institute for Medical Research,

Mill Hill, London NW7 1AA

&

University of London

Senate House, Malet Street, London, WC1E 7HU

November 1996

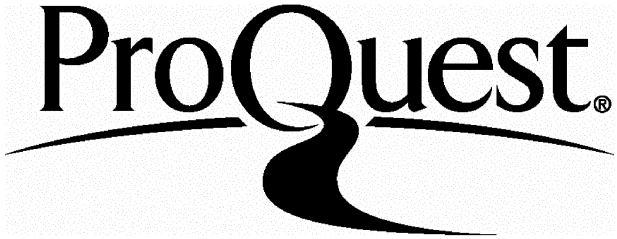

ABSTRACT

Calmodulin (CaM) inhibits mammalian phosphofructokinase (PFK) in a calcium dependent manner; however the putative CaM binding sequence is not homologous to those of other well characterized systems. This work addresses the structural and functional properties of complexes of CaM with selected target peptides from PFK using calcium binding and optical spectroscopic methods. Wild-type CaM, site-directed mutants of CaM, and cleaved domains of CaM were studied in complex with PFK target peptides of different length and amino-acid composition. Comparison of equilibria and structural data from these complexes allowed definition of the sequence involved in the interaction and conformation of the complexes.

The effect of binding different peptides on the calcium affinity of CaM has been determined by an indicator method. The presence of the PFK target peptide apparently causes a 200 fold increase in the affinity of the first two stoichiometric binding constants (K_1 & K_2), however there is little effect on K_3 & K_4. Interestingly the change in far-UV, near-UV CD, and fluorescence spectroscopic signals generated by the interaction of CaM with the target sequences are essentially complete on addition of two molar equivalents of calcium to 1 molar equivalent of CaM:PFK peptide complex, consistent with a differential function of the two domains.

The dissociation rates of calcium from CaM:PFK peptide complexes has been determined in stopped-flow experiments using the calcium chelators EGTA and Quin-2. Calcium dissociation kinetics are biphasic, with 2 sites having higher affinity. Enzyme activity studies show PFK inactivation to be CaM concentration dependent and the addition of PFK target peptide reverses the inhibition.

A mechanism for the calcium dependent interaction of CaM with the PFK target

sequence is presented. In comparison to the three closely related known CaM:target peptide structures the interaction of CaM with the PFK target sequence apparently results in a complex with a conformation of lower peptide helicity and with significantly less calcium dependence of interactions. Hence the CaM:PFK complex appears to define a new type of CaM interaction, distinctively different in structure from that currently considered for the binding of CaM in apo- or holo-form to sequences from other target enzymes. This novel interaction has also been addressed by crystallographic methods and details of optimal crystallization conditions for the CaM:PFK peptide complex are described.

CONTENTS

Section		Page
1.0	**ABBREVIATIONS**	A21
2.0	**INTRODUCTION**	
2.1	Calcium ion as a physiological regulator	2
2.2	Calmodulin	2
2.2.1	Calmodulin: structure	2
2.2.2.1	Calmodulin: calcium-binding	6
2.2.2.2	Specificity of calcium for calmodulin	10
2.2.2.3	Calcium induced conformational changes	10
2.2.2.4	Requirement of calcium binding for target recognition	12
2.2.2.5	Calcium binding in the presence of target enzymes	14
2.3	Target recognition by calmodulin	14
2.3.1	Similarities in properties of calmodulin binding targets	16
2.3.2	Peptides unlikely to conform to a basic amphipathic α-helical conformation	22
2.4	Phosphofructokinase	23
2.5	Calmodulin interaction with phosphofructokinase	25
2.6	Aims of this project	28
3.0	**MATERIALS AND METHODS**	
3.1	Sample preparations	30
3.1.1	Wild-type calmodulin purification	30
3.1.2	Wild-type calmodulin half molecule preparation	33

	and purification	
3.1.3	Preparation and purification of site-directed mutants of calmodulin	37
3.1.4	Apo-calmodulin studies	37
3.1.4.1	Preparation of calcium free buffers	37
3.1.4.2	Preparation of Apo-calmodulin	39
3.1.5	Peptide syntheses and purification	41
3.2	Spectroscopic studies	
3.2.1	Ultra-Violet and Visible Spectrophotometry	41
3.2.2	Fluorescence spectroscopy	43
3.2.3	Circular Dichroism	46
3.2.4	Stopped-Flow Kinetics	48
3.2.5	Crystallization	51
4.0	**RESULTS**	
4.1	**Interactions of calmodulin with PFK peptides involving aromatic amino acids studied by fluorescence spectroscopy**	
4.1.1	Experimental design for determination of dissociation constants by fluorescence spectroscopy.	53
4.1.2	Effects of peptide length	60
4.1.3	Peptide amino-acid substitutions	62
4.1.4	Affinity of complexes formed between site directed mutants of calmodulin or proteolytic fragments of calmodulin with	65

	phosphofructokinase target peptides.	
4.1.5	Accesibility of peptide tryptophan in the calmodulin:phosphofructokinase complex.	68
4.1.6	Influence of pH on fluorescence properties of the calmodulin:phosphofructokinase complex	72
4.1.7	Conclusions	75
4.2	**Conformational studies of secondary and tertiary structure in calmodulin, PFK peptides and the complexes formed by their interaction**	
4.2.1	Far-UV CD spectroscopy of CaM and its complexes with PFK target sequences	77
4.2.1.1	Peptide length effects (CaM bound and in trifluoroethanol treated)	77
4.2.2	Near-UV CD spectroscopy of calmodulin and its complexes with phosphofructokinase target sequences.	81
4.2.3	Structural studies using site directed mutants of calmodulin in complex with PFK peptide P9-26.	85
4.2.4	Conformational properties of the TR2C:P9-26 interaction.	87
4.2.5	pH related conformational effects in the CaM:P9-21 complex.	89
4.2.6	Effects of temperature on the secondary structure of phosphofructokinase target peptides.	89
4.2.7	Conclusions.	94

4.3	**The calcium dependence of CaM:PFKpep interactions**	
4.3.1	Determination of stoichiometric calcium binding constants in calmodulin complexed to a series of phosphofructokinase target peptides.	97
4.3.2	Structural changes of complex formation as a function of calcium concentration studied by fluorescence and circular dichroism.	104
4.3.2.1	Fluorescence spectroscopy.	104
4.3.2.2	Circular dichroism.	108
4.3.3	Conclusions.	113
4.4	**Stopped-flow kinetics of CaM:PFKpep complex dissociation**	
4.4.1	Quin-2 induced dissociation of calcium from complexes of calmodulin with target peptide sequences from phosphofructokinase.	116
4.4.2	EGTA induced dissociation of phosphofructokinase target peptides from calmodulin followed by changes in tryptophan fluorescence intensities.	121
4.4.3	Kinetic mechanism of calcium dissociation from the CaM:PFK peptide complexes.	124
4.5	**Enzyme activation studies**	
4.5.1	Materials and Methods.	133
4.5.1.1	Phosphofructokinase preparation.	133

4.5.1.2	Enzyme assay.	133
4.5.1.3	Enzyme assays involving calcium binding site mutants of CaM.	135
4.5.1.4	Data acquisition.	136
4.5.2	Effects of CaM and PFK target peptides on PFK activity.	136
4.5.3	Differential effects of calmodulin and calcium binding site mutants of calmodulin on activation properties of phosphofructokinase.	139
4.6	**Crystallization trials and crystallography**	
4.6.1	Introduction.	143
4.6.2	Sample preparation for crystallization.	143
4.6.3	Sample crystallization.	144
4.6.4	Vapour diffusion in hanging drops.	144
4.6.5	Optimal crystallization conditions for the complexes formed between CaM and either P9-21 or P1-26.	145
4.6.6	Structural data and interpretation.	145
5.0	**GENERAL DISCUSSION**	
5.1	Introduction.	149
5.2	CaM:PFK peptide complex.	149
5.2.1	Stoichiometry of interaction.	149
5.2.2	Conformation of CaM:PFK peptide complex.	151
5.2.3	Conformation of the bound PFK peptide.	153

5.2.4	Orientation of the calmodulin:target peptide complex.	155
5.3	Dissecting the role of specific peptide amino-acid residues involved in binding calmodulin.	158
5.3.1	The role of hydrophobic interactions in CaM:PFK peptide complexes.	160
5.3.2	The role of charge interactions in CaM:PFK peptide complexes.	162
5.4	Calcium binding studies of calmodulin in complex with PFK target peptides.	163
5.4.1	Consequences of mutation in Ca^{2+} binding sites of calmodulin upon CaM:PFKpeptide complex affinity and conformation.	164
5.4.2	The coupling of calcium and PFK peptide binding to CaM.	165
5.4.3	Characterizing the calcium binding sites of calmodulin influenced by target peptide.	168
5.4.4	Calcium dissociation mechanism.	169
5.5	Conclusions: Towards a working model of the CaM:PFK peptide complex.	172
5.5.1	How does calmodulin interact with the PFK target sequence?	172
5.5.2	What is the role of calcium binding in complex formation of CaM with PFK target peptides?	173
5.6	Questions arising from this work.	174
	Acknowledgments	178
	References	182

APPENDICES

1.0	Equilibrium studies: Methods for the determination of dissociation constants.	210
2.0	Determination of stoichiometric calcium binding constants for calmodulin.	217
3.0	Stopped-flow kinetic data analyses.	222
4.0	Relationship between stoichiometric and intrinsic association constants	223

FIGURES

Figure		Page
1.0	Scheme representing the synthetic peptides used in these studies.	A22
2.1.	Calcium transport systems in eukaryotic cells.	3
2.2.1.	X-ray crystal structure of Ca^{2+}CaM determined at 2.2 Å	5
2.3a.	Primary sequences of some known calmodulin binding domains of proteins.	17
2.3b.	Structure of the complex formed between calmodulin and peptide M13 from skeletal muscle myosin light chain kinase.	19
2.5.	Localization of calmodulin binding domains in the three dimensional model of phosphofructokinase.	27
3.1.1a.	Absorption spectrum of calmodulin.	31
3.1.2a.	Absorption spectra of calmodulin tryptic fragmants TR1C and TR2C.	34
3.1.2b.	Electrospray ionization mass spectra for the tryptic fragments generated by controlled proteolysis of calmodulin.	35
3.1.2c.	Polyacrylamide Gel Electrophoresis of calmodulin and tryptic fragments used in these studies.	36
3.2.2.	Fluorescence titration profile for the titration of calmodulin to peptide P9-26 at 2μM.	45
3.2.4.	Diagrammatic representation of a stopped-flow instrument.	50

4.1.1b.	Determination of the dissociation constant of the CaM:P9-21 complex using a χ^2 minimization approach.	56
4.1.1c.	Titration of peptide FFF to a complex of calmodulin bound to peptide P1-21.	59
4.1.5.	Titration of acrylamide to peptide P9-21 or a complex of calmodulin bound to peptide P1-26, P1-15, P9-26 or P9-21.	70
4.1.6a.	Fluorescence enhancements for the complexes formed between calmodulin and target sequence P9-21 at different pH values.	73
4.1.6b.	Fluorescence of peptide [P9-26 (Y14F)] at different pH values.	73
4.2.1.1a.	Far-UV CD spectra for calmodulin and complexes formed by the interaction of calmodulin and target peptides from PFK.	79
4.2.1.1b.	Far-UV CD difference spectra for complexes formed by the interaction of calmodulin and target peptides from PFK.	79
4.2.1.1c.	Far-UV CD spectra for target peptides P1-26, P9-26, and P9-21 in 50% trifluoroethanol.	79
4.2.1.1d.	Trifluoroethanol titration to calculate the number of helical residues in peptides P1-26, P1-21, P9-26 and P9-21.	79
4.2.2a.	Near-UV CD spectra of calmodulin and complexes formed by its interaction with peptides P1-26, P1-21, P9-26, P9-21 and P1-15.	83
4.2.2b.	Difference spectra generated for the complexes formed between calmodulin and peptides P9-26, [P9-26 (W12F)], and peptide WFF from sk-MLCK.	83

4.2.2c.	Near-UV CD difference spectra for the complexes formed between calmodulin and peptides P9-26, WFF (sk-MLCK) and RS20 (sm-MLCK).	84
4.2.3a.	Near-UV CD spectra for the complexes formed between peptide P9-26 and calmodulin or calcium-binding site mutants of calmodulin.	86
4.2.3b.	Near-UV CD difference spectra for the complexes formed between peptide P9-26 and calmodulin or calcium-binding site mutants of calmodulin.	86
4.2.4a.	Near-UV CD spectra of calmodulin, TR2C (CaM residues 78-148) and the complexes formed with peptide P9-26.	88
4.2.4b.	Near-UV CD difference spectra for the complexes formed between calmodulin and TR2C (CaM residues 78-148) with peptide P9-26.	88
4.2.5a.	Near-UV CD spectra of calmodulin in complex with peptide P9-21 at pH 5.0, 6.0, 7.0 & 8.0.	91
4.2.6.	Far-UV CD data corresponding to the helical propensities of PFK target peptides in 50% TFE over the temperature range 10-70°C.	92
4.3.1a.	Calcium binding to calmodulin and complexes of calmodulin with PFK target peptides P1-26, P9-26 and P9-21.	98
4.3.1b.	Calcium saturation curves produced from theoretical stoichiometric association constants for binding of 4 ligands to a protein.	100

4.3.2.	Calcium saturation curves for calmodulin in the presence of peptides WFF and WF10 from sk-MLCK, and peptides P1-26, P9-26 and P9-21 from PFK.	102
4.3.2.1a.	Fluorescence emission values for the titration of calcium to a 1:1 complex of calmodulin with either P1-26, P9-26 or P9-21.	107
4.3.2.2a.	Near-UV CD titration of calcium to apo-CaM.	110
4.3.2.2b.	Near-UV CD titration of calcium to a solution of apo-CaM and peptide P9-21.	110
4.3.2.2c.	Near-UV CD data at 295nm resulting from calcium titration to a mixture of apo-CaM and either P1-26, P9-26 or P9-21.	110
4.3.2.2d.	Far-UV CD data at 222nm corresponding to formation of helix as calcium is added to apo-CaM in the absence or presence of PFK target peptides.	112
4.4.1.	Experimental stopped-flow traces for the dissociation of calcium from calmodulin and calmodulin complexed to using fluorescent calcium chalator quin-2.	117
4.4.2a.	Experimental stopped-flow trace for dissociation of calcium from calmodulin complexed to P1-26 using the calcium chelator EGTA.	122
4.4.2b.	Arrhenius plot showing the calcium dissociation from calmodulin in the presence of peptide P9-21 as a function of temperature.	122
4.4.3	Formal kinetic scheme for dissociation of	126

	Ca_4CaM-PFK peptide complexes assuming that calcium ions dissociate in pairs.	
4.5a.	The reaction scheme from the glycolytic cascade which was used as a basis for a coupled enzyme assay system in these studies.	132
4.5.1.1.	Absorption spectra of phosphofructokinase enzyme before and after ATP removal by PD10 G-25 Sephadex gel filtration column.	134
4.5.2	Influence of calmodulin and PFK target sequence P9-26 on the activity of PFK monitored by the absorbance of NADH in the coupled enzyme assay	138
4.5.3.	Influence of calmodulin and calcium binding site mutants B2K and B4K on the rate of activation of PFK with time as determined by spectrophotometric assay.	141
4.6.5.	Crystals grown of the Ca_4CaM:PFK peptide complexes.	147
5.3a.	Secondary structure prediction of selected target sequences from the high affinity calmodulin binding region of phosphofructokinase.	156
5.3b.	Helical wheel diagramatic to assess the propensity of putative helical sequences from PFK to form amphipathic α-helix.	156
5.5.1.	Schematic representation of the potential contacts between terminal domains of calmodulin and PFK peptide P1-26. in complex with a target enzyme or peptide.	177

A1.1a. Theoretical binding curves for the reaction P + L ⇌ PL at 10μM concentration for reactions with affinity K_a 1 x 10^4 to 1 x 10^8. 211

A1.1b. Titration of TR2C to P9-21 at 5μM. 211

TABLES

Table		Page
1.	Schematic representation of synthetic PFK peptides used in these studies based on amino-acids 371-379 of rabbit muscle phosphofructokinase.	A22
2.2.1.	Stoichiometric calcium binding constants for wild-type calmodulin from Drosophila, Bovine, Xenopus, Ram, and Scallop sources.	7
2.2.2.5.	Stoichiometric calcium binding site constants for calmodulin in the presence of calcineurin, skeletal muscle myosin light chain kinase and troponin-I.	15
2.3.	Affinities of calmodulin for type I adenylylcyclase, smooth muscle myosin light chain kinase, skeletal muscle myosin light chain kinase, Ca^{2+}ATPase, phosphofructokinase and calmodulin dependent protein kinase II.	21
3.1.3.	Extinction coefficients for calcium binding site mutants of calmodulin at the tyrosine and phenylalanine absorbance maxima.	38
3.1.5.	Extinction coefficients of PFK peptides used in these studies.	42
4.1.1a.	Example of the data averaging procedures for the determination of protein:peptide affinities by fluorescence measurements.	57
4.1.2.	Dissociation constants and fluorescence enhancements for	61

	the complexes formed between calmodulin and target sequences from PFK.	
4.1.3.	Dissociation constants and fluorescence enhancements for the complexes formed between calmodulin and target sequences from PFK with specific single amino-acid substitutions within the sequence.	64
4.1.4.	Dissociation constants for the complexes formed between site-directed mutants or proteolytic fragments of calmodulin with target sequences from PFK.	66
4.1.5.	Acrylamide quenching data for the titration of acrylamide to peptide P9-21 or a complex of calmodulin bound to either P1-26, P1-21, P9-26 or P9-21.	71
4.1.6.	Dissociation constants for the complexes formed between calmodulin and target sequence P9-21 at different pH values.	74
4.2.1.	Far-UV CD extinction coefficients at 222nm of four PFK target peptides in either a calmodulin bound state or in the presence of 50% trifluoroethanol.	80
4.2.6.	Far-UV CD extinction coefficients at 222nm of four PFK target peptides over the temperature range 10-70°C.	93
4.3.1.	Stoichiometric calcium binding constants determined for calmodulin in complex with PFK target peptides.	99
4.3.1b.	Relationship between intrinsic and stoichiometric association constants.	100
4.3.2.1.	Amplitude of fluorescence signal complete for titrations of	106

calcium to apo-CaM and tryptophan containing target sequences.

4.4.1. Peptide dissociation constants and calcium dissociation rate constants of the complexes formed between calmodulin and PFK target peptides. 118

5.1 Sequences of target peptides used in these studies with summary of peptide properties, also on attatched sheet. 150

1

ABBREVIATIONS

ABBREVIATIONS

CaM, calmodulin; Ca_4CaM or holo-CaM, calcium saturated calmodulin; apo-CaM, calcium free calmodulin; PFK, phosphofructokinase; PFKpep, phosphofructokinase peptide; sk-MLCK, skeletal muscle myosin light chain kinase; sm-MLCK, smooth muscle myosin light chain kinase; CaMKII, CaM kinase II; 5,5'-Br_2BAPTA, 5,5'-dibromo-1,2-bis(O-amino-phenoxy)-ethane-N,N,N',N'-tetra-acetic acid; EGTA, [ethylenebis(oxyethylenenitrilo)]tetra-acetic acid; EDTA, ethylenediaminetetra-acetic acid; Quin-2, 2-[[2-bis(carboxymethyl)amino]-5-methyl-phenoxy]methyl]-6-methoxy-8-[bis-carboxymethyl)-amino]quinoline; SBTI, soy bean trypsin inhibitor; TPCK-trypsin, N-Tosyl-L-phenylalanine chloromethyl ketone trypsin; Tris, tris(hydroxymethyl)methylamine; CNBr, cyanogen bromide; TnC, troponin-C; TR1C, calmodulin residues 1-77; TR2C, calmodulin residues 78-148.

One and three letter codes for amino acid residues:

A=Ala=alanine, C=Cys=cysteine, D=Asp=aspartate, E=Glu=glutamate, F=Phe=phenylalanine, G=Gly=glycine, H=His=histidine, I=Ile=isoleucine, K=Lys=lysine, L=Leu=leucine, M=Met=methionine, N=Asn=asparagine, P=Pro=proline, Q=Gln=glutamine, R=Arg=arginine, S=Ser=serine, T=Thr=threonine, V=Val=valine, W=Trp=tryptophan and Y=Tyr=tyrosine.

Mutant notion

Calmodulin mutants: B2K= E67K calmodulin, B2Q= E67Q calmodulin, B4K= E140K calmodulin, B4Q= E140Q calmodulin.

Peptides: A variant of the peptide sequence is denoted as (X#Y), where X is the wild type residue, # is the number of the residue in the sequence, and Y is the residue which replaces the wild-type residue.

Figure 1

Scheme representing the synthetic peptides used in these studies based on amino-acid residues 371-397 from rabbit muscle enzyme.

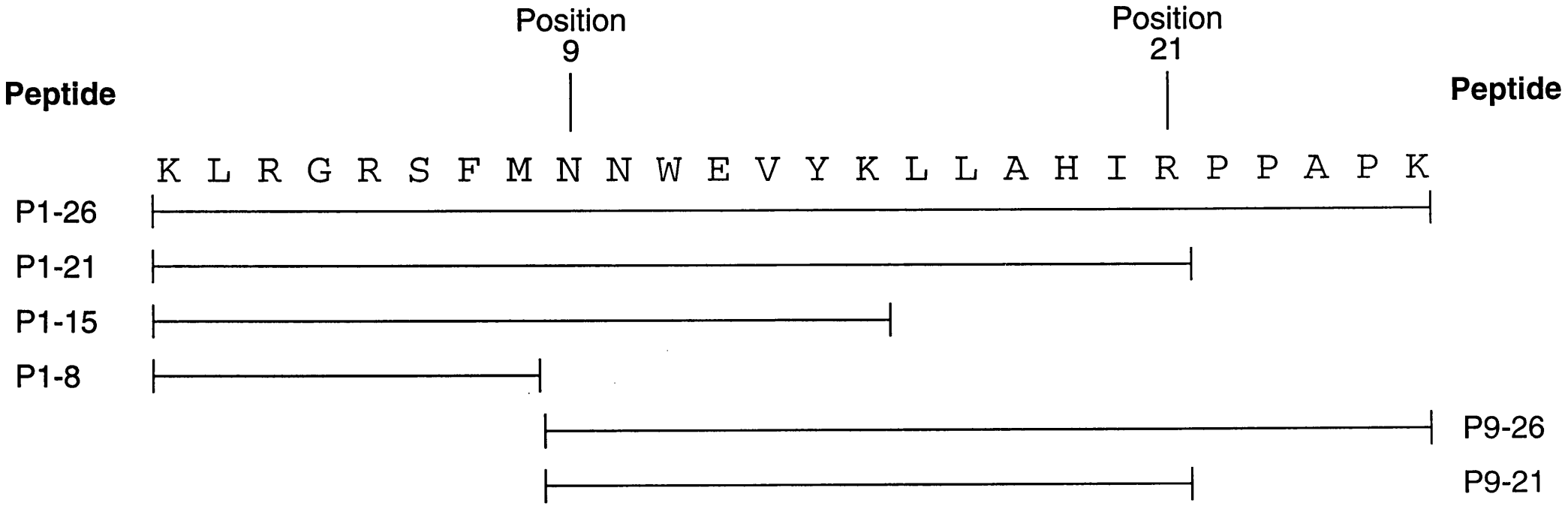
Position 9
Position 21
Peptide
Peptide
K L R G R S F M N N W E V Y K L L A H I R P P A P K
P1-26
P1-21
P1-15
P1-8
P9-26
P9-21

2

INTRODUCTION

2.1 Calcium Ion as a Physiological Regulator

Calcium ion has long been known as an important physiological regulator, particularly of processes related to nerve conduction and muscle contraction. The resting concentration of Ca^{2+} in the cytoplasm is low, at 10^{-7}-10^{-8} M whereas outside cells [Ca^{2+}] is 10^{-3} M. Induction, propagation and termination of the Ca^{2+} signal requires an elaborate system of channels, pumps, and exchangers, see figure 2.1. Specific channels that open in response to electrical or hormonal stimuli allow Ca^{2+} to enter the cytoplasm from outside the cell or from internal organelles, (Davis, 1992).

To control calcium within cells, evolution has selected reversible complexation by specific proteins which are either soluble, organized in non-membranous structures or intrinsic to membranes. One result of the increase in intracellular calcium concentration is binding of Ca^{2+} to regulatory proteins such as calmodulin or troponin-C. Conformational changes induced by calcium binding to these proteins provide binding surfaces for interactions with target receptors (see section 2.3), setting off a cascade of metabolic events. Immediately following Ca^{2+} release within the cell, the Ca^{2+} concentration is regulated by calcium buffering proteins such as recoverin and parvalbumin, (Kawasaki & Kretsinger, 1994). Termination of the calcium signal is achieved by the action of Ca^{2+}ATPases which actively pump Ca^{2+} out of the cytoplasm until the intracellular Ca^{2+} concentration returns to its basal level.

2.2 Calmodulin

2.2.1 Calmodulin structure

Calmodulin (**cal**cium **modul**ating prote**in**) is a ubiquitously expressed intracellular protein which mediates calcium induced effects through specific binding of calcium ions. The crystal structure of mammalian calmodulin, M_r = 16,800, was solved originally by

Figure 2.1

Calcium transport systems in eukaryotic cells are shown as characterized so far. Three systems are known in the plasma membrane: an ATPase, a sodium-calcium exchanger, which normally imports calcium but sometimes exports it, and calcium channels of several types, two in the sarcoplasmic reticulum (calcium-ATPase and a release channel sensitive to different effectors) and two in the inner membrane of the mitochondria (electrophoretic uptake and calcium-releasing sodium-calcium exchange). The soluble calcium-binding proteins of the cytosol have been included also in the figure since these mediate the physiological effect of intracellular calcium. The nuclear envelope is also depicted in the figure, however, the calcium transport systems in the nucleus are not understood, illustration adapted from Carafoli, (1994).

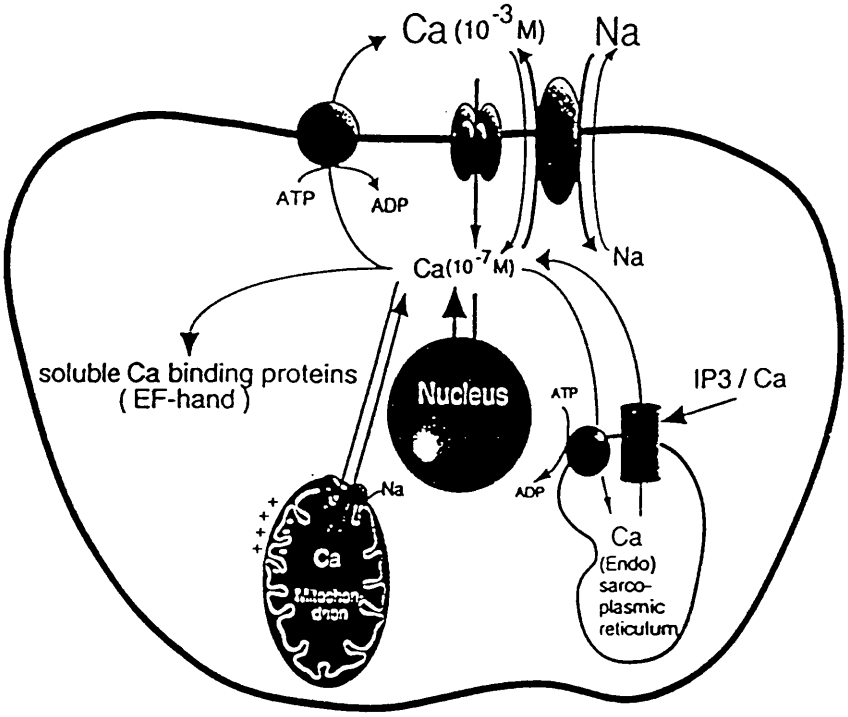
Ca (10-3 M)
Na
ATP
ADP
Ca(10-7 M)
Na
soluble Ca binding proteins
(EF-hand)
Nucleus
ATP
IP3 / Ca
Na
ADP
Ca
Ca
(Endo)
sarco-
plasmic
reticulum

Babu and coworkers in 1985 at 2.2Å and independently solved at 1.9Å by Kretsinger et al., (1986). Since this time further structural refinements have been published (Babu et al., 1988; Chattopadhyaya et al., 1992; Rao et al., 1993). The crystal structure of *Drosophila melanogaster* calmodulin, the species used in these studies, has been determined (Taylor et al., 1991). The sequence of *Drosophila melanogaster* calmodulin differs from the mammalian form in 3 amino acid positions (Watterson et al., 1987; Smith et al., 1987; Yamanska et al., 1987). In bovine calmodulin the *Drosophila melanogaster* calmodulin residues Phe 99, Thr 143, and Ser 147 are replaced by Tyr, Glu, and Ala respectively. The two structures are however closely similar, (Babu et al., 1988; Taylor et al., 1991). Ca_4CaM is a molecule composed of two very similar terminal domains. From the Ca_4CaM crystal structure two distinct globular domains are separated by an apparently continuous α-helix, see figure 2.2.1. The NMR structure, Barbato et al., (1990) is comparable to the crystal structure in most respects but shows that in solution (more representative of physiological conditions) the central α-helix is discontinuous, resulting in a flexible tether permitting closer proximity of the terminal domains, Barbato et al., (1990). Using CD spectroscopy, Bayley and Martin , (1992) showed that the helical content of calmodulin is increased under the solution conditions used in protein crystallization.

Each domain of calmodulin contains two helix-loop-helix, EF-hand, calcium ion binding sites. The EF-hand structural motif was first defined from the crystal structure of parvalbumin, (Kretsinger et al., 1973) and it has since been identified in numerous other proteins, including calmodulin. The EF-hand consists of two perpendicularly oriented α-helices and an interhelical loop, which together form a single Ca^{2+}binding site, (Ikura, 1996; Kawasaki & Kretsinger, 1995 for review). The 2 calcium sites within each

Figure 2.2.1

X-ray crystal structure of Ca^{2+}CaM determined at 2.2 angstroms resolution. Residues 78-81 of the connecting helix (comprising residues 65-93) show some deviations from ideal helix geometry, Babu et al., (1988).

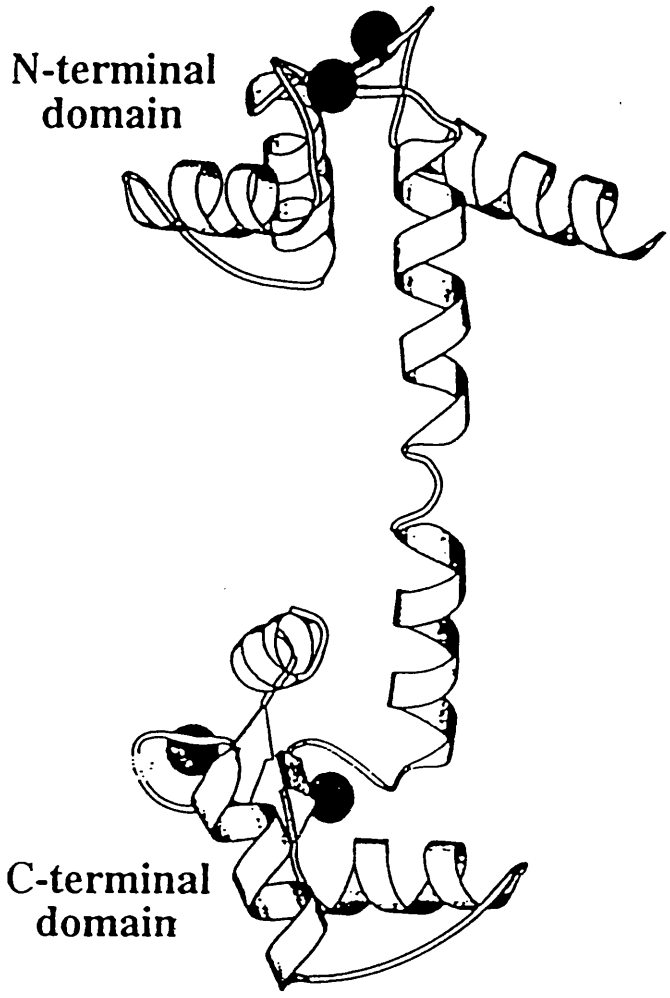
N-terminal
domain
C-terminal
domain

domain are connected via a short strand of beta-sheet such that the calcium binding sites are linked back to back. Recent studies, (Browne et al., ۱۹۹۶) suggest that point mutation of the individual beta-sheet residues in calmodulin destabilizes the wild type structure.

2.2.2 Calmodulin: Calcium-binding

In each of the four EF-hand calcium binding sites of calmodulin the calcium is chelated by seven oxygen ligands, five of these are provided by carboxylate side-chains. one by a backbone carbonyl and one by a water molecule. Positions 1, 3, 5, 7, 9, and 12 of the loop regions for all four EF-hands provide the calcium liganding positions. Position 12 is a glutamate in all EF-hands and provides a bidentate chelation. The glutamate at position 12 is considered important because it appears to enclose the calcium within the binding site, (Beckingham, 1991). Mutation of the glutamate to glutamine or lysine at position 12 demonstrates that the bidentate chelating glutamate has an important structural role in the calcium induced conformational changes of calmodulin, (Maune et al., 1992).

Since most intracellular calcium induced effects are mediated through the binding of calcium to calmodulin it is not surprising that there has been a great deal of interest in quantifying the binding of calcium to calmodulin. The stoichiometric binding constants for a number of calmodulins have been determined from a variety of techniques and these data are summarised in table 2.2.1. The constants are generally measured by flow-dialysis, (Porumb, 1994) or using a chromophoric calcium chelator, (Linse et al., 1991). Moderately good agreement is noted between independent determinations using either technique and with a number of different sources of calmodulin, see table 2.2.1. The binding of calcium to calmodulin has been described in a number of models.

Table 2.2.1

Stoichiometric calcium binding constants for wild-type calmodulin from *Drosophila*, Bovine, Xenopus, Ram, and Scallop sources. Binding constants are estimated using either the chromophoric chelator (CC) method, Linse et al., (1991) or by flow-dialysis (FD), Porumb, (1994). Data is presented as log K_1-K_4 or log $K_1.K_2$ and log $K_3.K_4$ to facilitate comparisons between species and techniques.

	Source	Method	log K_1	log K_2	log K_3	log K_4	log K_1K_2	log K_3K_4	Reference
CaM	*Drosophila*	CC	5.33	6.32	4.33	5.33	11.65	9.67	Martin et al., (1996)
CaM	Bovine	CC	4.9	6.6	4.4	5.6	11.5	10.0	Linse et al., (1991)
CaM	Xenopus	FD	5.3	5.95	4.5	5.0	11.25	9.5	Porumb (1994)
CaM	Scallop	FD	5.54	5.6	5.08	4.68	11.14	9.76	Yazawa et al., (1992)
CaM	Ram	FD	6.04	5.95	4.66	5.55	11.99	10.21	Stemmer & Klee, (1994)
TR2C	*Drosophila*	CC	5.32	6.21			11.53		Bayley et al., (1996)
TR1C	*Drosophila*	CC			4.62	5.17		9.79	Bayley et al., (1996)
TR2C	Bovine	CC	5.0	6.4			11.4		Linse et al., (1991)
TR1C	Bovine	CC			4.0	5.8		9.8	Linse et al., (1991)

An early model, (Milos et al., 1986) treated the binding as due to four independent sites and subsequently it has been treated as four identical sites with positive cooperativity, (Haiech et al., 1988; Porumb et al 1994). However, knowledge of the structure involved, and the results of more detailed analysis suggest that the binding is best characterized as two independent pairs of sites with cooperativity within each domain, (Forsen et al., 1986; Martin & Bayley, 1986; Linse et al., 1988). The validity of this model was further addressed by Linse and coworkers in 1991 using proteolytically cleaved domains of bovine calmodulin. The isolated domains of calmodulin can be generated by a controlled tryptic cleavage to yield TR1C (residues 1-77) and TR2C (residues 78-148) (N- and C-terminal domains respectively). The ion-binding properties of the intact calmodulin are effectively reproduced as the sum of those of the two domains, table 2.2.1. The NMR and CD properties of TR1C & TR2C may also be summed to give those of intact calmodulin, (Thulin et al., 1984; Martin et al., 1985). The binding constants of the fragments show that the average Ca^{2+} affinity is 6 fold higher for the C-terminal domain than for the N-terminal domain, (Linse et al., 1991) table 2.2.1.

From the data of the tryptic fragments the C-terminal domain sites evidently contain the higher affinity calcium binding sites. However, it is not possible to assign binding constants to individual sites. Stoichiometric binding constants take no account of the distribution of the calcium ions within individual binding sites on the protein, instead they represent the sum of the calmodulin species with a given number of calcium ions bound.

There have been attempts to describe the mechanism of calcium binding to calmodulin in terms of intrinsic binding site constants, eg: (Kilhoffer et al., 1988, 1992). However, meaningful mechanistic information requires the presence of a probe to reflect a change in a specific calcium binding site. Mutagenesis (eg: to insert Trp residues) or labelling could provide probes at any calcium binding sites; however protein functional integrity may be altered and one cannot exclude the possibility that the probe influences the calcium uptake mechanism of the other calcium binding sites.

The cooperative binding of calcium by calmodulin is an important biological feature of calmodulin. Cooperativity exists in a protein when occupancy of one binding site influences the affinity of remaining sites within the protein, ie: there must be some kind of structural interaction between the binding sites. The advantage of positive cooperativity of calcium uptake by calmodulin is that the regulatory effect of Ca_4CaM can be achieved over a smaller range of free calcium concentration than would otherwise be the case. Therefore a more rapid cellular response is achieved when intracellular calcium concentration increases *in vivo*. Positive cooperativity appears to exist for a number of the EF-hand proteins including troponin-C, (Grabarek et al., 1983; Teleman et al., 1983; Pearlstone et al., 1992), parvalbumin, (Cave et al., 1979), and calmodulin (Crouch & Klee, 1980; Linse et al., 1991).

It is typical for EF-hand sites to occur as tightly coupled pairs, with conservative hydrogen bonding and hydrophobic interactions between two sites providing stabilization and a potential bridge for cooperativity. One component of this coupling between EF-hands within a domain is an antiparallel β-sheet interaction between residues 7 to 9 of two adjacent calcium binding loops. In addition to this β-sheet communication the two coupled sites of a domain exhibit extensive interactions between their four helices, termed

A-D. The strongest interaction is between helices A and D (preceding EF-loop 1 and following EF-loop 2 respectively) as well as the analogous interaction between helices B and C.

2.2.2.2 Specificity of calcium for calmodulin

The question of the metal specificity of the four EF-hand binding regions for calcium was addressed by Chao and coworkers in 1984, who studied the activation of calmodulin by various metal cations as a function of ionic radius. In general, the closer the radius of a metal cation to that of calcium, the more effective was the cation in substituting for calcium. These ions include cadmium, mercury, and lead. The ability of calmodulin to bind magnesium and terbium has also been addressed, (Kilhoffer et al., 1981; Reid and Procshyn, 1995). In all these studies the metal succeeds in binding the EF-hand. The relative extents of stimulation of phosphodiesterase by cations and the ability of metal cations to inhibit calcium binding were also related to their ionic radii.

Calcium-proton antagonism has been studied in calmodulin, (Milos et al., 1986; Haiech et al., 1981), In the latter study the effect of pH on the affinity of calmodulin for calcium was studied. The number of moles of calcium bound per mole of protein (monitored by flow dialysis) was 4, 3, and 1 at pH values 7, 5, and 4 respectively.

2.2.2.3 Calmodulin: Calcium induced conformational changes

Since the activation of target enzymes by calmodulin is usually calcium dependent one presumes that the conformational change induced by the binding of calcium is the regulatory trigger for Ca_4CaM regulated activation. The lack of knowledge of the details of these structural changes has been a major barrier to understanding this critical aspect of Ca^{2+} signalling at the molecular level. Recently, this understanding improved when

the three-dimensional structure of the apo-protein was described. Two independent studies have determined the structure of intact apo-CaM (Zhang et al., 1995; Kuboniwa et al., 1995). In addition a structure of the isolated C-terminal domain of CaM has been reported (Finn et al 1995). Recent NMR studies of apo-calmodulin show that in analogy with the calcium ligated form of the protein, it consists of two small globular domains separated by a flexible linker, with no stable, direct contacts between the two domains. In the absence of calcium, the four helices in each of the two globular terminal domains form a highly twisted bundle, capped by a short anti-parallel β-sheet. It is evident from comparison of the apo- and holo-forms of the protein that calcium binding to calmodulin involves a marked decrease in protein dynamics.

Solution techniques such as small angle X-ray scattering, (Heidorn & Trewhella, 1988; Heidorn et al., 1989; Klevit et al., 1985), NMR (Barbato et al., 1992; Fisher et al., 1994; Ikura et al., 1992; Yazawa et al., 1987), fluorescence (Malencik & Anderson, 1982; Malencik and Anderson, 1983; O'Neill, et al., 1987; O'Neill & Degrado, 1990) and CD (Heidorn et al., 1989; Klevit et al., 1985; Maune et al., 1992) have been used to study the calcium induced conformational changes in calmodulin. These data, and the known structures of apo- and holo-calmodulin, support a model in which calcium binding to the two EF-hand calcium binding sites within a globular domain leads to pronounced changes in the inter-helical angles within the EF-hands of the domain. Specifically for apo-CaM, (Kuboniwa et al., 1995; Zhang et al., 1995) the EF-hands are in a closed conformation in contrast with an open conformation when calmodulin is calcium loaded, (Babu et al., 1988; Barbato et al., 1990). Furthermore, these data indicate that as a consequence of calcium binding two hydrophobic surfaces are exposed and these provide an environment suitable for binding hydrophobic targets.

2.2.2.4 Calmodulin: Requirement of calcium binding for target recognition

Binding of Ca^{2+} by CaM stimulates a major conformational change in the protein, leading to a more compact and more highly helical structure, which substantially increases the affinity of calmodulin for a number of regulatory target proteins, the exact details of target recognition are reserved for consideration later (section 2.3).

Upon binding of calcium, the interhelical angles of the calcium binding EF-hands change. The extent to which this happens appears to be different for the two domains of calmodulin. The C-terminal domain of calmodulin was recently described as having a semi-open conformation, (Swindells et al., 1996). Houdusse & Cohen, (1995) proposed earlier that such a conformation was feasible in apo-CaM and that it was induced as a result of binding IQ-motif peptides such as neuromodulin and unconventional myosin in a calcium independent way. The study, carried out by Swindells et al., (1996), used the NMR coordinates of apo-CaM, (Zhang et al., 1995) to study further the feasability of the C-terminal domain having a semi-open conformation. In contrast to the results of Houdusse & Cohen, (1995) Swindells et al., (1996) propose that the semi-open conformation of the C-terminal domain of apo-calmodulin is independent of interaction with IQ-motif peptides. However, despite this it is interesting to note that a semi-open conformation might explain the increased affinity of the C-terminal domain calcium binding sites for calcium compared with those sites in the N-terminal domain.

To date the only physiologically relevant target proteins which bind apo-calmodulin with high affinity are the neural specific proteins, neuromodulin and neurogranin (Masure et al., 1986; Apel et al 1990; Baudier et al 1991). In contrast to the other identified calmodulin binding enzymes (~30 to date, see Crivici & Ikura, 1995) for review) these proteins will not bind the calcium saturated form of calmodulin, but will

bind apo-calmodulin with nM affinity.

The majority of targets interact with calmodulin in a calcium dependent manner. The mechanism of the calcium dependent interaction was first proposed by Persechini & Kretsinger, (1988) in which through calcium binding of calmodulin each globular domain could interact with one of two hydrophobic patches approximately 180 degrees apart in the helical form of the sk-MLCK peptide, M13. The main concept of this model, which uses the central helix as a flexible tether, proved to be correct, but the detailed model of interaction between the peptide and globular domains of calmodulin was not accurately predicted. Strydnadka & James, (1990) later proposed a model which accurately described the orientation of the target peptide helix with respect to calmodulin although unlike the model of Kretsinger & Persechini, (1988) no attempt was made to alter the conformation of the calmodulin central helix. A detailed description of the interaction of calmodulin with its targets is reserved for section 2.3.

To determine the influence of a mutation in calcium binding on enzyme activation Gao et al., (1993) determined whether a series of calcium binding site mutants of calmodulin could activate the enzymes smooth and skeletal muscle myosin light chain kinase, adenylylcyclase, and plasma membrane Ca^{2+}-ATPase. In each mutant, the conserved bidentate glutamate of one of the Ca^{2+} binding sites is mutated to glutamine or lysine, Maune et al., (1992a). The glutamate at position 12 is considered important because it encloses the calcium within the binding site, (Beckingham, 1991). The effect of this study was mostly a decrease in enzyme activation. The effect of mutation at a site in the C-terminal domain appears more detrimental to activity than mutation of a site in the N-terminal domain, this is presumably reflective of the extent to which each mutant's competence to interact with target binding regions has been compromised.

2.2.2.5 Calmodulin: Calcium binding in the presence of target enzymes

To determine the calcium saturation of calmodulin necessary and sufficient to induce the conformational change which allows activation of enzymes, several groups have determined the stoichiometric binding constants for calmodulin in complex with target enzymes or peptides based on the calmodulin binding region. Specifically, the stoichiometric constants have been determined for calmodulin in complex with: calcineurin peptide, (Stemmer & Klee, 1994) sk-MLCK peptide, (Martin et al., 1995); melittin, (Maulet & Cox, 1983); troponin-I peptide, (Keller et al., 1982); and peptides from the plasma membrane Ca^{2+} pump, (Yazawa et al., 1992). For all of these complexes the presence of the target enhances the affinity of calcium for all 4 sites. Table 2.2.2.5 demonstrates the influence of calcineurin, troponin-I, and a target peptide from sk-MLCK on the stoichiometric calcium binding constants for calmodulin. Early models describing calmodulin activation of target enzymes suggested that calmodulin bound 4 calcium ions before it bound its target enzyme. A recent model proposes that a partly-calcium saturated calmodulin may bind its target but not necessarily activate it *in vivo*, (Bayley et al., 1996). The role of the partially calcium saturated CaM:Target species is to allow a more rapid cellular response to increases in intracellular calcium concentration.

2.3 Target recognition by calmodulin

Most calmodulin target proteins are large and multimeric, making CaM:target protein complexes difficult to study at the molecular level. Consequently, much of the structural information available has been obtained from the study of synthetic peptides or fragments of the CaM binding domains of several target proteins, (Crivici and Ikura, 1995).

Table 2.2.2.5

Stoichiometric calcium binding constants for calmodulin in the presence of calcineurin (CaN), skeletal-muscle myosin light chain kinase (sk-MLCK), and troponin-I. A target peptide derived from the calmodulin binding site of sk-MLCK enzyme was used for the sk-MLCK experiment. Binding constants are estimated using either the chromophoric chelator (CC) method, Linse et al., (1991) or by flow-dialysis (FD), Porumb, (1994). Data is presented as log K_1-K_4. $K_{CaM:T}$-K_{CaM} represents the difference in stoichiometric binding constants of calmodulin in the presence ($K_{CaM:T}$) or absence (K_{CaM}) of target peptide or protein.

	Peptide/ Enzyme	Method	CaM Source	log K_1	log K_2	log K_3	log K_4	Reference
CaM	Enzyme	FD	Ram	6.04	5.96	4.67	5.55	Stemmer & Klee, (1994)
CaM:Calcineurin				7.22	7	7.1	6.52	
($K_{CaM:T}$-K_{CaM})				1.18	1.04	2.42	0.97	
CaM	Peptide	CC	*Drosophila*	5.23	6.42	4.33	5.33	Martin et al., (1996)
CaM:sk-MLCK				6.79	7.91	6.57	6.53	
($K_{CaM:T}$-K_{CaM})				1.56	1.49	2.24	1.2	
CaM	Protein	CC	Rabbit	5.28	5.44	4.66	4.08	Keller et al., (1982)
CaM:troponin-I				6.42	5.2	6.72	4.70	
($K_{CaM:T}$-K_{CaM})				1.14	0.24	2.06	0.62	

2.3.1 Similarities in properties of calmodulin binding targets

When calcium is bound the structurally altered calmodulin reveals two hydrophobic patches that bind to a large number of proteins, (over 30 to date, Crivici & Ikura, 1995 for review). The calmodulin binding sequences share little homology, (figure 2.3a) however several share the propensity to form a basic amphipathic alpha-helix and these peptides have since been known collectively as the "BAA" peptides, (O'Neill and Degrado, 1990). This characteristic is observed in the NMR solution structure of calmodulin in complex with a sk-MLCK peptide, (Ikura et al, 1992), and crystal structures of complexes of CaM with sm-MLCK and CaM Kinase II peptides, (Meador et al,1992,93). For all of these structures the central helix of calmodulin is discontinuous, allowing its two terminal domains to engulf the helical target peptide. In the structures of CaM:sk-MLCKpep and CaM:sm-MLCKpep the helical peptides lie in a hydrophobic channel with the N-terminal portion of the peptides interacting primarily with the C-domain of CaM and the C-terminal portion of the peptides interacting primarily with the N-domain of CaM. The presence of two hydrophobic residues spaced 12 residues apart appears to be an important feature in the binding of the target peptide to calmodulin. These similarities also apply for the structure of calmodulin in complex with CaMKII, however it appears that the two important hydrophobic residues are spaced only 8 residues apart. These hydrophobic residues apparently make exclusive contacts with only one domain of calmodulin, anchoring the peptide to either domain of the protein. Figure 2.3b shows the interaction between calmodulin and the basic amphipathic α-helical peptide M13 from skeletal muscle myosin light chain kinase based on the NMR coordinates from the Brookhaven protein data bank.

Figure 2.3a

Primary sequences of some known calmodulin binding domains of proteins. Alignment of calmodulin binding domains was made by visual inspection based on the alignment of the putatively conserved hydrophobic anchors that interact with the hydrophobic patches on the C- and N-terminal domains of calmodulin, (Ikura et al., 1992; Crivici & Ikura, 1995). The alignment therefore is based on the premise that all peptides would adopt a basic amphipathic α-helical conformation. This is probably not the case for glucagon, secretin, and phosphofructokinase based on their primary sequence. Abbreviations: sk-, sm-MLCK, skeletal-, smooth-muscle myosin light chain kinase; CaMKinII, calmodulin dependent protein kinase II; PFK, phosphofructokinase; MARCKS, myristoylated alanine-rich C kinase substrate; F52, MARCKS like peptide.

References: 1) Blumenthal et al., (1987); 2) Lowenstein & Snyder, (1992); 3) Novack et al., (1991); 4) Zhang & Vogel, (1994); 5) Payne et al., (1988); 6) Vorherr et al., (1993); 7) Graff et al., (1991); 8) Dasgupta et al., (1989); 9) Blackshear et al., (1992); 10 & 11) Malencik & Anderson, (1983); 12) Buschmeier et al., (1987).

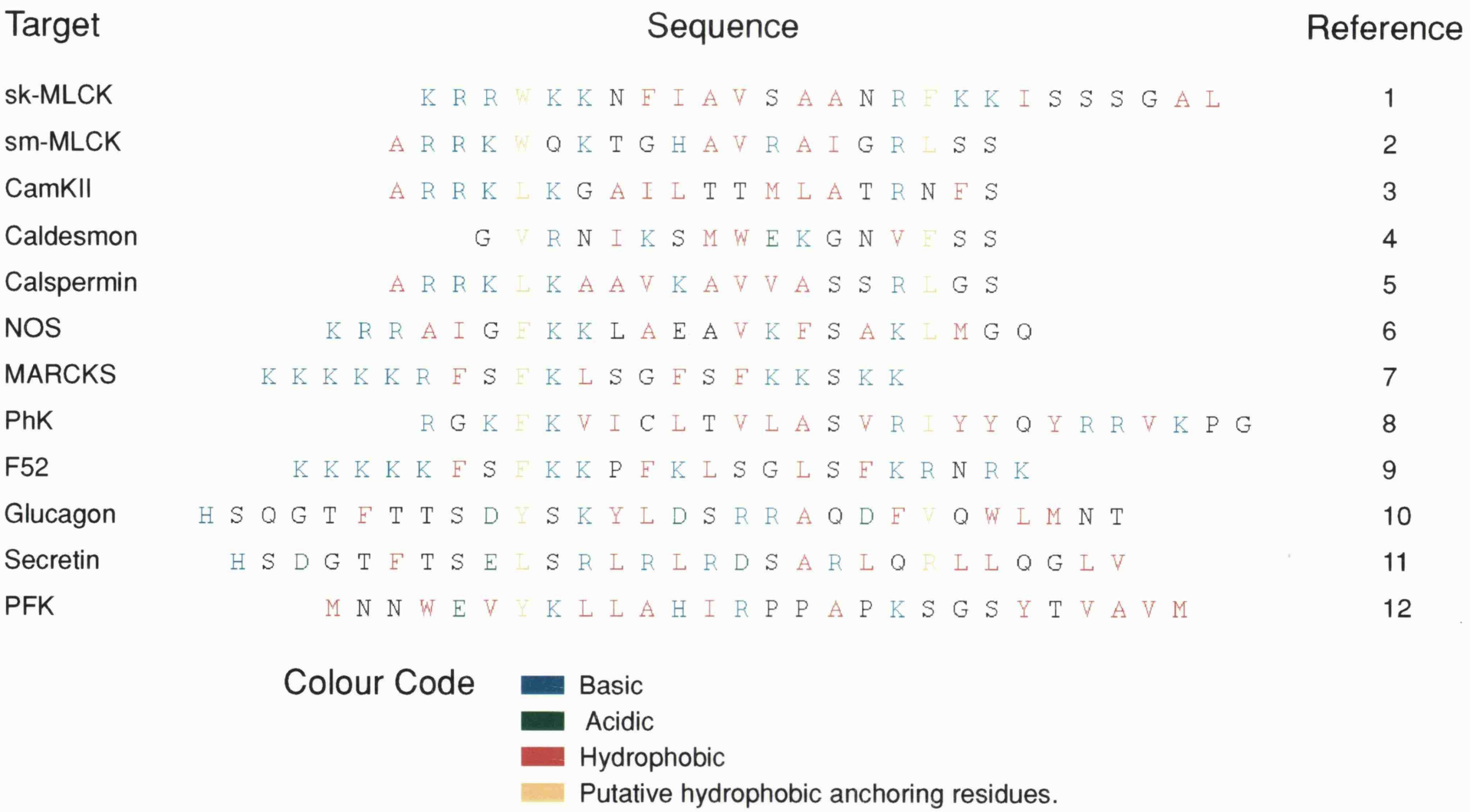
Target
Sequence
Reference
sk-MLCK K R R W K K N F I A V S A A N R F K K I S S S G A L 1
sm-MLCK A R R K W Q K T G H A V R A I G R L S S 2
CamKII A R R K L K G A I L T T M L A T R N F S 3
Caldesmon G V R N I K S M W E K G N V F S S 4
Calspermin A R R K L K A A V K A V V A S S R L G S 5
NOS K R R A I G F K K L A E A V K F S A K L M G Q 6
MARCKS K K K K K R F S F K L S G F S F K K S K K 7
PhK R G K F K V I C L T V L A S V R I Y Y Q Y R R V K P G 8
F52 K K K K K F S F K K P F K L S G L S F K R N R K 9
Glucagon H S Q G T F T T S D Y S K Y L D S R R A Q D F V Q W L M N T 10
Secretin H S D G T F T S E L S R L R L R D S A R L Q R L L Q G L V 11
PFK M N N W E V Y K L L A H I R P P A P K S G S Y T V A V M 12
Colour Code
Basic
Acidic
Hydrophobic
Putative hydrophobic anchoring residues.

Four points are characteristic of the structures of the three bound peptides solved to date. These characteristics are likely to prevail in several other targets based on their primary sequence;

1. The peptides are predominantly α-helical when bound.

2. The peptides generally bind so that the N-terminal position of the peptide interacts predominantly with C-terminal domain of calmodulin & vice versa.

3. The N-terminus of the peptide is rich in positive charge.

4. The interaction is predominantly hydrophobic. Two key hydrophobic interactions exist involving a N-terminal and a C-terminal peptide hydrophobic residue fitting into hydrophobic pockets in the C-terminal and N-terminal domains of calmodulin respectively.

The similarities in the complexes formed by interaction of calmodulin with sk-MLCKpep, sm-MLCKpep, and CaMKIIpep is not in peptide conformation only, but is also accounted for by the similar change in calmodulin conformation on binding target. Before the structures of calmodulin complexes were solved it was noted that binding of calcium to calmodulin stimulated exposure of a hydrophobic patch on each domain of calmodulin. Several groups therefore anticipated that each domain could bind a target peptide. However, the structures of the CaM-target peptide complexes determined so far (sm-MLCK, sk-MLCK or CaMKII) show that complex formation involves the protein engulfing the target in such a way that calmodulin binds a single target peptide. The overall structures of the three complexes are hence globular. This trend is not exclusive however since small angle x-ray scattering measurements reveal that for peptides from the plasma membrane calcium pump there is an elongated structural mode that is distinct from the compact form, Kataoka., (1991). Furthermore, O'Hara et al., (1994) have found

Figure 2.3b

Photograph depicting the complex formed between calmodulin and peptide M13 sequence (KRRWKKNFIAVSAANRFKKISSGAL) from skeletal muscle myosin light chain kinase. Picture generated from NMR coordinates, Ikura et al., (1992). Model generated from NMR coordinates using molecular graphics program Insight II.

using calmodulin with fluorophores attatched to each domain, that when calmodulin binds the target peptide from cyclic AMP phosphodiesterase the distance between the two fluorophores, one on each calmodulin binding domain, remains as great as in free calmodulin. In contrast, as expected from the crystal structure, the fluorophores move much closer together when calmodulin binds a MLCK target peptide.

It appears therefore that calmodulin may bind target peptides in several modes. The interaction of calmodulin with its target does not appear to be chirally selective since studies of calmodulin in solution with target peptides composed only of D-amino acids (D-melittin or D-sm-MLCK (RS20)) demonstrated that complex formation was 1:1 stoichiometry with comparable affinity to the natural L-peptides, (Fischer et al., 1994). The versatility of calmodulin in complex formation may arise through the flexible nature of the protein which is a consequence of the flexible tether region, (Ikura et al., 1992; Kretsinger 1992a & 1992b; Meador et al., 1995; Raghunathan et al., 1993)

The affinities of calmodulin for a series of target enzymes is provided in table 2.3. The association between calmodulin and these targets is strong and undoubtedly of physiological significance. Sometimes the affinities of calmodulin for target peptides derived from these high affinity enzymes is even greater than from that of the whole enzyme. This difference in affinities led several groups to believe that there may be an interacting surface unaccounted for in the whole enzyme which directly or indirectly inhibited the binding of calmodulin to the enzyme site. This effect has since been rationalised as a consequence of a pseudosubstrate sequence which is present in the whole enzyme. The enzymes are regulated by a form of molecular inhibition such that in the absence of calmodulin, substrate binding is competitively inhibited by a pseudosubstrate inhibitory sequence of the enzyme. Binding of calmodulin to the enzyme following an

Table 2.3

Affinities of calmodulin for Type I Adenylylcyclase, smooth muscle myosin light chain kinase, skeletal muscle myosin light chain kinase, Ca^{2+}ATPase, phosphofructokinase and calmodulin dependent protein kinase II (CaMKinII). K_{act} is the concentration of calmodulin required for half maximal activation of the enzyme. See references for method of K_{act} determination.

Enzyme	K_{act} (nM)	Reference
Type I Adenylylcyclase	49	Gao et al., (1993)
Smooth muscle myosin light chain kinase	0.34 0.8	Gao et al., (1993) George et al., (1996)
Skeletal muscle myosin light chain kinase	0.66	Gao et al., (1993)
Ca^{2+} ATPase	20	Gao et al., (1993)
Neuronal nitric oxide synthase	2.3	George et al., (1996)
Phosphofructokinase	3	Buschmeier et al., (1987)
CaMKinII	70	Malencik et al., (1986)

increase in intracellular Ca^{2+} results in a conformational change which relieves the autoinhibitory action and allows activation of the enzyme. Pseudosubstrate regions have been found in several enzymes eg: smooth muscle myosin light chain kinase, (Kemp et al., 1987; Blumenthal et al., 1985; Takio et al., 1985) and phosphorylase kinase Lanciotti & Bender, 1995; Dasgupta & Blumenthal, 1995).

2.3.2 Calmodulin binding targets: Peptides unlikely to conform to the BAA conformation

No single consensus sequence for recognition by CaM exists, yet the complexes formed are highly specific and have high affinity, see table 2.3. The three target sequences for which a structure in complex with CaM has been solved have basic amphipathic α-helical conformation, (Ikura et al., 1992; Meador et al., 1992, 1993).

This type of complex binding may not be the same for all calmodulin:target peptide interactions since there are target peptide sequences which have little or no propensity to form α-helical structure. In addition many sequences are not particularly rich in basic and/or hydrophobic residues, (Crivici and Ikura, 1995). Some target peptides even incorporate acidic residues within the sequence, e.g., glucagon, and secretin, (Malencik and Anderson 1982). The primary sequences of these target sequences are shown in figure 2.3a. The calmodulin-binding region derived from the mammalian phosphofructokinase enzyme is an example of a sequence quite different from the sequences of the "BAA" peptides for which a structure exists. The PFK target peptide M11 (MNNWEVYKLLAHIRPPAPKSGSYTVAV) is unusual in three respects: it contains a proline rich region of sequence, has few positively charged residues, and has an acidic glutamate neighbouring one of the putative hydrophobic anchors involved in

complex stabilization.

2.4 Phosphofructokinase

Phosphofructokinase (ATP: D-fructose-6-phosphate-phosphotransferase; EC 2.7.1.11) is a key element in glycolysis, catalysing the formation of fructose-1,6-bisphosphate and ADP from fructose-6-phosphate and ATP and is the main regulatory enzyme in glycolysis. Human PFK is a tetrameric enzyme, encoded by muscle, liver, and platelet genes. Deficiency of muscle PFK (glycogenosis type VII, Tarui disease) is an autosomal recessive disorder characterized by an exertional myopathy and a hemolytic syndrome, (Uyeda, 1979 for review).

Mammalian phosphofructokinase is regulated, in a pH dependent manner, by a number of ligands including substrates, reaction products, and various metabolites, (Uyeda, 1979; Kemp & Foe, 1983). Of these, fructose-2,6-bisphosphate and AMP are efficient positive effectors while ATP and citrate are potent inhibitors.

Phosphofructokinase exists in several polymeric forms, (monomer, dimer, tetramer, oligomer) and the association state is influenced by protein concentration, ionic strength, pH, temperature and a number of ligands, (Lad et al., 1973; Luther et al., 1985). The association state of the enzyme is directly related to its catalytic activity. The tetramer (Mol wt 320,000) is apparently the smallest active form of the enzyme, (Lad et al., 1973). At concentrations of about $0.2 mgmL^{-1}$, pH 8.0, 100mM phosphate buffer, the enzyme exists in the active tetrameric form. The association state changes to give dimers (and possibly monomers) at pH values below 8.0 and at low enzyme concentration, consequently a reduction in specific activity of the enzyme occurs (Pavelich & Hammes, 1973). Active aggregates larger than the tetramer but having the same specific activity are formed at higher pH values and at elevated concentrations ($> 0.2 mgmL^{-1}$). Since

the intracellular PFK concentration is estimated to be $1 mgmL^{-1}$ the predominant forms of the enzyme *in-vivo* are likely to be the tetramer and higher oligomeric species, (Lad et al., 1973).

Phosphofructokinase undergoes inactivation in the presence of several different proteins including Zn^{2+} dependent inactivating protein purified from rat liver, (Brond & Soling, 1986) and erythrocyte membrane band 3 protein, (Jenkins et al., 1985). Calmodulin undergoes a high affinity interaction with phosphofructokinase ($\sim$nM, see table 2.3) which is thought to be specific and physiologically relevant, (Mayr & Heilmeyer, 1983). Binding of calmodulin induces a shift from the highly active enzyme tetramer toward an inactive dimer (Mayr, 1984a,b). The influence of calmodulin on the association state of PFK implies that calmodulin binds to the PFK dimeric interface.

The molecular mechanism of allosteric regulation of mammalian phosphofructokinase is very complex and the influence of different effectors on enzyme structure has not clearly been established. One of the reasons is the lack of a three dimensional structure for mammalian phosphofructokinase.

Structures of phosphofructokinase from both *Bacillus stearothermophilus* and *Escherichia coli* have been reported (Evans & Hudson, 1979; Evans et al., 1986; Shirakihara & Evans, 1988). However, the bacterial enzymes are smaller proteins consisting of four identical subunits with a molecular weight of 34,000 per subunit. This is less than half of the size of the mammalian (rabbit muscle) enzyme which has a subunit molecular weight of 83,000, (Luther et al., 1985).

Since the nature of the bacterial enzymes is so different from that of the mammalian one, there is no reason to believe that these enzymes would share any mechanism of regulation. However, Poorman and coworkers (1984) demonstrate clear

homology among the N- and C- halves of rabbit muscle PFK and the *Bacillus stearothermophilus* enzyme and propose an evolutionary relationship by series gene duplication and divergance.

Doubling the *Bacillus stearothermophilus* PFK structure should therefore give a rabbit muscle PFK tetramer with 8 active sites and 8 allosteric sites. Equilibrium binding studies have revealed, however, that there are only 4 catalytic sites in rabbit muscle PFK. Poorman et al., (1984) propose that only one of the duplicated sequences has retained activity and that some of the catalytic and allosteric sites in mammalian PFK's may have differentiated, thereby producing a larger enzyme with an increased number of effectors. It would appear therefore that the structure of *Bacillus stearothermophilus* PFK can provide a basis for inferences concerning the structural organization of mammalian (rabbit muscle) PFK. Alignment of the sequences of the bacterial and mammalian sources of PFK demonstrate however that neither the high affinity (10nM) nor low affinity (1μM) calmodulin binding sites (see section 2.5) has a corresponding sequence in the bacterial enzyme. This is perhaps not surprising since bacterial PFK would not use eukaryotic calmodulin.

2.5 Calmodulin:Phosphofructokinase interaction

Phosphofructokinase, (PFK) was first identified as binding calmodulin in 1983 when Mayr & Heilmeyer noted the presence of a high molecular weight species present subsequent to an attempted purification of skeletal muscle myosin light chain kinase using a calmodulin-Sepharose column. The species was characterized as phosphofructokinase. The regulatory effect of calmodulin binding to a target enzyme usually manifests itself in an increase in enzyme activity. However it has been shown that calmodulin inhibits

the activity of phosphofructokinase, (Mayr, 1984a).

Calmodulin has been shown to influence PFK activity through a change in association state, preventing association of inactive dimers to active tetrameric enzyme, (Buschmeier et al, 1987). Each subunit of the enzyme can bind two calmodulin molecules. A cyanogen bromide cleavage of whole PFK identified the binding regions and the peptides were termed M11 and M22. The peptides M11 and M22 were used in equilibrium studies to determine their dissociation constants in complex with calmodulin as 11nM and 1μM respectively. The M22 site is situated at the extreme C-terminus of the PFK polypeptide. The M11 site is situated in the middle part of the polypeptide linking the duplicated sequences such that calmodulin binding prevents association of dimeric PFK to tetrameric PFK, see figure 2.5. It is presumably this structural feature that accounts for the inactivation effect of calmodulin on PFK since the dimeric form of PFK is inactive whilst the tetrameric form is active. Subsequent to Ca^{2+} dependent calmodulin binding to the high affinity site of dimeric PFK, a conformational change occurs in the subunits which is apparently hysteretic, (Mayr, 1984a). Dissociation of calcium by EDTA does not reconstitute active tetramers, (Mayr, 1984a). Instead, large inactive polymers of PFK devoid of calmodulin are formed (Mayr, 1984a). The induced polymerisation can be reversed, using a sufficient excess of Ca^{2+}CaM to saturate the low affinity (M22) CaM-binding sites, (Mayr, 1984b) plus an increase in ATP concentration so that an allosteric ATP binding site is saturated. The effect of the ATP saturation can however be mimicked by lowering the pH, (Mayr, 1984b).

Figure 2.5

Localization of calmodulin binding domains in the three dimensional model of phosphofructokinase. Two dimers are depicted in an orientation presumed necessary for association to tetrameric enzyme, Buschmeier et al., (1987). Dark and light grey cylinders represent the N- and C- terminal halves of each polypeptide subunit. CBS corresponds to the high affinity calmodulin binding sites. The asterices depict the position of the low affinity calmodulin binding sites.

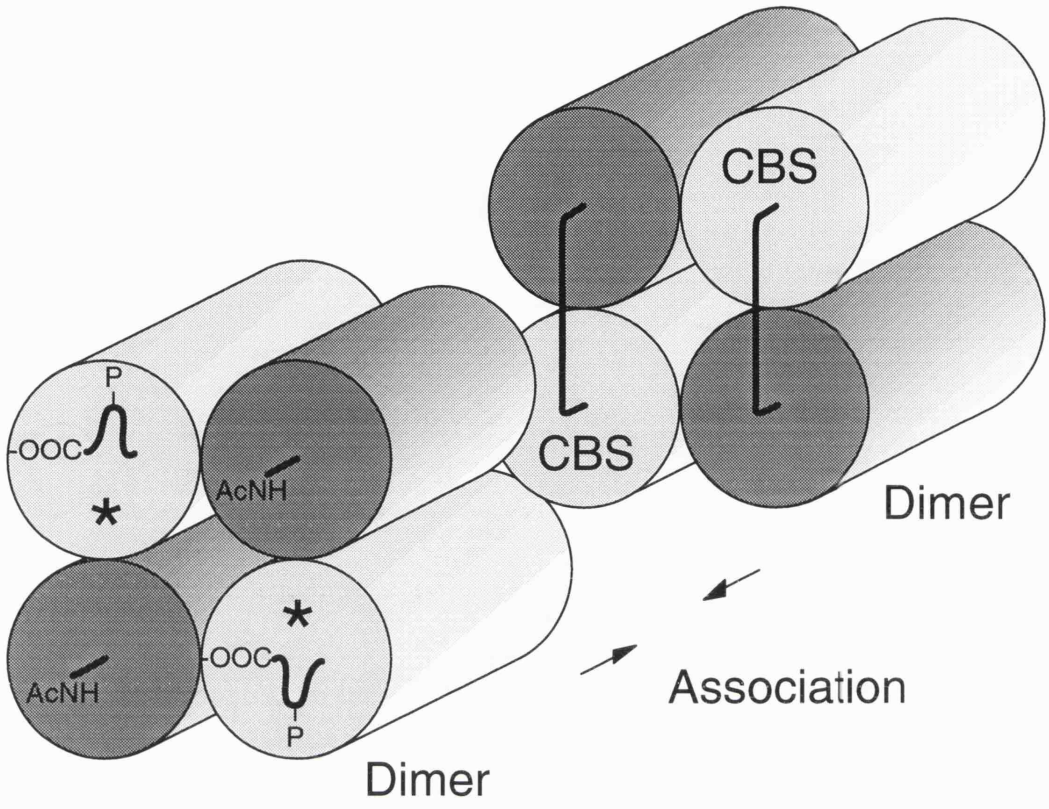
CBS
CBS
Dimer
P
-OOC
AcNH
*
AcNH
*
-OOC
P
Association
Dimer

2.6 Aims of the project

The aim of this project is to study the interaction of calmodulin and the high affinity calmodulin binding region of mammalian phosphofructokinase. The primary sequence of the calmodulin binding region of phosphofructokinase is unlike the sequences which give rise to the common basic-amphipathic α-helical structure present in the target regions of sk-MLCK, sm-MLCK, or CaMKII complexed to calmodulin. An alternative conformation thus seems possible and even likely in the CaM target sequence.

Equilibrium, structural and kinetic studies were therefore performed on the calmodulin:phosphofructokinase system using peptides of different length and composition corresponding to the high affinity CaM binding region of PFK in order to investigate:

1. The conformational properties of the two components under calcium-free and calcium saturated conditions and the affinity of calcium dependent peptide binding to calmodulin, specifically: the role of specific charged and hydrophobic residues in the target peptide sequence and the effect of peptide length on calmodulin binding properties and protein:peptide complex interaction.
2. The macroscopic calcium binding constants of calmodulin in the presence of several PFK target sequences and the kinetics of calcium dissociation reactions from complexes of CaM plus PFK peptides.
3. The concentration dependence of PFK inactivation by calmodulin and the ability of target peptides in reversing this inhibition.
4. The crystallization conditions and x-ray diffraction structure of calmodulin in complex with target sequences from PFK.

3

MATERIALS & METHODS

3.1 Sample preparations

Buffers

The working buffer is 25mM Tris, 100mM KCl, 1mM $CaCl_2$, pH 7.0. All buffers are prepared with distilled water and are filtered before use. For pH studies the buffer was 25mM sodium acetate (pH < 6) or 25mM borate (pH > 8) in place of 25mM Tris.

3.1.1. Wild Type protein purification

Drosophila melanogaster calmodulin was cloned by Dr Dai-Rong Su and was a gift from Dr Kathy Beckingham, (Rice University). The calmodulin was overexpressed in *Escherichia.coli* using the method described by Maune et al., (1992a). A 40L culture of cells was grown in rich medium and the cells were spun down and resuspended in 1.5L of 25mM Tris, 50mM KCl, and 1mM $CaCl_2$. The cells were lysed immediately using a French press and the cell debris was spun down and the supernatant was stored at -70°C. To purify calmodulin, the supernatant (250mL) was diluted 1:1 with 25mM Tris, 50mM KCl, and 1mM $CaCl_2$. This sample was then applied to a 350mL DEAE-Sephacel column. The column was washed with buffers containing 100mM and 200mM KCl. Calmodulin was eluted with buffer containing 400mM KCl, and applied to a 100mL phenyl Sepharose affinity column. After washing with buffer containing 1mM $CaCl_2$ the calmodulin was eluted using a 1mM EDTA buffer. A small amount of a high molecular weight impurity was removed by a G50 Sephadex gel-filtration column in 25mM Tris, 100mM KCl, and 1mM $CaCl_2$. Purified calmodulin was stored at -20°C. The amount and purity of calmodulin at each stage of purification was assessed using sodium dodecyl sulphate gel electrophoresis, and the characteristic absorption spectrum of calmodulin, see figure 3.1.1a for spectrum. The concentration of holo-CaM was calculated using

Figure 3.1.1a

Absorption spectra of calmodulin. Top spectum is the absorbance scan uncorrected for light scattering. Lowest curve represents the calculated contribution of light scattering to the top spectrum. The remaining spectrum represents the true calmodulin absorbance, corrected for the light scattering contribution.

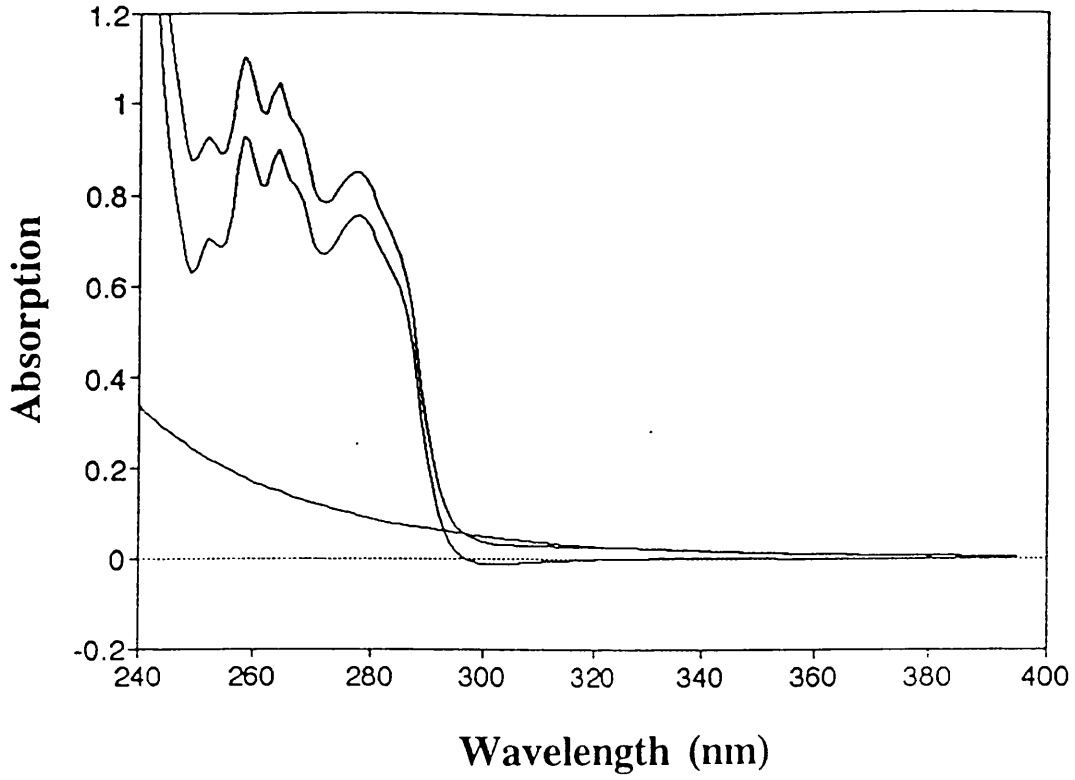
Absorption
1.2
1
0.8
0.6
0.4
0.2
0
-0.2
240
260
280
300
320
340
360
380
400
Wavelength (nm)

extinction coefficients calculated previously by Maune et al., (1992), see table 3.1.3.

3.1.2. Wild type calmodulin half molecule preparation.

A 20mg sample of calmodulin prepared as described above in 25mM Tris, 100mM KCl, 1mM $CaCl_2$, pH7.0, 25°C was cleaved at position 77-78 by N-tosyl-L-phenylalanine chloromethyl ketone (TPCK) trypsin (Sigma) at 1:80 weight ratio to yield two half molecules of calmodulin, TR1C and TR2C corresponding to residues 1-77 and 78-148 respectively, using procedures modified from Findlay and Sykes, (1991) and Persechini et al., (1994). After 1 hour incubation at room temperature a 25 fold excess (100μL) of soy bean trypsin inhibitor (SBTI) (Sigma) was added to the 4.5mL solution to stop the proteolysis. The sample was applied to a 350mL G-50 Sephadex gel filtration column equilibrated and eluted with 25mM Tris, 1mM $CaCl_2$ pH7.0. The first peak contains the high molecular weight trypsin-SBTI complex, free SBTI, and uncleaved CaM. The second peak contains a mixture of the two fragments. The mixture was then loaded onto a Mono Q anion exchange column (Pharmacia Biotech Inc.) equilibrated in 25mM Tris, 1mM $CaCl_2$, pH 7.3. Bound proteins were eluted at a flow rate of 1mLmin^{-1} by linearly increasing the NaCl gradient from 0 to 500mM at a rate of 1%min^{-1}. The absorbance of the eluate was monitored at 254nm, and column fractions containing protein were monitored by absorption spectroscopy between 240-400nm to identify the tyrosine containing TR2C fragment from the TR1C fragment (which lacks tyrosine and has no aromatic absorbance signal at 280nm), figure 3.1.2a. Each fragment was pooled, concentrated and desalted on a PD10 Sephadex column to remove NaCl from the buffer. The final products were made 100mM in KCl and stored at-20°C. This preparation yielded 10% TR1C and 35-40% TR2C. Purification was assessed at each stage by absorption spectroscopy, figure 3.1.2a; mass spectrometry

Figure 3.1.2a

Absorption spectra of fragments TR2C (CaM residues 78-148), top spectrum and TR1C (CaM residues 1-75) generated by limited proteolysis. Spectra are corrected for the contribution of light scattering.

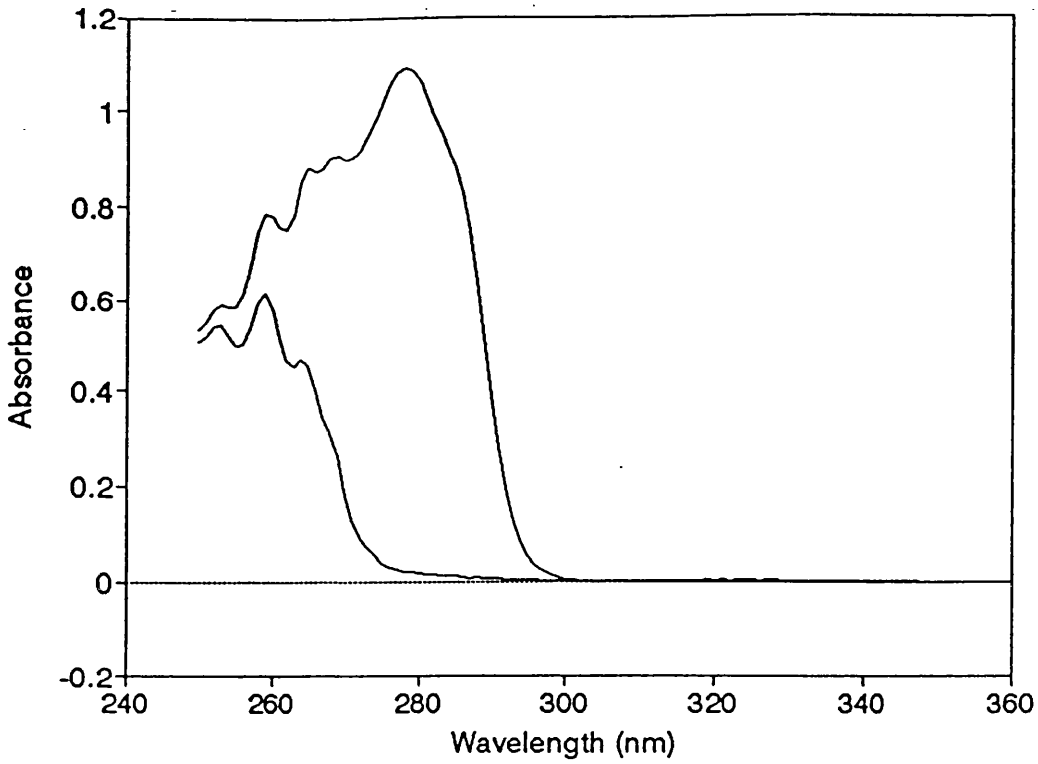
1.2
1
0.8
0.6
0.4
0.2
0
-0.2
Absorbance
240
260
280
300
320
340
360
Wavelength (nm)

Figure 3.1.2b

Electrospray ionization mass spectra for *Drosophila melanogaster* calmodulin tryptic fragments. Species generated from the proteolysis were (a) a mixture of N-terminal fragment residues 1-75 and 1-76; (b) a mixture of C-terminal fragments residues 75-148 and 78-148. Spectrum (c) corresponds to the pure C-terminal fragment 78-148. The spectral peaks are designated AX or BX where A and B correspond to two types of fragments A & B within one sample. X is the net charge associated with the mass, hence true molecular mass is calculated by multiplying the mass/charge ratio by the charge. The TR1C fragments are proposed to have a formyl methionine group at the N-terminus. Because calmodulin is over-expressed in E.coli cells during protein preparation it is possible that the enzyme responsible for cleaving the N-formyl methionine is not present at sufficiently high concentration to operate effectively. The molecular weight of the N-formyl methionine is 161, however on binding the N-terminus of calmodulin 2 protons will be lost as a consequence of the N-terminus not binding hydrogen, hence the apparent difference in molecular weight is 159. The two species in the sample corresponding to spectrum (a) molecular weight's 8475 and 8652 correspond to fragments 1-75 (+ 159 mass units) and 1-76 (+159 mass units) respectively.

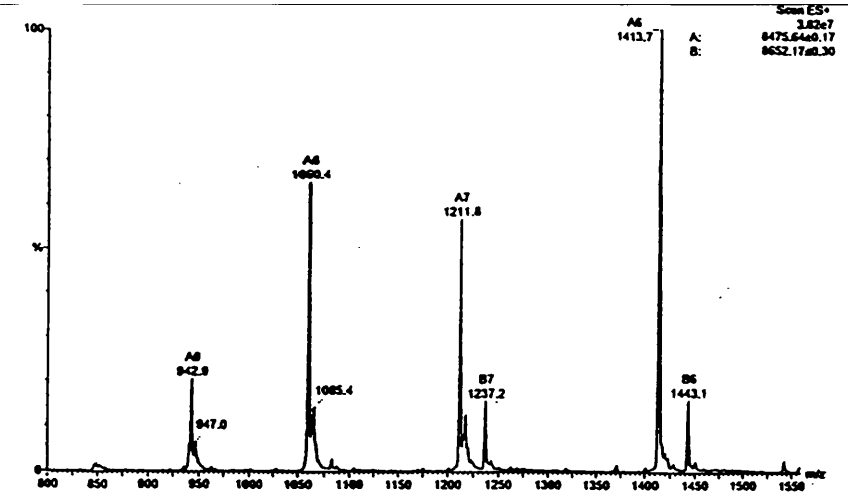
Scan ES+
3.82e7
A: 8475.64±0.17
B: 8652.17±0.30
A6
1413.7
A8
1060.4
A7
1211.8
A9
942.9
1085.4
947.0
B7
1237.2
B6
1443.1
100
%
0
800 850 900 950 1000 1050 1100 1150 1200 1250 1300 1350 1400 1450 1500 1550
m/z

A

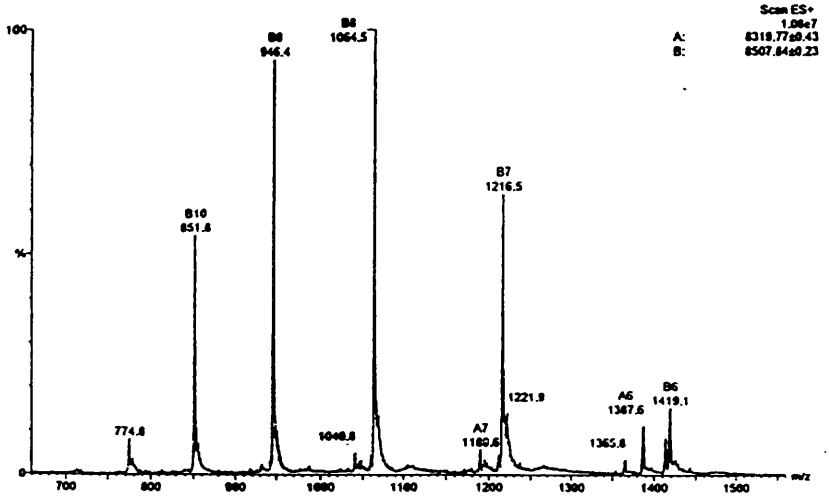
Scan ES+
1.08e7
A: 8318.77±0.43
B: 8507.84±0.23
B8
946.4
B8
1064.5
B7
1216.5
B10
851.8
774.8
1048.8
A7
1180.6
1221.9
A6
1387.6
1365.8
B6
1419.1
100
%
0
700 800 900 1000 1100 1200 1300 1400 1500
m/z

B

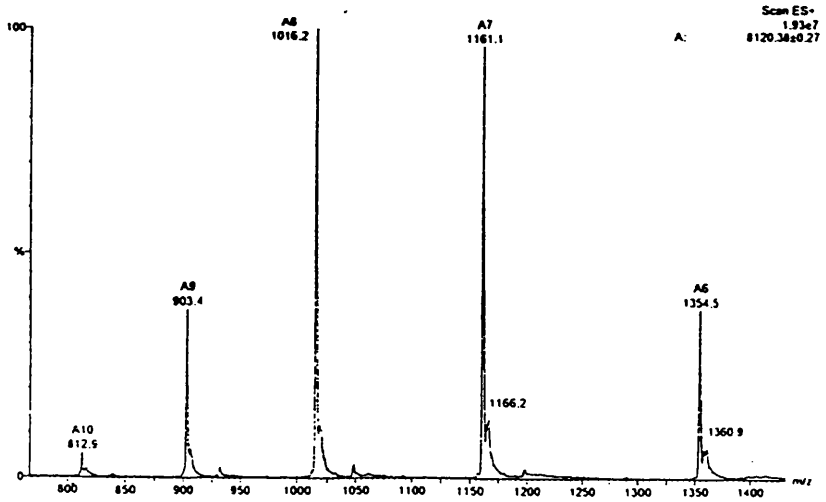
Scan ES+
1.93e7
A: 8120.38±0.27
A8
1016.2
A7
1161.1
A9
903.4
A6
1354.5
1166.2
A10
812.5
1360.9
100
%
0
800 850 900 950 1000 1050 1100 1150 1200 1250 1300 1350 1400
m/z

C

Figure 3.1.2c

Polyacrylamide gel electrophoresis, Laemmli, (1971) of calmodulin fragments after purification. The farthest right lane of PAGE (A) corresponds to the mixture of fragments obtained after purification by G-75 sephadex gel-filtration. PAGE (B) shows the separation of the fragments purified in PAGE (A). Only TR2C residues 78-148 (lane nearest right) was used in spectroscopic studies.

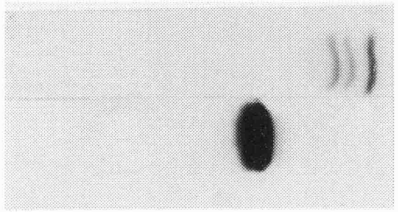
TR1C/TR2C
CaM

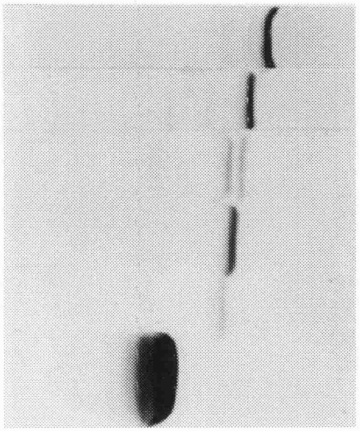
TR2C (78-148)
TR2C (76-148)
TR1C/TR2C
TR1C (1-75)
TR1C (1-75)
CaM

figure 3.1.2b and PAGE, figure 3.1.2c.

3.1.3. Preparation and purification of site directed mutants of calmodulin

The calcium-binding site mutants used in this study, (B2Q; B2K; B4Q; and B4K), were cloned and expressed in *Escherichia.coli* and were a gift from Kathy Beckingham, (Rice University). The point mutations are indicated in table 3.1.3. The mutants were purified by Pete Browne using the protocol described by Maune et al (1992). Mutant proteins were stored at -70°C in 25mM Tris, 100mM KCl, and 1mM $CaCl_2$ at pH7.5. The protein concentrations were assessed using extinction coefficients obtained by Maune et al, (1992a).

3.1.4. Apo-Calmodulin studies.

3.1.4.1. Preparation of calcium free buffers

Calcium free buffer was 25mM Tris, 100mM KCl, pH7.0 with Chelex beads (Sigma) added to chelate any residual calcium. To ensure that calcium was removed the calcium concentration in the buffer was calculated using the high affinity calcium chelator, 1,2-bis (o-aminophenoxy) ethane -N,N,N',N'- tetraacetic acid, (BAPTA). The absorbance of BAPTA reflects the extent to which BAPTA is calcium saturated. Calcium concentration in the buffer was determined as follows:

1. A stock solution of BAPTA is prepared in water and the concentration is calculated using an extinction coefficient of 1.6×10^4 $M^{-1}cm^{-1}$ at 239nm in the presence of excess calcium.
2. 600μL of Chelex treated calcium free buffer is placed in a cuvette and a spectrum of the buffer is recorded, this is used as a baseline. 10μL of BAPTA is added to

Table 3.1.3

Extinction coefficients for calcium binding site mutants of calmodulin at the tyrosine and phenylalanine absorbance maxima. Extinction coefficients were obtained by measuring the UV absorbance spectrum of a stock solution whose concentration was determined by each native protein in 6M guanadine HCl, 25mM KCl, 10mM HEPES, pH7.6, and determination of the protein concentration for this denatured aliquot from the extinction coefficient at 276nm of a 9:1 molar mixture of the N-acetyl methyl esters of tyrosine and phenylalanine in the same 6M guanadine HCl buffer, Maune et al., (1992a).

Mutant	Mutation	Extinction coefficient ϵ at (λnm) $(M^{-1}cm^{-1})$	
CaM	*Drosophila* CaM (wild-type)	1578 (278.9)	2120 (258.9)
B2K	*Drosophila* CaM (E67K)	1582 (278.8)	2088 (258.8)
B2Q	*Drosophila* CaM (E67Q)	1599 (278.4)	2109 (258.9)
B4K	*Drosophila* CaM (E140K)	1599 (277.2)	2180 (258.8)
B4Q	*Drosophila* CaM (E140Q)	1541 (277.2)	2116 (258.9)

the cuvette to give a final concentration of 25μM and the absorbance at 263nm is measured (A_1).

3. A small volume (~ 10μL) EGTA is added to give a final EGTA concentration of 20μM and absorbance at 263nm is remeasured (A_2).

4. 10μL of 10mM calcium is then added to the cuvette to give a calcium concentration of 150μM and the absorbance at 263nm is remeasured (A_3).

The effect of dilution on concentration is accounted for and buffer [Ca^{2+}] is then calculated as:

$$\frac{A_2-A_1}{A_1-A_3} \cdot [\text{BAPTA}]$$

The addition of Chelex to the buffer removes residual calcium ions present. Calcium concentration was always less than 2μM after Chelex treatment.

3.1.4.2. Preparation of Apo-Calmodulin

Apo-CaM was generated by adding 5mM EGTA pH7.0 (approximately 10μL) to a concentrated calmodulin solution (~ 600μM) in a total volume of 0.5mL. The sample was then loaded to a 25mL PD10 Sephadex gel filtration column prequilibrated in buffer prepared according to section 3.1.4.1. Once the sample has run onto the column the protein is eluted in the same buffer. Apo-CaM elutes between 2.8 - 3.8mL. Salts are eluted after 4mL. Apo-CaM is determined as being calcium free using atomic absorption and absorption spectroscopy, the extinction coefficients for *Drosophila melanogaster* apo-calmodulin were determined by Maune et al., (1992a) to be 1874 at 278.7 and 2179 at

258.6nm respectively.

3.1.4.3 Titrations of Apo-Calmodulin with calcium

Stoichiometric calcium binding constants for apo-calmodulin and apo-calmodulin in the presence of target peptides derived from the calmodulin binding region of phosphofructokinase were performed using the chelator method described by Linse et al., (1991). The chelator used for binding was 5,5'Br_2BAPTA. 5,5'Br_2BAPTA is prepared in water and the concentration of the solution is calculated using an extinction coefficient of $1.6x10^4$ $M^{-1}cm^{-1}$ at 239nm in the presence of excess calcium. The determination of calcium binding is based on the absorbance difference resulting from whether the chelator is calcium bound or not, ie: the titrations involve calmodulin competing with the chromophoric chelator for calcium. Calcium titration is performed as follows:

1. A 300μL solution containing 25μM apo-CaM $\pm$ 75μM PFK peptide and 25μM 5,5'Br_2BAPTA is held in a 1cm quartz cuvette in a thermostatted cuvette holder at 20°C, solution A. The peptide is at 3 fold excess to ensure saturation of protein. The same solution is prepared in the presence of 1mM $CaCl_2$, the latter solution, solution B, is kept in an Eppendorf at 20°C.
2. The absorbance of solution A at 263nm is recorded when a stable reading is reached. An aliquot of solution B is then added, the solution is mixed using a plastic Pasteur pipette and the absorbance at 263nm is recorded again.
3. Step 2 is repeated until there is no further significant change in absorbance indicating the end of the titration.

The analyses of the titration data to give calcium binding constants was performed using

a program written by Dr S Martin (NIMR) as described in Appendix 2.

3.1.5. Peptide syntheses and purification

The phosphofructokinase, myosin light chain kinase, and Degrado peptides used in this work were synthesized as unprotected sequences on an Applied Biosystems 430A peptide synthesizer and purified by reverse phase HPLC by Peter Fletcher, NIMR. Peptides P9-21 and P1-26 were synthesized at the Alberta Peptide Institute, Canada and peptide P1-21 was synthesized by Prof R Ramage at Edinburgh University using similar methods of synthesis and purification. Peptide purity was never less than 95%. Peptide concentration is calculated using absorption spectroscopy. All the peptides used in this study are listed in table 3.1.5 with extinction coefficients which were calculated as the sum of the individual amino-acid contributions at a particular wavelength, see section 3.2.1.

3.2 Spectroscopic Analyses

3.2.1. Ultraviolet and Visible Spectra

Absorption spectroscopy has been used to determine protein and peptide concentrations using known or calculated extinction coefficients. Extinction coefficients for peptides were calculated as the sum of the contributions of individual aromatic amino acid residues using the method of Gill and von Hippel, (1989). Thus, $\epsilon_{280nm} = N_{Trp} \times 5559 + N_{Tyr} \times 1197$, for a peptide containing N_{Trp} and N_{Tyr} residues. Extinction coefficients for holo *Drosophila melanogaster* calmodulin at 259 and 279nm are 1578 and 2120$M^{-1}cm^{-1}$ respectively, (Maune et al., 1992a) and the extinction coefficients for calcium binding site mutants of calmodulin are reported in table 3.1.3, (Maune et al., 1992a). The

Table 3.1.5

Sequences of peptides used in this study with extinction coefficients used for calculation of concentration. Extinction coefficients for peptides were calculated using the method of Gill & Von Hippel (1989). sk-, sm-MLCK corresponds to skeletal or smooth muscle myosin light chain kinase. Degrado is the model peptide prepared by Degrado et al., (1986).

Peptide *(From PFK unless otherwise stated)*	Sequence	$\Delta\epsilon$ $M^{-1}cm^{-1}$ at 280nm
P9-21 P9-21 (H-N) P9-21 (E-Q) P9-21 (E-K)	N N W E V Y K L L A H I R N N W E V Y K L L A N I R N N W Q V Y K L L A H I R N N W K V Y K L L A H I R	6756
P9-26 P9-26 (W-F) P9-26 (Y-F)	N N W E V Y K L L A H I R P P A P K N N F E V Y K L L A H I R P P A P K N N W E V F K L L A H I R P P A P K	6756 1197 5559
P1-26	K L R G R S F M N W E V Y K L L A H I R P P A P K	6756
P1-21	K L R G R S F M N N W E V Y K L L A H I R	6756
P1-15	K L R G R S F M N N W E V Y K	6756
Degrado	K L W K K L L K L L K K L L K L G	5690
sm-MLCK (RS20)	A R R K W Q K T G H A V R A I G R L S S	5690
sk-MLCK (WFF)	K R R W K K N F I A V S A A N R F	5690

extinction coefficients for peptides are listed in table 3.1.5.

Absorption spectroscopy was also used in calcium binding studies, sections 3.1.4 & 4.3 and in monitoring the purification of calmodulin from cell extract, and proteolytically cleaved fragments of calmodulin from tryptic digestion. Since *Drosophila melanogaster* calmodulin contains one tyrosine residue and eight phenylalanine residues but no tryptophan residues it fortuitously has a very characteristic spectrum, see figure 3.1.1a.

3.2.2. Fluorescence Spectroscopy

A Spex fluorolog fluorimeter was used for fluorescence studies described in this thesis. The instrument has a xenon lamp providing continuous light output from 270-700nm, and features double monochromators and automated data collection.

Fluorescence emission spectroscopy was used for ligand binding studies of the CaM:PFKpep complex. The fluorescence emission properties of a tryptophan residue depend upon its environment. The emission maximum (λ_{max}) for free tryptophan in solution is approximately 356nm, the λ_{max} moves to shorter wavelength, typically 330nm, when the residue is in a more apolar environment such as the interior of a protein. In addition to the spectral shift an increase in fluorescence intensity frequently occurs. Therefore fluorescence spectroscopy can be used to quantify the affinity of the calmodulin binding site for the target sequence and determine the stoichiometry of binding.

A full example of the the binding of peptides to calmodulin determined by either direct or competition methods is provided in sections 4.1.1. Titrations of calcium to apo-CaM were also performed by fluorescence spectroscopy. Here, 5μL aliquots of a stock solution of calcium (mM) were titrated into a 4mL plastic fluorescence cuvette containing 60μM apo-CaM, thermostatted at 20°C. The stock solution of calcium is prepared at a

concentration such that after approximately 20 aliquots of calcium the protein will have 4 molar equivalents of calcium present. Protein concentration is typically 60μM, this is high in comparison to the previously described ligand binding experiment since saturation of signal is being monitored here and not affinities of calcium for calmodulin.

Emission spectra for all the mentioned titrations were recorded from 290-400nm with λ_{ex}=280 or 295nm. Excitation and emission monochromator slits were set at 0.4 and 2.35mm respectively, corresponding to spectral bandpasses of 1.51 and 8.86nm respectively.

An increase in fluorescence intensity at 330nm was used to quantify binding of peptide to protein. A profile of the titration of peptide P9-26 to protein B2Q is shown in figure 3.2.2. Note the shift in λ_{max} toward the blue when the peptide tryptophan is buried. Dissociation constants for all calmodulin:peptide complexes were determined using a computer program written by Dr S Martin (NIMR) based on standard non-linear least squares techniques, see appendix 1.

Fluorescence spectroscopy was also used in acrylamide quenching studies to determine solvent accessibility of the peptide tryptophan in the PFK peptide or the CaM:PFKpep complex. The instrumental parameters were similar for this experiment although λ_{ex}=296nm and emission at 340nm were used. In acrylamide titrations the peptide or CaM:PFKpep complex was 0.5μM, (5μM for the weaker binding P1-15) and the sample was held in a glass cuvette to which aliquots of concentrated acrylamide (5.3M) were added. The spectrum was recorded and the procedure repeated until the titration appeared to be complete. The data were then analysed by fitting to the modified Stern-Volmer equation, (Eftink & Ghiron, 1976).

$$F_o/F = (1 + K_{sv}[Q])e^{V[Q]}$$

Figure 3.2.2

Fluorescence titration profile for the titration of calmodulin to peptide P9-26 at 2μM. Buffer used was 25mM Tris, 100mM KCl, 1mM $CaCl_2$ at pH 7.0 using an excitation wavelength of 280nm. Titration performed such that calmodulin aliquots ($< 10\mu$L) were added to 2mL of peptide in buffer. Curves were digitised directly on Spex fluorolog fluorimeter. The contribution of a raman signal has been subtracted.

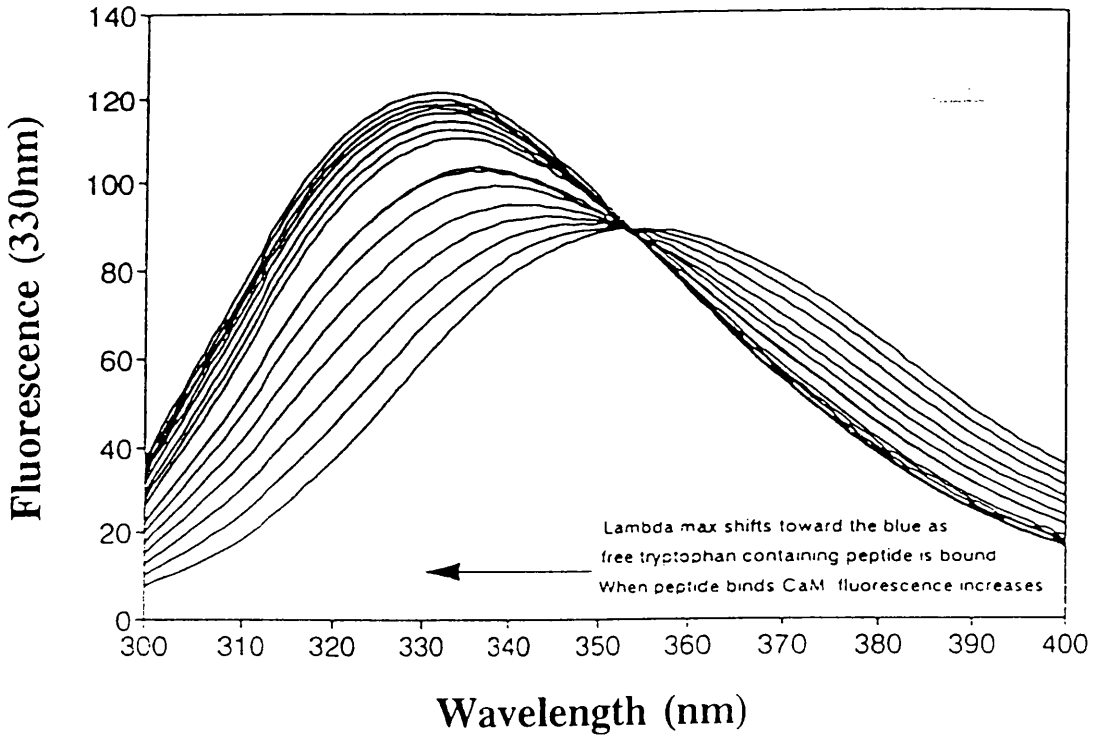
Fluorescence (330nm)
140
120
100
80
60
40
20
0
300
310
320
330
340
350
360
370
380
390
400
Lambda max shifts toward the blue as
free tryptophan containing peptide is bound
When peptide binds CaM fluorescence increases
Wavelength (nm)

In this equation F_o and F are the fluorescence intensities in the absence and the presence of quencher, respectively, [Q] is the concentration of acrylamide, K_{SV} is the Stern-Volmer constant for collisional quenching, and V is the static quenching constant.

3.2.3. Circular Dichroism

Absorption and fluorescence spectroscopy measurements are helpful in following molecular changes. In order to interpret the measurements in terms of protein secondary structure, techniques involving the use of plane polarized light have become important. There are various ways in which light can be polarized. Most familiar is plane polarized, in which the varying electric field of the radiation has a fixed orientation. Circular polarization is also a means by which light can be polarized. Here the electric field rotates either clockwise or anticlockwise with the frequency of the radiation. Symmetric molecules exhibit a preference for the absorption of left or right circularly polarized light and the resulting spectrum will reflect the symmetry of the molecule in question. CD is therefore of particular use in the study of protein secondary and tertiary structure. Specifically, far-UV CD experiments (200-250nm) were performed to quantitate the secondary structure of the protein and peptide under various conditions. Near-UV CD experiments (250-320nm) were performed to study the environment and mobility of the aromatic residues of calmodulin, the peptides, and their complexes.

Circular dichroism spectra were recorded using a Jasco J-600 spectropolarimeter at room temperature with 1mm path length fused silica cuvettes for far-UV CD and 1cm fused silica cuvettes for near-UV CD. Protein concentrations used for far and near-UV CD were 10 and 60μM respectively. For studies of protein in complex with peptide, a 1.1 fold excess was generally used. The band widths and time constant used were 2nm

and 0.5s respectively. Multiple (16) scans were averaged, baselines were subtracted and a small degree of numerical smoothing applied. Temperature was controlled using a Neslab RT-111 water bath. To determine the secondary structure of the PFK peptides when complexed to calmodulin, equation 3.2.3a is applied. $\Delta\epsilon_{MRW}$ is related to $\Delta\epsilon_M$ through equation 3.2.3c and to molar ellipticity by equation 3.2.3b. The molar calmodulin concentration is used in the calculation of $\Delta\epsilon_{M\ (complex)}$ and $\Delta\epsilon_{M\ (CaM)}$. Spectra are presented as $\Delta\epsilon$ in mean residue weight for far-UV CD spectra (see equation 3.2.3c) in order to facilitate quantitative calculation of secondary structure for the different peptides in solution, solvent, or in complex with calmodulin. In order to apply the models for the helix → coil transition to the raw data, the mean residue ellipticity must be converted into fractional helicity. This conversion requires a knowledge of $[\theta]_{222nm}$ for the completely helical and completely coiled forms of the peptide; we employ the method of Scholz et al., (1993) to do this. The expressions $[\theta]_H$ and $[\theta]_C$ correspond to the ellipticity at 222nm measured for model peptides in 100% or 0% helical form respectively. The values of $[\theta]_H$ and $[\theta]_C$ are calculated according to equations 3.2.3d and 3.2.3e. Temperature, T is in °C, n is the number of residues in the peptide chain and x is a constant (2.5) used to correct for non-hydrogen bonded carbonyls that do not contribute to $[\theta]_H$. Knowing the ellipticity for a fully helical peptide the actual peptide helicity is calculated from this.

Equation 3.2.3a. $\Delta\epsilon_{M\ (peptide)}=\Delta\epsilon_{M\ (complex)}-\Delta\epsilon_{M\ (CaM)}$

Equation 3.2.3b. $\Delta\epsilon_{MRW} \cdot 3300 = [\theta]_{MRW}$

Equation 3.2.3c. $\Delta\epsilon_{MRW}=\Delta\epsilon_M/$no of peptide bonds

Equation 3.2.3d. $[\theta]_H=-40000.(1-x/n)+100.T$ deg.cm^{2}decimole^{-1}

Equation 3.2.3e. $[\theta]_C = +640\text{-}45.T$ deg.cm^{2}decimole^{-1}

Equation 3.2.3f. % α-helicity = $\Delta\epsilon_{MRW(act)} / \Delta\epsilon_{MRW(100\%)}$

Part of the CD studies described later involve calculation of percentage peptide helicity in the calmodulin bound form or in the presence of the helicogenic solvent trifluoroethanol (TFE). The following example illustrates how helicity can be quantitated for the 13 residue peptide P9-21 when complexed to calmodulin:

Equation 3.2.3d is used to determine the ellipticity of a fully helical peptide comprising n residues. Therefore if P9-21 were completely helical in complex with CaM at 20°C:

$$[\theta]_H = -40000.(1\text{-}2.5/12) + 100.20 \text{ deg.cm}^2\text{decimole}^{-1}$$

$$= -29666.7$$

$$[\theta]_C = +640\text{-}45.20 \text{ deg.cm}^2\text{decimole}^{-1}$$

$$= -260$$

The $\Delta\epsilon_{MRW}$ is calculated for the fully helical peptide as -8.911, using equation 3.2.3b, taking into account the contribution to ellipticity of random coil, see equation 3.2.3e. The $\Delta\epsilon_{MRW}$ has been calculated for the calmodulin bound peptide as -3.5 (see results), the value is calculated using: equation 3.2.3a, assuming no change in calmodulin secondary structure. $\Delta\epsilon_{MRWpeptide}$ is calculated using equation 3.2.3c, therefore the % α-helicity of the bound peptide is calculated according to equation 3.2.3f as 39%.

3.2.4 Stopped-Flow Kinetics

A stopped-flow spectrophotometer is essentially a conventional spectrophotometer

with the addition of a system for rapid mixing. Figure 3.2.4 is provided to illustrate the mixing and observation system. Two syringes (B_1) and (B_2) contain the reactants to be mixed. Flow is initiated by the drive plate (A) which operates pneumatically to drive the reactants from the syringes. The solutions from the syringes pass from the syringe filled valves (C) into the mixing chamber (D). The solution passes to the observation cell (E) and the fluorescence is amplified by a photomultiplier (F). Flow is stopped when the solution reaches the back syringe and this hits a metal stopping bar (I). In order to record the signal with time a trigger switch is used which allows the signal to be observed before flow stops. Stopped-flow experiments were performed on a High-Tech SF61-MX stopped-flow spectrofluorimeter. A xenon lamp was used and excitation was 295 or 330nm for tryptophan or Quin-2 experiments respectively. Emission was measured using cut-on filters corresponding to 330 or 360nm for tryptophan or Quin-2 experiments respectively. All concentrations quoted are those prior to 1:1 volume stopped-flow mixing. The dead time of the instrument is ~3ms at a drive pressure of about 4 bar. Any loss of fluorescence signal during the dead time of the instrument is corrected for.

Dissociation of calcium by EGTA was achieved by mixing 2μM CaM:PFKpep complex in 100μM $CaCl_2$ with an equal volume of 20mM EGTA, PFK peptide was 1.1 fold in excess of protein. The observed rates were independent of EGTA concentration between 0.5-20mM. Dissociation of calcium by Quin-2 was studied by mixing 3μM CaM:PFKpep complex in 20μM $CaCl_2$ with an equal volume of 90μM Quin-2, PFK peptide was 1.1 fold in excess of protein concentration. Analysis of stopped-flow data is considered in Appendix 3.

Figure 3.2.4

Diagrammatic representation of a stopped-flow instrument. (a) Plan view of an instrument stopped to the back syringe. A, drive; B, reactant syringes; C, filling valves; D, mixer; E, observation cell; F, photomultiplier; G, emptying valve; H, back syringe; I, stopping-bar. Diagram taken from Stopped-flow spectrophotometric techniques, J.F. Eccleston, in Spectrophotometry & spectrofluorimetry: a practical approach, IRL press, 1987.

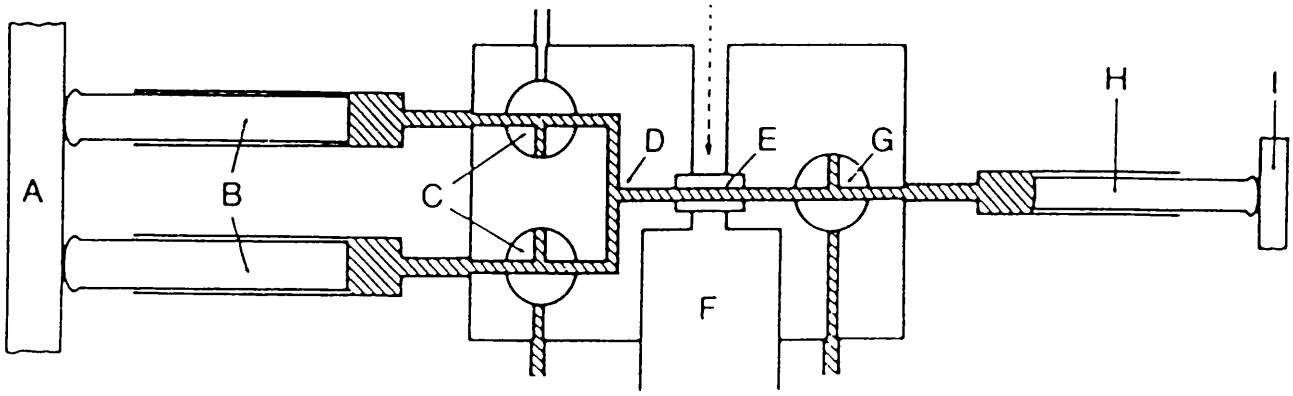
A
B
C
D
E
F
G
H
I

3.2.5 Crystallography

Note: Crystallographic studies were performed in collaboration with Dr's K Henrick, M Hirshberg, B Xiao and Professor G Dodson from the Division of Protein Structure (NIMR).

For crystallographic studies single, untwinned crystals of at least 1mm in size are ideally required. In these studies crystals of proteins were grown using the hanging drop method, (McPherson, 1984). Crystals were produced by slowly and continuously increasing the concentration of both the protein and a solute that encourages crystallization, typically polyethylene glycol, see results for crystal growing conditions.

The crystals used were mounted and placed in the beam of x-rays. The protein is frozen in the beam using a stream of liquid nitrogen vapour. The beam of x-rays was usually produced by striking a target of copper with electrons accelerated in a high voltage. A copper target provides x-rays with wavelength 0.154nm. Diffraction patterns have also been obtained by using the intense x-rays available from a synchrotron source. In this system, accelerated electrons are injected into an electron storage ring and these orbiting electrons emit synchrotron radiation.

4

RESULTS

4.1 Interactions of calmodulin with PFK peptides involving aromatic amino acids studied by fluorescence spectroscopy.

Fluorescence spectroscopy was used to assess the interaction of calmodulin with PFK peptide targets, see table 1 or 5.1 for sequences. The affinity of calmodulin for target peptides was studied by either direct or competition methods. The experimental design and limitations of these techniques with reference to two specific examples are discussed. The accessibility of Trp residues in various complexes was studied using acrylamide quenching.

4.1.1 Experimental Design for determination of the dissociation constants by fluorescence spectroscopy

The absence of a tryptophan in *Drosophila melanogaster* calmodulin provides a simple method for estimating calmodulin affinity for tryptophan containing target sequences. All sequences studied have a tryptophan reporter probe at position 11 except for peptide P1-8 which has been modified to include a tryptophan at position 7 in place of the native phenylalanine residue. As the tryptophan containing peptide is titrated with calmodulin the fluorescence emission spectral characteristics change, see figure 3.2.2. This fluorescence characteristic was used in both direct and competition methods to determine dissociation constants. The method of titration was governed by peptide affinity for calmodulin, and the limit of the fluorescence signal itself. The quality of the data obtained on the Spex fluorolog instrument permits working at concentrations as low as 100nM. The estimation of affinities below nM however requires that one works at a concentration lower than 0.1μM, since the concentration of the peptide used determines the range of K_d which may be determined. A detailed example of how dissociation constants were obtained follows for calmodulin in complex with peptides P9-21 (32nM)

and P1-21 (1nM) assessed by direct and competition techniques respectively.

4.1.1.1. Direct Binding Technique for determination of dissociation constants

In this experiment a plastic or quartz cuvette containing buffer is held in a thermostatted holder at 20°C. The fluorescence emission spectrum of the buffer is recorded over the wavelength range 300-400nm with excitation at 295nm. The Raman contribution was then subtracted from subsequent spectra. An aliquot of peptide P9-21 is added to the cuvette, and the spectrum of the peptide sample is recorded. The concentration of peptide ideally needs to be relatively close to its K_d - but this is unknown, therefore the optimal working concentration is estimated in preliminary experiments and then raised or lowered depending on the degree of protein saturation noted from the experimental data. A concentration is used so free ligand concentration during titration and stoichiometry of interaction can be determined see section 3.4.1. A concentration of 0.5μM was chosen for the CaM:P9-21 titration. The protein is titrated into the peptide in aliquots of approximately 5μL and at least 25 points contribute to the titration with at least 15 points prior to a 1:1 concentration of protein:peptide complex. Following each addition the spectrum of the CaM:P9-21 is recorded. Despite previous findings involving titration of calmodulin to peptide WFF from sk-MLCK, (Findlay et al., 1995) it was found that there was no binding of peptide or protein to the walls of either type of cuvette. The spectra for a complete titration of CaM to peptide P9-26 are illustrated in figure 3.2.2. The presence of the isoemissive point indicates a simple process for the binding of peptide by calmodulin. For all peptides the complete 300-400nm spectrum is recorded for each aliquot. Having ensured that the process has an isoemissive point, the repeat titrations (n = 4) are performed by measuring fluorescence

intensity at 330nm and the fluorescence enhancement at this wavelength is used to determine the dissociation constant. Single wavelength titrations are advantageous when proteins are unstable with time or if samples are photobleached. These were not problems in this research, single wavelength was used to reduce experimental time, and exposure was minimized with narrow excitation slits.

When the titration was completed the fluorescence emission values at 330nm for known protein and peptide concentration were imported into a spreadsheet where data was manipulated into a format suitable for inputting to the data analysis program. The fitting of the experimental data to an equation and subsequent determination of dissociation constant is described appendix 1. The program has been developed by Dr S Martin, NIMR. The program, EQFIT4A is a non-linear least squares fit to a single dissociation constant. The dissociation constant and fluorescence enhancement are obtained by a χ^2 minimization procedure. Figure 4.1.1b shows the variation of χ^2 as a function of the K_d for the CaM:P9-21 titration. The minimum χ^2 is at K_d = 30nM. The values of four independent titrations of CaM to peptide P9-21 under identical conditions with the average and the corresponding standard deviation are shown in table 4.1.1a.

4.1.1.2. Competition Binding Technique for determination of dissociation constants

The competition experiment follows a similar principle to the direct method. In the competition experiment of CaM with P1-21 or P1-26 one begins the titration with a complex of protein and peptide at a ratio of 1:3. The elevated ratio is important to ensure in subsequent analysis of the data that there is negligible free calmodulin present during titration. Absolute calmodulin concentration is generally 0.5μM. The CaM:PFKpep

Figure 4.1.1b

Determination of the dissociation constant of the CaM:P9-21 complex using a χ^2 minimization approach.

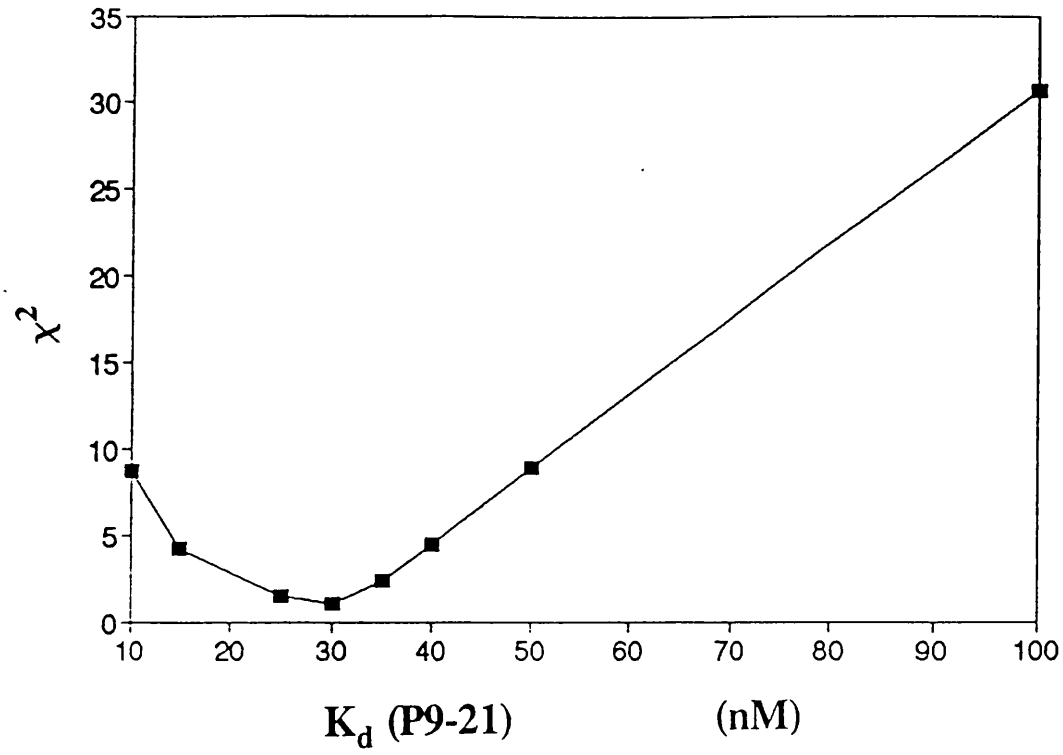
35
30
25
20
15
10
5
0
χ^2
10
20
30
40
50
60
70
80
90
100
K_d (P9-21) (nM)

Table 4.1.1a

Example of data averaging procedures for the determination of CaM:PFK peptide affinities by fluorescence measurements by either direct or competition techniques. The dissociation constant (direct titration) or ratio of dissociation constants (competition titration) for each experiment is determined using χ^2 minimization procedure. Experimental procedures described in section 4.1.1.

Peptide used in CaM complex	Titn	Competing peptide (K_d) of competing peptide for CaM	(1) K_d determined by direct method M	(2) K_d(PFKpep)/ K_d(FFFpep) determined by competition method	Average of 4 titrations with standard deviation
P9-21	1 2 3 4		3.1×10^{-8} 4.2×10^{-8} 3.1×10^{-8} 2.7×10^{-8}		3.2×10^{-8} M ± 5.1×10^{-9} M
P1-21	1 2 3 4	sk-MLCK (FFF) (40pM)		25 25 30 40	Average ratio from column 2 is 30. Therefore K_d (P1-21) = 1.2×10^{-9} M ± 2.0×10^{-10} M

species is then titrated with a competing "silent" peptide which does not contain a tryptophan. The peptide used (FFF) is derived from the high affinity calmodulin binding region of skeletal muscle myosin light chain kinase, sequence KKRFKKNFIAVSAANRFK. The peptide has a dissociation constant of 40pM as determined by competition experiment with peptide WFF, sequence KKRWKKNFIAVSAANRFK. This is the calmodulin binding site of skeletal muscle myosin light chain kinase and has a K_d of 150pM for calmodulin, (Martin et al., 1996). When FFF is titrated in CaM:PFKpep the FFF competes with the PFK peptide for the high affinity binding site. Subsequent to each FFF addition the solution is mixed and allowed to compete and requilibrate for five minutes. The dissociation of the tryptophan containing PFK peptide from calmodulin is observed as a loss of fluorescence signal at 330nm. As in the direct method of analysis, initial titrations cover the wavelength region 300-400nm with excitation at 295nm to check that the titration curves show an isoemissive point. Repeat titrations (n = 4) were performed by measuring the fluorescence intensity at 330nm. The data are corrected for dilution and are analysed in a non-linear least squares fit to peptide competition data, the fitting of the experimental data and full data analysis method is described in Appendix 1. Figure 4.1.1c shows the titration data and fit to the titration data for the competition of CaM:P1-21 by peptide FFF. The program EQFIT6 (Dr S Martin, NIMR) provides the fluorescence enhancement and the ratio of the dissociation constants of the "silent" peptide and the PFK peptide. Since the dissociation constant of the silent peptide for calmodulin is known the dissociation constant of the PFK peptide for calmodulin can be calculated. Table 4.1.1a shows the ratios, calculated dissociation constants, averaged dissociation constant and corresponding standard deviation results of four independent titrations of peptide FFF to

Figure 4.1.1c

Titration of peptide FFF to a complex of calmodulin bound to peptide Pi-21 at a ratio of 1:3. Peptide FFF has sequence KKRFKKNFIAVSAANRFK and is a spectroscopically silent peptide derived from the high affinity calmodulin binding sequence of skeletal muscle myosin light chain kinase. The experiment is performed at 0.5μM protein concentration. The graph illustrates the experimental data (symbols) with the non-linear least squares fit to the competition data (curve), see section 3.4.1. Excitation wavelength was 280 or 295nm. Emission was measured at 330nm. Monochromators were adjusted to 1 and 9nm for excitation and emission slits respectively.

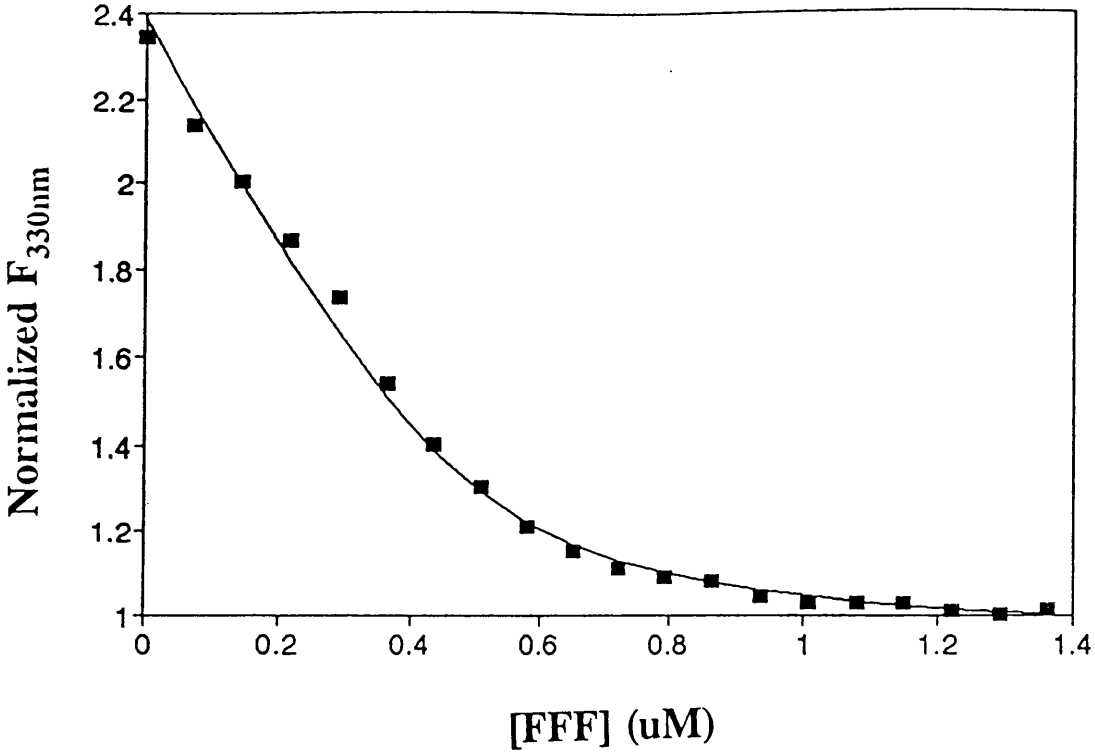
Normalized F_{330nm}
2.4
2.2
2
1.8
1.6
1.4
1.2
1
0
0.2
0.4
0.6
0.8
1
1.2
1.4
[FFF] (uM)

CaM:P1-21.

4.1.2. Effects of peptide length.

The affinities of calmodulin for six PFK peptides (P1-26; P1-21; P1-15; P1-8; P9-21; and P9-26) derived from the sequence of mammalian (rabbit muscle) PFK (see scheme 1) were determined by fluorescence spectroscopy. The dissociation constants for the complexes of the peptides with calmodulin are reported in Table 4.1.2 with the standard deviation from four independent titrations. Stoichiometry is 1:1 under all circumstances.

The affinity of binding generally increases with increasing number of residues, except for peptide P1-15 which has markedly lower affinity for calmodulin. It is possible that the 15 residue peptide is not long enough to interact with both domains of calmodulin. The full length 26 residue sequence has high affinity (280pM) compared with peptide P9-26 (11nM) indicating the potential importance of residues P1-8. However, supplementing peptide P9-26 with peptide P1-8 only increases the apparent affinity of P9-26 to 1nM. Thus the peptide sequence P1-26 must consist of a single entity for optimal high affinity interaction. Comparison of dissociation constants of CaM complexed to either peptide P9-21 or peptide P9-26 indicates that inclusion of the 5 C-terminal peptide residues in the target sequence increases affinity by 3 fold. This may appear surprising, since the C-terminal region is rich in proline residues and since CaM targets are often alpha-helices, such a region was not anticipated to contribute significantly in binding.

Table 4.1.2

Dissociation constants with standard deviations calculated from four independent titrations and fluorescence enhancements for the complexes formed between calmodulin and target sequences from rabbit muscle phosphofructokinase between 0.1 and 10μM. All titrations performed at 20°C in 25mM Tris, 100mM KCl, 1mM $CaCl_2$, pH 7.0. Excitation wavelength was 280 or 295nm. Emission was measured at 330nm. Monochromators were adjusted to 1 and 9nm for excitation and emission slits respectively. All dissociation constants were assessed using the direct non-linear least squares fit to a single dissociation constant except for complexes with peptides P1-21, P1-26 and P1-8 which were determined by a competition method, see section 3.4.1. The dissociation constant for peptide P1-8 was determined using the competition method with peptide [P1-8 (F7W)] for which the dissociation constant was calculated (by change in tryptophan fluorescence on binding CaM) to be 10μM using an experimental calmodulin concentration of 25μM.

Peptide	pH	Dissociation Constant (M)	Method of K_d Analysis	λ_{max}	F/Fo
P1-26	7.0	$2.8 \times 10^{-10} \pm 1.0 \times 10^{-11}$	Competition	333	2.22
P1-21	7.0	$1.0 \times 10^{-9} \pm 9.0 \times 10^{-10}$	Competition	332	2.31
P1-15	7.0	$1.0 \times 10^{-6} \pm 1.3 \times 10^{-7}$	Direct	338	2.42
P1-8	7.0	$1.0 \times 10^{-5} \pm 3.0 \times 10^{-6}$	Competition	N/D	1.7
P9-26	7.0	$1.2 \times 10^{-8} \pm 3.0 \times 10^{-9}$	Direct	334	2.18
P9-21	5.0	$7.5 \times 10^{-10} \pm 3.9 \times 10^{-10}$	Direct	333	2.3
P9-21	6.0	$3.0 \times 10^{-9} \pm 5.0 \times 10^{-10}$	Direct	333	2.32
P9-21	7.0	$3.2 \times 10^{-8} \pm 5.1 \times 10^{-9}$	Direct	334	2.38
P9-21	8.0	$6.0 \times 10^{-8} \pm 1.9 \times 10^{-9}$	Direct	333	2.41
[P9-21 (H20N)]	5.0	$6.0 \times 10^{-9} \pm 4.0 \times 10^{-10}$	Direct	333	2.38
[P9-21 (H20N)]	7.0	$5.0 \times 10^{-8} \pm 2.2 \times 10^{-8}$	Direct	333	2.38
P9-26 + P1-8	7.0	$1.0 \times 10^{-9} \pm 2.6 \times 10^{-9}$	Direct	333	2.34

4.1.3 Peptide Amino-Acid substitutions.

Interaction of the PFK target sequences with calmodulin was studied using synthetic peptides based on the wild-type sequence containing specific amino-acid substitutions. Fluorescence titrations were performed as described in section 4.1.1. The target peptides are: [P9-26 (W11F)]; [P9-26 (Y14F)]; [P9-26 (E12Q)]; [P9-21 (E12K)]; and [P9-21 (H20N)].

The rationale for the choice of each peptide follows.

1. [P9-26 (W11F)] and [P9-26 (Y14F)]

In view of the importance of bulky hydrophobic groups in interactions involving calmodulin, peptides [P9-26 (W11F)] and [P9-26 (Y14F)] were prepared to determine effects of specific aromatic amino-acid residues W11 and Y14 on affinity for calmodulin.

2. [P9-21 (E12Q)]; [P9-21 (E12K)]; and [P9-21 (H20N)].

In order to study the importance of charge-charge interactions the above peptides were synthesized. The presence of negatively charged glutamate acidic residues in CaM binding targets is unusual. The role of this glutamic acid residue was studied by substitution to either a conservative neutral glutamine or a non-conservative basic lysine. The importance of the histidine residue was also examined; since the sequence is not predominantly basic, the histidine could be important as a putative basic residue.

The fluorescence enhancement and dissociation constants of each peptide variant in complex with CaM is given in table 4.1.3 along with the standard deviation of four independent titrations for each complex. The affinity of the spectroscopically silent P9-26 (W11F) was assessed using competition with the tryptophan containing peptide WF10,

sequence KKRWKKNIAV, from skeletal muscle myosin light chain kinase (K_d = 790nM, Findlay et al., 1995).

From specific amino-acid substitutions of the wild-type calmodulin-binding target sequence of PFK the following conclusions may be drawn:

(a). Replacement of the tryptophan residue at position 12 by phenylalanine caused a surprisingly large decrease in affinity, K_d increasing >800 fold from 12nM to more than 10μM. The presence of a tryptophan as a bulky hydrophobic anchor seems characteristic in several target interactions, (Meador et al., 1993; Ikura et al., 1992). It is interesting to note that for sk-MLCK peptide WFF the tryptophan can be substituted for phenylalanine with only 8 fold reduction in affinity, (Findlay et al., 1995). Therefore the tryptophan of the PFK target peptide appears residue specific for target interaction with calmodulin.

(b). The substitution of Tyr → Phe at position 14 has a lesser effect (~ 3 fold): The dissociation constant of [P9-26 (Y14F)] (K_d 40nM) is only slightly higher than that of the wild-type P9-26 sequence (K_d 11nM).

(c). There is little effect on affinity when the glutamate residue of wild-type P9-21 (K_d 32nM) is substituted to either a glutamine (K_d 20nM) or a lysine (K_d 5nM), although a slight increase is noted in both instances. Despite the small change in affinity, the fluorescence enhancement is increased by 1.43 fold when the glutamate is substituted with either a glutamine or a lysine. This suggests that the tryptophan fluorescence is partially quenched by the acidic glutamate residue.

Table 4.1.3

Dissociation constants with standard deviations calculated from four independent titrations and fluorescence enhancements for the complexes formed between calmodulin and target sequences from rabbit muscle phosphofructokinase with specific single amino-acid substitutions within the sequence. Protein concentration varies between 0.1 and 10μM. All titrations performed at 20°C in 25mM Tris, 100mM KCl, 1mM $CaCl_2$, pH 7.0. Excitation wavelength was 280 or 295nm. Emission was measured at 330nm. Monochromators were adjusted to 1 and 9nm for excitation and emission slits respectively. All dissociation constants were assessed using the direct non-linear least squares fit to a single dissociation constant except for complexes with peptide [P9-26 (W12F)] which was determined by a competition method, using the native peptide see section 3.4.1.

Peptide derivative	Dissociation constant (M) wild-type sequence	Dissociation constant (M) variant peptide	K_d(wt)/ K_d(v)	λ_{max}	F/Fo
[P1-8 (F7W)]	$1.0 \times 10^{-5} \pm 3.0 \times 10^{-6}$	$1.0 \times 10^{-5} \pm 9.3 \times 10^{-6}$	1.0		1.7
[P9-26 (W12F)]	$1.2 \times 10^{-8} \pm 3.0 \times 10^{-9}$	$> 1.0 \times 10^{-5}$	>800	334	
[P9-26 (Y14F)]	$1.2 \times 10^{-8} \pm 3.0 \times 10^{-9}$	$4.0 \times 10^{-8} \pm 2.3 \times 10^{-9}$	3.3	334	2.36
[P9-21 (E13Q)]	$3.2 \times 10^{-8} \pm 5.1 \times 10^{-9}$	$2.0 \times 10^{-8} \pm 5.7 \times 10^{-9}$	0.65	333	3.25
[P9-21 (E13K)]	$3.2 \times 10^{-8} \pm 5.1 \times 10^{-9}$	$5.0 \times 10^{-9} \pm 1.1 \times 10^{-10}$	0.15	333	3.25
[P9-21 (H20N)]	$3.2 \times 10^{-8} \pm 5.1 \times 10^{-9}$	5.1×10^{-8}	1.6	334	2.3

(d). Peptide [P9-21 (H20N)] (K_d 51nM) bound with very similar affinity to the P9-21 sequence, (K_d = 32nM) at pH 7.0. The pH dependence of the interaction of P9-21 and [P9-21 (H20N)] is fully considered in section 4.3.

4.1.4 Affinity of complexes formed between site directed mutants of CaM or proteolytic fragments of CaM with PFK peptides.

Site-Directed Mutants: The calcium binding site mutants (prepared by Pete Browne, (NIMR) according to the method of, Maune et al., 1992a) have the conserved glutamic acid residue in the twelfth position of one of the four calcium ion binding loops mutated to either a glutamine or a lysine. Mutations in site 2 and 4 result in a major reduction in calcium affinity for the mutated site whether the mutation is E-Q or E-K. The mutants have been termed BnQ or BnK where n is the number of the mutated calcium binding loop.

These mutants were used to investigate the requirement of an intact calcium saturated site in the interaction of the mutant CaM with peptide P9-26, and to try to identify the domain which interacts with the tryptophan of the target peptide by comparing the affinities of the mutant CaM:peptide complexes.

Table 4.1.4 shows that the mutations have a marked effect on the affinity of the calmodulin for peptide P9-26. Affinities of the mutants for peptide P9-26 were determined at 0.5 or 2.0μM peptide concentration. The higher concentration (2.0μM) was used in titrations involving peptide binding to site 4 mutants, since the effect of the mutation in site 4 is far more detrimental to peptide binding than that in site 2. Compared to wild-type calmodulin, the affinity decreases 3 fold and 13 fold for the site 2 mutants, B2Q and B2K respectively, and 133fold or 83 fold for the site 4 mutants B4Q and B4K.

Table 4.1.4

Dissociation constants with standard deviations calculated from four independent titrations and fluorescence enhancements for the complexes formed between site-directed mutants and proteolytic fragments of calmodulin with target sequences from rabbit muscle phosphofructokinase. Protein concentration varies between 0.1 and 10μM. All titrations performed at 20°C in 25mM Tris, 100mM KCl, 1mM $CaCl_2$, pH 7.0. Excitation wavelength was 280 or 295nm. Emission was measured at 330nm. Monochromators were adjusted to 1 and 9nm for excitation and emission slits respectively. All dissociation constants were assessed using the direct non-linear least squares fit to a single dissociation constant, see section 3.4.1.

Protein		P1-26	K_d/ K_d wt	P9-26	K_d/ K_d wt	P9-21	K_d/ K_d wt
wild type CaM (wt)	Kd (M) F/Fo λ_{max}	$2.8 \times 10^{-10} \pm 0.1 \times 10^{-11}$ (2.22) [333]	1.0	$1.2 \times 10^{-8} \pm 3.0 \times 10^{-9}$ (2.18) [333]	1.0	$3.2 \times 10^{-8} \pm 5.0 \times 10^{-9}$ (2.38) [334]	1.0
B2Q	Kd (M) F/Fo λ_{max}			$4.0 \times 10^{-8} \pm 5.0 \times 10^{-9}$ (2.25) [333]	3.3		
B2K	Kd (M) F/Fo λ_{max}			$1.6 \times 10^{-7} \pm 1.1 \times 10^{-8}$ (2.14) [336]	13		
B4Q	Kd (M) F/Fo λ_{max}			$1.6 \times 10^{-6} \pm 1.0 \times 10^{-6}$ (2.55) [336]	133		
B4K	Kd (M) F/Fo λ_{max}			$1.0 \times 10^{-6} \pm 4.0 \times 10^{-7}$ (2.31) [350]	83		
TR2C	Kd (M) F/Fo λ_{max}	$4.0 \times 10^{-7} \pm 1.1 \times 10^{-8}$ (2.22) [333]	1400	$1.0 \times 10^{-7} \pm 3.0 \times 10^{-8}$ (2.19) [334]	8.0	$1.0 \times 10^{-7} \pm 2.3 \times 10^{-8}$ (2.31) [335]	3.1

This implies that the C-domain contains the more important elements for P9-26 target sequence binding. In addition to affinity data it is noticeable from the emission spectra that the peptide tryptophan is more buried when bound to the B2 mutants than when bound to the B4 mutants. The wavelength maximum at 350nm for B4K suggests that the peptide tryptophan is significantly solvent exposed.

Proteolytic fragments: Studies of the isolated domains of calmodulin have previously yielded information regarding the Ca_4CaM:Target peptide interaction which would have been difficult to interpret using the whole calmodulin. The isolated domains not only yield data regarding inter-site and inter-domain cooperativity, but also indicate sites of interaction between whole calmodulin and its targets. The question of orientation in the peptide:calmodulin interaction was addressed by comparing affinities of TR2C (the C-terminal domain of calmodulin, residues 78-148) for PFK target sequences of differing length.

The titrations and affinity determinations were assessed using the method described in sections 4.1.1. TR2C concentration used in these titrations was 0.5μM. Table 4.1.4 shows the affinity of the C-terminal domain (TR2C) for PFK target sequences P1-26, P9-26, and P9-21. Stoichiometry was 1:1 for all TR2C:PFK peptide complexes.

Using P9-21 as a control it is possible to deduce the effect on affinity of extending at either the N- or C-terminal domain of the peptide. The affinity of P1-26 is reduced by 1400 fold compared with the interaction of the same peptide with intact calmodulin. This indicates that the N-terminal domain of calmodulin is required for high affinity interaction. The first 8 residues of the target sequence must be particularly important since the affinities of CaM:P1-26 and TR2C:P1-26 differ by 1400 fold whereas the

affinities of CaM:P9-26 and TR2C:P9-26 differ by only 8 fold. From this data it would seem that the tryptophan at position 11 is located in the C-terminal domain of calmodulin yet some or all of the first 8 residues of the target peptide make important contacts with the N-terminal domain of calmodulin. Consistent with this interpretation, there was no detectable interaction between TR1C and peptide P9-26 in experiments performed using a P9-26 concentration of 10μM, data not shown.

This is strikingly different to the mode of binding found when CaM Kinase II, sk-MLCK or sm-MLCK targets bind calmodulin, (Quiocho et al., 1992; Meador et al., 1992, 1993). Since the dissociation constants of peptides P9-21 and P9-26 with TR2C are the same (100nM) one can say that the residues -Pro-Pro-Ala-Pro-Lys- interact with residues in the calmodulin N-terminal domain. The affinity of peptide P1-26 shows slightly lower affinity for TR2C (400nM) this indicates that for optimum binding of P1-26 the opening 8 N-terminal residues -Lys-Leu-Arg-Gly-Arg-Ser-Phe-Met- require the presence of the CaM N-terminal domain.

The F/Fo values for all three peptides show fluorescence enhancements similar to the interaction of the peptides with the intact protein. Since the F/Fo is based on the fluorescence arising from the bound tryptophan spectra this indicates that the peptide tryptophan for the PFK target sequence interacts with the calmodulin C-terminal domain.

4.1.5 Accessibility of peptide tryptophan in the CaM:PFK complex.

Quenching studies were used in order to reveal the localization of fluorophores in proteins and their accesibility to quenchers, specifically acrylamide was used as a quencher to compare the accesibility of the calmodulin bound peptide tryptophan for peptides P1-26, P1-15, P9-26, and P9-21.

Acrylamide quenching studies were performed by adding small aliquots of concentrated acrylamide to a complex comprising calmodulin (0.5μM) and the peptide of interest (0.6μM) or peptide alone (0.6μM) The results were analyzed using the modified Stern-Volmer equation (Eftink & Ghiron, 1976), see section 3.2.2.

The values of the Stern-Volmer and static quenching constants for the complexes of CaM:P1-26, CaM:P1-15, CaM:P9-26, CaM:P9-21, and peptide P9-21 are given in table 4.1.5 as an average of four independent titrations with standard deviations on the four calculations. The titration data is illustrated in figure 4.1.5. It is evident that the tryptophan is buried to a similar extent in bound peptides P1-26, P9-26, and P9-21. However the tryptophan of peptide P1-15 is significantly more exposed to solvent (K_{sv}= 3.4M^{-1}) although less so than the tryptophan of the free peptide P9-21 in solution (K_{sv}= 9.1M^{-1}), both show relatively large values of the static quenching constant. This indicates two possibilities:

1. Peptide P1-15 is bound to calmodulin in a manner different from peptides P1-26, P9-26, or P9-21.

2. Peptide P1-15 is bound to calmodulin in a manner similar to peptides P1-26, P9-26, and P9-21, but is more exposed to solvent.

Peptide P1-15 has sequence K L R G R S F M N N W E V Y K. It appears that the tryptophan residue generally interacts with the C-terminal domain of calmodulin whilst the preceding N-terminal residues may make contacts with the N- and C-terminal domains. There are only 4 residues C-terminal to the tryptophan in peptide P1-15 and therefore any regular structure which might exist in C-terminal extended peptides such as P1-21 or P1-26 may not be present in the P1-15 peptide. This conformational effect may itself influence the hydrophobic nature of the tryptophan in the CaM:P1-15 complex,

Figure 4.1.5

Representative titrations of acrylamide to peptide P9-21 (x) or a complex of calmodulin bound to peptide P1-26 (*), P1-15 (+), P9-26 (□) or P9-21 (■) at equimolar concentration. Peptide concentration is 10μM for P1-15 and 0.5μM otherwise. Excitation wavelength was 296nm. Emission was measured at 340nm. Monochromators were adjusted to 1 and 9nm respectively. Data is for single representative titrations, experiments were repeated 3 times. The Stern-Volmer static quenching constants, V and collisional quenching constant, K_{SV} are listed with standard deviations in Table 4.1.5.

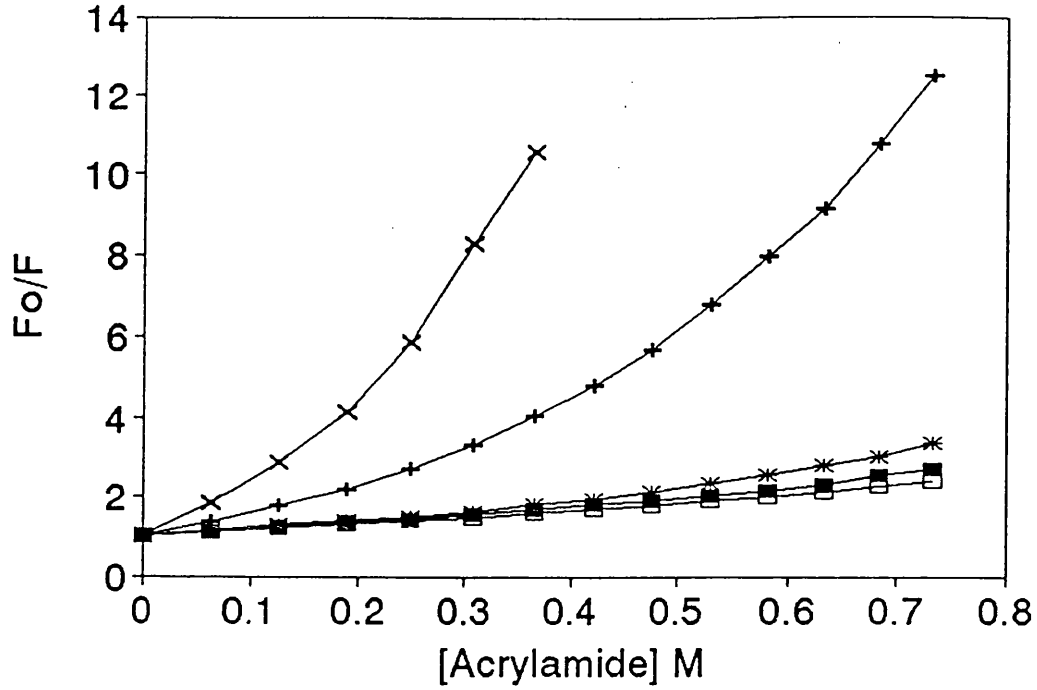
14
12
10
8
6
4
2
0
Fo/F
0
0.1
0.2
0.3
0.4
0.5
0.6
0.7
0.8
[Acrylamide] M

Table 4.1.5

Acrylamide quenching data for the titration of acrylamide to peptide P9-21 or a complex of calmodulin bound to peptide P1-26, P1-21, P1-15, P9-26 or P9-21 at equimolar concentration. Peptide concentration is 10μM for P1-15 and 0.5μM otherwise. Buffer is 25mM Tris, 100mM KCl, 1mM $CaCl_2$, pH 7.0. Excitation wavelength was 296nm. Emission was measured at 340nm. Monochromators were adjusted to 1 and 9nm for excitation and emission slits respectively.

Peptide/Peptide:Protein complex	Stern-Volmer constant K_{SV} M^{-1}	Static quenching constant V M^{-1}
CaM:P1-26	1.144 ± 0.281	0.1441
CaM:P1-15	3.437 ± 1.961	1.382
CaM:P9-26	0.958 ± 0.253	0.0487
CaM:P9-21	0.9634 ± 0.295	0.2953
P9-21	9.128 ± 0.5652	1.701

alternatively the effect may be due to the inability of the "short" P1-15 peptide to bind to calmodulin in such a way that the calmodulin can provide the hydrophobic environment characteristic of CaM in complex with P1-26, P1-21, P9-26 or P9-21.

4.1.6 Influence of pH on fluorescence properties of the CaM:PFK complex.

The pH dependence of the affinity of peptide P9-21 for calmodulin was studied in the range 5.0-8.0. Table 4.1.6 shows the dissociation constants (measured at 0.5μM CaM) for CaM:P9-21 decrease significantly at lower pH. Figure 4.1.6a shows the pH dependence of the fluorescence enhancements of CaM:P9-21. An F/Fo value >1 reflects that the peptide is bound to some extent since the increase in absolute intensity reflects the solvent accessibility of the tryptophan residue in the target peptide. The wavelength maximum also reflects the peptide environment since the wavelength maximum for free and bound tryptophan are approximately 350 and 330nm respectively, see section 3.2.2. The pH dependence of peptide [P9-26 (W12F)] fluorescence reveals that there are three distinct pH dependent processes, figure 4.1.6b. The first shift at pH 3.5-4.3 correlates with protonation of the α-carboxyl groups of the peptide. The histidine protonation could explain the change in intensity between 6.0 and 7.0 (His pK_a 6.04). The third fluorescence dependent pH process is the ionization of the tyrosine to the negatively charged tyrosinate species, pH $>$ 8.0.

The large decrease observed in affinity for peptide P9-21 binding to calmodulin between pH 5.0 and 7.0 suggested a possible involvement of the histidine residue present in the PFK peptide since His has a pK_a = 6.04. The residue would be protonated at pH 5.0 and could contribute an additional positive charge for interaction with the net negatively charged calmodulin. This prompted synthesis of a P9-21 peptide analogue with

Figure 4.1.6

(A) Fluorescence enhancements for the complex formed between calmodulin and target sequence P9-21 from rabbit muscle PFK at equimolar concentration. Protein concentration is 0.5μM. All titrations performed at 20°C in100mM KCl, 1mM $CaCl_2$. Buffer is 25mM sodium acetate (< pH 7.0), 25mM Tris (pH 7.0-8.5), and 25mM sodium borate (pH > 8.5). Excitation wavelength was 295nm. Emission was measured at 330nm.

(B) Fluorescence of peptide [P9-26 (W12F)] at 10μM. Fluorescence is normalized so that the lowest value (pH 12.8) = 1. The buffers used are as described in the legend for figure 4.1.6a. Excitation wavelength is 280nm, emission was measured at 320nm.

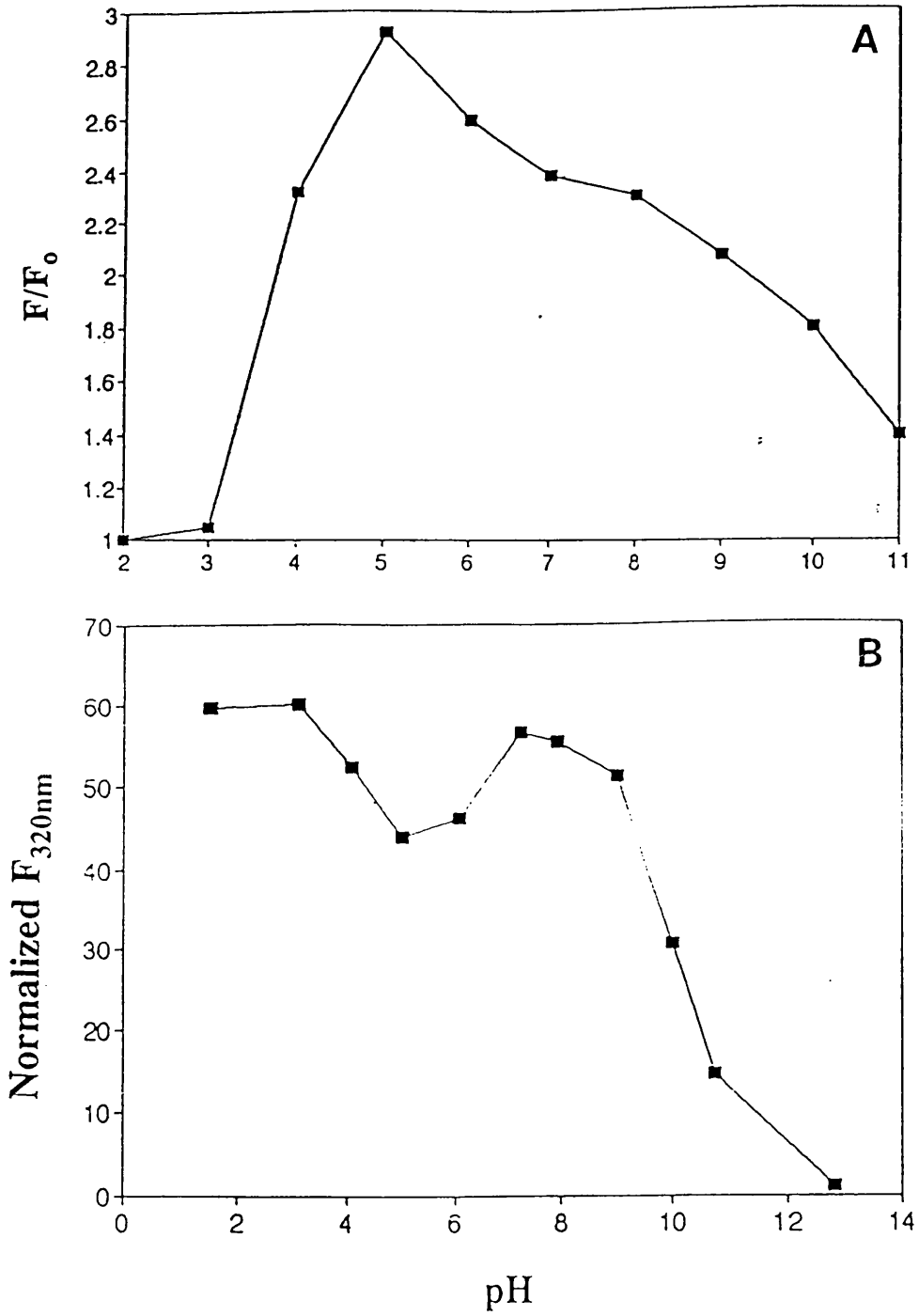
A
F/F$_o$
3
2.8
2.6
2.4
2.2
2
1.8
1.6
1.4
1.2
1
2
3
4
5
6
7
8
9
10
11
B
Normalized F$_{320nm}$
70
60
50
40
30
20
10
0
0
2
4
6
8
10
12
14
pH

Table 4.1.6

Dissociation constants with standard deviations calculated from four independent titrations and fluorescence enhancements for the complexes formed between calmodulin with target sequence P9-21 at different pH values. Calmodulin and peptide concentrations are 0.5 and 0.55μM respectively. Experimental buffer is 25mM Tris, 100mM KCl, 1mM $CaCl_2$ for studies between pH 7.0 and 8.5. For studies above and below these pH values 25mM sodium borate or 25mM sodium acetate was used in place of 25mM Tris. Excitation wavelength was 280 or 295nm, emission was measured at 330nm.

pH	K_d (M)	F/Fo
2.0		1.00
3.0		1.00
4.0		2.32
5.0	$7.5 \times 10^{-10} \pm 3.9 \times 10^{-10}$	2.92
5.5	$5.0 \times 10^{-10} \pm 1.0 \times 10^{-10}$	2.69
6.0	$3.0 \times 10^{-9} \pm 5.0 \times 10^{-10}$	2.59
6.5	$1.0 \times 10^{-8} \pm 1.4 \times 10^{-9}$	2.40
7.0	$3.2 \times 10^{-8} \pm 5.1 \times 10^{-9}$	2.38
7.5	$4.5 \times 10^{-8} \pm 1.2 \times 10^{-9}$	2.31
8.0	$6.0 \times 10^{-8} \pm 1.9 \times 10^{-9}$	2.30
8.5	$2.5 \times 10^{-7} \pm 4.6 \times 10^{-8}$	1.91
9.0	$3.9 \times 10^{-7} \pm 7.4 \times 10^{-8}$	2.07
10.0		1.8
11.0		1.4

His-Asn substitution, [P9-21 (H20N)]. The dissociation constant for the peptide variant is reported in table 4.1.3 The affinity of peptide [P9-21 (H20N)] for calmodulin is 10 fold weaker at pH 5.0 and 1.5 weaker still at pH 7.0 compared with peptide P9-21; however the affinity of [P9-21 (H20N)] for calmodulin is still pH dependent, having approximately 10 fold stronger affinity at pH 5.0 than 7.0, (6nM cf. 50nM). The greater than 30 fold increase in affinity for the P9-21 peptide over the same pH range suggests that protonation of the histidine residue is involved in high affinity binding. However the effect is small since in addition to this other pH dependent processes exist. The fluorescence of peptide [P9-21 (H20N)] is not dependent on pH and the fluorescence of its complex with calmodulin exhibits fluorescence characteristics similar to the complex formed with the P9-21 peptide. Thus it does not appear that the presence of a protonated histidine residue is a very significant part in the binding of the peptide by calmodulin.

4.1.7 Conclusions

From study of the interaction of calmodulin with target sequences from phosphofructokinase by fluorescence it can be concluded that:

(1). Peptide P1-26 has picomolar affinity for calmodulin, the first eight residues of which evidently make important contribution to binding. However, the full affinity of binding is only seen when the sequence is composed as one intact peptide. Surprisingly, the 5 C-terminal residues of the P1-26 sequence contribute to the affinity, this may involve the PPAPK sequence or may be a result of the arginine binding more strongly when protected by the additional 5-residue portion of sequence. The tryptophan of peptide P1-15 may bind to calmodulin in a different mode to the same tryptophan in peptides P1-26,

P1-21, P9-26 and P9-21, since the environment of the peptide tryptophan is far more solvent exposed in the complex of CaM:P1-15 than for the complexes formed between CaM and the other tryptophan containing peptides.

(2). It is likely that the tryptophan of the target peptide makes its most important (if not all contacts) with the C-terminal domain of calmodulin. The tryptophan residue is specific for binding since substitution for phenylalanine severely impairs affinity. Tyrosine, (another aromatic amino-acid in the PFK target sequence) is a less critical determinant in sequence recognition by calmodulin since the peptide tyrosine at position 14 was substituted for phenylalanine with little effect on affinity.

(3). Residues 16-26 of the PFK sequence are required to provide the correct environment for the binding of the peptide tryptophan to calmodulin. It may be that this is through binding to the calmodulin N-terminal domain, providing a conformational change in the protein which in turn provides a hydrophobic channel between the domains for peptide to bind.

(4). The PFK target sequence is not particularly basic, and a protonated histidine might provide some minor additional binding affinity. The fluorescence of the tryptophan is quenched by a neighbouring acidic group; but, surprisingly, substitution of the acidic group to a neutral or basic amino acid had little effect on affinity.

4.2. Conformational studies of secondary and tertiary structure in calmodulin, PFK peptides and the complexes formed by their interaction

As mentioned previously in chapter 2, consideration of the primary sequence of the calmodulin binding region of PFK suggests that it is very unlikely to adopt the basic amphipathic α-helical conformation that is noted in the calmodulin bound forms of sk-MLCK, Ikura et al., 1992), sm-MLCK, (Meador et al., 1992) and CaMK II, (Meador et al., 1993).

To investigate the conformational features of the PFK target sequence, circular dichroism techniques were used; specifically, far-UV CD was used for study of the peptides in solution, in the helicogenic solvent trifluoroethanol (TFE) and in the calmodulin bound form. Near-UV CD was used also in these studies to assess the environment of peptide aromatic amino acids in complexes of different PFK peptides with calmodulin.

4.2.1.Far-UV CD spectroscopy of CaM and its complexes with PFK target sequences.

4.2.1.1. Peptide length effects (CaM bound and in TFE)

PFK peptides in aqueous solution and on binding to CaM

The PFK peptides, P9-21, P9-26, P1-21, and P1-26 display predominantly random structure in aqueous solution, data not shown. Calmodulin alone has a far-UV CD spectrum characteristic of a mainly α-helical protein (maxima at 207 and 222nm). Intensification of the signal at 222nm indicates that the α-helical content of the complex increases when any of the three peptides are bound to calmodulin, see Fig 4.2.1.1a. The increase shown is relatively small since calmodulin contains substantial α-helix. The far-

UV CD spectra of the bound peptides were calculated, assuming no conformational change in calmodulin on binding peptide. The far-UV CD difference spectra is calculated as {[CaM:$PFK_{peptide}$] - [CaM]} and show that for all four peptides some α-helical structure is induced on binding, Fig 4.2.1.1b. In order to apply the models for the helix-coil transition to the mean residue ellipticity at 222nm. $[\theta]_{222nm}$ were converted into fractional helicity, using the method of (Scholz et al., 1991) see section 3.2.3.

The extent of α-helical structure in the calmodulin bound PFK peptides is shown in table 4.2.1. The P9-26 peptide (n_H = 7.5) is somewhat more helical than the P9-21 peptide (n_H = 5) when bound to calmodulin. It is unlikely that the additional five residues "PPAPK" at the C-terminus can become helical. This might indicate that a sequence within the P9-21 region has higher α-helical propensity when further residues are added to its C-terminal end.

The bound P1-26 peptide (n_H = 6.7) has little extra helicity compared to the P9-26 peptide, this suggests that the extra 8 residues at the N-terminus do not adopt an α-helical conformation upon binding to calmodulin. The increased intensity at 205-212nm is consistent with these additional residues being unstructured (random coil).

Structure of the PFK peptides in trifluoroethanol (TFE)

To determine the propensity of the peptides to form helix in solution trifluoroethanol, (TFE), was added to the peptides and the intensity at 222nm was recorded in 50% TFE, (Figure 4.2.1.1c, (Table 4.2.1). The helical propensities were calculated using the same method as above. The 26 residue peptide appears to have the greatest propensity to form helix, although in terms of peptide size the proportion of helix per peptide is quite similar suggesting that neither the high affinity P1-26 peptide or the lower affinity P9-21 peptide are predominantly helical in TFE unlike many other

Figure 4.2.1.1

(a) Far-UV CD spectra for calmodulin and complexes formed by the interaction of CaM and target peptides from PFK. Calmodulin concentration is 10μM, peptide concentration is 11μM. The buffer used was 25mM Tris, 100mM KCl, 1mM $CaCl_2$, pH7.0. Spectra were collected at room temperature. For each experiment a spectrum is an average of 16 scans.

(b) Far-UV CD difference spectra for complexes formed by the interaction of CaM and target peptides from PFK. Experimental conditions as above.

(c) Far-UV CD spectra for target peptides P1-26, P1-21, P9-26 and P9-21 from PFK in 50% trifluoroethanol. 50μM peptide is dissolved in 50% trifluoroethanol in 25mM Tris, 100mM KCl, pH7.0 at 20°C. For each experiment a spectrum is an average of 16 scans.

(d) The number of helical residues in peptides P1-26 (□), P1-21 (*), P9-26 (▲) and P9-21 (■) calculated in a solution with 50% trifluoroethanol, experiments performed at 50μM peptide. Sample buffer is 25mM Tris, 100mM KCl, pH 7.0. Spectra are recorded at 20°C. Helicity is quantitated using the method of Scholz et al., (1993) as described in section 3.2.3.

a
CaM
+P9-21
+P1-21
+P9-28
+P1-28
Δε_M (M⁻¹.cm⁻¹)
Wavelength (nm)
b
P9-21
P9-28
P1-28
Δε_M (M⁻¹.cm⁻¹)
Wavelength (nm)
c
P9-21
P9-28
P1-28
Δε_M (M⁻¹.cm⁻¹)
Wavelength (nm)
d
helical residues
% TFE (v/v)

Table 4.2.1

Far-UV CD extinction coefficients at 222nm of four PFK target peptides in either a calmodulin bound state or in the presence of 50% trifluoroethanol (TFE). For experiments in the presence of calmodulin the value of the mean residue CD of the CaM:peptide complex is related to the molar CD by the equation $\Delta\epsilon_{MRW} = \Delta\epsilon_M/n$, where n is the number of peptide bonds in the complex of calmodulin (147) plus the number of peptide bonds from the target sequence. The CD arising from calmodulin alone can similarily be calculated, and the signal arising from the bound peptide calculated as ([CaM:peptide]-[CaM]). The CD signal for the peptide (50μM) in trifluoroethanol is obtained directly. All samples were prepared in 25mM Tris, 100mM KCl, 1mM $CaCl_2$, pH7.0, 20°C. The signal obtained for an individual experiment is an average of 16 scans and values quoted at 222nm are an average of four independent experiments with standard deviation. The percentage helicity is calculated using the method of Scholz et al., (1993) described in section 3.2.3.

	CALMODULIN BOUND 20°C			PEPTIDE IN 50% TFE 20°C		
	$\Delta\epsilon_{MRW}$ (222nm)	% α-helix	# helical residues (n_H)	$\Delta\epsilon_{MRW}$ (222nm)	% α-helix	# helical residues (n_H)
P9-21	3.5 ± 0.2	39.0	5.0	3.4 ± 0.6	37	4.8
P9-26	4.3 ± 0.4	41.6	7.5	4.5 ± 0.3	43	7.8
P1-21	3.8 ± 0.4	35.4	7.4	4.1 ± 0.7	39	8.1
P1-26	2.8 ± 0.1	25.7	6.7	3.6 ± 0.4	33	8.6

calmodulin binding target peptides, (O'Neill and Degrado, 1990). The helicity induced as a function of TFE concentration is reported in Figure 4.2.1.1d. The maximum inducable helicity occurs at approximately 30% TFE. The helicity of the PFK peptides bound to calmodulin was comparable with the helicity of the PFK peptides in 50% TFE, see table 4.2.1.

These findings are important for the recognition of the PFK target sequence by calmodulin. It would appear that the higher affinity of P1-26 can probably be attributed to the extra 3 basic residues of the P1-26 peptide compared with the P9-21 and P9-26 peptides. The increased affinity of calmodulin for the longer peptides is probably not associated with an increased propensity of the longer peptides to form helix. This suggests that the CaM:P1-26 interaction may be quite distinct from the basic amphipathic α-helical calmodulin binding peptides discussed in the review by (O'Neill and Degrado, 1990).

4.2.2. Near-UV CD spectroscopy of CaM, and its complexes with PFK target sequences.

Figure 4.2.2a shows the near-UV CD spectra of calmodulin alone and in complex with each of the five PFK peptides, P1-26, P1-21, P1-15, P9-26, and P9-21. A single tyrosine residue at position 138 in calmodulin contributes to the signal at 280nm. The large difference in peptide CD signals at 280 and 295nm present upon peptide binding to calmodulin is characteristic of the immobilization of the aromatic residues (1 Tyr, 1 Trp) in the target sequence. The spectra for the complexes formed between CaM and peptides P1-26, P1-21, P9-26, and P9-21 are relatively intense and show similar characteristic spectra, this indicates that the environment of the immobilized tryptophan residue of P9-21, P9-26, P1-21 and P1-26 is similar and the mode of binding to

calmodulin is independent of peptide length. Any small differences in spectra are likely to be attributable to either baseline alignment problems or uncertainty in protein concentration. The spectrum of peptide P1-15 in complex with calmodulin is very different at 280 and 295nm, this suggests that the tryptophan of this peptide is in a different environment. It is possible that because residues 16-21 are not present in this peptide that insufficient interaction occurs between the peptide and the two domains of calmodulin so that the peptide tryptophan is in a different environment. The spectra for the free peptides show very little near-UV CD intensity as anticipated for unstructured polypeptides (data not shown).

The interaction of calmodulin with peptide WFF from sk-MLCK using near-UV CD has been described by Findlay et al (1995). In the sk-MLCK peptide there is no tyrosine residue, however, in sk-MLCK peptide (and target sequences from several other sources) a tryptophan residue near the N-terminus is implicated in the high affinity interaction. To determine whether the spectrum of the bound Trp in the CaM:P9-26 complex resembles the Trp spectrum resulting from interaction of calmodulin with sk-MLCK target sequence the contribution of the tyrosine and tryptophan to the CaM:P9-26 spectrum were deduced. Figure 4.2.2b shows the spectra of bound P9-26 and [P9-26 (W12F)], each with the calmodulin contribution subtracted, the difference of the two curves is also shown to illustrate the apparent contribution of the bound Trp. These calculations assume (1) additivity of the tyrosine and tryptophan signals, and (2) the spectrum representing the peptides P9-26 and [P9-26 (W12F)] bind in analogous fashion. On this basis Trp of the bound PFK peptide was quite different from that of Trp of the bound sk-MLCK peptide, see figure 4.2.2c. This suggests that the sk-MLCK and PFK target sequences bind in different modes.

Figure 4.2.2

(a) Near-UV CD spectra of calmodulin and complexes formed by its interaction with peptides P1-26, P1-21, P1-15, P9-26 and P9-21. Protein concentration is 50μM and peptide is 1.1 fold in excess. Spectra collected at 20°C in buffer comprising 25mM Tris, 100mM KCl, 1mM $CaCl_2$.

(b) Difference spectra generated for the complexes formed between calmodulin and peptides P9-26, [P9-26 (W12F)] and peptide WFF from sk-MLCK.

(i) = ([CaM:P9-26]-[CaM])

(ii) = ([CaM:P9-26 (W12F)]-[CaM]

(iii) = (i) - (ii)

(iv) = ([CaM:WFF]-[CaM])

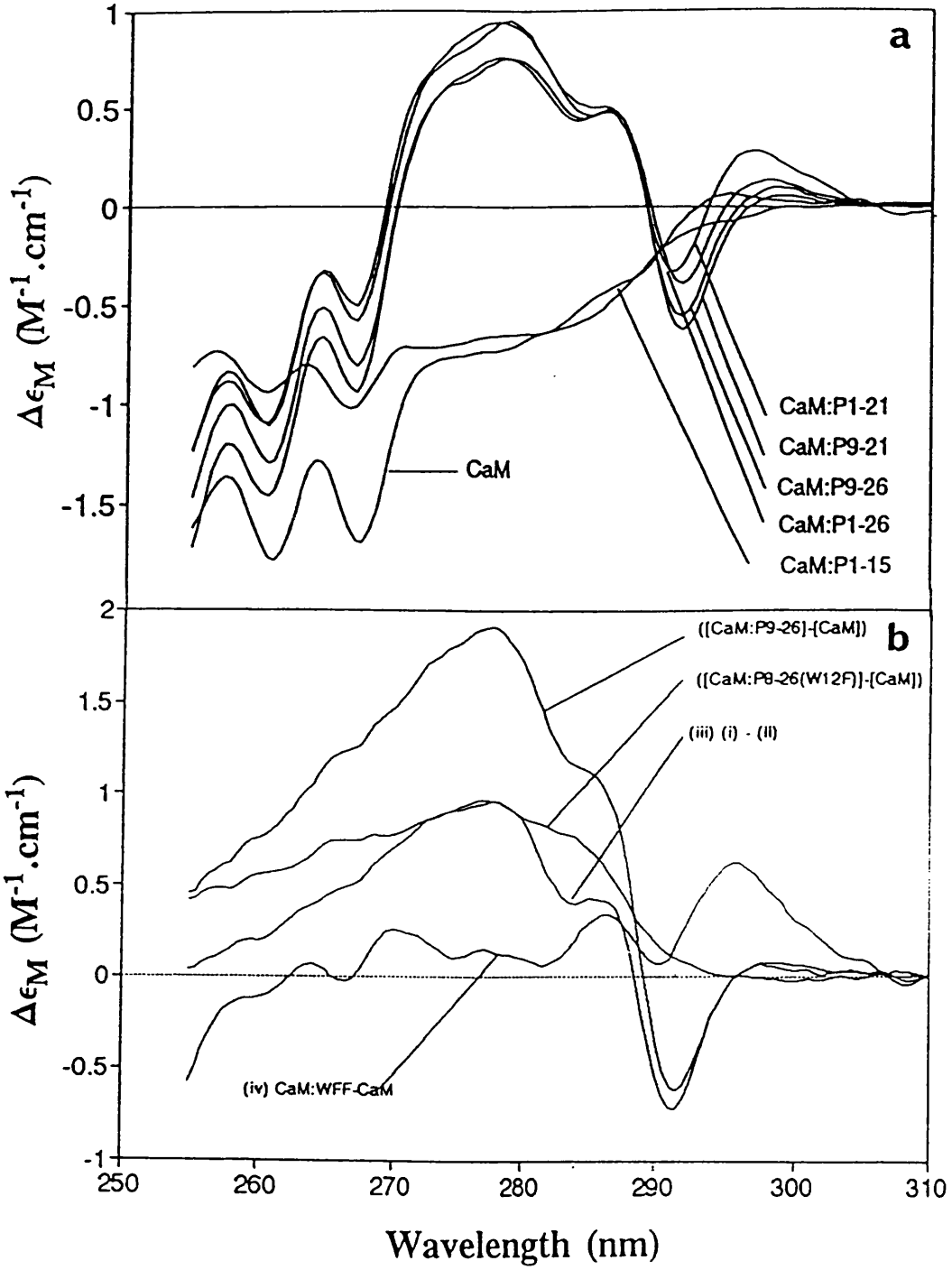
a
b
CaM
CaM:P1-21
CaM:P9-21
CaM:P9-26
CaM:P1-26
CaM:P1-15
([CaM:P9-26]-[CaM])
([CaM:P8-26(W12F)]-[CaM])
(iii) (i) - (ii)
(iv) CaM:WFF-CaM
Δε_M (M^-1.cm^-1)
Wavelength (nm)

Figure 4.2.2c

Near-UV CD difference spectra for the complexes formed between calmodulin and peptides P9-26, WFF, and RS20 from the calmodulin binding regions of phosphofructokinase, sk-MLCK, and sm-MLCK respectively. Calmodulin spectra was collected at 50μM with a peptide concentration of 55μM. For each experiment protein and protein:peptide complex spectra were collected as an average of 16 scans. Samples were dissolved in a buffer comprising 25mM Tris, 100mM KCl, 1mM $CaCl_2$, pH 7.0 at 20°C.

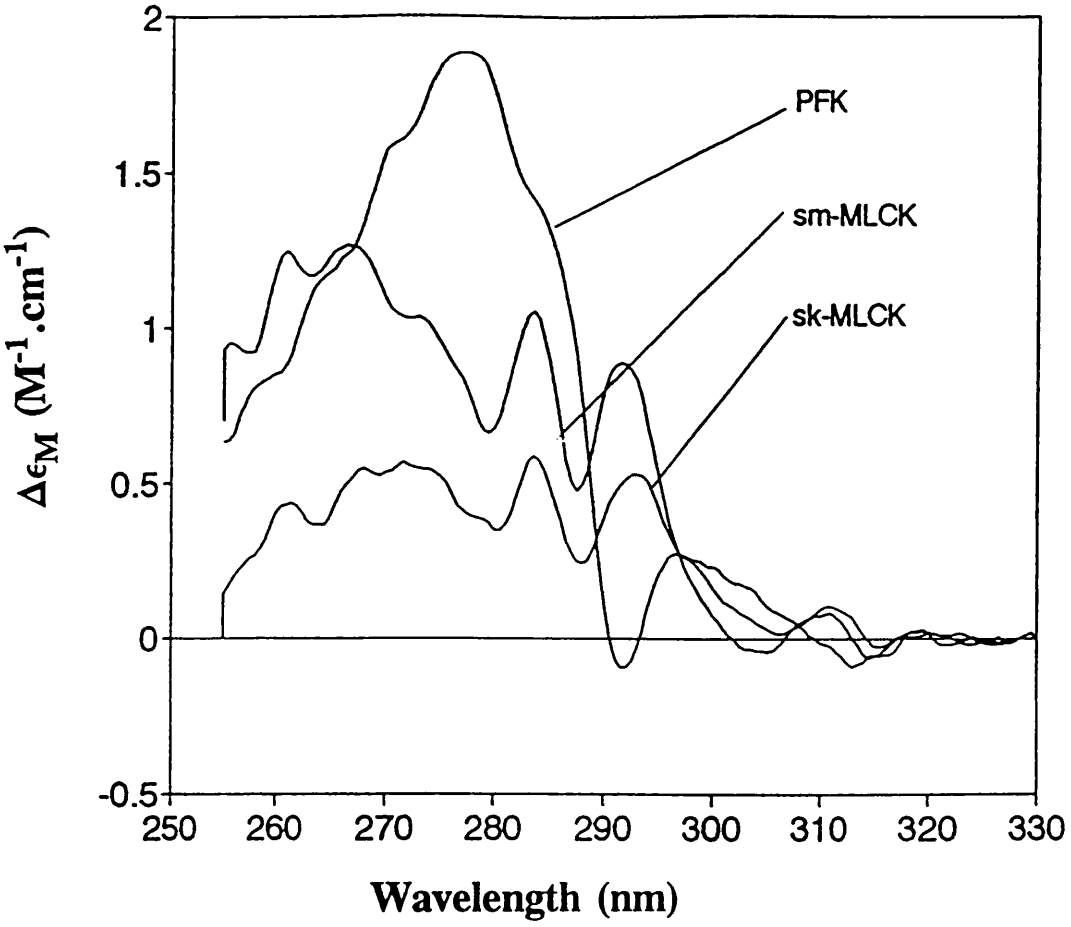
2
1.5
1
0.5
0
-0.5
250
260
270
280
290
300
310
320
330
PFK
sm-MLCK
sk-MLCK
$\Delta\epsilon_M$ ($M^{-1}.cm^{-1}$)
Wavelength (nm)

To demonstrate that near-UV CD reflects tryptophan environment, near-UV CD was used to compare the calmodulin bound conformations of the target peptides from sm-MLCK and sk-MLCK. The 3D structures of the complexes with CaM indicate that the bound peptides make similar contacts with calmodulin and the tryptophan of the two peptides resides in the same hydrophobic pocket provided by calmodulin, (Ikura et al., 1992; Meador et al., 1992). On the basis of the 3D structural evidence one would therefore expect the environment of the calmodulin to be very similar for the sk- and sm-MLCK peptides when bound to calmodulin. The difference spectra of CaM:sk-MLCK and CaM:smMLCK shows that this is so, figure 4.2.2c.

Because near-UV CD is extremely sensitive to the environment of the chromophore it can be concluded that all peptides P1-26, P1-21, P9-26 & P9-21 from PFK bind to CaM in a similar manner, however the environment of the Trp sidechain of the bound PFK peptide is probably quite different from that of the Trp in the bound sk or sm-MLCK target peptides.

4.2.3. Structural studies using site-directed mutants of calmodulin in complex with PFK peptide P9-26

A series of single calcium-binding site mutants of *Drosophila melanogaster* calmodulin were used to determine the effect of mutation in calcium binding site on interaction with peptide P9-26, (Maune et al., 1992a,b) also see table 3.1.3.

Near-UV CD (see section 3.2.3) was used to assess the environment of the putative important hydrophobic tryptophan anchor in the PFK target sequence using binding site mutants of calmodulin in complex with peptide P9-26. The effective elimination of calcium binding in site 4 of calmodulin appears to effect the environment

Figure 4.2.3

(a) Near-UV CD spectra for complexes formed between peptide P9-26 and either calmodulin or one of the calcium binding site mutants of calmodulin, B2K, B2Q, B4K or B4Q. Spectra collected at 20°C in 25mM Tris, 100mM KCl, 1mM $CaCl_2$, pH 7.0. CaM or calcium binding site mutants of CaM concentration is 50μM. Peptide P9-26 concentration is in 1.1 fold excess over protein.

(b) Near-UV CD difference spectra for the complexes in legend (a). Difference spectra are calculated as ([Protein:P9-26]-[Protein]) where protein is CaM or a calcium binding site mutant of CaM.

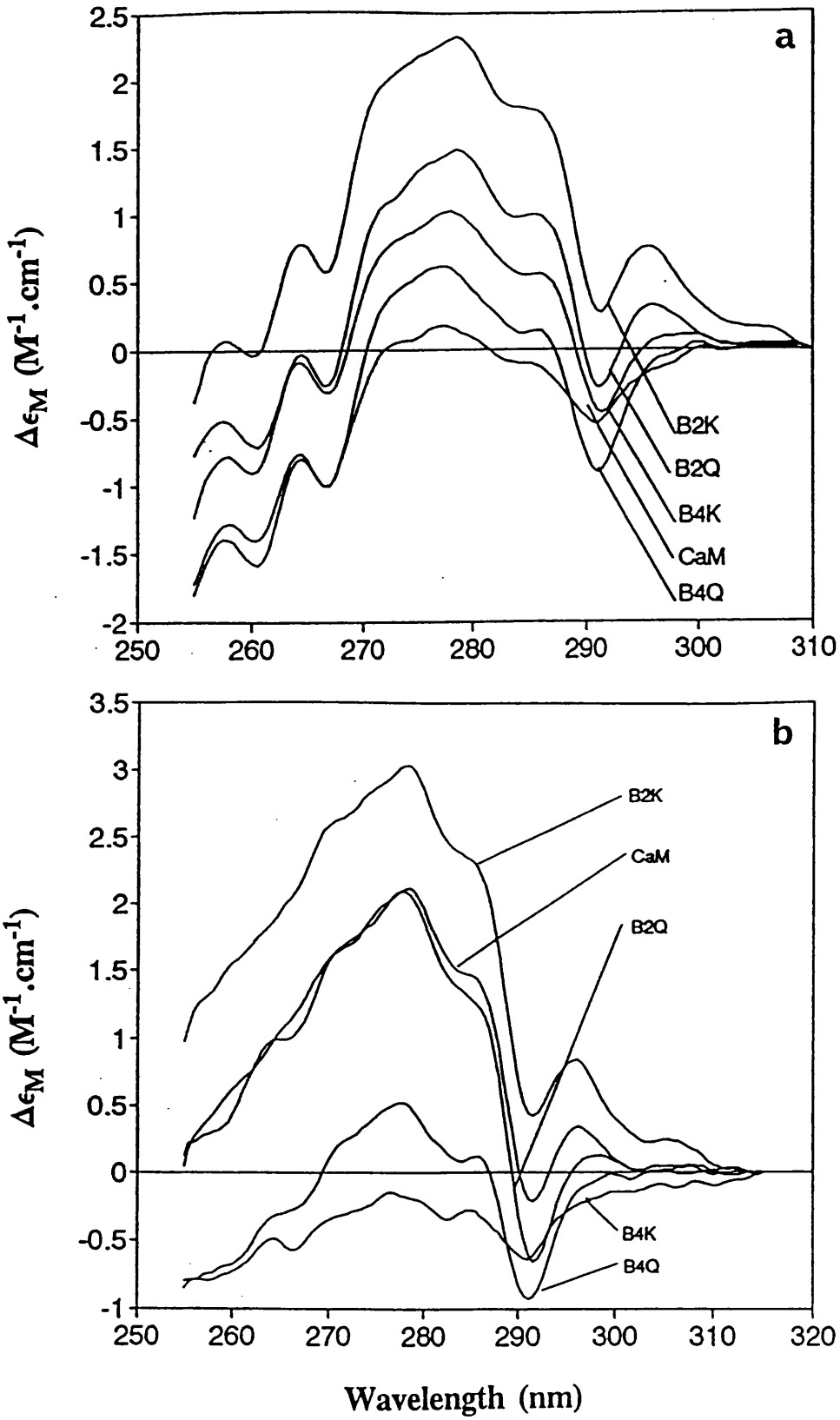
a
b
B2K
B2Q
B4K
CaM
B4Q
$\Delta\epsilon_M$ ($M^{-1}.cm^{-1}$)
Wavelength (nm)

of the tryptophan in the bound peptide more significantly than the B2 mutants. Figure 4.2.3a shows the complexes formed upon interaction of calcium binding site mutants of calmodulin with peptide P9-26. Figure 4.2.3b shows the difference spectra for each of the calcium binding site mutants of calmodulin in complex with peptide P9-26. The spectra indicate that the effect of mutation at site 4 in the C-domain is more detrimental to complex formation than mutation of site 2 in the N-terminal domain. These spectra are also consistent with the deduction that the peptide tryptophan is buried in a hydrophobic pocket within the C-domain of calmodulin.

4.2.4 Conformational properties of the TR2C:P9-26 interaction

Figure 4.2.4a shows the near-UV CD spectra for Ca_4CaM, Ca_2TR2C and the complexes formed with peptide P9-26. The spectra for the Ca_2TR2C and Ca_4CaM are closely similar at 280nm suggesting that the tyrosine at position 138 in the protein is in the same environment whether the N-terminal domain of the protein is present. The spectra resulting from the complex of each protein with peptide P9-26 are similar in shape implying that the overall interaction is similar, there is however a substantial difference in intensity of the two signals and this may reflect the extent to which the peptide tryptophan and possibly tyrosine are buried when complexed to protein. It is easier to make deductions regarding the nature of the tryptophan, since there is only one tryptophan in the system and it is in the peptide, furthermore this single tryptophan has a characteristic signal arising only from a transition in the aromatic residue itself at 295nm. The signal at 280nm is more difficult to interpret since there are two tyrosines in the complex system, one in the peptide and another in the C-domain of calmodulin at position 138, furthermore the signal at 280nm arises from electronic transitions in tyrosine and tryptophan.

Figure 4.2.4

(a) Near-UV CD spectra for calmodulin, TR2C (CaM residues 78-148) and the complexes formed with peptide P9-26. Spectra collected at 20°C using a buffer comprising 25mM Tris, 100mM KCl, 1mM $CaCl_2$, pH 7.0. Protein concentration is 50μM and peptide P9-26 is 55μM.

(b) Near-UV CD difference spectra for the complexes formed between calmodulin and TR2C (CaM residues 78-148) with P9-26. Difference spectra calculated as ([CaM:P9-26]-[CaM]) or ([TR2C:P8-26]-[TR2C]). Spectra collected under conditions specified in legend for figure 4.2.4a.

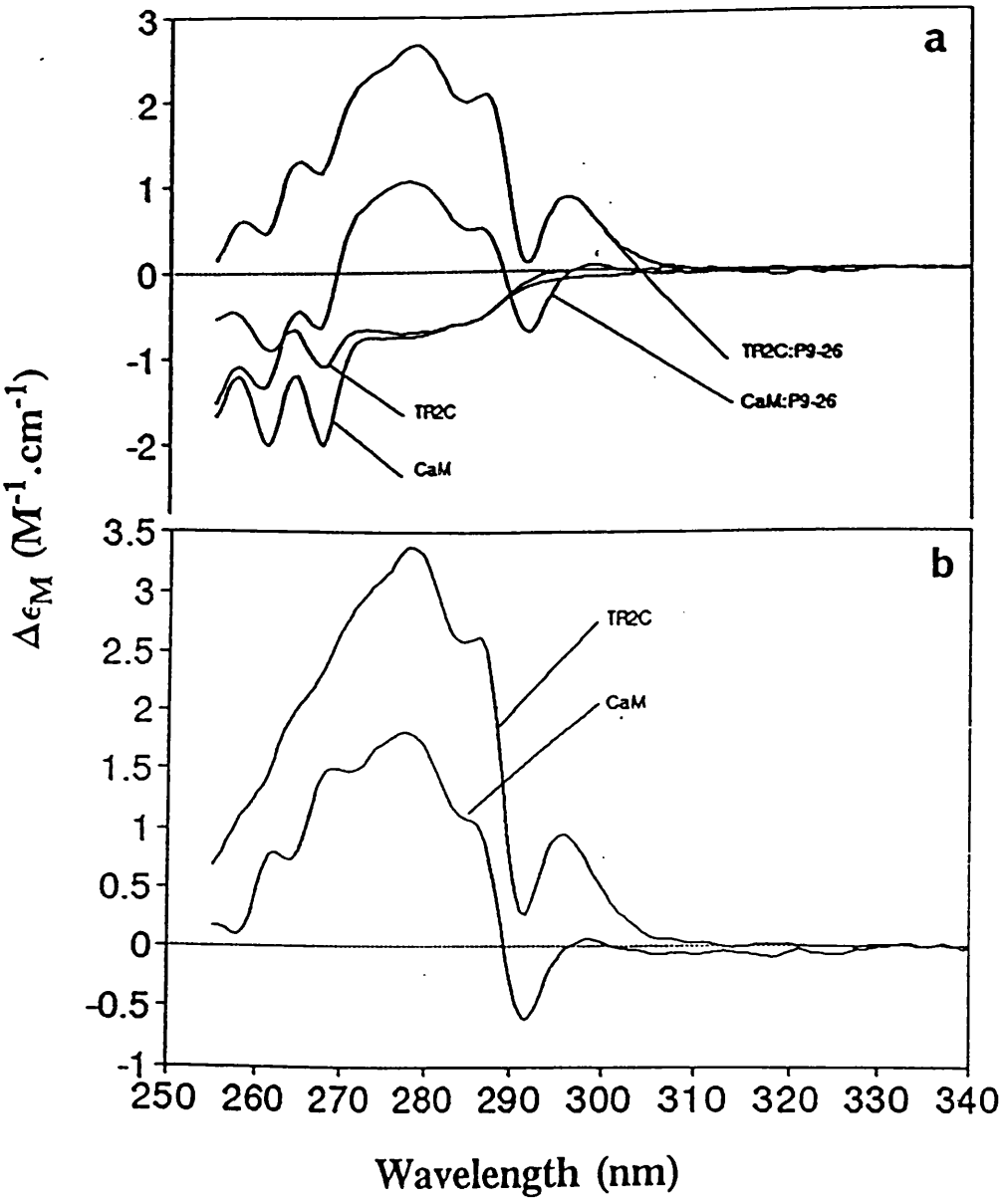
a
b
TR2C:P9-26
CaM:P9-26
TR2C
CaM
TR2C
CaM
$\Delta\epsilon_M$ ($M^{-1}.cm^{-1}$)
Wavelength (nm)

The difference spectra for CaM:P9-26 and TR2C:P9-26 complexes calculated as [(Protein:P9-26)-(Protein)] (see figure 4.2.4b) supports these findings. It would appear therefore that the tryptophan and possibly the tyrosine of the PFK peptide interacts with the C-terminal domain of the protein.

4.2.5 pH related conformational effects in CaM:P9-21 system

To probe whether the pH dependance of CaM:P9-21 interaction corresponds to a different mode of peptide binding, calmodulin and CaM:P9-21 complexes were studied using CD techniques. There is no difference in the tertiary structure of calmodulin over the pH range 5.0-8.0 as judged by near-UV CD, see figure 4.2.5a, however in the complexes the intensity arising from the peptide tryptophan at 290-300nm is significantly affected by a decrease in pH over this range. This correlates with a decrease in Kd indicating that the tryptophan immobilization correlates with high affinity interaction.

Far-UV CD was used to study the conformation of the P9-21 peptide over the pH range 5.0-8.0. There was little difference in peptide structure in aqueous solution, or TFE in this pH range. This indicates that the pH dependent affinity of P9-21 for CaM is not related to changes in secondary structure.

4.2.6 Effects of temperature on the secondary structure of the PFK peptides.

The PFK target sequences; P1-26, P1-21, P9-21 and P9-26 were prepared in 50% TFE and monitored by far-UV CD at 222nm over a wide temperature interval to assess helical propensities under these conditions.

Figure 4.2.6a-d illustrates measurements taken at 222nm for four PFK peptides in 50% TFE, 25mM Tris, 100mM KCl, pH7.0 at different temperatures. The data

collected at 10μM show that the helix → coil transition is approximately linear in the temperature range 5-80°C. It was not possible to determine an equilibrium constant associated with the transition for any of the peptides since this requires a knowledge of $[\theta]_{222nm}$ for which the peptide is completely helical or completely coiled, and these conformational states were not observed over the temperature range studied. The temperature titrations were repeated three times and the average value of $\Delta\epsilon_{MRW}$ along with the corresponding number of helical residues in the peptide calculated as described in section 4.2.1 is shown with standard deviation in table 4.2.6, NB: $[\theta]_{MRW} = \Delta\epsilon_{MRW}.3300$.

These studies indicate that the peptide has greater propensity to form α-helical structure at lower temperature in the presence of 50% TFE than at higher temperatures in the temperature interval 5-80°C, however the magnitude of the effect is relatively small.

Figure 4.2.5a

Near-UV CD spectra collected for calmodulin and the complexes it forms with peptide P9-21 at pH 5.0, 6.0, 7.0 and 8.0. For each experiment the spectrum is an average of 16 scans. Spectra collected at 20°C in a buffer comprising 100mM KCl and 1mM $CaCl_2$ and either 25mM sodium acetate for experiments at pH 5.0 and 6.0 or 25mM Tris for experiments at pH 7.0 and 8.0.

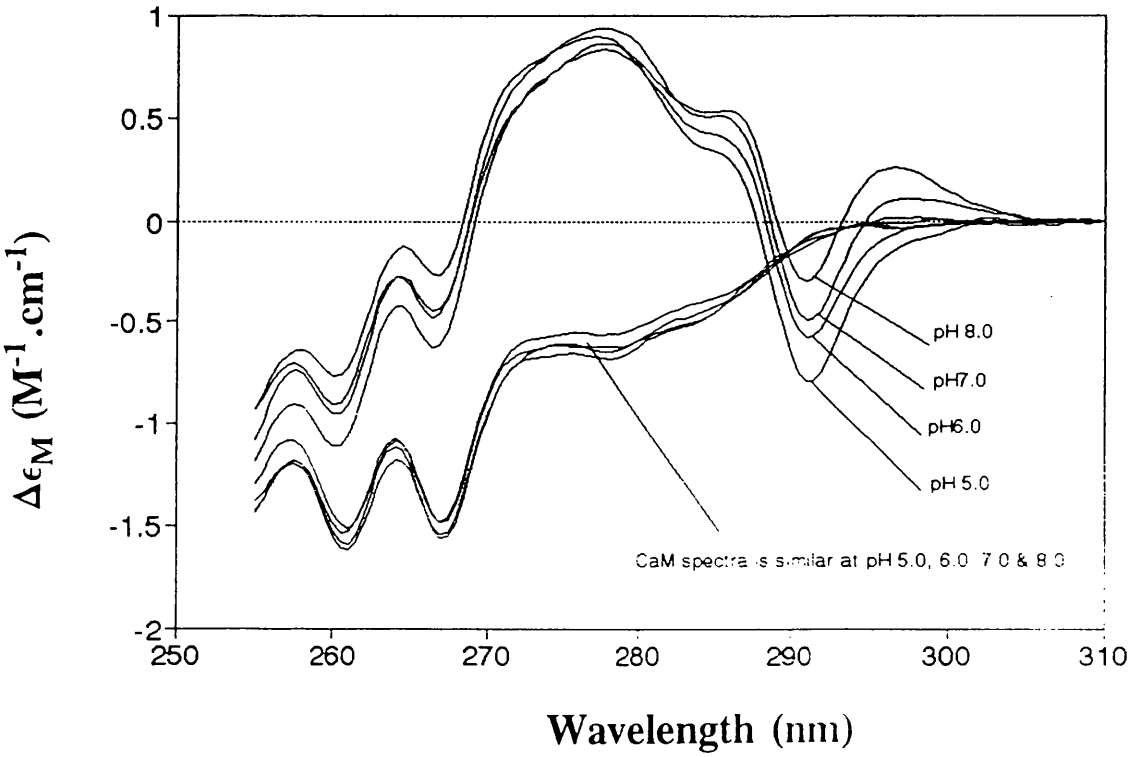
1
0.5
0
-0.5
-1
-1.5
-2
250
260
270
280
290
300
310
pH 8.0
pH7.0
pH6.0
pH 5.0
CaM spectra is similar at pH 5.0, 6.0 7.0 & 8.0
$\Delta\epsilon_M$ ($M^{-1}.cm^{-1}$)
Wavelength (nm)

Figure 4.2.6

Far-UV CD data corresponding to the helical propensities of peptides P1-26 (a), P1-21 (b), P9-26 (c) and P9-21 (d) in 50% TFE over the temperature range 10-70°C. Peptides were prepared at 50μM concentration in 25mM Tris, 100mM KCl at pH 7.0. The CD intensity was measured at 222nm and is reported as $\Delta\epsilon_{MRW}$. The titrations were typically performed by raising temperature, however the effect of temperature on far-UV CD is fully reversible.

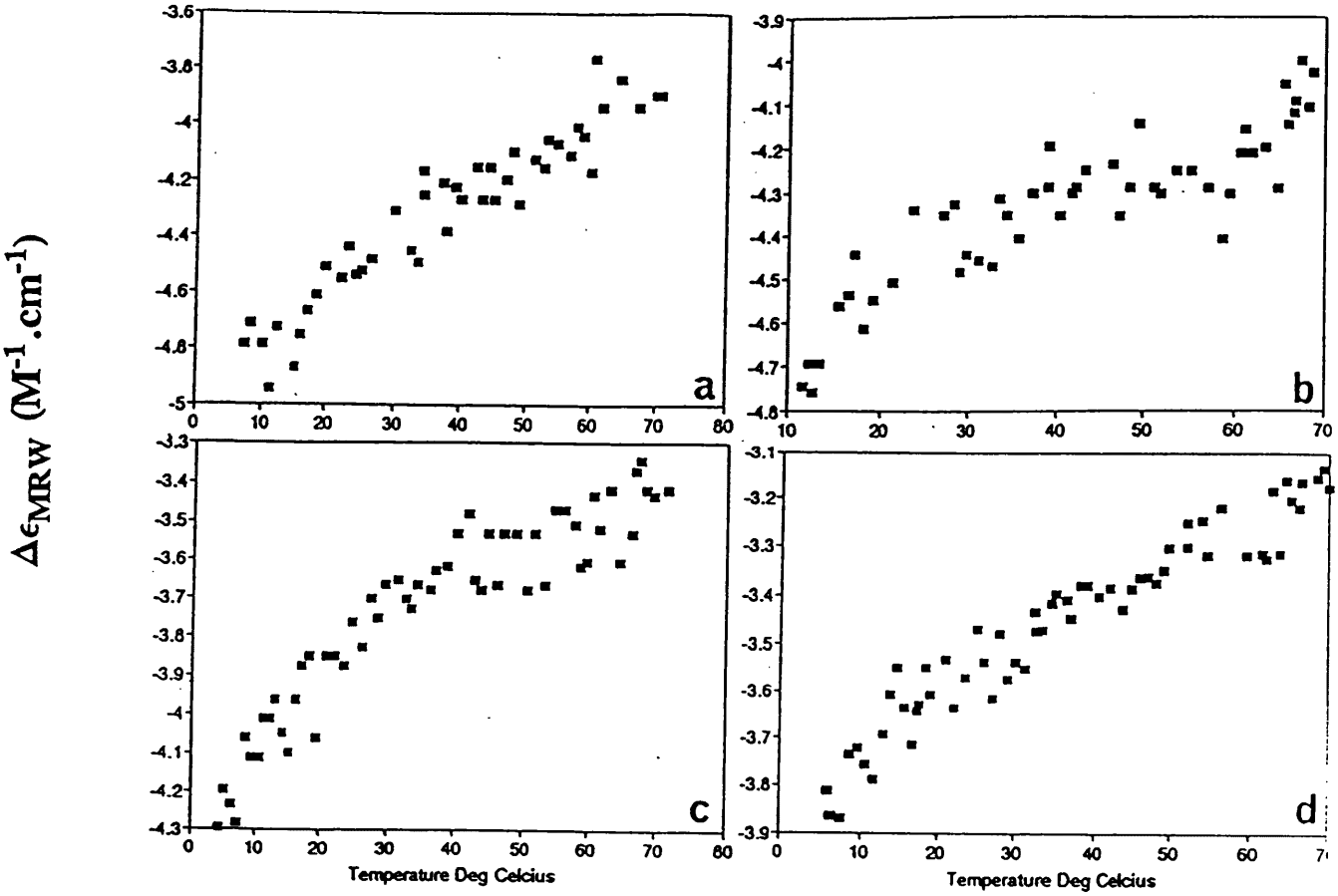
$\Delta\epsilon_{MRW}$ ($M^{-1}.cm^{-1}$)
a
b
c
d
Temperature Deg Celcius
Temperature Deg Celcius

Table 4.2.6

Far-UV CD extinction coefficients ($-\Delta\epsilon_M$) at 222nm of four PFK target peptides (50μM) at temperatures 10, 20, 30 and 70°C. All samples prepared in 25mM Tris, 100mM KCl, pH7.0. The values quoted at 222nm are an average of four independent single wavelength scans with standard deviation, adjacent to the ($-\Delta\epsilon_M$) in brackets is the calculated number of helical residues in the peptides, see text.

	$-\Delta\epsilon_M$ ±SD (# α-helical residues)			
	Temperature °C			
	10°C	20°C	30°C	70°C
P9-21	58.8 ± 8 (6.1)	55.2 ± 3 (5.8)	52.8 ± 8 (5.5)	45.6 ± 5 (4.8)
P9-26	81.1 ± 7 (7.8)	75.7 ± 7 (7.3)	73.4 ± 5 (7.1)	68.0 ± 5 (6.6)
P1-21	86.0 ± 4 (8.1)	79.0 ± 4 (7.4)	74.0 ± 9 (7.0)	68.0 ± 8 (6.4)
P1-26	96.9 ± 10 (8.9)	91.3 ± 9 (8.4)	89.4 ± 5 (8.1)	79.4 ± 6 (7.3)

4.2.7 Conclusions

From this work several structural features have been determined which describe the interaction of CaM and PFK target peptide, specifically;

(1). The PFK peptides have a low propensity to form α-helix whether bound to calmodulin (maximally 42%) or in the presence of helicogenic solvent (maximally 45%). Furthermore the effect of temperature on the transition of random coil to α-helix is small (an increase in approximately 2 helical peptide residues is typical on lowering a solution of peptide in 50% TFE from 70°C to 10°C.

(2). By adding residues P22-P26 to peptide P9-21 one notes a small increase in α-helical content (approximately 2-3 residues) consistent with residues in peptide P9-21 becoming α-helical, through a stabilization of the C-terminal end of the peptide.

(3). Residues 1-8 within the longer sequences have no α-helical conformation in the calmodulin bound conformation or in the presence of 50% TFE.

(4). Target peptides of different length have similar tryptophan conformation when complexed to calmodulin. The conformation is unlike the conformation of the peptide tryptophan in peptides WFF or RS20 from sk- and sm-MLCK respectively. However, like the peptide tryptophan of the two MLCK peptides the peptide tryptophan of the PFK sequence interacts with the C-terminal domain of calmodulin. Target peptide P1-15 binds calmodulin in a different manner to peptides P1-26, P1-21, P9-26 or P9-21 indicating that residues 16-21 are important in interaction. It may be that these residues make contacts

necessary for the target peptide to span both domains of calmodulin.

5. The environment of the peptide tryptophan when bound to calmodulin is somewhat sensitive to pH in the range 5.0-8.0.

4.3 The calcium dependence of CaM:PFKpep interactions

Studies to determine the affinity of calcium for calmodulin using absorbance, fluorescence, CD and NMR techniques show that sites 3 and 4 of the C-domain bind more tightly and with strong positive cooperativity in calcium binding, (Martin and Bayley, 1986; Forsén et al., 1986; Linse et al., 1990; Pedigo and O'Shea, 1995). Data from tryptic fragments of calmodulin, (Linse et al., 1991) demonstrate that sites 3 and 4 in the C-terminal domain of CaM have 6 fold greater average affinity for calcium than sites 1 and 2 in the N-terminal domain.

Early models describing calmodulin activation of target enzymes assumed that both domains of the fully saturated holo form of calmodulin (Ca_4CaM) were necessary for activation of several enzymes. More recently, interest has focused on the role of individual domains, raising the possibility that partially calcium saturated CaM:target complexes may have a potential role in regulation, (Klee, 1988; Persechini et al., 1994, 1996; Bayley et al., 1996).

The work described so far has indicated the unusual features of the interaction of CaM with PFK target sequences. The role of individual calmodulin domains can be further examined by determining the influence of the target region of PFK on calcium binding to calmodulin. In this section, this question is examined by quantifying calcium binding in the presence of PFK target sequences. It is known that calcium binds to the C-domain sites with higher affinity compared with the N-domain sites for apo-CaM and this is thought to be preserved in the presence of the WFF peptide from sk-MLCK, (Martin et al., 1996). It is clearly of interest to know whether this is also the case for the PFK target peptides.

4.3.1 Determination of stoichiometric calcium binding constants in calmodulin complexed to a series of PFK target peptides

The effect of the target peptide on the stoichiometric calcium binding constants of calmodulin was determined using the chelator indicator method, (Linse et al., 1987) as described in section 3.1.4.3.

Titrations of calcium to protein or protein plus peptide were performed 6 times for each sample. An example of the titration for apo-CaM and its complexes with peptides P1-26, P9-26 and P9-21 is shown in figure 4.3.1a. The presence of any of the target peptides appears to increase the affinity of calmodulin for calcium. In order to quantify this effect of target peptides the stoichiometric calcium binding constants for calmodulin and its complexes with target peptides were determined. A full description of the data analysis procedure is provided in Appendix 3. The stoichiometric constants are presented in table 4.3.1. The binding constants are an average of 6 independent analyses with standard deviations.

Figure 4.3.1 and Table 4.3.1 show that the first stoichiometric calcium binding constant (K_1) is substantially increased in the presence of the target peptide (120 fold for P1-26); the effect on the other stoichiometric calcium binding constants is much smaller, though K_3 is increased in the presence of target peptide also ($\sim$30 fold for P1-26). This is in marked contrast with the WFF peptide from sk-MLCK where all four stoichiometric constants are increased by the presence of target peptide, (Bayley et al., 1996).

The relationship between the intrinsic (k_i) and stoichiometric (K_i) association constants is described in Appendix 4. In its simplest form, the relationship represents binding of four ligands to a protein and takes no account of cooperativity between sites. It is, however, relevant in interpreting the binding data.

Figure 4.3.1a

Calcium binding to calmodulin and complexes formed between peptides P1-26, P9-26, and P9-21. Protein concentration is 25μM, peptide concentration is 75μM, BAPTA concentration is 25μM. Samples dissolved in 25mM Tris, 100mM KCl calcium free buffer prepared according to section 3.1.4 and temperature is maintained at 26°C. Absorbance measured at 263nm reflects the extent to which calmodulin and BAPTA compete for the binding of calcium.

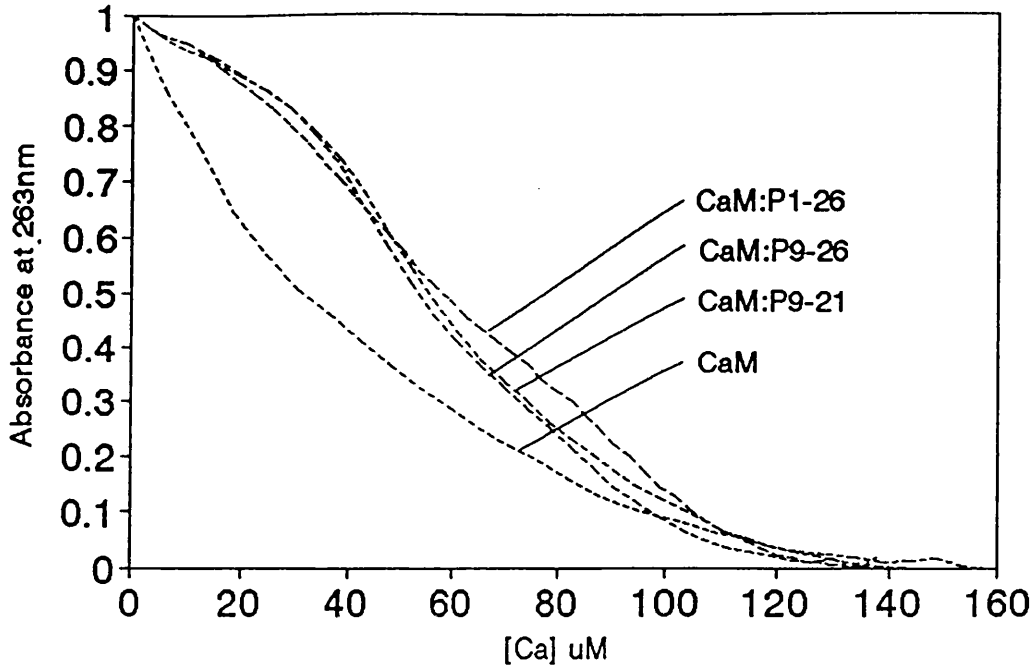
Absorbance at 263nm
1
0.9
0.8
0.7
0.6
0.5
0.4
0.3
0.2
0.1
0
0
20
40
60
80
100
120
140
160
[Ca] uM
CaM:P1-26
CaM:P9-26
CaM:P9-21
CaM

Table 4.3.1

Stoichiometric binding constants determined for calmodulin and calmodulin in the presence of 3 target peptides (P1-26, P9-26 and P9-21) from PFK. The dissociation constants for the complexes calmodulin forms with the target peptides is also shown, these were determined as described in section 4.1.1. Stoichiometric binding constants were determined at 25μM CaM, 25μM BAPTA (and 75μM peptide if applicable) using the chromophoric chelator method described in section 4.3. Each set of macroscopic binding constants K_1-K_4 is determined 6 times for calmodulin or a calmodulin:peptide complex and the standard deviation is calculated and is quoted directly below the K value.

CaM:P complex	$Ca_4CaM:P$ K_d	K_1	K_2	K_3	K_4
CaM:P1-26	2.8×10^{-10}	2.77×10^7	1.77×10^6	4.80×10^5	4.51×10^5
S.D.		14%	23%	16%	42%
CaM:P9-26	1.2×10^{-8}	1.39×10^7	8.21×10^5	2.38×10^5	7.36×10^4
S.D.		6%	8%	15%	31%
CaM:P9-21	3.2×10^{-8}	1.01×10^7	1.77×10^6	1.14×10^5	1.90×10^5
S.D.		14%	35%	8%	39%
CaM		2.39×10^5	1.17×10^6	1.25×10^4	6.02×10^5
S.D.		5%	13%	9%	16%

Table 4.3.1b

Relationship between intrinsic and stoichiometric association constants. The relationship (described in Appendix 4) holds for a 4 ligand binding site protein with no interaction between sites.

Figure 4.3.1b

Calcium saturation curves produced from theoretical stoichiometric association constants for the binding of four ligands (calcium) to a protein. The curves correspond to the stoichiometric binding constants described in table 4.3.1b above. Therefore curve 1 corresponds to the data of line 1 in table 4.3.1b etc. Curve 5 is described by $\log_{10}$ stoichiometric binding constants $K_1 = 8$, $K_2 = 7$, $K_3 = 7$, $K_4 = 7$.

	INTRINSIC association constants $\log_{10}$				STOICHIOMETRIC association constants $\log_{10}$			
	k_1	k_2	k_3	k_4	K_1	K_2	K_3	K_4
1	5	5	5	5	5.6	5.18	4.82	4.4
2	6	6	5	5	6.34	5.81	5.17	4.68
3	7	7	5	5	7.3	6.71	5.29	4.7
4	8	8	5	5	8.3	7.7	5.3	4.7

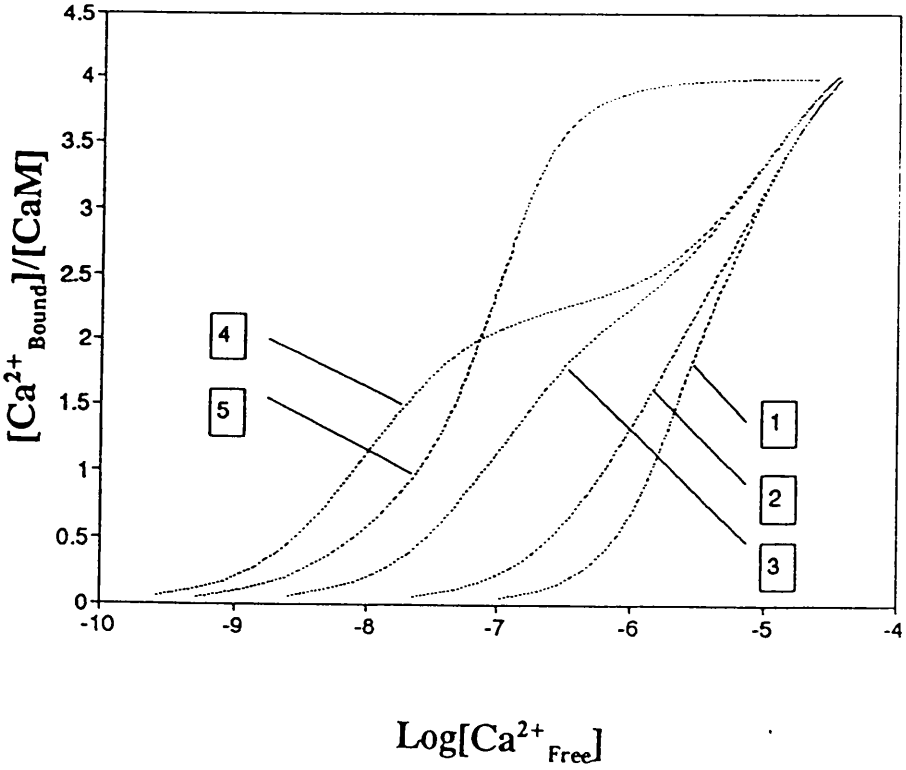

For illustration, for a range of theoretical intrinsic constants the corresponding stoichiometric constants were calculated, see table 4.3.1b. The data in line 1 represents a system for which the affinity of the four sites are equal. Line 2 represents a protein which exhibits ligand binding similar to that of calcium binding by calmodulin, for which binding is best described as two pairs of sites with one pair exhibiting higher affinity.

The pCa curves for the stoichiometric association constants calculated from theoretical intrinsic constants are shown in figure 4.3.1b. Comparison of the data from lines 1 and 2 of table 4.3.1b shows that increasing the intrinsic constants k_1 and k_2 mainly affects the first two stoichiometric constants. This is also evident from the corresponding pCa curves 1 and 2. As k_1 and k_2 increase further and k_3 and k_4 remain constant only two out of the four (K_1 and K_2) stoichiometric constants are influenced. This correlation is seen in figure 4.3.1b curves 3 and 4. The effect of an increase in all four stoichiometric association constants is depicted by curve 5. Since the effect of PFK target peptide on calcium binding is associated with increases predominantly in K_1 and K_2 these calculations suggest that the PFK target peptide influences predominantly 2 intrinsic calcium binding constants for calmodulin only.

Previously determined stoichiometric binding constants for CaM in complex with peptide WFF from sk-MLCK and those determined here for calmodulin in complex with peptides P1-26, P9-26 and P9-21 have been used to calculate the degree of saturation versus Log [Ca free], see figure 4.3.2.

The increased affinity of calmodulin for calcium in the presence of target peptide represents the effect of the PFK (or sk-MLCK) target peptides on the cooperative uptake of calcium by calmodulin. The effect is more pronounced in the case of sk-MLCK for which the binding of all four sites seem to be influenced. In the case of the PFK target

Figure 4.3.2

Calcium saturation curves for calmodulin in the presence of peptides WFF & WF10 from sk-MLCK and peptides P1-26, P9-26, and P9-21 from PFK. The pCa curves are created using the determined stoichiometric calcium binding constants for calmodulin in complex with the peptide, see section 3.1.4. The protein concentration is 25μM, peptide concentration is 75μM. Samples are dissolved in calcium free buffer (section 3.1.4) comprising 25mM Tris, 100mM KCl, pH 7.0. Panel A shows the influence of target peptides P1-26, P9-26 or P9-21 (b) on calcium saturation of calmodulin (a). Panel B demonstrates the influence of target peptides WFF (a), WF10 (b) and P1-26 (c) on calcium saturation of calmodulin (d).

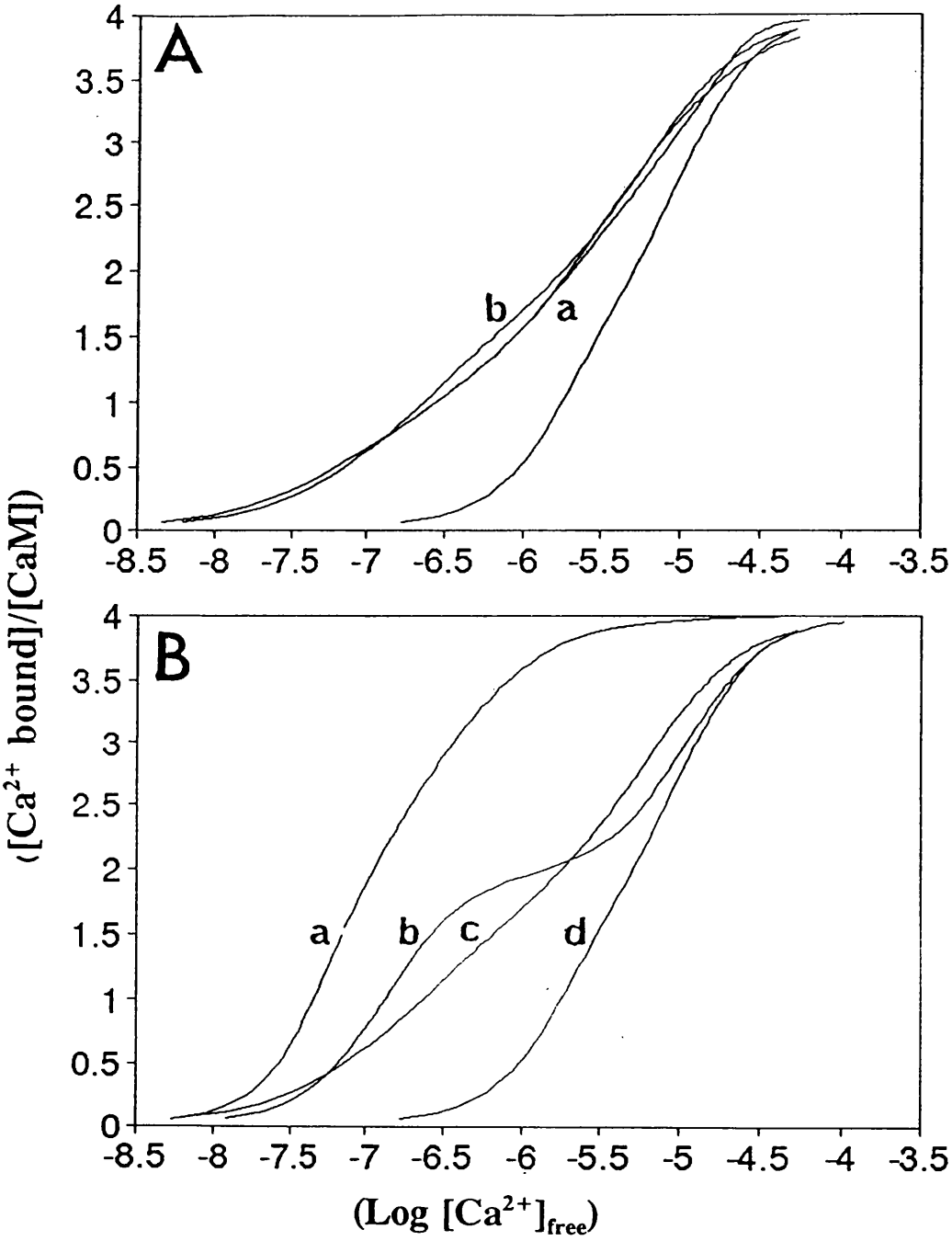
A
B
a
b
c
d
([Ca2+ bound]/[CaM])
(Log [Ca2+]free)

peptides it appears that only the affinity of the first two calcium ions for calmodulin are increased substantially, see table 4.3.1. Although it is not necessarily valid to assume that the two sites affected are those in the C-domain, the result is analogous to the effect of the shorter peptide WF10 (first 10 residues of WFF) where the more marked effect on the calcium binding to the C-domain results in a biphasic calcium binding curve, (Bayley et al., 1996) also see figure 4.3.2.

The calcium induced increase in the affinity of calmodulin for a particular peptide may, in principle, be calculated from experimentally determined dissociation constants for the peptide in the presence (K_d) and absence of calcium (K'_d). However, because the latter value is not generally accessible experimentally, an estimate of the ratio of the dissociation constants $(K'_d)/(K_d)$ may be obtained from the measured stoichiometric calcium binding constants determined for calmodulin alone (K1,...,K4) and for calmodulin in the presence of excess peptide (K1',...,K4') through the following equation, (Yazawa et al., 1992).

$$K'_d/K_d = (K_1'K_2'K_3'K_4')/(K_1K_2K_3K_4)$$

The K'_d/K_d values calculated for calmodulin in complex with P1-26, P9-26, or P9-21 are 5054, 952, and 184 respectively. These are significantly lower than the value of 3.1×10^6 calculated for calmodulin in complex with peptide WFF from sk-MLCK, (Bayley et al., 1996) or the value of 6.2×10^8 for calmodulin in complex with peptide C28W from the calcium pump, (Yazawa et al., 1992).

These results imply that the binding of calcium to calmodulin makes a contribution to the overall calcium induced increase in peptide affinity, although not as significant a contribution as peptides derived from sk-MLCK and calcium pump. The ratios can be

used with experimentally determined K_d values to calculate a value for K'_d. The dissociation constants calculated for apo-calmodulin in complex with P1-26, P9-26, and P9-21 are 1.42, 10.4, and 6μM respectively. However, titrations of apo-calmodulin to peptides were performed at 50μM, and no appreciable binding was observed. It should be noted however that these calculations give only a lower limit for the ratio of the dissociation constants since the true values of K_1'-K_4' will only be measured under conditions where the protein can be totally saturated with peptide in the absence of calcium (Dr S Martin, NIMR, personal communication). This is not generally achievable because the affinity of the peptide for calmodulin in the absence of calcium is very low, (Crivici & Ikura, 1995).

4.3.2 Structural changes of complex formation as a function of calcium concentration studied by Fluorescence and Circular Dichroism

4.3.2.1 Fluorescence spectroscopy

The characteristic increase in emission intensity of the bound tryptophan of the peptide was used to follow the calcium dependence of complex formation.

Apo-CaM was generated from Ca_4CaM as described in section 3.1.3. Chelex treated buffer (25mM Tris, 100mM KCl, pH 7.0) was used in all solutions. 3mL of apo-CaM or apo-CaM plus PFK peptide (60-100μM) were mixed by plastic pasteur pipette in a 10mm pathlength cuvette. A 1:1 ratio of protein:peptide was used in these experiments. The spectrum was recorded between 300-400nm with λ_{exc} at 295nm. Calcium was then added in approximately 10μL aliquots from mM stock. After each addition the spectrum was recorded. Emission at 330nm was used to follow calcium

binding.

Figure 4.3.2.1a shows the calcium titrations for apo-CaM in the presence of peptides P1-26, P9-26, and P9-21. The data have been normalized between 0 and 1 to aid comparisons. In addition table 4.3.2.1 shows the fluorescence change at various calcium concentrations. Each value in the table is the average of 4 titrations with the standard deviation.

The titrations are similar for all three complexes; the fluorescence signal change is non-linear but is effectively complete after binding of the first two calcium ions. The binding of the first calcium ion contributes approximately 50% of the total fluorescence intensity characteristic of the Ca_4CaM:PFKpep species for peptides P9-26 and P9-21, and 75% of the total signal in the case of the Ca_4CaM:P1-26 complex. This indicates that in the presence of the target peptide, calmodulin requires fewer than 4 calcium ions bound to saturate the fluorescence signal characteristic of the bound peptide.

After the first and second mole of calcium is added to calmodulin in solution with peptide P1-26 the fluorescence is enhanced to a greater extent than when CaM is in complex with peptides P9-21 or P9-26. This correlates with the greater affinity of peptide P1-26 for calmodulin than peptides P9-21 and P9-26 since the specificity by which calmodulin interacts with its many targets in the cell is governed by affinity of the target for calmodulin and the calcium saturation state of the protein. This suggests that targets which have high affinity for calmodulin may bind and be activated by calmodulin in a partially saturated state in preference to lower affinity targets at low calcium ion concentration, (Bayley et al., 1996).

Table 4.3.2.1

Amplitude of fluorescence signal complete for titrations of calcium to mixtures of apo-CaM and tryptophan containing peptide at 60μM protein concentration using a 1.1 fold excess of target peptide. Four molar equivalents are required to fully saturate calmodulin under these conditions.

Molar Equivalents of Calcium	Apo-CaM:P1-26	Apo-CaM:P9-26	Apo-CaM:P9-21
0	0	0	0
1	70 ± 3	50 ± 5	46 ± 3
2	92 ± 3	85 ± 4	83 ± 3
3	100 ± 2	96 ± 2	94 ± 3
4	100	100	100

Figure 4.3.2.1a

Fluorescence emission values for the titration of calcium to a 1:1 complex of calmodulin with either P1-26 (■), P9-26 (x) or P9-21 (▲). Protein concentration is 60μM. Samples are dissolved in calcium free buffer prepared according to section 3.1.4. Buffer comprises 25mM Tris, 100mM KCl, pH 7.0. Spectra are collected at 20°C using an excitation wavelength of 295nm and fluorescence emission is measured at 330nm. Data has been normalized between 0 and 1 to aid comparisons for th three titrations.

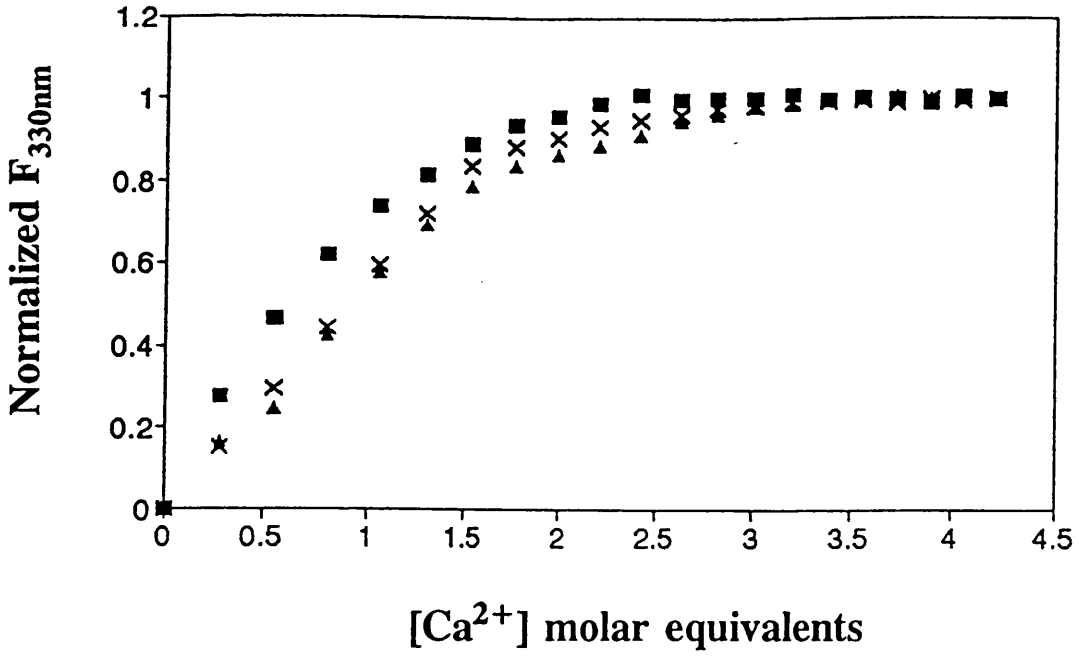
Normalized F_{330nm}
1.2
1
0.8
0.6
0.4
0.2
0
0
0.5
1
1.5
2
2.5
3
3.5
4
4.5
[Ca^{2+}] molar equivalents

4.3.2.2 Circular Dichroism spectroscopy to detect changes in complex structure

It appears from the fluorescence experiments (previous section) that the majority of the signal characteristic of bound tryptophan is generated after the addition of 1-2 equivalents of calcium to the mixture of apo-CaM and peptide. Further examination of the environmental changes of calcium titration was made using far and near-UV CD methods.

Near-UV CD

Near-UV CD has previously been used to demonstrate that peptides P1-26, P1-21, P9-26 and P9-21 bind to Ca_4-calmodulin in a similar conformation, at least so far as the residues tyrosine and tryptophan are concerned. In this section calcium titrations were performed in order to study the conformational transitions associated with calcium binding to apo-CaM and the complexes it forms with peptides from PFK.

Experiments were performed at 60μM, protein:peptide ratio being 1:1 for all experiments. The sample for study is placed in a 10mm path length quartz cuvette which is held in a thermostatted cuvette holder. After each calcium addition the spectrum was recorded over the wavelength range 250-340nm. The calcium induced changes in near-UV CD reflect the changes in environment of the aromatic residues in the protein and peptide as a function of the degree of calcium saturation.

Figure 4.3.2.2a shows a calcium titration with apo-CaM, there is a characteristic decrease in CD intensity at 280nm associated with the change in the environment of the single tyrosine of the protein. The decrease is greatest upon the first addition of calcium to the protein indicating that the first calcium ion is likely to go into the C-domain since the tyrosine residue is situated in calcium-binding site 4 of the C-domain.

Figure 4.3.2.2b. shows the calcium titration of apo-CaM plus P9-21. The

environment of the peptide tryptophan is reflected in changes at 280 and 295nm. The signal at 280nm increases initially, however the addition of the third and fourth calcium ions result in loss of CD signal, this could be attributed to an effect of the tyrosine in the protein, to determine whether this was the case the same experiment was performed using peptide [P9-26 (Y14F)], The same loss of signal at 280nm was observed on calcium addition to apo-CaM:[P9-26 (Y14F)]. This indicates that the effect results from an environmental change of the protein tyrosine as calcium is titrated to the protein:peptide mix, although additivity of the peptide tyrosine, and protein tyrosine is assumed and the effect of peptide tryptophan is ignored since the change in signal at 295nm is consistently a negative increase as calcium is titrated to the CaM:PFK peptide mix.

Figure 4.3.2.2c shows the CD signal at 295nm for calcium titrations to mixtures of apo-CaM and peptides P1-26, P9-26, [P9-26 (Y14F)] and P9-21. For all complexes it appears that the large increase in tryptophan intensity at 295nm is associated with the binding of the first 2 calcium ions to the calmodulin. Further addition of calcium results in plateau of signal or slight decrease in signal. The loss of signal after addition of the second molar equivalent of calcium suggests that the presence of peptide might influence order of calcium binding therefore data is reported in terms of absolute values and calmodulin contribution cannot be subtracted.

Figure 4.3.2.2

(a) Near-UV CD titration of calcium to apo-CaM at 60μM. Spectra recorded in calcium free buffer (section 3.1.4) comprising 25mM Tris, 100mM KCl, pH 7.0 at 20°C. Addition of 1-4 calcium ions to 1 calmodulin. The top spectrum with $\Delta\epsilon_{280nm}$ = $+0.5M^{-1}cm^{-1}$ is apo-CaM and the addition of 1,2,3 or 4 molar equivalents of calcium is shown by the signal at 280nm progressively increasing negatively. The predominant effect is on addition of the first calcium ion, since this binds to the high affinity site in the C-domain near to Y138 from which the signal is derived.

(b) Near-UV CD titration of calcium to a solution of apo-CaM and peptide P9-21 at 60μM protein and 66μM peptide. Spectra recorded in calcium free buffer (section 3.1.4) comprising 25mM Tris, 100mM KCl, pH 7.0 at 20°C. Apo-CaM:P9-21 complex spectrum has a signal of $+0.75M^{-1}cm^{-1}$ at 280nm. The additional spectra represent the addition of 1, (A), 2, (B), 3, (C), or 4, (D) molar equivalents of calcium to calmodulin complexed to P9-21.

(c) Near-UV CD data at 295nm resulting from titration of calcium to a solution of apo-CaM and either peptide P1-26 (□), P9-26 (+), P9-21 (■) or P9-26 (Y14F) (*) at 60μM apo-CaM and 66μM peptide. Spectra recorded in calcium free buffer (section 3.1.4) comprising 25mM Tris, 100mM KCl, pH 7.0 at 20°C.

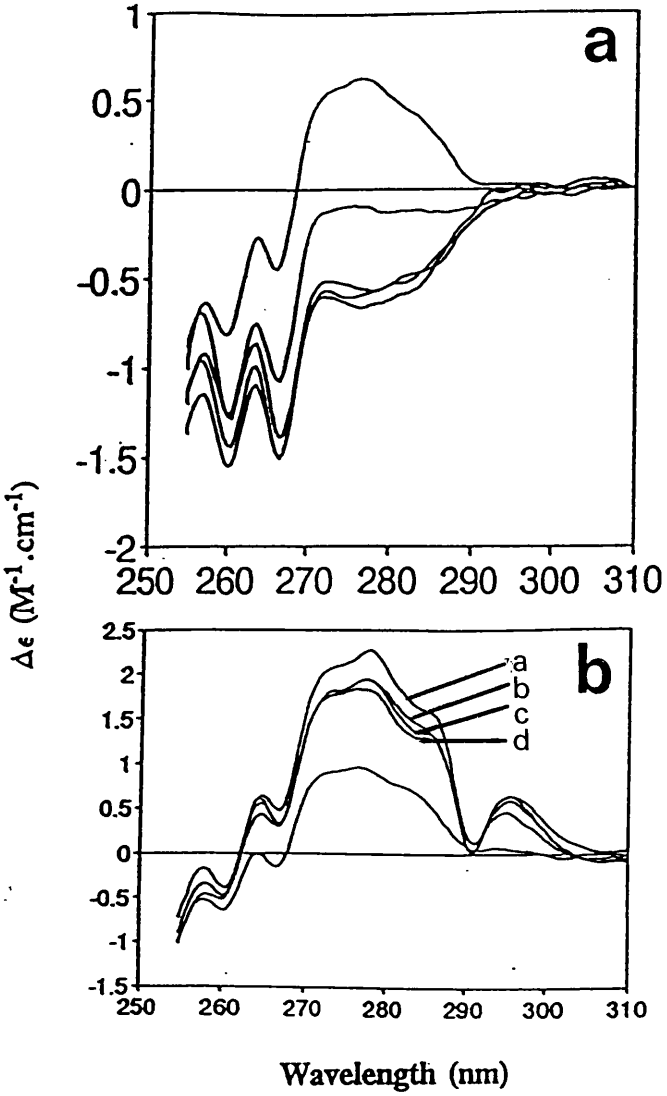
a
b
c
d
Δε (M-1.cm-1)
Wavelength (nm)

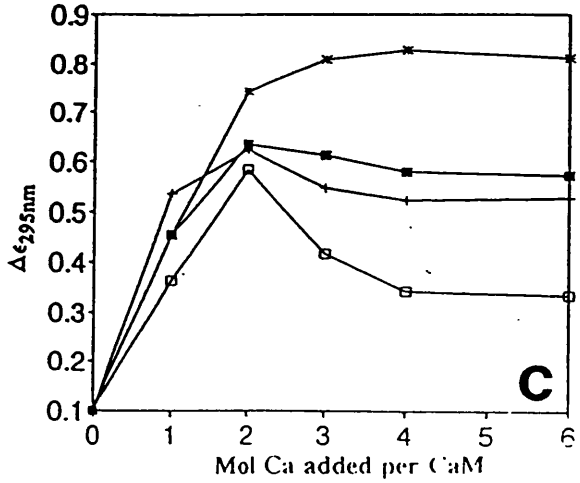
c
Mol Ca added per CaM

Far-UV CD

Calcium titrations were performed using apo-CaM and calcium free solutions prepared as described in section 3.1.3. A 300μL solution of protein or protein plus peptide (10μM) was placed in a 1mm path length quartz cuvette. A 1:1 ratio of protein:peptide is sufficient for peptide to saturate protein at 10μM protein. The spectra of each sample was recorded over the wavelength range 200-260nm. An increase in α-helical structure is associated with increasingly negative CD intensity at 222nm. Therefore, the change in α-helical structure of the protein or protein plus peptide mixture on binding calcium was determined by recording the signal at 222nm as a function of calcium concentration, see figure 4.3.2.2e.

For calmodulin in solution the increase in α-helical structure detected at 222nm induced by calcium binding is approximately linear between 0 and 4 moles of calcium per calmodulin. In the presence of the target sequences from PFK there is a greater increase in α-helicity at all stages of the calcium titration compared with the α-helicity induced by calcium titration to calmodulin. This is especially greater in the binding of the first and second molar equivalent of calcium.

Upon complex formation the peptides will also adopt partial α-helical conformation, (see section 4.2) therefore comparisons of total α-helicity are made, although the increases in α-helicity in the peptides are themselves very small, maximally 6/161* ($\sim$4%) residues at 20^{0}C calculated for CaM 148 residues plus peptide P9-21 13 residues). As with the fluorescence experiment described previously, section 4.3.2.1, the uptake of the first two calcium ions appears to generate a signal which is characteristic of the fully calcium saturated protein:peptide complex. Furthermore, as in the fluorescence experiment, the major change in the process of Ca_0CaM:PFKpep -

Figure 4.3.2.2e

Far-UV CD data at 222nm resulting from titration of calcium to a solution of apo-CaM, (■) and either peptide P1-26 (□), P1-21, P9-26 (*) or P9-21 (▲) at 60μM apo-CaM and 66μM peptide. Spectra recorded in calcium free buffer (section 3.1.4) comprising 25mM Tris, 100mM KCl, pH 7.0 at 20°C.

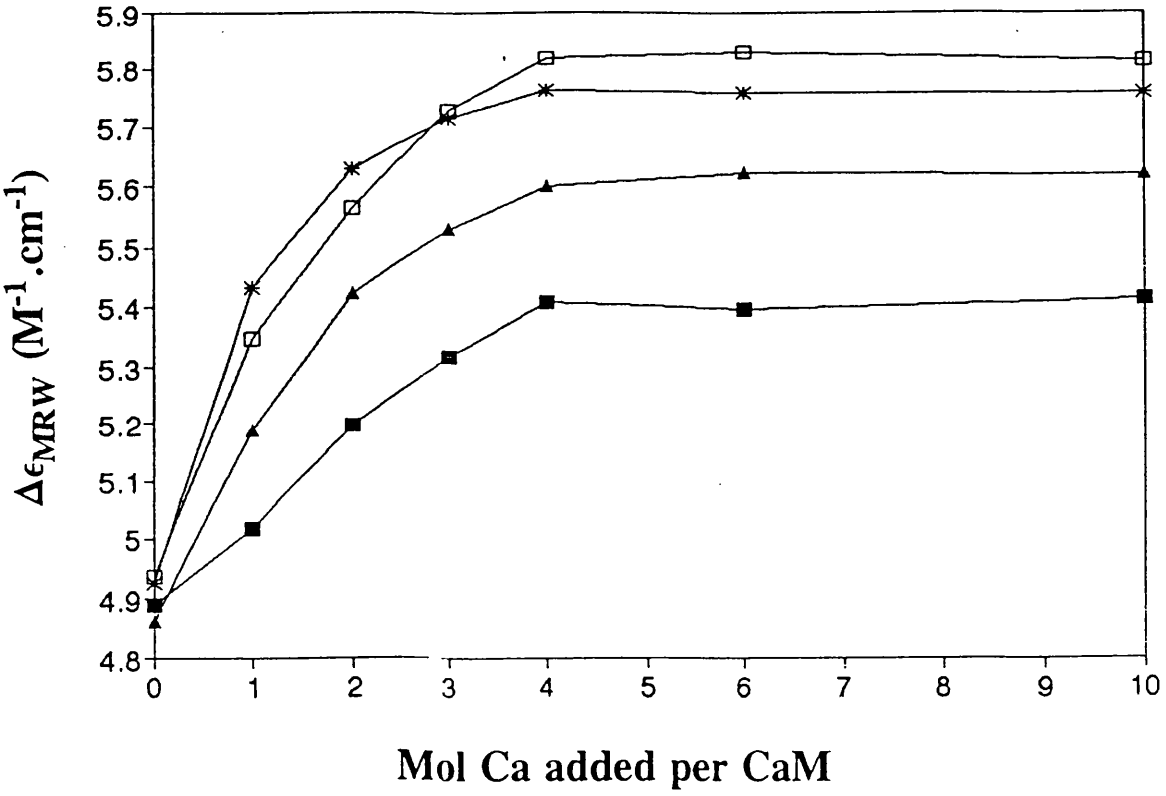
5.9
5.8
5.7
5.6
5.5
5.4
5.3
5.2
5.1
5
4.9
4.8
0
1
2
3
4
5
6
7
8
9
10
$\Delta\epsilon_{MRW}$ ($M^{-1}.cm^{-1}$)
Mol Ca added per CaM

Ca_4CaM:PFKpep appears to occur upon addition of 1 mole of calcium per calmodulin. Change of signal after addition of 1 molar equivalent of calcium for calmodulin in complex with peptides P1-26, P9-26, and P9-21 are 42%, 50%, and 44% respectively compared with 25% for the apo-CaM protein alone.

4.3.3 Conclusions

(1) The presence of a PFK target sequence results in an increased affinity of calmodulin for the first two calcium ions, by approximately 200 fold. Binding of the third and fourth calcium ions are little affected by the presence of the target sequence; this is in contrast with other targets which exhibit increased affinity of binding for all four sites.

(2) Fluorescence and CD spectroscopy indicate that after the second mole of calcium is added to calmodulin in solution with the PFK target a spectrum similar in amplitude to that of the fully calcium saturated protein:peptide complex is produced. The effect is more pronounced for complexes for which the peptide exhibits greater affinity for calmodulin. Fluorescence studies of calcium binding to calmodulin in the presence of PFK target sequences show that approximately 50% of total signal associated with binding occurs after addition of one molar equivalent of calcium to the calmodulin:PFK target mixture. Since the assay of binding is based on the change in environment of the peptide tryptophan it is likely that either site 3 or 4 or both sites are filled preferentially to sites 1 or 2. This proposed order of binding is supported by the similar F/Fo values (approximately 2.3) for the interaction of PFK target sequence with either TR2C or intact CaM, implying the majority of the signal change associated with CaM binding a PFK target sequence arises from the tryptophan of the peptide binding the C-domain of the protein.

4.4 Stopped-flow kinetics of CaM:PFKpep complex dissociation

4.4.1 Introduction

The overall mechanism of calcium binding to calmodulin and target recognition of an enzyme by calmodulin can be depicted as scheme 4.4a (standard abbreviations, E = target peptide or enzyme). The pathway implies that calcium saturation of calmodulin is required in order that calmodulin may bind to its target. It is known that calcium binding is certainly required in most cases to increase the affinity of calmodulin for its target, see (Falke et al., 1994) for review. However it is unclear what extent of calcium saturation is necessary and sufficient to induce the conformational change which allows the activation of enzymes. This section uses kinetic studies to examine the possible underlying mechanisms.

Scheme 4.4a:

$$\underset{}{\overset{}{}} \quad \overset{+4Ca}{} \qquad \overset{+E}{}$$

$$CaM \rightleftarrows Ca_4CaM \rightleftarrows Ca_4CaM\text{-}E$$

Stopped-flow fluorescence kinetic studies using EGTA and the fluorescent Ca^{2+} indicator Quin-2 (8-amino-2-[(2-amino-5-methylphenoxy)-methyl]-6-methoxyquinoline-N,N,N',N'-tetraacetic acid) have previously permitted quantitation of calcium dissociation rate constants and have thus provided insight into the kinetic aspects of calcium binding to calmodulin, (Martin et al., 1985, 1986).

The chelator Quin-2 (Tsien, 1980) has a backbone similar to that of EGTA and, like EGTA, it chelates Ca^{2+} with high affinity with $K_d = 2 \times 10^{-8}M$ at low ionic strength. Moreover, the molecule contains aromatic rings that interact electronically and sterically with the chelating backbone. Thus calcium chelation results in fluorescent

spectral changes and Quin-2 provides a method for the direct quantitation of the number of calcium ions associated with each phase observed in the fluorescence stopped-flow dissociation experiments.

The dissociation of calcium from calcium saturated calmodulin occurs in 2 distinct steps. In previous studies, (Bayley et al., 1984; Martin et al., 1985) using bovine brain calmodulin, the calcium dissociation rates for the isolated N-terminal domain (TR1C, CaM residues 1-75) were found to be approximately 60 fold faster than those for the C-terminal domain, see table 2.2.1. These results using tryptic fragments are conserved in studies with the intact protein in which the C-terminal sites have similarly higher affinity than the N-terminal sites, (Thulin et al., 1984; Martin et al., 1985; Linse et al., 1991; Bayley et al., 1996). Each dissociation process accounts for approximately 50% of the total reaction amplitude, and each process corresponds to the release of two calcium ions. The calcium dissociation constants are reported in table 4.4.1, and are specific for the buffer conditions employed here. In the absence of KCl the slow phase rate is two-fold slower, whilst the fast phase rate is three fold faster, (Martin et al., 1985).

Calcium binding studies described in section 4.3 suggest that in the case of PFK target peptides, calmodulin need not be fully saturated with calcium in order to generate spectral characteristics like those of Ca_4CaM. Stoichiometric constants imply that the presence of target peptide increases the affinity associated with the binding of the first two calcium ions to calmodulin. These two pieces of information suggest that a Ca_nCaM:PFKpep species with $n<4$ might be structurally and functionally significant. A more realistic representation of calcium dependent target binding is shown in scheme 4.4b to include a number of possible intermediates in which it is evident that calcium and peptide binding by calmodulin can follow a multitude of possible routes. Both calcium

and peptide binding are known to be extremely fast (approximating the diffusion limited bimolecular rate of ~ $10^9 M^{-1}s^{-1}$) and hence they are extremely difficult to study by stopped-flow techniques. However the reverse reaction in which calcium is removed by chelator can provide some information on the route of dissociation. In these studies Quin-2 was used to directly quantify calcium dissociation in calmodulin and complexes with PFK target peptides, Changes in tryptophan fluorescence induced by EGTA dissociation of calcium from calmodulin in complex with tryptophan containing target peptides were also used to investigate features of the peptide dissociation mechanism.

Scheme 4.4b:

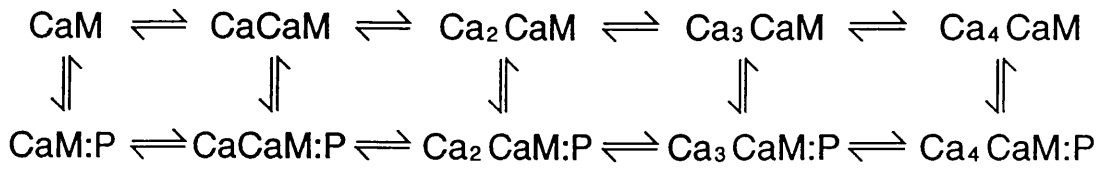

4.4.1 Quin 2 induced dissociation of calcium from complexes of calmodulin with target sequences from PFK

The experimental method is described in section 3.2.4. Quin-2 fluorescence was measured using an excitation wavelength of 334nm and an emission cut-on filter of 360nm with [CaM]= 3μM, [PFK peptide] 3.3μM, 30μM total Ca^{2+} and [Quin-2]= 130μM. All concentrations quoted are prior to stopped-flow mixing. A full description of the stopped-flow experiment is provided in section 3.2.4. Data analysis is considered in Appendix 3.

The stopped-flow mixing of Quin-2 to Ca_4CaM complexes leads to an increase in fluorescence associated with the formation of Ca:Quin-2, see Figure 4.4.1. The

Figure 4.4.1

Experimental stopped-flow traces for the dissociation of calcium from calmodulin (A) and calmodulin complexed to peptide P9-26 (B) using the fluorescent calcium chelator Quin-2. Concentrations and experimental parameters are provided in the text. For any single experiment n=9 individual stopped-flow traces. The fit to the experimental data is shown by the smooth curve. (A) Dissociation of calcium from calmodulin. There was little difference in fitting to either a one or two exponential process for calcium dissociation from calmodulin alone since only 3% of the fluorescence signal deriving from the fast dissociation of the N-domain Ca^{2+} ions is seen owing to the majority of the dissociation occuring within the dead-time of the instrument (5ms). Data shown here is fitted to a single exponential, the amplitude for the process is 0.136 and the corresponding rate is $6.9s^{-1}$. The data fits with a χ^2 of 1.22. (B) The trace showing dissociation of calcium from the complex of with PFK peptide P9-26, the amplitudes (A) and rates (k) associated with the fit to the trace here are A_{fast}= 0.0614, k_{fast}= $18s^{-1}$, A_{slow}= 0.134, k_{slow}= $2.4s^{-1}$ The dissociation of calcium from Ca_4CaM:P9-26 is best fit as biphasic as shown by the residuals calculated for a one or two exponential fit (inset). The χ^2 values for the two fits are 2.3 and 1.01 for the single and double exponential fits respectively.

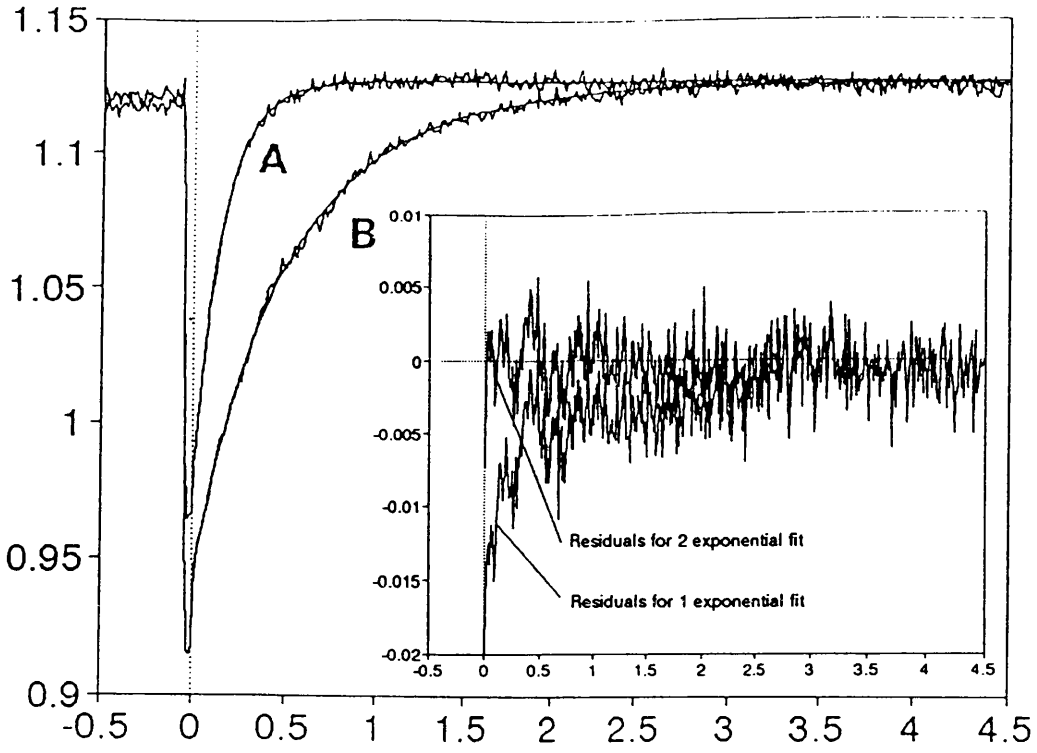
1.15
1.1
1.05
1
0.95
0.9
-0.5
0
0.5
1
1.5
2
2.5
3
3.5
4
4.5
A
B
0.01
0.005
0
-0.005
-0.01
-0.015
-0.02
Residuals for 2 exponential fit
Residuals for 1 exponential fit

Table 4.4.1

Dissociation constants (K_d) (calculated in section 4.1.1) and calcium dissociation rate constants for the complexes formed between calmodulin and target peptides from PFK obtained by stopped-flow kinetic methods with Quin-2 or EGTA at 20°C. Calcium dissociation by EGTA is monitored at 2μM protein with a 1.1 fold excess of peptide EGTA concentration is 20mM with an excitation wavelengths of 295nm and an emission cut-on filter at 330nm. Calcium dissociation by Quin-2 is monitored at 3μM CaM with peptide 1.1 fold in excess. Quin-2 concentration is 130μM, fluorescence is determined using an excitation wavelength of 330nm and an emission cut-on filter at 360nm. Calcium dissociation is best fit by a biphasic model for CaM and its complexes with PFK target peptides.

a) Data from Martin et al., (1986) at 5°C.

b) Data from Brown et al., (1996) at 20°C.

c) % signal is calculated for data where the slow phase corresponds to 0.136V as determined in control experiments with calmodulin alone. This is 50% of the total amplitude for Ca_4CaM.

d) The EGTA experiment is not quantitative in terms of calcium ions, % signal refers to the amplitude of bound tryptophan fluorescence lost in the corresponding phase.

e) The fluorescence values reported are corrected for the fluorescence lost in the dead-time of the instrument using $A_t = A_0 \exp(-kt')$, where A_t and A_0 are amplitudes at time t and time zero k is the rate constant and t' is the dead-time of the instrument (5ms). Hence for a process occuring at $k = 18s^{-1}$, 9% of the fluorescence amplitude is lost in the instrument, hence the observed rate is corrected for by the appropriate factor in table 4.4.1.

	K_d (nM)	Quin-2				EGTA		
		Dissociation rates. (k_f & k_s) ± S.D (s^{-1})	Flu (V)[c]	% signal[c]	Calcium ions in phase	Dissociation rates. (k_f & k_s) ± S.D (s^{-1})	Flu (V)[c]	% signal[d]
CaM		*6.9 ± 0.5*	*0.136*	*50*	*2*			
CaM:P1-26	0.28	11 ± 4 *1.2 ± 0.4*	0.0522 *0.135*	28 *50*	1.12 *2*	13 ± 4 *1.6 ± 0.2*	0.059 *0.1206*	33 % *67 %*
CaM:P9-26	12.0	18 ± 6 *2.4 ± 0.2*	0.0621 *0.134*	32 *49*	1.28 *2*	14 ± 5 *2.2 ± 0.5*	0.065 *0.1214*	35 % *65 %*
CaM:P9-21	32.0	16 ± 2 *2.6 ± 0.3*	0.0565 *0.136*	29 *50*	1.16 *2*	17 ± 3 *2.5 ± 0.6*	0.050 *0.1189*	29 % *71 %*
CaM[a]		700 ± 200 *8.5 ± 0.5*			N/D *2*			
CaM:WFF[b]	0.12	10 ± 1 *1.4 ± 0.1*			2 *2*	12 ± 3 *1.5 ± 0.2*		10% *90%*

dissociation of calcium from calmodulin has previously been demonstrated to be biphasic with rates of $700s^{-1}$ and $8.5s^{1}$, the fast phase rates correspond to the 2 N-terminal calcium ions (Bayley et al., 1984; Martin et al., 1985, 1986). The fast phase of calcium dissociation from calmodulin can only be measured at low temperatures with an instrument with a shorter dead-time than the one used here (5ms).

In experiments reported here (at 20°C) the dissociation of calcium from the low affinity binding sites of calmodulin alone is not observed since most of the signal is lost in the dead-time of the instrument (5ms). Since $A_t = A_o \exp(-kt')$, where A_t and A_o are the amplitudes at time t and time zero respectively, k is the rate constant, and t' is dead-time, for a process with $k = 700s^{-1}$ only 3% of the total signal would remain at the end of the 5ms dead-time. Thus the small contribution of the N-terminal sites is negligible and the observed calcium dissociation from calmodulin at 20°C can be fit as a single exponential process; the resulting fluorescence amplitude corresponds to dissociation of 2 calcium ions from the C-terminal domain. The data for the dissociation of calcium from calmodulin C-terminal sites determined here ($6.9s^{-1}$), agrees well with the previous literature value of $8.5s^{-1}$, (Bayley et al., 1984; Martin et al., 1985, 1986).

The rates determined for the CaM:PFKpep complexes are shown in table 4.4.1. The behaviour is similar for the three PFK complexes with a fast phase of $11\text{-}18s^{-1}$ and a slow phase of $1.2\text{-}2.6s^{-1}$, see figure 4.4.1. By analogy with Ca_4CaM, the fast phase is assumed to correspond to dissociation of the N-terminal calcium ions. The rates are closely similar to the rates of Ca^{2+} dissociation from the Ca_4CaM:sk-MLCK (WFF) complex, ($k_f = 10s^{-1}$ $k_s = 1.5s^{-1}$), [CaM= 2μM, WFF= 2.2μM, [Quin-2]= 90μM, [Ca]= 20μM, (Martin et al., 1996)), suggesting a general result that the rate of calcium dissociation from calmodulin is reduced in both fast and slow phases by the presence of

these target peptides.

The amplitudes correspond directly to the chelation of calcium by the Quin-2 and are proportional to the number of ions involved in a particular phase. The amplitude is calibrated from the slow phase of the Ca_4CaM/Quin-2 reaction. The PFK target peptides slows the fast dissociation phase, which can thus be quantified. However, the fast rates are still sufficiently fast that it is necessary to correct for part of the amplitude lost in the dead-time of the instrument. For example the observed fluorescence amplitude determined for a fast rate of k_f of $18s^{-1}$ will according to $A_t = A_o \exp(-kt')$ represent only 91% of the actual fluorescence amplitude associated with that phase. The traces shown in figure 4.4.1 are not corrected for this loss in amplitude, however all amplitudes given in table 4.4.1 are corrected.

Table 4.4.1 shows that the maximum total amplitude is less than 4 calcium ions after correction of amplitudes for dead-time. A possible reason is that under the experimental conditions used here the CaM:PFK peptide complexes are not fully calcium saturated and hence that the N-terminal sites are not completely filled.

Using the stoichiometric calcium binding constants determined in section 4.3.1 it is possible to calculate the degree of calcium saturation under particular experimental conditions. These calculations show that the number of calcium ions bound per calmodulin are 3.22, 3.24, and 3.28 in the presence of peptides P1-26, P9-26 and P9-21 respectively. These calculations show why the fast phase is less than the theoretical maximum. Raising the calcium concentration would avoid this problem, however this would in turn require increasing the total quin-2 concentration which is a limiting factor in the fluorescence experiment.

It can be concluded from these kinetic studies that calcium dissociation from

calmodulin in complex with a series of PFK target peptides (affinities K_d= 32nM to 280pM) are similar and are best described as biphasic, each phase involving loss of 2 calcium ions. The calcium dissociation characteristics are very similar to those of calmodulin in complex with target peptide WFF from sk-MLCK, (Martin et al., 1996). For this complex it appears that the fast phase by analogy with calmodulin alone involves dissociation of the N-terminal calcium ions.

4.4.2 EGTA induced dissociation of PFK target peptides from calmodulin followed by change in tryptophan intensity.

Changes in tryptophan fluorescence emission were studied following EGTA induced calcium dissociation from Ca_4CaM:PFKpep complexes. This experimental method uses the known calcium dependence of calmodulin interaction with peptide to quantify calcium dissociation rates and probe peptide dissociation mechanism. The experimental method is described in section 3.2.4. Tryptophan fluorescence was measured using an excitation wavelength of 295nm and an emission cut-on filter of 330nm. Typical experimental concentrations were [CaM]= 2μM, [PFK peptide]= 2.2μM, and 100μM total Ca^{2+}. EGTA was prepared at 20mM, however fluorescence signal is independent of [EGTA] in the range 1-20mM. All concentrations quoted are prior to stopped-flow mixing. A full description of the stopped-flow experiment is provided in section 3.2.4. For all EGTA stopped-flow experiments described here data is reported as an average of three independent experiments and each experiment involves the averaging of at least 9 traces. Data analysis is considered in Appendix 3.

The addition of EGTA to Ca_4CaM complexes leads to a decrease in fluorescence characteristic of the environment change associated with the tryptophan of the target peptide. Figure 4.4.2a illustrates the intensity of fluorescence emission at 330nm as a

Figure 4.4.2

(A) Experimental stopped-flow trace for the dissociation of calcium from calmodulin complexed to peptide P9-26 using the calcium chelator EGTA. Concentrations quoted are prior to 1:1 stopped-flow mixing. Data is never less than an average of 9 stopped-flow traces. The fit to the experimental data is shown by the smooth curve. Concentrations and experimental parameters are described in the text. The dissociation of calcium from Ca_4CaM:P9-26 is best fit as biphasic as shown by the residuals calculated for a one or two exponential fit (inset). The corresponding χ^2 values for the single and double exponential fit are 2.03 and 1.2 respectively. The amplitudes (A) and rates (k) of the two exponential fit are A_{fast}= 0.065, k_{fast}= 14s^{-1}, A_{slow}= 0.1214, k_{slow}= 2.2.

(B) Arrhenius plot showing the calcium dissociation from calmodulin in the presence of peptide P9-21 as a function of temperature. Rates were determined from the average of at least 9 traces at a given temperature. Data was analysed as described above. Since the process of calcium dissociation from CaM:P9-21 is biphasic two sets of data are presented corresponding to the fast and slow dissociation rates. The gradient of the line was calculated from regression analysis, the top line represents the fast dissociation process, activation energies associated with each dissociation are reported in the text.

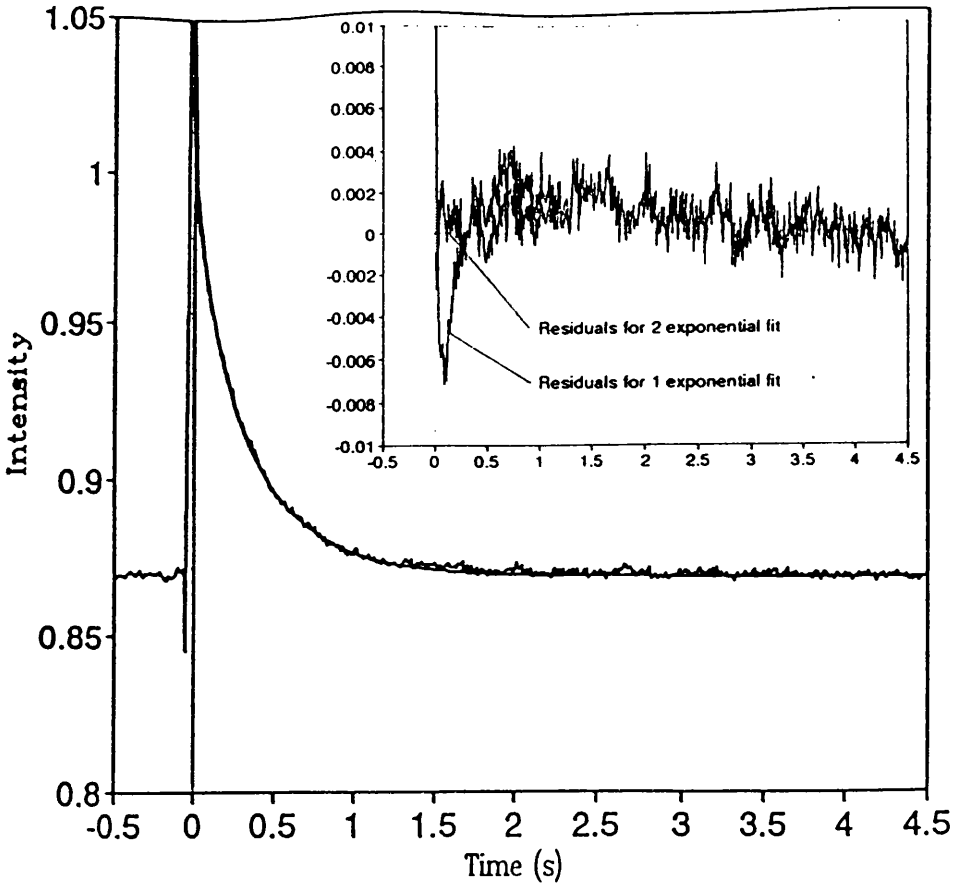
Intensity
Time (s)
Residuals for 2 exponential fit
Residuals for 1 exponential fit

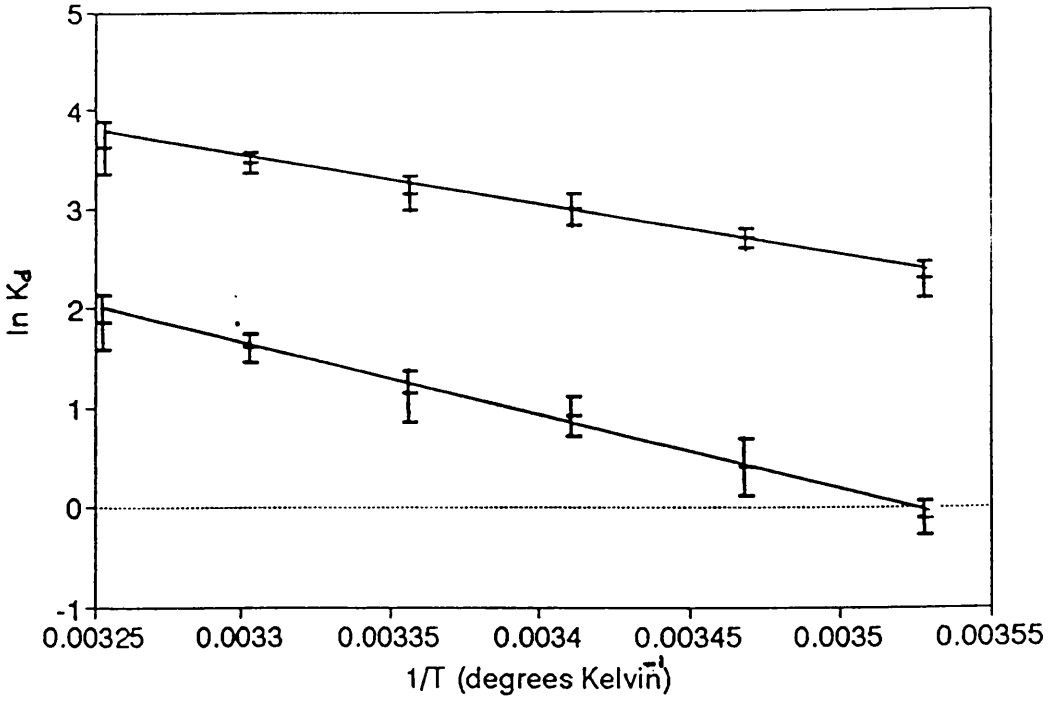
ln Kd
1/T (degrees Kelvin)

function of time for the calcium dissociation observed in the Ca_4CaM:P9-26 complex. The dissociation of calcium from this complex (figure 4.4.2a) is very similar to the Ca_4CaM:P1-26 and Ca_4CaM:P9-26 complexes, see table 4.4.1 for values. The rates are similar for the three PFK peptide complexes with a fast phase of $\sim$13-17s^{-1} and a slow phase of 1.6-2.5 s^{-1}, the presence of all peptides reduces the rate of calcium dissociation from calmodulin consistent with the Quin-2 experiment (section 4.4.1).

Table 4.4.1 shows the rates and amplitudes and corresponding rates and amplitudes for the same experiment using peptides from other sources including peptide WFF from sk-MLCK.

The amplitudes of the fast phase for the EGTA induced calcium dissociation of calmodulin in complex with P1-26, P9-26, or P9-21 corresponds to 30-34% of the total fluorescence, implying that the calcium dissociation mechanism follows a similar route in all three complexes. The majority ($\sim$70%) of the fluorescence is associated with the slow phase. Since the tryptophan binds to calmodulin C-domain, it follows that k_s corresponds to dissociation of calcium ions in CaM C-domain since this is the phase for which the majority of the fluorescence is associated. The same experiment was performed using peptide WFF from sk-MLCK in which the peptide tryptophan also binds calmodulin C-domain, (Martin et al., 1996; Ikura et al., 1992), in this case 90% of the tryptophan fluorescence amplitude corresponds to the slow phase.

For calmodulin in complex with peptide P9-21 the activation energies for the fast and slow phases were calculated in experiments over the temperature range 5-40°C to be 49 $\pm$ 2 and 68 $\pm$ 3 kJ mol^{-1} respectively. Figure 4.4.2b shows the Arrhenius plot from which the apparent activation energies are derived, linear regression of the averaged data from 3 experiments was used to draw a line. Martin et al., (1985) have previously

reported values of 42 and 63kJ mole^{-1} for dissociation of the N- and C-terminal calcium ions from calmodulin in the absence of peptide. Brown et al., (1996) performed a similar study with calmodulin in the presence of peptide WFF and reported values of 52 and 70kJ mole^{-1} The activation energies determined for the peptide complexes are higher than the values observed for Ca_4CaM alone, consistent with the enhanced binding of calcium to calmodulin in the presence of peptide (Olwin and Storm, 1985; Yagi et al., 1989; Yazawa et al., 1987), however the WFF exerts a greater effect, this result supports calcium binding experiments see section 4.3.

These kinetic studies using EGTA indicate that the calcium dissociation rates for calmodulin in complex with P1-26, P9-26, or P9-21 are similar with a fast phase of $\sim$13-17s^{-1} and a slow phase of 1.6-2.5s^{-1}. The majority (70%) of the fluorescence is lost in the slow dissociation process which is consistent with loss of the C-domain calcium ions this would presumably account for majority of the fluorescence change since the peptide tryptophan binds the CaM C-domain, see section 4.2. Assuming the fast dissociation process corresponds to loss of the N-domain calcium ions, this implies that loss of calcium from the N-domain sites accounts for approximately $\sim$30% of the fluorescence, this may be a consequence of altered tryptophan environment in the Ca_2CaM:PFK peptide kinetic transient alternatively it might be explained in the kinetic model which follows.

4.4.3 Kinetic mechanism of calcium dissociation from Ca_4CaM:PFK peptide complexes

Calcium dissociation from calmodulin has previously been described as biphasic, each phase involves dissociation from a pair of sites within one domain, (Martin et al.,

1985; Forsen et al., 1986). The differential affinities of the pairs of sites within each domain was determined by Martin et al., (1985). The N-terminal sites apparently have dissociation rates of $\sim 700s^{-1}$, whilst the C-domain sites have greater affinity for calcium and dissociation rates are $8.5s^{-1}$. Based on these data for calmodulin and experimental data presented in section 4.4.1 & 4.4.2 a model of calcium dissociation from Ca_4CaM:PFKpep is presented.

The reaction mechanism is shown in figure 4.4.3. The top line of the scheme demonstrates the equilibrium established for calmodulin C in complex with peptide P, with 2 N, and 2 C, calcium sites filled. Equilibrium binding studies previously determined that the complexes formed between calmodulin and PFK peptides, P1-26, P9-26, or P9-21 were of high affinity (K_d 32nM-280pM), see table 4.1.1. Under typical stopped-flow experimental conditions (CaM $=2\mu$M, PFK peptide $= 2.2\mu$M), calmodulin is fully saturated with peptide.

Like the dissociation of calcium from calmodulin, the loss of calcium from complexes of calmodulin with PFK target peptides is best described as biphasic, with each phase involving two calcium ions. Consequently, the first stage of calcium dissociation from $C_{N,C,P}$ can be described as following either path 1 or 2, see figure 4.4.3a. Dissociation to $C_{N.C,\_}$ + $_P$ (path A) is not possible under stopped-flow conditions, (see above).

Equilibrium calcium binding studies of calmodulin in the presence of PFK target peptides indicate that the binding of the first two calcium ions is to the C-domain of calmodulin, therefore these are the high affinity calcium binding sites, (see section 4.3). It seems very likely that the initial fast phase of dissociation of calcium from $C_{N,C,P}$ involves loss of the N-terminal (low-affinity) calcium ions, ie: step 2, not step 1. The

Figure 4.4.3

Formal kinetic scheme for dissociation of Ca_4CaM-PFK peptide complexes assuming that Ca^{2+} ions dissociate in pairs. C represents calmodulin and the subscripts P, N, and C represent peptide, N- and C-terminal Ca pair, respectively. NB: All steps involving Ca^{2+} dissociation have been assumed to be irreversible, as outlined in the results section.

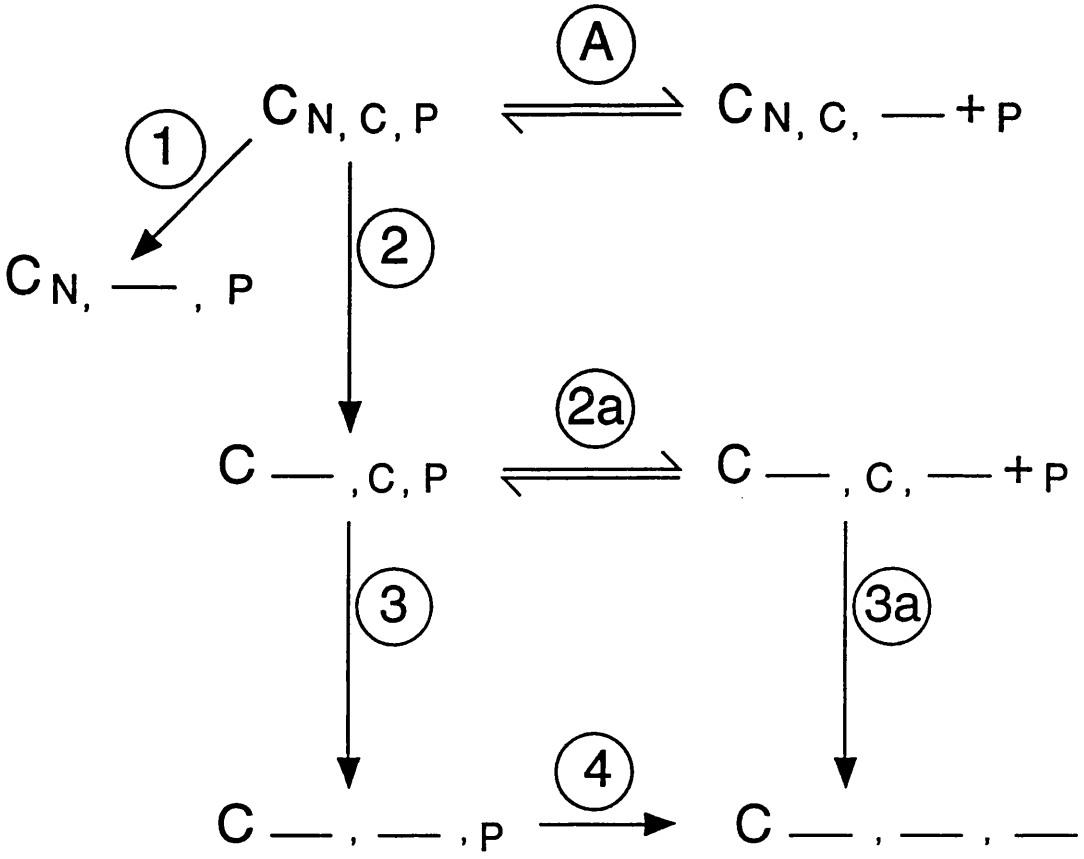
A
$C_{N,C,P}$
$C_{N,C,}$ — + P
1
$C_{N,}$ — , P
2
2a
C — , C, P
C — , C, — + P
3
3a
4
C — , — , P
C — , — , —

consequent calcium dissociation must involve the C-domain calcium ions, ie: via steps 3 and 4, (Johnson et al., 1996). Step 3 will reflect the rate of the slow phase however, since the affinity of apo-calmodulin for PFK peptide is very low, and the corresponding rate of step 4 would be indistinguishable ($>1000s^{-1}$).

This model presents two problems however based on experimental findings, specifically:

(1). EGTA stopped-flow dissociation experiments indicate that up to 30% of fluorescence amplitude is contributed by the fast dissociation phase. However, according to calcium binding experiments for CaM plus P1-26 it appears that the fluorescence signal is essentially complete on addition of two calcium ions (ie: both calcium ions in the C-domain). It might therefore be expected that there would be little or no fluorescence amplitude associated with the initial loss of 2 N-domain calcium ions from the $C_{N,C,P}$ complex. This is not the case. It is of course possible that Trp signal in $C_{N,C,P}$ and the kinetic transient species $C_{-,C,P}$ are significantly different.

(2). The second problem concerns the apparent inconsistency that PFK peptides of different affinity (32nM-280pM) for calmodulin have apparently very similar dissociation rate constants for calcium. Since the target peptide increases the calcium affinity of calmodulin, one would anticipate on a simple model that the greater the affinity of the target peptide, the more slowly would the calcium ions dissociate. This is not the case.

These two inconsistencies suggest that a simple model for peptide dissociation is not adequate. A more detailed kinetic model has been presented by Brown et al., (1996) which includes a relaxation stage in the calcium dissociation mechanism. As previously discussed the equilibrium of step A will lie predominantly to the left-hand side. The complex resulting from dissociation of N-terminal calcium ions complex $C_{-,C,P}$ must

therefore also exist in an equilibrium such that $C_{\_,C,P} \rightleftharpoons C_{\_,C,\_} + {}_P$, (step 2a).

Since the affinity of the isolated C-domain of calmodulin (TR2C) has significantly reduced affinity for target peptide compared with the intact protein, (CaM:P1-26, K_d= 0.28nM cf TR2C:P1-26, K_d= 40μM), then under stopped-flow protein and peptide concentrations used in these experiments one can expect the equilibrium to be of kinetic significance. Step 2a can therefore be designated as a reversible step, and constitutes a relaxation process in the kinetic mechanism, as opposed to a uni-directional irreversible step such as calcium dissociation in the presence of a chelator, Brown et al., (1996). However it is coupled to unidirectional steps 2 and 3a.

Bayley et al., (1996) & Brown et al., (1996) account for this equilibrium in similar studies using calmodulin in complex with target sequences of sk-MLCK. The mechanism is also applicable to calcium dissociation from Ca_4CaM:PFKpep. Specifically, the mechanism can account for questions 1 and 2 posed above.

In response to why there is an apparent fluorescence amplitude associated with the N-domain calcium ions, According to this mechanism, the fast phase of calcium dissociation represents calcium dissociation from the N-domain binding site (step 2), however the coupling to reversible step 2a accounts for the observation of the associated change in tryptophan fluorescence since step 2a involves dissociation of the peptide. Note, however that in this mechanism rate of the fast process is mainly a consequence of dissociating N-domain calcium ions.

The reason why there is relatively little influence on the target peptide affinity for calmodulin upon the calcium dissociation rate constants can also be explained by this equilibrium stage (step 2a) in the reaction mechanism. The reversible equilibrium of step 2a provides two routes by which calcium dissociation can occur, ie: from $C_{\_,C,P}$ (via step

3) or from $C_{\_,C,\_}$ (via step 3a). Calcium dissociation from the latter is effectively the same as calmodulin in the absence of the target peptide. Hence, for there to be a large effect of target peptide on the calcium dissociation from C-domain sites, it is necessary that the equilibrium of step 2a is favoured to the left hand side, ie; peptide rebinding is efficient. Given the drastic reduction in K_d for the complexes formed between the C-domain and PFK target peptide compared with intact protein, it is unlikely that under experimental conditions used that rate of calcium dissociation from the C-domain sites of the Ca_2CaM:PFK peptide kinetic transient species will be strongly affected by differences in target peptide affinity for intact calmodulin.

In support of the existence of a relaxation step, (Bayley et al., 1996) and Brown et al., (1996) suggest that the observed rates should be affected by [peptide]/[CaM] ratio. Experimentally, studies with calmodulin in complex with target peptides from sk-MLCK and mastoparan show that the fast phase can be reduced and eliminated by repeating experiments at raised [peptide]/[CaM] ratios. Furthermore, the slow phase rate is also reduced, (Bayley et al., 1996; Brown et al., 1996), consistent with a significant contribution to the mechanism from steps 2a and 3a.

In conclusion, the effect of the PFK target peptides studied was to decrease calcium dissociation rate from calmodulin. PFK target peptides of different affinities were studied, (K_d= 32nM-280pM) however the effect of the target peptide on calcium dissociation rates appears to be independent of these differences in affinity. Calcium dissociation from the Ca_4CaM:PFKpeptide is biphasic, each phase involves two calcium ions. The fast phase ($\sim$ 10-20s^{-1}) correlates with loss of calcium from the sites within the N-domain, dissociation of the C-domain calcium ions is slower (1-2s^{-1}). According to the model proposed, subsequent to loss of the N-domain calcium ions the Ca_2CaM:PFK

peptide kinetic transient species will be in rapid equilibrium with Ca_2CaM and free peptide, hence the slow phase of calcium dissociation likely represents dissociation from Ca_2CaM:PFK peptide and Ca_2CaM.

4.5 Enzyme activation studies

The dynamic processes of assembly and disassembly of enzyme complexes provides a system for the potential control of the flux of metabolic pathways, (Ovadi, 1988). The enzyme phosphofructokinase can exist in several oligomeric states, (Mayr, 1984a). The monomeric and dimeric forms of the enzyme are inactive, whilst the larger tetrameric form is active. Higher polymeric forms are partially active but not particularly well understood, (Mayr, 1984a, 1984b).

A number of physiological effects and small molecular weight effectors such as the adenosine phosphates and citrate exist to regulate the enzyme. Calmodulin regulates activity presumably through preventing association of the inactive dimers to active tetramers through high affinity binding to the dimeric interface.

Since PFK is itself a large (monomer = 86kDa) multimeric enzyme, the complex formed between PFK and CaM is difficult to study at the molecular level. Consequently, investigations of the interaction described in sections 4.1-4.4 of this thesis have used target sequences of the enzyme based on the high affinity calmodulin binding site. In support of existing studies, the following section shows that the calcium dependent inactivation effect of calmodulin corresponds to interaction with the sequences previously studied, see table 1.

The method follows NADH oxidisation by coupling fructose-1,6-bisphosphate formation to aldolase, glyceraldehyde 3-P dehydrogenaseand triose-phosphate isomerase reactions, (Racker et al., 1964). This yields 2 moles of NADH oxidized for each mole of fructose-1,6-bisphosphate formed, see figure 4.5a. The methods used in this section are quite different from those in previous chapters and are therefore to assist the reader the experimental methods are incorporated into this results section.

Figure 4.5a

The reaction scheme from the glycolytic cascade from which the coupled enzyme assay system is based. The method follows NADH disappearance by coupling fructose-1,6-bisphosphate formation to aldolase, glyceraldehyde 3-P dehydrogenase & triose-phosphate isomerase reactions. Scheme from Harper's Biochemistry, (1985).

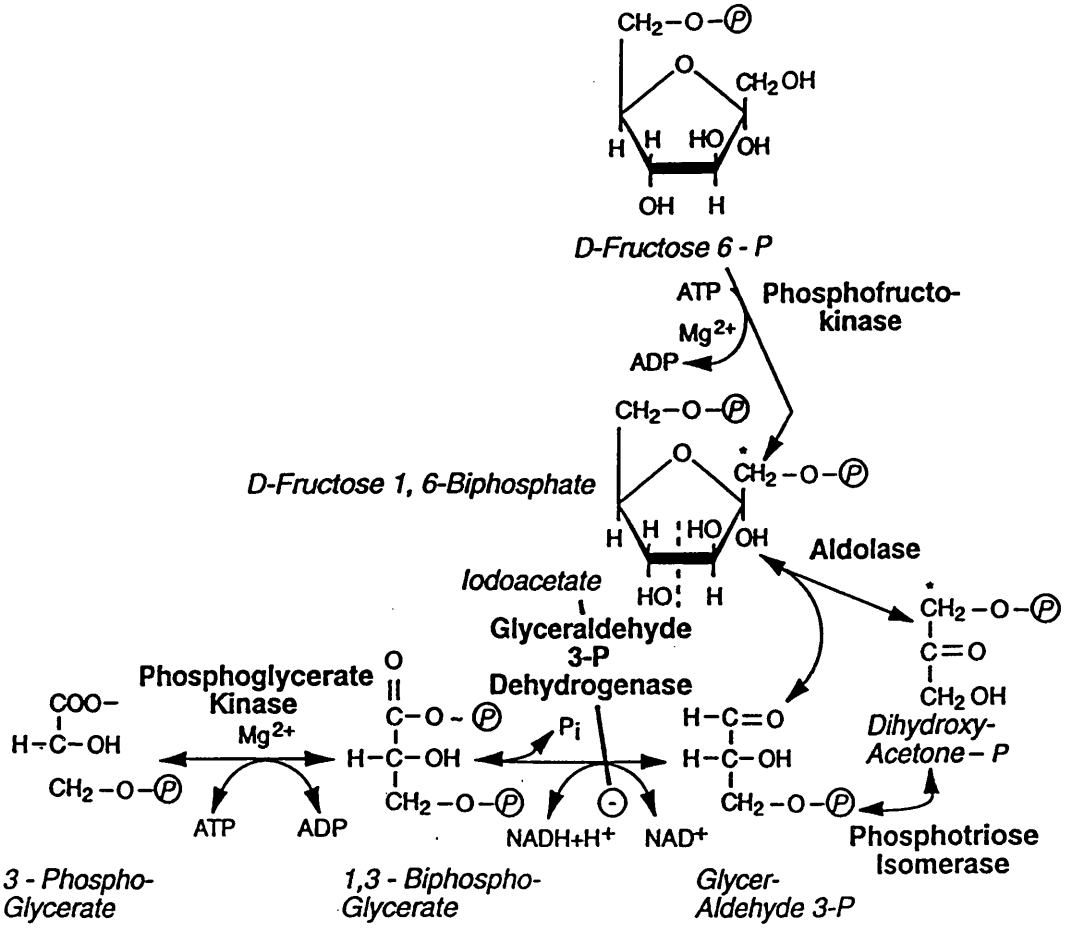
D-Fructose 6 - P
ATP
Mg2+
ADP
Phosphofructo-
kinase
D-Fructose 1, 6-Biphosphate
Aldolase
Iodoacetate
Glyceraldehyde
3-P
Dehydrogenase
Phosphoglycerate
Kinase
Mg2+
Pi
ATP
ADP
NADH+H+
NAD+
Dihydroxy-
Acetone - P
Phosphotriose
Isomerase
3 - Phospho-
Glycerate
1,3 - Biphospho-
Glycerate
Glycer-
Aldehyde 3-P

4.5.1 Materials and Methods

4.5.1.1 Phosphofructokinase preparation

An ammonium sulphate crystalline suspension of rabbit skeletal muscle phosphofructokinase was purchased from Sigma chemicals and stored at 4°C. PFK was centrifuged at 10000g for 10min to remove ammonium sulphate. The pellet was then resuspended in enzyme dilution buffer (see below). Residual $(NH_4)_2SO_4$ and ATP were removed using a prepacked G25-Sephadex PD10 column (Pharmacia). The column was equilibrated in 50mL 100mM phosphate, 0.5mM EDTA, 3mM DTT at pH 8.0, 4°C. 0.75mL of PFK was applied to the column and the enzyme was eluted in 4mL. Aliquots of 500μL were collected and a 1mL sample, essentially free of ATP (judged by $\frac{A_{280}}{A_{260}}$) was collected between 2-3mL, see figure 4.5.1.1 for absorption spectra. This method gave a 75% yield based on manufacturers initial concentration and the concentration of the ATP free sample determined using $A_{280} = 1.07$ for a solution of 1mgmL^{-1}, (Parmeggian et al., 1966).

The specific activity of the enzyme at 4°C was typically 250 units/mg, however this has been noted to decrease after about 4 weeks, (Lad et al., 1973). Only enzyme at high specific activity was employed for the measurements reported here. Care must be exercised in dilution and selection of the dilution media of the enzyme before assay, because PFK is extremely sensitive to low pH, monovalent anions and protein concentration.

4.5.1.2 Enzyme assay

PFK activity and its variation were determined by a coupled enzyme system basically in accordance with Mayr's procedure, (Mayr, 1984a).

(1). Depending on the number of assays between one and six 10mm path length quartz

Figure 4.5.1.1

Absorption spectra of the PFK enzyme used in these studies before and after gel-filtration chromatography. The spectrum with λ_{max} at approximately 260nm is the PFK purchased from Sigma chemicals in 1.4M $(NH_4)_2SO_4$, pH 7.2, with 0.05M β-glycerophosphate, 0.004M ATP, 0.001M DTT and 0.002M EDTA. The spectrum with λ_{max} at 280nm is the PFK enzyme after gel-filtration on a G25-Sephadex PD10 column to remove ATP and $(NH_4)_2SO_4$. The buffer for the ATP free sample is 0.1M Phosphate, 0.003M DTT, 0.0005M EGTA.

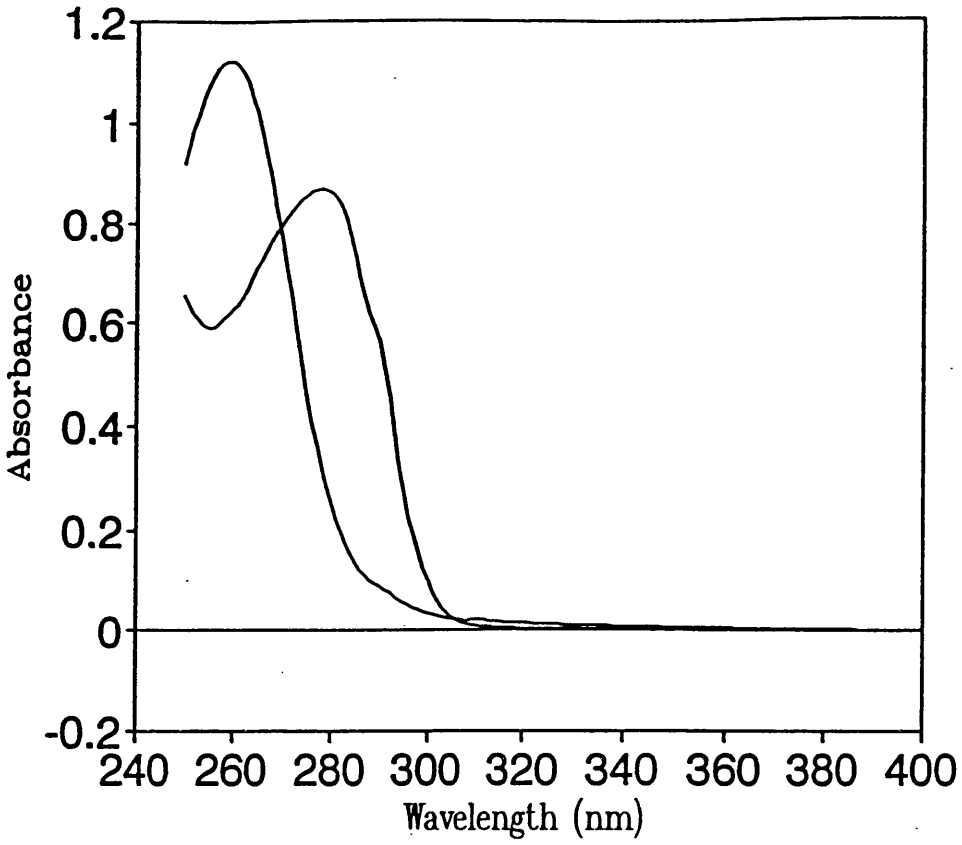
1.2
1
0.8
0.6
0.4
0.2
0
-0.2
Absorbance
240 260 280 300 320 340 360 380 400
Wavelength (nm)

cuvettes were filled with 790μL of the auxiliary enzyme solution containing; 1mM ATP, 3mM $MgCl_2$, 3mM DTT, 2mM fructose-6-phosphate, 0.2mM NADH, 0.1mM EGTA, 50mM Tris (pH 8.0), 0.05 units of aldolase ml^{-1}, 3 units of glycerol-3-phosphate dehydrogenase ml^{-1}, and 12 units of triose-phosphate isomerase ml^{-1}. This solution was equilibrated at 26°C in the thermostatted cuvette holder of the spectrophotometer.

(2). To 125μL of preincubation buffer in capped Eppendorf tubes, a solution of calcium saturated calmodulin$\pm$peptide and water to a total volume of 245μL are added to give the desired calmodulin concentration. The tubes are incubated at 26°C for 20 minutes. The preincubation buffer comprises 20mM HEPES, 1.5mM $MgCl_2$, 200mM KCl, 0.05mM ATP, 0.1mM $CaCl_2$, 5mM DTT. The concentration of calmodulin and target peptide used are stipulated in the results section.

(3). 40μL of PFK at approximately 100 fold times the desired final concentration is prepared, see earlier. To start the incubation, 6μL of this solution is added to each Eppendorf and mixed by a vortex.

(4). From each preincubation sample a 20μL aliquot was withdrawn after 1 minute and diluted into the cuvette. The curves are similar for preincubation times of 1, 5, or 10 min. The absorbance of the solution is then followed with time at 365nm and the activity of the enzyme is determined, either alone, or in the presence of calmodulin and target peptide.

4.5.1.3 Enzyme assays involving calcium-binding site mutants of calmodulin

In studies using calcium-binding site mutants of calmodulin the enzyme activity

was determined using the method described above but with some minor modifications. The major difference in the studies is that the preincubation stage is not used. Since mutant calmodulins have a lower affinity for target peptides derived from the enzyme it was anticipated that they would also exhibit a similarly decreased affinity for the intact enzyme. Therefore, the PFK and protein samples were introduced directly into the cuvette at higher concentration. PFK was dissolved in 100mM phosphate, 0.5mM EDTA, 3mM DTT, pH 8.0 and was added to the cuvette, subsequent to the addition of calmodulin, to give a total concentration of 1.1μM. Wild-type CaM, B2K, and B4K were dissolved in 25mM Tris, 100mM KCl, 0.1mM $CaCl_2$, pH 7.5 and were added to the cuvette to give a total protein concentration of 22μM (ie: 20 fold in excess over PFK).

4.5.1.4 Data aquisition

The decrease in absorbance at 365nm was recorded using a Cary 3E UV Vis spectrometer. The assays were initiated by addition of phosphofructokinase to the assay mixture, or after preincubation of 1 min (see above). Cuvettes were maintained at 26^{0}C using a thermostatted cuvette holder.

4.5.2 Effect of calmodulin on phosphofructokinase activity

The central aim of studying the interaction of calmodulin with the intact enzyme was to question the physiological significance of the interaction, ie: exactly how effective is calmodulin as an inhibitor of PFK activity. The intracellular PFK concentration is 1mgml^{-1}, (Uyeda, 1979). This concentration is two orders of magnitude too high for the standard optical spectroscopic techniques used in the study of PFK activity. A two step preincubation assay was performed as a compromise to analyze PFK activation. For the preincubation assay first concentrated PFK was incubated together with Ca_4CaM and other effectors but with one substrate missing. The rate of activity was then measured in

a second step by dilution of an aliquot into an optimal assay, (Mayr, 1984).

In the following experiments, the influence of calmodulin on the activity of phosphofructokinase was assessed, in addition the competitive inhibition of the target sequence derived from the enzyme was determined.

Figure 4.5.2 shows the decrease in absorbance with time for PFK under different assay conditions. The PFK concentration is 1.1μM (0.1mgmL^{-1}) subunits in the preincubation buffer, which is lacking in fructose-6-phosphate, preventing any prior reaction. The enzyme was diluted 40 fold to 2.5ugmL^{-1} into a quartz cuvette containing the enzyme dilution buffer, see methods. This concentration corresponds to approximately 5 units of PFK specific activity in each cuvette. The change in absorbance was then followed with time at 365nm to determine the effects of calmodulin and target peptides on PFK activity.

The concentration of calmodulin used is 3μM, target peptide concentration is 15μM, concentrations quoted are those in the preincubation buffer. Although calmodulin is in 2.7 fold excess over enzyme, it has been shown previously, (Buschmeier et al., 1987) that calmodulin interacts with 1:1 stoichiometry to PFK protomers under these experimental concentrations, (Mayr, 1984a; Lan & Steiner, 1991). Target peptide is in 5 fold excess over calmodulin and in 13.6 fold excess over enzyme. Given the similarity in dissociation constants for the complex of calmodulin with target sequence (P1-26 = 0.28nM) or target enzyme (3nM, Buschmeier et al., 1987), this molar ratio was thought to be sufficient to determine whether the target sequence competitively inhibits the interaction of calmodulin with the enzyme.

The curves in figure 4.5.2 correspond to the change in NADH absorption with time. The rate of this reaction (ie: the slope) is controlled by the concentration of

Figure 4.5.2

Influence of calmodulin and PFK target sequence on the activity of PFK monitored by the absorption of NADH in the coupled enzyme assay described in text. Data is absorption at 365nm plotted with time. Phosphofructokinase is prepared at 1.1μM concentration in preincubation buffer (*) (see methods) and with 3μM Ca_4CaM (+), and in the presence of 3μM Ca_4CaM plus 15μM target peptide (-).

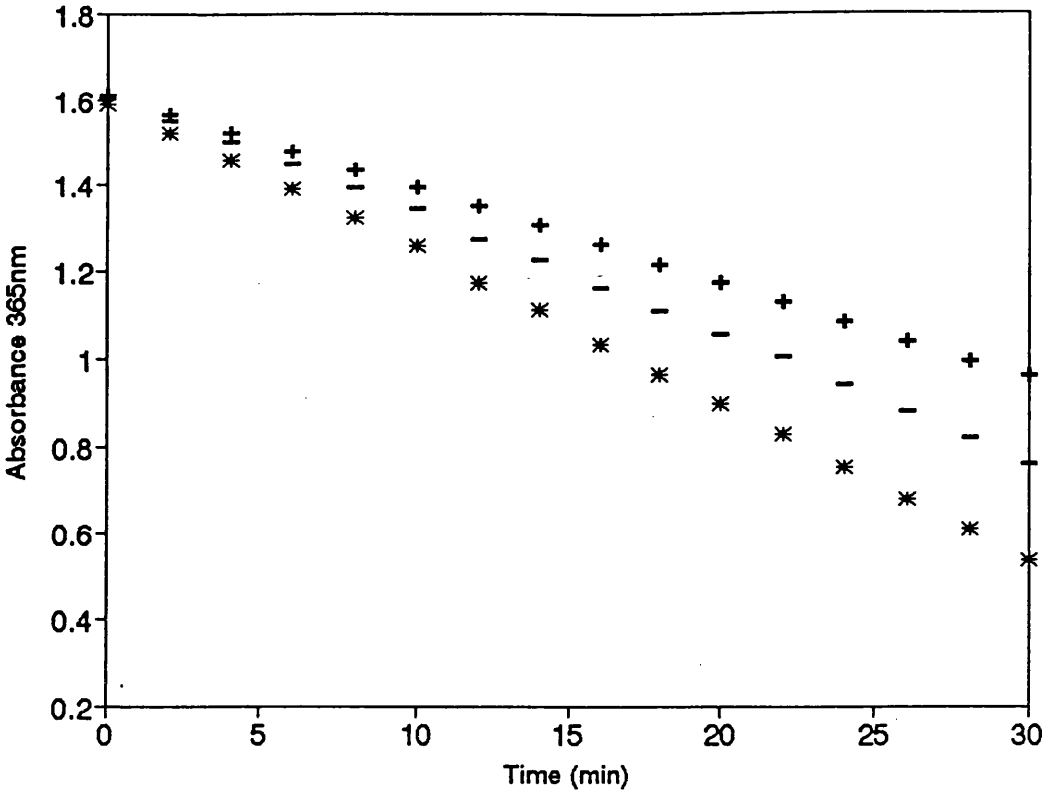
Absorbance 365nm
1.8
1.6
1.4
1.2
1
0.8
0.6
0.4
0.2
0
5
10
15
20
25
30
Time (min)

reactants and substrates and by the activity of the PFK which catalyzes the conversion of fructose-6-phosphate to fructose-1,6-bisphosphate. Figure 4.5.2 shows the influence of calmodulin and a target sequence derived from PFK on the rate of reaction.

The curve depicted by (*) symbols illustrates the absorption change in NADH for PFK in the absence of calmodulin and target peptide. The (+) symbols show that the rate of this reaction is slower in the presence of calmodulin, ie: the PFK activity is reduced. The (-) symbols show the effect of adding calmodulin and the target sequence P9-26. The target clearly competes with the enzyme for binding to calmodulin. However, even at the elevated peptide concentration used in this experiment restoration of the full PFK activity was not observed, hence the curve depicted by the (-) symbols in figure 4.5.2 demonstrates a reaction which is still inactivated to some extent by calmodulin.

Given that calcium has been shown to inhibit PFK activity it was necessary to maintain a calcium free environment in PFK preparations. PFK is therefore prepared in 0.5mM EDTA, and is not added to the Ca^{2+}-containing preincubation buffer until 1 minute before dilution into the enzyme assay buffer. The absence of calcium from the PFK preparation and the optimal conditions employed fully activate tetramers present and prevent them from dissociation before reaction commences, (Mayr, 1984a).

4.5.3 Differential effects of calmodulin and calcium binding site mutants of calmodulin on activation properties of PFK

Previous studies have indicated that the structural and functional integrity of calmodulin in complex with target peptides derived from PFK, (see section 4.2) are impaired by mutation of the conserved glutamate residue at position 12 of the EF-hand calcium binding loop to a lysine residue. The inactivating effects of B2K and B4K on

PFK were compared with those of wild-type CaM using the assay method described in section 4.5.1.

Figure 4.5.3 shows that the activation of PFK is decreased in the presence of calmodulin and both the B2K and B4K calcium-binding site mutants of calmodulin. Total enzyme concentration was 1μM, calmodulin and calcium-binding site mutants were 20 fold in excess over enzyme. The reason for using higher PFK and protein concentrations in this experiment is rationalised by the results of a fluorescence experiment in section 4.1.5 which demonstrates that the affinity of the calcium-binding site targets for PFK target peptide P9-26 is greatly reduced; (CaM:P9-26 Kd = 11nM, B2K:P9-26 Kd = 160nM; B4K:P9-26 Kd = 1μM).

The activity of the kinase alone increases with concentration as is evident from comparison of this experiment and the similar experiment described in section 4.5.1 using 0.011μM enzyme.

It is difficult to estimate free intracellular calmodulin concentration especially since in the cell, it reacts with many species other than PFK. Therefore it may be that this concentration is unphysiologically high. The results from these experiments are however intended only to be used quantitatively in terms of comparisons between calmodulin and the site-directed mutants of calmodulin.

It appears from figure 4.5.3 that both mutants can reduce the activity of PFK, but they are clearly less effective than CaM itself. The B4 mutant is less effective than the B2 mutant, consistent with the known affinities of these proteins for peptide P9-26, (CaM:P9-26= 11nM; B2K:P9-26= 160nM; B4K:P9-26= 1000nM).

Figure 4.5.3

Influence of calmodulin and calcium-binding site mutants, B2K and B4K on the rate of activation of PFK with time as determined by a coupled enzyme spectrophotometric assay. Data is absorption at 365nm plotted with time. Phosphofructokinase is prepared at 1.1μM concentration in cuvette (filled squares). The effect of 22μM calmodulin is demonstrated by the open squares. The effects of 22μM B2K or B4K are illustrated by filled triangles or asterices respectively.

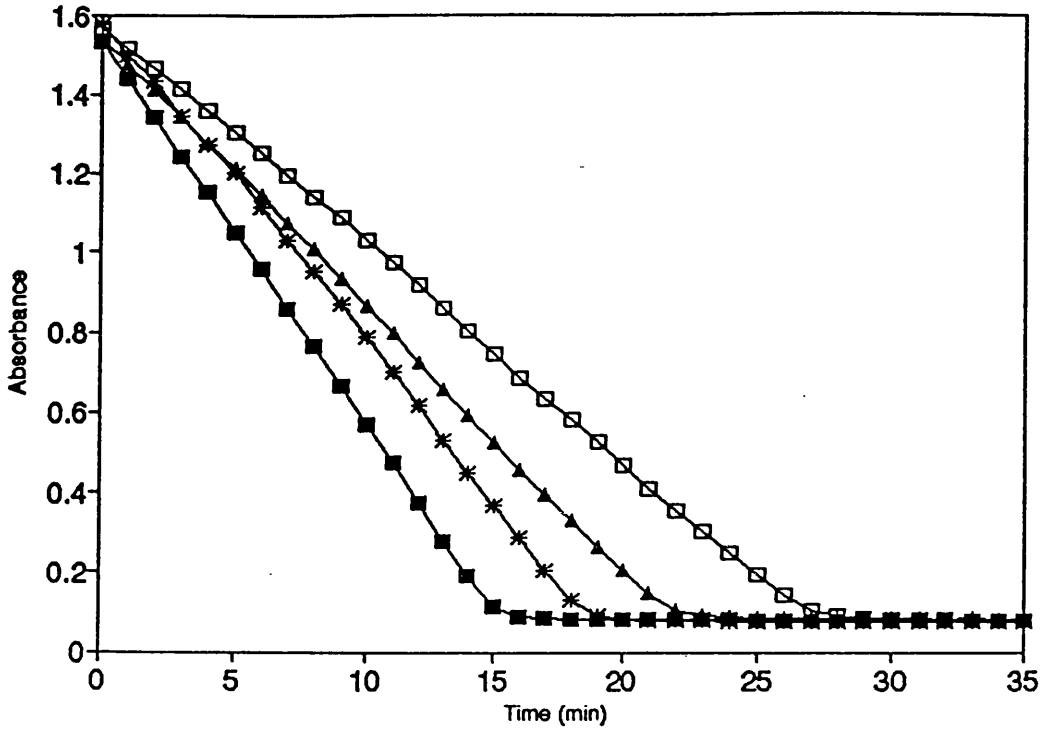
1.6
1.4
1.2
1
0.8
0.6
0.4
0.2
0
Absorbance
0
5
10
15
20
25
30
35
Time (min)

Further experiments were prevented by shortage of materials and also by difficulties in obtaining quantitative information in this complex system. However, it is possible to make qualitative deductions from this series of experiments:

(1). Wild-type calmodulin is able to inhibit PFK activity.

(2). As expected the target peptide P9-26 derived from the high affinity binding site of PFK competetively inhibits the effect of calmodulin on the target enzyme.

(3). Mutation of the conserved bidentate calcium chelating residue glutamate to lysine in either site 2 or 4 results in calmodulins which are less effective in inhibiting PFK than is wild-type CaM. The B2 mutant is more effective in inactivating PFK thn the B4 mutant, consistent with structural and affinity studies described in section 4.1.2 and 4.2.

These results support the findings of Mayr, (1984) and Buschmeier et al., (1987) however the scope of calmodulin as a potential inhibitor of PFK appears to be considerably less than its ability to modulate numerous other enzyme activities through calcium dependent control. These include MLCK, CaMKII, calcineurin, phosphorylase kinase, phosphodiesterase, and adenylate cyclase (Manalan & Klee, 1987; Soderling, 1990). Nonetheless the affinity of calmodulin for PFK implied by the evidence of Mayr (1984a) and supported by the peptide binding data of section 4.1.1 of this work suggest that CaM could indeed function as a calcium dependent modulator of PFK and hence contribute to regulation of glycolytic processes.

4.6 Crystallization of the complex formed between CaM and PFK target peptide.

4.6.1 Introduction

The essential feature of a crystal is its ordered and three dimensionally periodic internal structure. A system of asymmetric objects that spontaneously declines its dynamic flexibility and arranges itself with extraordinary precision in a fixed lattice appears to be in contradiction to usual entropic tendencies. The crystallization of molecules from solution is a reversible equilibrium phenomenon, and the specific kinetic and thermodynamic parameters depend upon the chemical and physical properties of the solvent and solute used. Although the individual molecules lose rotational and translational freedom, thereby lowering the entropy of the system, they, at the same time, form many new stable chemical bonds. This reduces the potential or free energy of the system and provides the driving force for the ordering process.

Note: The crystallization and diffraction studies presented here were part of a collaborative project with members of the Protein Structure Division within NIMR, specifically, Dr's Kim Henrick, Miriam Hirshberg, Steve Gamblin and Bing Xiao.

4.6.2 Sample preparation for crystallization

Samples of Ca_4CaM:P9-21 and Ca_4CaM:P1-26 were prepared in a similar manner. Calmodulin from the preparation described in section 3.1 was in 25mM Tris, 100mM KCl, 1mM $CaCl_2$, pH 7.0. This calmodulin was applied to a PD10 G25-Sephadex gel filtration column prequilibrated in 25mM $NH_4(CO_3)_2$ pH 7.0. The resulting calmodulin was lyophilized and made 5-20mgmL^{-1} in water and 100μM free calcium was added as $CaCl_2$. An appropriate amount of lyophilized peptide was weighed which would in

solution give a concentration 1.8 fold over CaM. The peptide was dissolved by the protein solution. The pH of the solution was adjusted accordingly, crystallization was best achieved at acidic pH 4.8-5.2. The complex samples were centrifuged (4000rpm for 3 min) to remove any dust particles. Fluorescence spectroscopy was used to ensure that peptide was bound to protein, see section 4.1.1. For preparation of heavy metal derivatives of the CaM:PFK peptide complexes the sample preparation varied slightly. In preparation of samples crystallised in the presence of lead, 1.8mg of P9-21 was dissolved in 500μL (10mM) PbAc to give a resulting peptide concentration of 2.14mM (3.53mgmL^{-1}). This solution was used to dissolve 10mg of calmodulin to give a concentration of 1.19mM (20mgmL^{-1}), the sample pH was 5.1.

4.6.3 Sample Crystallization

The solubility of a protein depends on the concentration of the protein, pH, temperature and a variety of other influences and as a result finding the point at which supersaturation occurs involves screening over a variety of chemical conditions. There are several methods for attaining supersaturation including dialysis, free interface diffusion and vapour diffusion on plates or slides. In these studies vapour diffusion in hanging drops was used. Through the vapour phase, the concentration of salt or organic solvent in the buffer reservoir equilibrates with that in the sample by distillation of water out of the droplet and into the reservoir.

4.6.4 Vapour Diffusion in Hanging Drops

This crystallization technique involves suspending a microdroplet of mother liquor solution (4-10μL) from the underside of a microscope coverslip, which is placed over a

small well containing 200-1000μL of the precipitating solution. The mother liquor comprises a mixture of the CaM:peptide complex and the buffer reservoir solution, typically 2-10μL complex was mixed with 2-10μL buffer reservoir solution in a drop on the coverslip. An important point to note is that the coverslips must be thoroughly and carefully coated with nonwetting silicone to ensure proper drop formation and prevent spreading. The coverslips are held to the surface of the well airtight by a thin application of silicone grease.

4.6.5 Optimal crystallization conditions for the complexes formed between CaM and peptides P1-26 and P9-21

Crystals were grown under a variety of experimental conditions; generally, the best crystals were grown in 40-45% polyethylene glycol 4K, 0.005M CaOAc, 0.04M NaOAc. The pH optimum for crystal formation from the drop was 4.8-5.2. Crystals have also been grown using 0.005M PbOAc instead of calcium, however the calmodulin already had calcium bound. Crystals prepared under these conditions have been redissolved in buffer and analysed by fluorescence spectroscopy to ensure that peptide is bound to calmodulin, for method see section 4.1. Photographs of several CaM:P1-26 and CaM:P9-26 crystals were taken and two of these are shown in figure 4.6.5, the figure legend describes the experimental conditions used to produce these crystals.

4.6.6 Structural data and Interpretation

The diffraction pattern of complex of Ca_4CaM:P9-21 has been collected at 2.2Å resolution, (data not shown). The structure could not be solved using isomorphous replacement from existing CaM:sm-MLCK peptide or CaM:CaMKII peptide structures.

However, this does not necessarily imply that the conformation of the CaM:PFK peptide structure is significantly different, since even the CaM:CaMKII peptide complex structure could not be solved from the structurally similar CaM:sm-MLCK structure.

Consequently crystallization trials of CaM:P9-26 have been performed in the presence of the heavy metals Pb and Tb in order to solve the phase problem and produce a crystal structure of the complex.

Figure 4.6.5

Crystals grown of the Ca_4CaM:P1-26, (a) & Ca_4CaM:P9-21. (b) complexes. Crystals grown in 42% polyethylene glycol 4000, 0.005M CaOAc, 0.04 NaOAc, pH 5.1, 4°C. Protein and peptide concentration were 1.19mM and 2.14mM respectively.

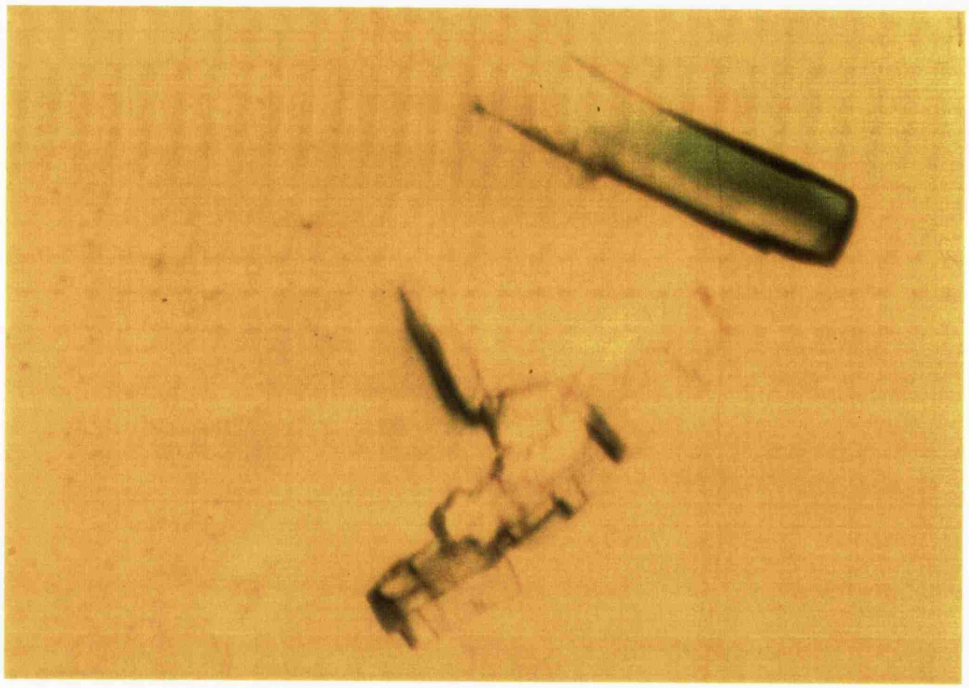

A

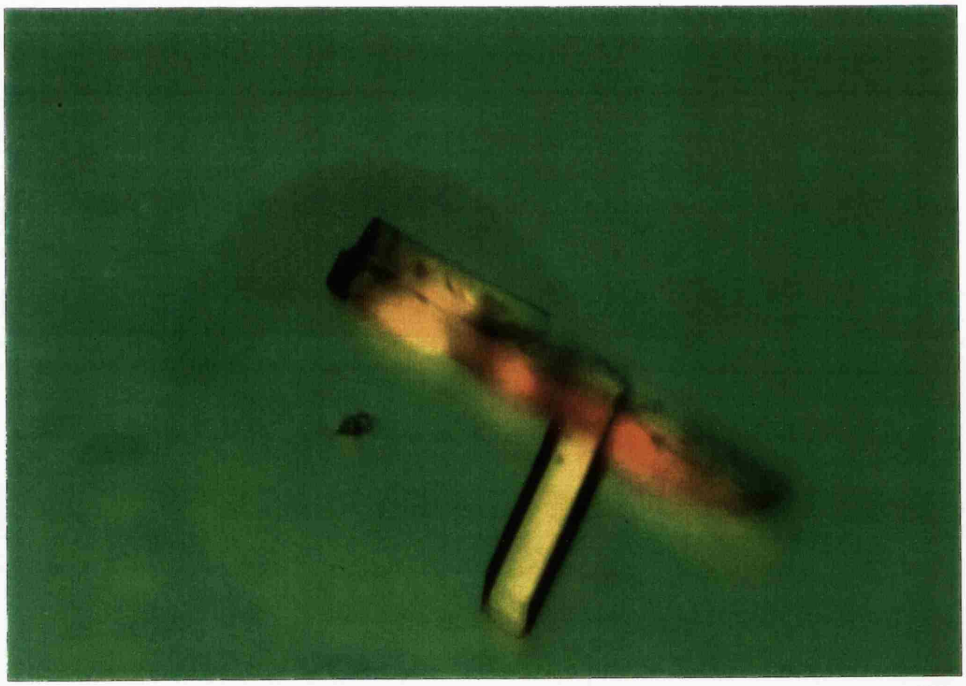

B

5

GENERAL DISCUSSION

5.1 General Discussion

The aim of this project is to study the interaction of PFK target sequences with calmodulin using a number of biophysical techniques. The experiments presented in this thesis establish that the mode of interaction of calmodulin with target peptides derived from PFK is significantly different from that observed in the CaM:peptide complexes whose structures have been solved. The most important experimental findings are summarized in table 5.1 for easy reference.

This discussion addresses the 3 main objectives of the work, which are to determine:

1. The conformation of the peptide in the calmodulin-PFK target peptide complex.
2. The importance of different residues and regions of the PFK target sequence in the interaction with calmodulin.
3. The calcium dependence of the calmodulin-PFK target peptide interaction, addressed by equilibrium calcium binding studies and stopped-flow kinetic studies of calcium dissociation.

5.2 CaM:PFK peptide complex

5.2.1 Stoichiometry of Interaction

Target enzymes or peptides derived from the calmodulin binding site of enzymes generally bind calmodulin with high affinity and 1:1 stoichiometry, (O'Neill & Degrado, 1990). There are examples of calmodulin binding targets for which the binding is contiguous eg: sk-MLCK, sm-MLCK, CaMKII and in contrast there also exist binding sites which are non-contiguous, eg: caldesmon (Marston et al., 1994).

There are cases known where calmodulin can apparently bind more than one peptide. For example, peptides derived from plasma membrane Ca pump, (Yazawa et al.,

Table 5.1

Summary of selected experimental findings.

Summary of Selected Experimental Findings

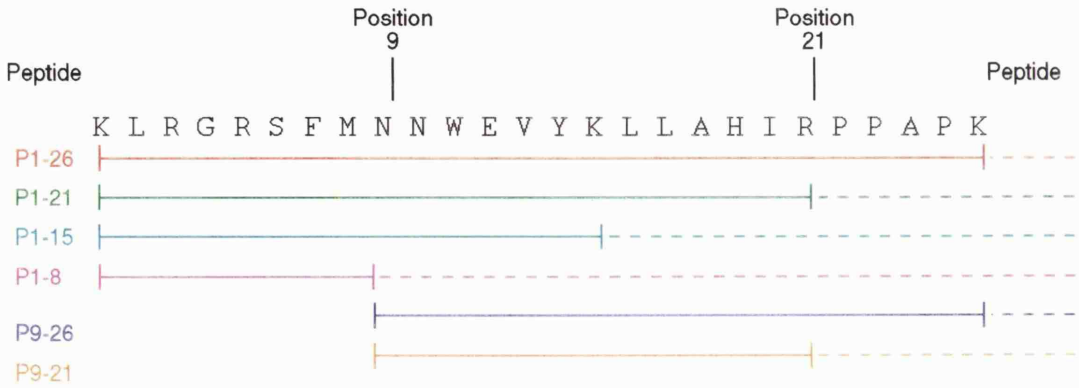

	K_d (CaM) M, pH7.0 Note 2	K_d(TR2C) M, pH7.0 Note 2	K_{SV} M^{-1} Note 3	# HEL Residues Note 4	CaM:Peptide Calcium Dissociation Rates (Q2) Note 5	CaM:Peptide Calcium Dissociation Rates (EGTA) Note 5
P1-26	2.8×10^{-10}	4.0×10^{-7}	1.14	6.7(8.6)	11(1.2)	13(1.6)
P1-21	1.0×10^{-9}	-	-	7.4(8.1)	-	-
P1-15	1.0×10^{-6}	-	3.44	-	-	-
P1-8	1.0×10^{-5}	-	-	-	-	-
P9-26	1.2×10^{-8}	1.0×10^{-7}	0.96	7.5(7.8)	18(2.4)	14(2.2)
P9-21	3.2×10^{-8}	1.0×10^{-7}	0.96	5.0(4.8)	16(2.6)	17(2.5)

Notes

1. Peptide length, name and biophysical parameters highlighted in specific colour.
2. K_d's calculated in section 4.1
3. K_{SV}'s calculated in section 4.1
4. Number of peptide helical residues are calculated for difference spectra as ([CaM : PFK peptide complex])-[CaM] value in brackets is for peptide in 50% TFE, see section 4.2 for calculations of α-Helicity
5. For quin-2 (Q2) and EGTA induced calcium dissociation two rates are given.The slower rate (k_S) is in brackets. NB: k_f and k_S for calcium dissociation from CaM are ≃700 and 6.9s^{-1} respectively, see section 4.4.

1992) and the wasp venom peptide mastoparan, (Linse et al., 1986; Ohki et al., 1991).

There are also examples of target proteins that can apparently bind multiple (2 or 3) calmodulin molecules simultaneously eg; synapsin I, (Goold & Baines, 1994) skeletal muscle ryanodine receptor, (Menegazzi et al., 1994) and phosphofructokinase, (Buschmeier et al., 1987).

Studies of the fragments generated by cyanogen bromide cleavage of phosphofructokinase demonstrate that two calmodulin binding sites exist, (Mayr & Heilmeyer, 1983). Analysis of these fragments show that the fragments have affinities of 11nM and 3μM (Buschmeier et al., 1987). Binding of calmodulin to the high affinity site, termed peptide M11 reduces enzyme activity, presumably through prevention of the conversion of inactive dimeric enzyme to active tetrameric form, (Buschmeier et al., 1987). Studies in this thesis have focused on the high affinity target binding site of rabbit muscle PFK, residues 371-397. The physiological significance of the lower affinity calmodulin binding site, termed M22, situated at the extreme C-terminus of the enzyme polypeptide is questionable given its low micromolar affinity, (Buschmeier et al., 1987).

In this work, a series of peptides derived from the rabbit muscle PFK sequence 371-397 have been studied using fluorescence and circular dichroism techniques. The peptides P9-21, P9-26, P1-21 and P1-26 all bind calmodulin in a calcium dependent manner with 1:1 stoichiometry and high affinity (K_d 3 x 10^{-8} to 3 x 10^{-10}M), see table 4.1.2.

5.2.2 Conformation of CaM:PFKpep

The near-UV CD spectra of the PFK peptides (except P1-15, see later) in complex with calmodulin were similar, see figure 4.2.2a. The intense signals present at 280/295nm indicate that the tryptophan residue from the peptide is immobilized in the

same hydrophobic environment for peptides P1-26, P1-21, P9-26 and P9-21. This view was further supported by acrylamide quenching studies. Stern-Volmer quenching constants of 1.14, 0.958 and 0.96 M^{-1} for bound peptides P1-26, P9-26 and P9-21 respectively indicated that the tryptophan was buried to the same extent in the three complexes. For comparison the K_{sv} for Trp in free P9-21 was $9.13M^{-1}$, figure 4.1.5.

The near-UV CD difference spectra were used to obtain information about the environment of the aromatic residues in target peptides. The calmodulin bound target peptides of sk-MLCK and sm-MLCK have similar near-UV CD, consistent with the tryptophan of each peptide being in a very similar environment, as judged by the three dimensional structures, which show tryptophan to have hydrophobic contacts with CaM residues L105, M124, and M144 in the C-domain, (Ikura et al., 1992; Meador et al., 1992). By contrast, the near UV CD for PFK peptides P1-26, P1-21, P9-26 & P9-21 shows that the environment of the tryptophan of the bound PFK peptides is similar in all cases, indicating a consistent mode of interaction. However, this interaction is substantially different from that of Trp 4 in the MLCK peptides, see figure 4.2.2c.

The near-UV CD signal derives from the precise geometry of the chromophoric residues and from the electronic interaction with other side chains and polypeptide backbone. The magnitude of the CD signals (which can be + or -) indicates the degree of immobilisation, but precise structural information is not easily obtained. The identity of the well defined signals with peptide P1-26 etc is however a good indication that all interact in similar environments. Although this is different from the MLCK peptide complexes, the PFK peptide tryptophan clearly also interacts with the C-domain of calmodulin, as shown by experiments involving the isolated domain TR2C, see section 5.2.4 for discussion.

5.2.3 Conformation of the bound PFK peptide

The tendency for calmodulin target sequences to adopt α-helical conformation has been well recognized (Crivici & Ikura, 1995 for review). In these studies far-UV CD has been used to investigate the conformation of PFK peptides bound to calmodulin and their propensity to form α-helical structure in the helicogenic solvent, trifluoroethanol.

The PFK peptides exhibit little α-helical conformation in the calmodulin bound form (maximally 5-8 residues, see table 5.1) and there is a similar low helical propensity for the peptides in trifluroethanol (5-8 residues). The similar values of peptide α-helicity noted on binding CaM or with trifluoroethanol indicates that there is little change in calmodulin α-helicity when calmodulin interacts with the peptide.

The higher α-helicity of peptide P9-26 (7.4 residues in the CaM bound form) compared with P9-21 (5.1 residues) is surprising since residues 22-26 are Pro-Pro-Ala-Pro-Lys, see table 5.1. Proline has a low probability of occurence in alpha-helical structures particularly at the C-terminus, (Williamson, 1994). The additional Pro-Pro-Ala-Pro-Lys sequence at the C-terminus must terminate the helix but may stabilise α-helix formation in residues preceding the first proline residue ie: in the P9-21 sequence, assuming that residues 22-26 effectively "end-protect" the C-terminus of peptide P9-21. The effect of N-terminal acetylation and C-terminal amide end-protection of the WFF sequence has previously been demonstrated to have a small but significant effect in increasing peptide α-helicity, (Martin et al., unpublished data). The presence of prolines in calmodulin binding peptides is unusual because of the inability of proline stretches to form α-helix. Known instances where prolines are found within CaM target sequences are MARCKS protein, (Graff et al., 1991) and phosphorylase kinase, (Dasgupta et al., 1989) and in these sequences there exists a single proline, not a proline rich cluster as

for the PFK target sequence. The presence of proline residues can be accomodated in a predominantly α-helical peptide as demonstrated in NMR studies of the interaction of troponin-C with troponin-I peptides containing proline residues, (Campbell and Sykes, 1991; Campbell et al., 1992). In these cases cardiac and skeletal TnI peptides form a discontinuous amphiphilic α-helix with the helix distorted around two central proline residues. In these NMR studies it is shown that the central bend in the peptide functions to bring the residues on the hydrophobic face into closer proximity with each other, thereby forming a small hydrophobic pocket.

From the CD data it is not possible to deduce the conformation of residues 22-26 of the PFK peptide and whether this unique cluster is important in the function of the intact enzyme. There is in fact a putative phosphorylation site in the enzyme sequence at residue 30, just 5 residues from proline 25 at the C-terminus of the sequence, (Buschmeier et al., 1987). The proline cluster may therefore have a conformational role in providing a suitable enzyme phosphorylation environment.

The P1-26 peptide might have been expected to show closer similarity to the archetypal basic amphipathic α-helical peptide, (O'Neill & Degrado, 1990) than either the P9-21 or P9-26 peptides since the added region at the N-terminus is relatively rich in basic residues, although with different disposition compared to many other calmodulin binding targets. However, the far-UV CD shows that the additional residues 1-8 of P1-26 do not adopt α-helical secondary structure, despite the high affinity interaction of this peptide with calmodulin.

The program SEQSEE, (Wishart et al., 1994) was used by Dr W Findlay, (Concordia University) to perform secondary structure prediction on the PFK peptides, based on several algorithms. The helical propensities assessed by three different methods

are shown in figure 5.2.3. It appears at first sight that the methods predict different propensity for the target sequences. However, both the Momany and Holley Karplus methods share the prediction that residues -NWEVYKLLAHI- have some tendency to form α-helix. Although far-UV CD spectroscopy demonstrates that only 7.5 residues of peptide P9-26 are α-helical, this sequence was placed on a helical wheel to detect whether the helical portion had any amphiphilic character. Figure 5.2.3 shows that 3 hydrophobic residues (V13, L16, L17) cluster on one side of the PFK residue peptide (in fact opposite to W11) implying a degree of amphiphilicity involving maximally 2 to 3 turns of helix. Thus there is some supporting evidence for the ability of a limited part of the sequence to adopt an α-helical conformation.

5.2.4 Orientation of the Calmodulin:Target peptide complex

The structures of complexes formed between calmodulin and target peptides solved at present time (ie: CaM:sk-MLCKpep, (Ikura et al., 1992), CaM:sm-MLCKpep, (Meador et al., 1992), CaM:CaMKIIpep, (Meador et al., 1993)) indicate that orientation of calmodulin with respect to target peptide is the same. The C-domain of the protein makes predominant contacts with the peptide N-domain (in particular peptide tryptophan) and vice-versa, the only exception known to date is mellitin.

Assuming that intact wild-type calmodulin was essential for optimal interaction with the PFK target sequences, calcium-binding site mutants of calmodulin and the isolated C-domain of calmodulin were used as a strategy to determine the structural orientation of peptide with respect to protein.

Fluorescence studies demonstrate that the characteristic F/Fo of peptide P9-26 tryptophan becoming bound to calmodulin is also found for fragment TR2C, (section 4.1)

Figure 5.2.3

Secondary structure prediction of selected target sequences from the high affinity calmodulin binding region of phosphofructokinase. Algorithms used are Momany, (1977); Holley-Karplus, (1978); Garnier, Osguthorpe & Robson, (1978). Sequence NWEVYKLLAHI was predicted to have some α-helical propensity by Momany and Holley Karplus methods, therefore this sequence was placed on a helical wheel to assess the propensity of the putative helix to be amphipathic.

Peptide	Secondary struture prediction method	Residues with propensity to form α-helix are underlined in bold
P9-21	Momany	NNW*EVYKLLA*HIR
	Holley/Karplus	NN*WEVYKLLA*HIR
	G-O-R (see legend)	NNWEVYKL*LAHIR*
P9-26	Momany	NNW*EVYKLLAHI*RPPAPK
	Holley/Karplus	NN*WEVYKLLA*HIRPPAPK
	G-O-R	NNWEVYKLL*AHIRP*PAPK
P1-26	Momany	KLRGRSF*MNNWEVYKLLAHI*RPPAPK
	Holley/Karplus	KLRGRSFMN*NWEVYKLLA*HIRPPAPK
	G-O-R	KLRGRSFMNNWEVYKLL*AHIRP*PAPK

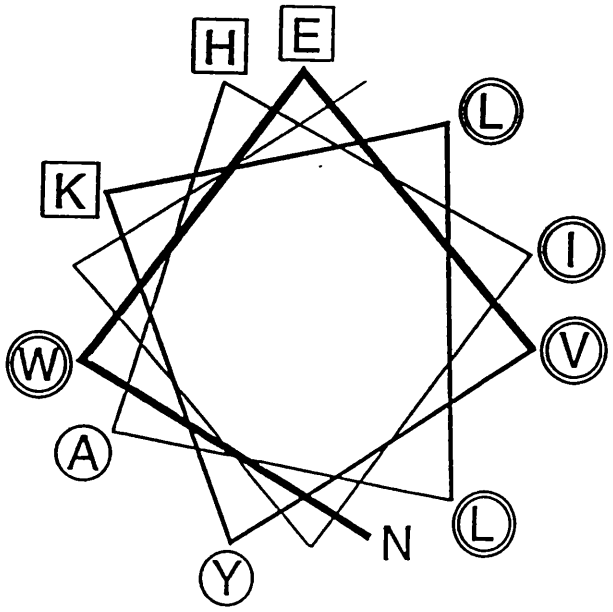

Polar

Hydrophobic

Very hydrophobic

though the affinity is significantly less. Near-UV CD properties of TR2C in complex with peptide P9-26 demonstrate that the spectrum characteristic of bound peptide is the same as that of intact calmodulin. These results indicate that the tryptophan interacts with the C-domain of calmodulin. In further support of this finding are the near-UV CD results of the interaction of calcium-binding site mutants of calmodulin with target peptide P9-26 which show that mutation in binding site 4 of the C-domain is far more detrimental to complex structure and affinity than the corresponding mutation in site 2 of the N-domain of calmodulin, (section 4.1 and figures 4.2.3 & 4.2.4).

Fluorescence studies demonstrate that the affinity of peptides P1-26, P9-26, and P9-21 with TR2C are reduced significantly compared with the interaction with intact calmodulin, table 4.1.4. Interestingly, despite the markedly stronger affinity of CaM:P1-26 (0.28nM) compared with CaM:P9-26 (11nM) and CaM:P9-21 (32nM), the TR2C:P1-26 affinity is similar to that of the corresponding TR2C:P9-26 and TR2C:P9-21 complexes. This suggests that the affinity for the interaction of P1-26 with TR2C can be accounted for by residues in the range of 9-21; further the strikingly increased affinity of P1-26 for intact CaM compared with TR2C is a strong indication that the first 8 residues of the target sequence interact at least in part with the N-domain of calmodulin. This is significantly different from the "classical" model where the C terminal portion of the peptide binds to CaM N-domain. It would appear to require the target sequence to fold back on itself, and this seems quite possible, since the first 8 residues have no rigid α-helical conformation and hence could presumably adopt this structure.

Steady-state fluorescence, and acrylamide quenching studies described earlier see section 4.1, for the interaction of calmodulin with peptide P1-15, indicate that the peptide tryptophan in this peptide is in a different environment from the other PFK peptides. This

peptide lacks residues 16-26, suggesting that residues following Trp11 have a defining role in determining the conformation of the bound peptide

5.3 Dissecting the role of specific peptide amino-acid residues involved in binding calmodulin.

Having established that the different lengths of PFK target sequence (with the exception of P1-15, see later) bound calmodulin in similar conformation by near-UV CD (see figure 4.2.2a) this made comparisons between affinity and conformation of the peptides in complex with calmodulin feasible. Table 4.1.2 lists the affinities determined for PFK target peptides in complex with wild-type calmodulin. Comparison of affinities of calmodulin for P1-26, P1-21, P9-26 and P9-21 (table 5.1) show that peptide P9-21 had lowest affinity for calmodulin (32nM), and this correlates with its relatively short length. It appears that this target peptide represents only part of the calmodulin binding domain of PFK. The affinity of peptide P9-26 for calmodulin is 3 fold higher than peptide P9-21, (11nM). The additional residues -Pro-Pro-Ala-Pro-Lys- therefore constitute some extra binding free energy for interaction. The P9-21 peptide is not end protected and so there is a negative carboxyl charge on the positively charged Arg21. The effect of adding residues 22-26 might therefore be simply associated with the removal of this negative charge, enhancing an electrostatic interaction with calmodulin.

The sequence of peptides P1-21 and P1-26 are more similar to the archetypal calmodulin binding sequence proposed by O'Neill and Degrado, (1990) since they contain a cluster of three basic residues within the first eight residues at positions 1, 3, and 5 of the N-terminus of the peptide. However, unlike the sequences from sk-MLCK or sm-MLCK (see figure 2.3a) it appears that the basic residue cluster is more distant from the

hydrophobic tryptophan residue in PFK as compared to the MLCK peptides in which the tryptophan of the peptide is situated within the basic sequence. Also for the MLCK peptides several N-terminal basic residues interact with residues on the N-domain of CaM, (eg; sk-MLCK peptide WFF residues R2, K5 & K6 interact with CaM N-domain). These residues are important in sk-MLCK target interaction since their removal greatly reduces the peptide affinity, (Blumenthal & Krebs, 1987). However the crystallographic B values of these basic residues are unusually high, (M Hirshberg, personal communication) suggesting either static or dynamic disorder. Thus it may be unwise to oversimplify the analogy between the N-terminal basic residues of the PFK sequence and the MLCK sequences since other evidence indicates a different mode of interaction with CaM for the PFK target.

Comparison of the affinities of P1-21 (1nM) and P1-26 (0.28nM) for calmodulin further demonstrate that the proline rich region (residues 22-26) is involved in interaction, table 4.1.2. Interestingly, the addition of the proline rich region to either peptide P9-21 (→ P9-26) or P1-21 (→ P1-26) increases the affinity by the same factor, approximately 3 fold. This is only a small effect, corresponding to an increase in free energy of binding of ~ 0.7kcal.

Conformational studies using fluorescence and near-UV CD described earlier on complexes of TR2C or of calcium-binding site mutants of calmodulin with various PFK peptides have demonstrated that the W11 of the peptide most probably interacts with the C-domain of the protein, (section 4.1.4, 4.2.3 & 4.2.4). Part at least of the following C-terminal residues 12-26 were thought likely to make contact with the N-terminal domain of the protein. To test this hypothesis the peptide P1-15 was prepared. Since this peptide ends 4 residues after the Trp it was thought to have only 4 residues with which to span

the N-domain. This was anticipated to be insufficient for interaction. The spectroscopic properties of the CaM:P1-15 complex were examined to test whether this structural proposal was correct.

Steady state fluorescence studies demonstrate that peptide P1-15 (K_d = 1μM, λ_{max}= 338nm) has approximately 100 -1000 fold weaker affinity for calmodulin relative to complexes of the other PFK peptides which are extended to residue 21 or 26, see table 4.1.2. Acrylamide quenching specifically demonstrates that the tryptophan is far more solvent exposed in a different environment compared with the trytophan of peptides P1-26, P1-21, P9-26 and P9-21, and the K_{sv} for CaM:P1-15 of 3.44M^{-1} approaches the value of 9.7M^{-1} for fully exposed tryptophan in the PFK target peptide, this may be a consequence of the C-terminal portion of the peptide preceding residue 16 not binding to the N-domain of calmodulin. The near-UV CD of CaM:P1-15 is quite different to that of CaM in complex with P1-26, P1-21, P9-26 or P9-21. Peptide P1-21 is only 6 residues longer yet has an affinity of 1 nanomolar indicating an important effect of residues 16-21 of which 4 are hydrophobic and two are basic.

5.3.1 The role of hydrophobic interactions in CaM:PFKpep complexes

The basis of the ability of CaM to interact with a diversity of structures has been attributed to 1) calcium induced exposure of hydrophobic residues in N- and C-domains and 2) the flexibility of the central linker region (expansion joint) allowing CaM to accomodate hydrophobic peptides of different length, (Meador et al., 1993). Since the hydrophobic surface patches on the 2 domains of CaM are rich in methionine it has been suggested that this "sticky" surface may consequently not place high demands on the specificity of interaction. Consistent with this, the conservative substitution of tryptophan

to phenylalanine in a sk-MLCK target peptide has little effect on affinity of the target peptide for calmodulin (K_d 0.2nM → 0.7nM, Findlay et al., 1995). By contrast sm-MLCK enzyme activation is impaired by more than 20 fold when the corresponding Trp at position 800 is substituted by Phe, (Matsushima et al., 1994). Applying the same strategy to the PFK peptides, substitution of the tryptophan of peptide P9-26 by phenylalanine results in a 1000x loss in affinity (K_d 11nM → 10μM). In fact hydrophobicity should be conserved in this substitution since Phe is ranked even more hydrophobic than Trp, (Eisenberg et al., 1984). One cannot exclude also that the reduction in affinity may be a structural consequence, since tryptophan is larger than phenylalanine being a conjugated two aromatic ring system, hence the contacts of the phenylalanine with the hydrophobic region in calmodulin may not be as great.

Like the tryptophan of either the sm- or sk-MLCK target, the tryptophan of the PFK peptide interacts with calmodulin C-domain and therefore might constitute a similar peptide anchoring role, though near-UV CD spectra suggest a different environment for the bound tryptophan of PFK peptides (previously discussed in section 5.2) compared with the bound Trp of the sk-MLCK and sm-MLCK peptides.

Using the available coordinates of the NMR solution structure of CaM:sk-MLCK peptide, (Ikura et al., 1992) a molecular model of binding was presented by Afshar et al., (1994). Afshar and coworkers note that the binding surface is formed by residues from both N- and C-domains. It displays a groove with 4 deep pockets which can accomodate hydrophobic peptide residues at relative positions 4 & 8 in pocket A; 11 in pocket B; 13 in pocket C; 14 & 17 in pocket D. Pocket A is derived from the C-domain whilst pockets B, C and D are derived from residues of the N-domain. Assuming the same polarity of binding and the correspondence of Trp11 of the PFK peptide with position 4, then the

hydrophobic residues which would fit this mode of binding would be Ala18 in pocket B, Ile20 in pocket C and ignoring Pro22, Pro23 one would find Ala24 in pocket D. Alignment of the PFK peptide to fit this model of binding appears possible for residues 11-21 assuming this stretch of residues is helical then the helical wheel model (figure 5.2.3) would place residues Ala18 and Ile20 in interaction with the N-domain. In addition Leu16 and Leu17 would correspond to residues I9 and I10 of sk-MLCK peptide which are seen in the NMR structure to interact predominantly with the N-domain: Thus although the potential helical region of PFK residues 1-26 is relatively short, it appears that key residues Trp11 and hydrophobic residues in the sequence 16 to 20 could provide simultaneous interactions with C- and N-domains respectively.

5.3.2 The role of charge interactions in CaM:PFKpep complexes

Despite the usual predominance of hydrophobic interactions in CaM:peptide interactions it has been demonstrated using analogues of the synthetic peptide Ac-W K K L L K L L K K L L K L L K K L L K L- that electrostatic interactions contribute to binding and stability of complex formation, (O'Neill & Degrado, 1990). In 0.15M NaCl at pH 7.0, the peptide containing only Trp, Lys and Leu binds calmodulin with a dissociation constant of 0.4nM (13.0kcal [54.6kJ]mol^{-1}) while the corresponding peptide in which all the Lys residues have been changed to neutral Gln residues binds with a dissociation constant of 10nM (11.0kcal [46.2kJ]mol^{-1}), ($\Delta G = -RTln(1/K_d)$. In this particular example about 15% (54.6-46.2/54.6) of the total binding energy is contributed by electrostatic interactions.

Fluorescence studies on the PFK target sequence over the pH range 2.0-13.0, show that there are three distinct pH sensitive fluorescence processes in the peptide which

may be attributed to protonation of carboxyl groups, protonation of histidine and ionization of tyrosine to tyrosinate at alkaline pH. These results do not appear to relate to the progressively weaker binding of target sequence P9-21 to calmodulin from pH 7.0 up to pH 9.0. Increases in affinity of calmodulin for P9-21 between pH 7.0 and 5.0 can be explained partially by the protonation of peptide histidine, with a pK_a of 6.

The interaction between whole PFK and calmodulin is pH sensitive over the range pH5.0-8.0 also, (Bazaes and Kemp, 1990; Shearwin and Masters, 1990), it may perhaps follow that the pH dependent protonation of histidine may account in part for this relationship. Alternatively pH dependent changes in conformation seen in the near-UV CD of the PFK peptides in complex with calmodulin (but not for CaM alone) over the pH range 5.0 to 8.0 may account for the pH sensitivity of intact PFK enzyme activity.

5.4 Calcium binding studies of calmodulin in complex with PFK target peptides

It is well established that the interaction of CaM with many target enzymes and proteins is calcium dependent and this accounts for the role of CaM in converting the changes in intracellular [Ca] into processes of enzyme activation regulation. In the model systems studied the calcium dependent binding of a target constitutes a coupled system:

$$\begin{array}{ccccc} & +Ca & & +P & \\ CaM & \rightleftharpoons & CaCaM & \rightleftharpoons & CaCaM{:}P \end{array}$$

Because of this coupling the apparent affinity of calcium is necessarily increased in the presence of the peptide. The fundamental mechanism introduces the questions of the nature of the interaction of the target sequence with calmodulin and the possible role of intermediate species, with partial saturation by calcium of the calmodulin binding sites. Differences in these properties may determine the selectivity of CaM interaction with

different targets; which is central to its action as a calcium dependent intracellular regulator. The calcium dependence of interaction of CaM with PFK target peptides was therefore examined to address these questions.

5.4.1 Consequences of mutation in Ca^{2+} binding sites of calmodulin upon CaM:PFKpep complex affinity and conformation.

Studies by Findlay et al., (1995) using the calcium binding site mutants of CaM; B2Q, B2K, B4Q & B4K, (Maune et al., 1992a) suggest that the structural influence of a mutation in any of the four calcium binding site mutants can be largely reversed by binding of sk-MLCK target peptide WFF. Despite this structural consequence the affinities of the calmodulin mutants for target peptide were all markedly lower than that of the wild-type protein, especially in the case of the C-terminal domain calcium binding site mutants, (CaM:WFF K_d = 0.2nM, B4K:WFF K_d = 48nM). These distinguishably different effects of calcium-binding in different domains upon target binding raises the question of the specific role of calcium binding to calmodulin in interaction with target sequences. Furthermore, one should consider whether four binding sites need be filled for a functionally viable CaM:target peptide complex.

In the case of the PFK peptides it appears that the affinity of CaM:PFKpep complex formation is less affected by mutation in site 2 than site 4, (see table 4.1.4). Furthermore near-UV CD of P9-26 in complex with B2Q,B2K, B4Q or B4K shows that the conformation characteristic of the wild-type CaM:P9-26 interaction more closely resembles the interaction of P9-26 with the B2 mutants than the B4 mutants, (figure 4.2.3). These results suggest that the different affinities of PFK target sequences for calmodulin with calcium binding site mutation are consistent with the independent

function of each calmodulin domain in interaction with PFK target sequence.

5.4.2 The coupling of calcium and PFK peptide binding to CaM.

Direct studies of the binding of calcium to calmodulin and its tryptic fragments shows little evidence of cooperativity between the two domains of calmodulin, (Linse et al., 1991). The calcium affinities of the sites in the C-terminal domain are on average 6-fold higher than those of the sites in the N-domain. The different affinities of the calcium binding sites for calcium in the two domains of calmodulin is strongly conserved and may indicate specific roles for individual domains in target binding and enzyme activation.

The discussion of calcium binding to calmodulin and the effect of target peptides or enzymes on calcium binding by CaM is necessarily based on stoichiometric association constants rather than site association constants, which cannot be determined unambiguously in a complex system. For intact calmodulin in the presence of either peptide P1-26, P9-26 or P9-21 the stoichiometric binding constant K_1 is seen to increase significantly in the presence of target peptide. The stoichiometric calcium binding constants K_2, K_3 and K_4 were less affected by the presence of target peptide, although a small increase was noted in K_3. Consideration of the relationship between stoichiometric and site association constants for a simple model system (see table 4.3.1b, figure 4.3.1b & appendix 4) indicates that the effect of PFK target peptide on calcium binding by calmodulin is consistent with increased affinity of calcium in principally two calcium binding sites. This result is in marked contrast with previous studies with targets derived from calcineurin, (Stemmer & Klee, 1994); troponin I, (Keller et al., 1982); plasma membrane calcium pump, (Yazawa et al., 1992); and skeletal muscle

MLCK, (Bayley et al., 1996). In all these cases the target sequence influences calcium binding to calmodulin by increasing all four stoichiometric binding constants, consistent with increased calcium affinity in all 4 calcium binding sites. Thus the calcium binding properties of calmodulin in complex with PFK peptides may represent possibly for the first time an interaction which exhibits Ca^{2+} dependent target binding through binding of only 2 calcium ions to calmodulin.

Until now binding of targets by calmodulin usually involves the holo protein. For the examples given above (calcineurin, sk-MLCK etc) calcium binding in all sites acts to increase target affinity. However, the neural specific proteins neuromodulin and neurogranin are unusual in that they bind calmodulin more strongly in the absence of Ca^{2+}, (Andreasen et al., 1983; Baudier et al., 1991). Thus the corresponding enzyme activation by calmodulin is seen as either calcium dependent or calcium independent respectively. It thus appears likely that PFK enzyme inactivation by calmodulin may be calcium dependent with respect to binding of calcium to only 2 calcium binding sites in calmodulin, ie; it is partially calcium dependent.

Recently, Bayley et al., (1996) used short peptides based on the 18 residue WFF sequence from sk-MLCK to determine the influence of the first 10 residues of the sequence upon calcium binding characteristics of calmodulin. The rationale behind this investigation lies in the knowledge that the first 10 residues of sk-MLCK (WFF) makes the majority of its interactions with CaM C-domain. Hence, it was of interest to determine to what extent binding of this target increased the stoichiometric calcium binding constants for calmodulin. Interestingly, the calcium binding profile for WF10 indicates a marked shift in the binding of the first two calcium ions only. This suggests calcium binding within a domain of calmodulin can be independent of the target peptide

binding to the other domain. Comparison of the calcium saturation curves of Ca_4CaM:WF10 and Ca_4CaMPFK peptide complexes further support the existence of a CaM:PFK peptide target complex for which the calcium dependence of CaM:PFK peptide interaction can be achieved by saturation of 2 calcium binding sites to give a Ca_2CaM:PFK peptide complex.

In contrast to the findings of Bayley et al., (1996), Yazawa et al., (1992) note a biphasic saturation curve in calcium binding studies of a mixture of TR1C, TR2C and peptide C28W from the plasma membrane Ca^{2+}pump. The biphasic Ca^{2+} binding was explained by decreased binding of the N-domain sites. This suggests that interdomain effects possibly involving the central helix as a connection between domains are important in complexes of calmodulin with some target peptides. These considerations suggest that affinity of a target peptide for apo-calmodulin needs to be considered explicitly in any quantitative model for activation.

The calcium induced increase in affinity of a target for a particular peptide may, in principle, be calculated from dissociation constants for the peptide in the presence (K_d) and absence (K'_d) of calcium. However, because the latter value is not generally accessible experimentally, an estimate of the ratio of the dissociation constants (K'_d)/(K_d) may be obtained from the measured stoichiometric calcium binding constants determined from calmodulin alone (K_1,....,K_4) and for calmodulin in the presence of excess peptide (K_1',....,K_4') through the equation used in section 4.3, (Yazawa et al., 1992).

$$K'_d/K_d = (K_1'K_2'K_3'K_4')/(K_1K_2K_3K_4)$$

The K'_d/K_d values calculated for calmodulin in complex with P1-26, P9-26 or P9-

21 are 5054, 952 and 184 respectively, these are significantly lower than the value of 3.1 x 10^6 calculated for CaM in complex with peptide WFF from sk-MLCK, (Bayley et al., 1996) or the value of 6.2 x 10^8 for calmodulin in complex with peptide C28W from the calcium pump, (Yazawa et al., 1992). These results imply that the binding of calcium to calmodulin makes a contribution to the overall calcium induced increase in peptide affinity, although not as significant a contribution as peptides derived from sk-MLCK and calcium pump.

The calcium binding data for calmodulin in the presence of PFK peptides apparently presents something of a paradox. On the basis of the demonstrated nM affinity of PFK peptides with Ca_4CaM, the apparent enhancement of the calcium binding affinity of calmodulin in the presence of peptide is unexpectedly low. However, this is based on the assumed low affinity of the peptides for apo-CaM. In fact experiments to measure this affinity have been unsuccesful over the accessible range of 0-50μM peptide. Thus these arguments are not at present fully quantitative.

5.4.3 Characterizing the calcium binding sites of calmodulin influenced by target peptide.

Several studies presented provide evidence of the domain in which calcium binding is increased in the presence of PFK target peptide. It is far more difficult to assign effects of target peptide to actual calcium binding sites, since one cannot say to what extent cooperative effects prevail between sites and possibly between domains in the presence of target peptide, (Yazawa et al., 1992).

Steady-state studies of tryptophan fluorescence and circular dichroism using

calmodulin, TR2C, and calcium binding site mutants of calmodulin indicate that the tryptophan of the PFK target sequence makes its most important contacts with the C-terminal domain of CaM. Using the same techniques when apo-calmodulin and target peptide were titrated with calcium, 50-75% of the signal was completed on addition of one calcium ion to the solution at high (60μM) concentration, (see figure 4.3.2.1a note: 90-100% signal was complete upon addition of 2 calcium ions per calmodulin). Since the spectroscopic signal arises through changes in peptide tryptophan environment on binding the calmodulin C-domain, (see section 4.3) it is clear that the two high affinity calcium binding sites of calmodulin in the presence of PFK target peptide correspond to those sites in the C-domain.

5.4.4 Calcium dissociation mechanism for CaM:PFKpep.

Rates for the chelator induced dissociation of several calmodulin-peptide and calmodulin-enzyme complexes have been reported in the literature, In the presence of target enzymes or target peptides derived from the intact enzymes of smooth muscle MLCK, (Johnson & Snyder, 1993; Kasturi et al., 1993); skeletal muscle MLCK, (Johnson et al., 1981; Persechini et al., 1996; Brown et al., 1996); caldesmon & calponin, Kasturi et al., (1993) and nitric oxide synthase, Persechini et al., (1996) the calcium dissociation rate constants are all reduced. For some of these studies only one rate is reported, possibly as a consequence of the inability to resolve the two similar exponential processes.

Using a variety of probes including tyrosine 138 of *Drosophila* calmodulin, target peptide tryptophan, site-directed mutants of calmodulin incorporating tryptophan, and tryptic fragments of calmodulin, (Bayley et al., 1996; Martin et al., 1996 and Brown et

al., 1996) demonstrate that the distinctive calcium affinity differences noted in the domains of calmodulin are conserved in the presence of peptides from MLCK, the extent to which is strictly governed by the specific target sequence. This supports the analysis in terms of the effect of peptide binding on the calcium affinity of individual domains.

The interaction of calmodulin with a target peptide from sk-MLCK was recently studied by Persechini et al., (1996). Using Quin-2 stopped-flow kinetic studies, tryptic fragments of calmodulin were used to quantify the (chelator-induced) calcium dissociation from calmodulin domains in the absence and presence of peptide. The apparent calcium dissociation rate constants for 2 sites in the C-domain of calmodulin were reduced from 12.6-1.6s^{-1} and the rate constant for 1 site in the N-domain is reduced from $>1000s^{-1}$ to 1.6s^{-1}. Similar studies were performed by Brown et al., (1996) who note that the effect of peptide on calcium affinity is similar, however their estimation of the calmodulin calcium dissociation rate constants are slower (k_f = 700s^{-1}, k_s = 6.9s^{-1}).

In studies here, the PFK target peptide sequence acts to increase the affinity of calcium for calmodulin. The rate constants of calcium dissociation from calmodulin in the absence of target peptide are 700s^{-1} and 8.5s^{-1}, these rates each correspond to dissociation of 2 calcium ions. In the presence of target peptide P1-26 the dissociation rates are 11s^{-1} and 1.2s^{-1}. The amplitudes correspond to apparently 2 calcium ions for the fast phase and 2 calcium ions from the slow phase.

A mechanism of calcium dissociation from the Ca_4CaM:PFK peptide complex was proposed in section 4.4.3. The mechanism is based on the calcium dissociation mechanism described for Ca_4CaM in complex with sk-MLCK peptide or mastoparan, (Bayley et al., 1996; Brown et al., 1996). The model, figure 4.4.3 describes the biphasic dissociation of calcium from Ca_4CaM:PFK peptide consisting of a fast dissociation of 2

N-terminal calcium ions ($11\text{-}18s^{-1}$) followed by a slower dissociation of calcium ions ($1.2\text{-}2.8s^{-1}$). Under stopped-flow conditions used here (2μM CaM, 2.2μM PFK peptide) it was noted for a PFK peptide with a dissociation constant in the order of nM for calmodulin that at the beginning of the stopped flow experiment there should be negligible dissociation of target peptide from calcium saturated Ca_4CaM. However upon addition of EGTA the intermediate formed (Ca_2CaM:PFK peptide) by dissociation of the N-terminal calcium ions was, according to the affinity of Ca_2CaM for PFK peptide (Ca_2TR2C:P1-26, K_d = 400nM), in rapid equilibrium with a mixture of Ca_2CaM and free PFK target peptide. Hence, in the EGTA stopped-flow experiment which uses the release of target peptide from Ca_4CaM:PFK peptide complex to determine the rate of calcium dissociation, one apparently observes more complex kinetics than a simple 2 step calcium dissociation. This finding accounts for the observation of fluorescence amplitude arising from dissociation of calmodulin N-terminal calcium ions when the target peptide tryptophan interacts with CaM C-domain. Since, under experimental conditions the fast-phase is apparently coupled to a fast reversible equilibrium of Ca_2CaM:PFK peptide with Ca_2CaM and free PFK peptide. This model also explains the intriguing fact that the dissociation of the 2 C-domain calcium ions generally occurs with a rate of $1\text{-}2s^{-1}$. For two target peptides of different affinity for calmodulin one would expect the difference in peptide affinity to influence the calcium dissociation rate from the CaM:peptide complex. However, the dissociation of Ca_2CaM:PFK peptide to Ca_2CaM and free PFK peptide in effect provides two species from which calcium can dissociate. Therefore, the slow phase will reflect the sum of the dissociation of calcium from Ca_2CaM:PFK and Ca_2CaM. Consequently, under stopped-flow conditions the rates of calcium dissociation are only slightly slower for dissociation of Ca_2CaM:PFK compared with Ca_2CaM.

In support of the existence of a relaxation step, (Bayley et al., 1996 & Brown et al., 1996) suggest that the observed rates should be affected by [peptide]/[CaM] ratio. Experimentally, studies with calmodulin in complex with target peptides from sk-MLCK and mastoparan show that the fast phase can be reduced and eliminated by repeating experiments at raised [peptide]/[CaM] ratios. Furthermore, the slow phase is also significantly reduced, (Bayley et al., 1996 & Brown et al., 1996).

It is clear from equilibrium and kinetic calcium binding studies that the interaction of calmodulin with PFK target peptides can be approximated as an interaction of target sequence involving two functionally distinct domains. It is evident from determination of stoichiometric binding constants in the presence of PFK target peptide that binding of two calcium ions exert a larger increase in target peptide affinity than do the remaining two sites. This finding does not imply that the sites are rendundant in function, it probably implies that they play a different role in complex interaction. Such a concept has also been discussed in recent work, (Bayley et al., 1996; Ikura, 1996; Persechini et al., 1994, 1996).

5.5 Conclusions

Towards a working model of the CaM:PFK peptide complex

This work can be seen to address 2 questions: 1) How far can we define the specific interactions involved in the formation of the CaM:PFKpeptide complex? and 2) What is the role of calcium binding in complex formation of CaM with PFK target peptides?.

5.5.1 How does calmodulin interact with the PFK target sequence?

Figure 5.5.1 summarises the likely interactions of calmodulin domains with

peptide amino-acid residues and the probable occurrence of the α-helical conformation present when calmodulin complexes with peptide P1-26 from PFK. The limited α-helicity of the target sequence is likely to occur maximally through residues Asn10-Ile20. The first 8 N-terminal peptide residues have no α-helical structure and this allows the peptide to make contacts at least with the N-domain, possibly via electrostatic interactions involving basic residues in positions 1-5. It appears that Trp11 is the major interacting residue with the calmodulin C-domain, and the interaction shows considerable specificity for this residue. Some residues from position 16 onwards are important in maintaining the hydrophobic environment of the Trp, probably further enhanced as a result of the hydrophobic residues in the region 16-20 in binding the N-terminal domain. Irrespective of the precise extent of the helical region of the target sequence, such a set of interactions would allow a relative short sequence of the target sequence to interact with both domains, as is found for the central region of the MLCK and CaMKII sequences. This would possibly allow the formation of the more globular conformation, characteristic of several CaM:pep complexes, but involving a different peptide conformation and interaction mechanism. The proline rich segment of the sequence (residues 22-26) acts to increase affinity for calmodulin although this may be an indirect end-protection effect stabilizing α-helix or charged residues in the sequence preceding residue 21. The specific conformation of residues 22-26 remains undetermined. Such a model, deriving from different lines of evidence is necessarily speculative; it is hoped that related structural work with NMR and X-ray analysis will help to define the structure of the complex more precisely.

5.5.2 What is the role of calcium binding in complex formation of CaM with PFK target peptides?

Equilibrium Ca^{2+} binding studies indicate that the effect of PFK target peptide on calcium binding to calmodulin apparently increases only the first two stoichiometric calcium binding constants significantly, in contrast with sk-MLCK peptide WFF, for which increases in all four stoichiometric binding sites are observed. These studies, in addition with spectroscopic studies of calcium induced conformational changes in the CaM:pep complex, indicate that binding of PFK peptide target to a semi-saturated calmodulin is feasible. Indeed, the spectroscopic signal associated with CaM binding P1-26 target is essentally complete on addition of 1-2 calcium ions. This does not imply that the remaining two sites are necessarily redundant in function. It is possible that in complex formation of calmodulin with intact PFK that the N-terminal domain still has a function in producing the inactivating effect of calmodulin on PFK.

The problems of assigning equilibrium and kinetic calcium binding data to actual sites have been discussed. Calcium dissociation is biphasic for all the PFK target complexes with each phase corresponding to apparently two calcium ions. Equilibrium calcium binding experiments and calcium dissociation kinetic experiments illustrate that calcium is likely to bind to both C-domain sites initially followed by binding of 2 calcium ions to the N-domain. Target peptide apparently binds to a Ca_2CaM species with the tryptophan of the target peptide interacting with the calcium loaded C-domain of calmodulin. Therefore it appears that calcium dissociation mechanisms are similar for CaM:PFKpep and CaM:sk-MLCKpep complexes in that the intermediate Ca_2CaM:peptide complex is involved. However, the stoichiometric calcium binding constants indicate that calcium binding clearly has a different role in the two complexes.

5.6 Questions arising from this work

The results of this project to investigate the interaction of calmodulin with its target binding region on PFK confirm the principles that different targets show different modes of interaction with CaM, and this opens up new and wider possibilities for future work.

Although the calcium binding studies show the selective enhancement of 2 out of 4 calcium binding sites by the PFK peptide, the quantitative understanding of the coupling of this process to peptide binding is still incomplete. This selectivity effectively distinguishes the steps of CaM binding to a target and the subsequent enzyme activation and this question is clearly accessible to further experimental investigation. It would be of great interest to ascertain exactly how CaM interacts with the PFK target given the apparent partial calcium dependence of interaction. This is particularly important since calcium binding to sites within both N- and C-domains has previously been presumed necessary for the exposure of hydrophobic surfaces on CaM required in interaction of target peptides other than those derived from PFK, eg sm-MLCK, CaMKII, (Meador et al., 1992, 1993) & sk-MLCK, (Ikura et al., 1992). It is not clear from the results of this thesis whether interactions of the PFK peptide with the N-domain involve a calcium dependent exposure of hydrophobic groups. If so, it is not easy to explain the apparent lack of effect of peptide binding on the affinity of the calcium sites in this domain.

Clearly a high resolution CaM:PFK peptide complex structure will be extremely useful. Despite succesful crystallization trials the structure of the Ca_4CaM-PFK peptide complex remains unsolved at present time. In due course, this structure will hopefully be solved by collaborators at NIMR (M Hirshberg, G Dodson), and it will be of great interest to find how well the optical spectroscopy data here correlates with the crystal

structure. The three dimensional structure of the complex is also being determined by NMR techniques in another collaborative project at NIMR (R. Biekofsky, J Feeney) and will provide another independent assessment of the interaction.

Until now there has been no structure reported of calmodulin in complex with an intact enzyme. Despite the similarities in K_d values for intact enzymes and target peptides derived from the enzymes, it is likely that other parts of the enzyme structure influences the interaction of calmodulin. Indeed it is known that pseudosubstrate sites exist in CaM targets for example; sm-MLCK and CaMKII, (Soderling, 1990 for review). Only a full CaM:Enzyme complex structure can address this question unambiguously. It would therefore be useful to determine what the effect of the rest of the enzyme is on structure, interaction and function of the CaM:Enzyme interaction. Trials to crystallize mammalian PFK in the absence of calmodulin have been unsuccesful (G. Dodson, personal communication), this is possibly because of its large size. The structure of *Bacillus stearothermophilus* PFK has been solved but is half the size of mammalian PFK and has no calmodulin binding sequence, (calmodulin is a eukaryotic protein). Since calmodulin functions to dissociate naturally occuring tetrameric PFK to inactive dimers it may be feasible in terms of molecular weight to attempt to crystallize mammalian PFK dimer in the complex with CaM.

Studies in this thesis implied that the Ca^{2+} binding properties of calmodulin in complex with PFK target peptides may represent distinctive features by which calmodulin could selectively recognize PFK over its other (over 30) intracellular targets. It would therefore be informative to determine whether the unique features of the CaM:PFK peptide interaction are observed in interaction of calmodulin with intact PFK. Experimentally it would be difficult to follow the calcium binding properties of this

interaction since intact PFK is inhibited by free calcium, (Uyeda, 1979) but structure investigations of PFK enzyme with spectroscopically labelled CaM mutants appear feasible.

Figure 5.5.1

Schematic representation of the potential contacts between the terminal domains of calmodulin with peptide P1-26 from rabbit muscle phosphofructokinase based on experimental findings. The central helix of calmodulin has been omitted for purposes of clarity. The circled h and + symbols correspond to hydrophobic and positively charged amino-acids respectively. Justification of the interactions are detailed in section 5.5.1. The dotted lines correspond to potential interactions. The dotted line is heavy between W11 and the C-domain of calmodulin since this represents a residue specific interaction.

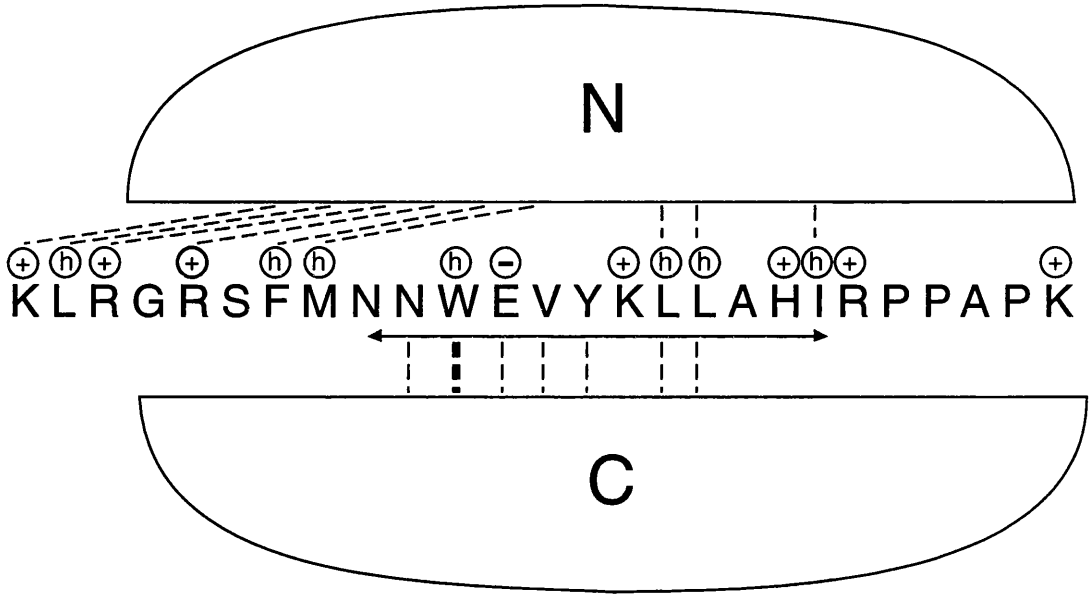
N
K L R G R S F M N N W E V Y K L L A H I R P P A P K
C

ACKNOWLEDGMENTS

I would like to express my gratitude to the following people:

First of all I should like to thank the Director, Sir John Skehel, and the Head of the Division, Dr David Trentham, for enabling me to work at the National Institute for Medical Research.

I wish to thank all my friends and colleagues who have worked with me in the laboratory, I address special thanks to:

My supervisor, Dr Peter Bayley, for his enthusiasm, encouragement and helpful criticism of this work.

Dr Stephen Martin to whom I am deeply grateful for introducing me to equilibrium and kinetic studies, for guidance, patience, and for use of his computer programs.

Pete Browne for preparation of mutant proteins and for loan of the PC which I am this very moment using.

Dr's Wendy Findlay, Sue Brown and Andreas Barth, post-doc's past and present for their useful discussions of literature and happy times.

Several people have been involved in aspects of the CaM:PFKpep project not directly related to this work:

I would like to thank Professor Guy Dodson for allowing me to work in his

crystallization laboratory. I would specifically like to thank Dr's Bing Xiao, Miri Hirshberg and Kim Henrick, who taught me the "spells" commonly used in crystallization and for collecting structural data, especially when it meant going to Daresbury!.
I would also like to thank Dr's Jim Feeney and Rolf Biekofsky for useful discussions and for sharing interesting PFK peptide NMR experimental data.

Special thanks to my very close caffeine buddies Treestan Rodriguez and Tasmilly (M) Khan, who have shared coffee breaks, tooth dilemmas and phone bills. Finally, I would like to say a big thankyou to Diane Macarthur a very special lady, who will be delighted to see her name printed in something other than the Daily Record.

REFERENCES

Afshar, A., Caves, L. S. D., Guimard, L., Hubbard, R. E., Calas, B., Grassy, G. & Haiech, J. (1994) Journal of Molecular Biology **244**, 544-71. Investigating the High Affinity and Low Sequence Specificity of Calmodulin Binding to its Targets.

Akke, M. & Forsen, S. (1990) Proteins: Structure, Function and Genetics **8**, 23-9. Protein stability and electrostatic interactions between solvent exposed charged side chains.

Allen, B. G. & Walsh, M. P. (1994) Tibs **19**, 42-8. The biochemical basis of the regulation of smooth muscle contraction.

Anagli, J., Hofmann, F., Quadroni, M., Vorherr, T. & Carafoli, E. (1995) Eur J Biochem **233**, 701-8. The calmodulin binding domain of the inducible (macrophage) nitric oxide synthase.

Apel, E.D., Byford, M.F., Au, D., Walsh, K.A. & Storm, D.R. (1990) Biochemistry **29**, 2330-36. Identification of the protein kinase C phosphorylation site in neuromodulin.

Armstrong, K. M. & Baldwin, R. L. (1993) Proc.Natl.Acad.Sci USA **90**, 11337-40. Charged histidine affects a-helix stability at all positions in the helix by interacting with the backbone charges.

Auzat, I. & Garel, J.-R. (1992) Protein science **1**, 254-8. pH dependence of the reverse reaction catalyzed by phosphofructokinase I from Escherichia coli: Implications for the role of Asp 127.

Babu, A., Rao, V. G., Su, H. & Gulati, J. (1993) Journal of Biological Chemistry **268**, 2619232-8. Critical minimum length of the central helix in troponin-C for the Ca2+ switch in muscle contraction.

Babu, Y. S., Bugg, C. E. & Cook, W. J. (1988) Journal of Molecular Biology **204**, 191-204. Structure of calmodulin refined at 2.2 Å resolution.

Babu, Y. S., Sack, J. S., Greenhough, T. J., Bugg, C. E., Means, A. R. & Cook, W. J. (1985) Nature **315**, 37-40. Three-dimensional structure of calmodulin.

Balendiran, K., Tan, Y., Sharma, R. K. & Murthy, K. H. M. (1995) Molecular and

Cellular Biochemistry **149; 150**, 127-30. Preliminary crystallization studies of calmodulin dependent protein phosphatase (calcineurin) from bovine brain.

Ban, C. & Ramakrishnan, B. (1994) Acta Crystallography **D50**, 50-63. Structure of the recombinant Paramecium tetraurelia calmodulin at 1.68A resolution.

Barbato, G., Ikura, M., Kay, L. E., Pastor, R. W. & Bax, A. (1990) Biochemistry **31**, 5269-78. Backbone dynamics of calmodulin studied by 15N relaxation using inverse detected two-dimensional NMR spectroscopy. The central helix is flexible.

Barden, J. A., Sehgal, P. & Kemp, B. E. (1996) Biochimica et Biophysica acta **1292**, 106-12. Structure of the pseudosubstrate recognition site of chicken smooth muscle myosin light chain kinase.

Baudier, J., Deloulme, J.C, Dorsaaelaer, A.V., Black, D. & Matthes, H.W.D. (1991) Journal of Biological Chemistry **266**, 229. Purification and characterization of a brain specific protein kinase C substrate, neurogranin.

Bayley, P. M. & Martin, S. R. (1992) Biochimica et Biophysica acta **1160**, 16-21. The α-helical content of calmodulin is increased by solution conditions favouring protein crystallization.

Bayley, P. M., Ahlstrom, P., Martin, S. R. & Forsen S. (1984) BBRC **120**, 185-91. The kinetics of calcium binding to calmodulin: Quin-2 and ANS stopped-flow fluorescence studies.

Bayley, P.M., Findlay, W.A. & Martin, S.R. (1996) Protein Science **5**, 1215-28. Target recognition by calmodulin: Dissecting the kinetics and affinity of interaction using short peptide sequences.

Bazaes, S. E. & Kemp, R. G. (1990) Metabolic Brain Disease **5**, 3. Resistance of Brain Phosphofructo-1-kinase to pH Dependent Inhibition.

Beckingham, K. (1991) Journal of Biological Chemistry **266**, 6027-30. Use of site-directed mutagenesis in the individual calcium-binding sites of calmodulin to examine calcium-induced conformational changes.

Bevington, P. R. (1969) Data Reduction and Error Analysis for the Physical Sciences,

McGraw-Hill, New York.

Blackshear, P.J., Verghese, G.M., Johnson, J.D., Haupt, D.M. & Stumpo, D.J. (1992) Journal of Biological Chemistry **267**, 13540-47. Characteristics of the F52 protein, a MARCKS homologue.

Blumenthal, D. K. & Stull, J. T. (1980) Biochemistry **19**, 5608-14. Activation of skeletal muscle myosin light chain kinase by calcium and calmodulin.

Blumenthal, D. K. & Stull, J. T. (1982) Biochemistry **21**, 2386-91. Effects of pH, Ionic Strength, and Temperature on Activation by Calmodulin and Catalytic Activity of Myosin Light Chain Kinase.

Blumenthal, D.K., Takio, K., Edelmann, A.M., Charbonneau, H., Titani, K., Walsh, K.A. & Krebs., (1985) Proc. Natl. Acad. Sci. U.S.A. **82**, 3187-91.

Blumenthal, D.K. & Krebs, E.G. (1987) Methods Enzymol **139**, 115-45. Preparation and properties of the calmodulin binding domain of skeletal muscle myosin light chain kinase.

Blumenthal, D. K. (1993) Molecular and Cellular Biochemistry **127**, 45-50. Development and characterization of fluorescently labeled myosin light chain kinase calmodulin-binding domain peptides.

Bray, D. (1995) Nature **376**, 307-12. Protein molecules as computational elements in living cells.

Brzeska, H., Venyamino, S.V., Grabarek, Z. & Drabikowski, W. (1983) Biochem Biophys Res Commun **153**, 169-173. Comparative studies of thermostability of calmodulin, skeletal muscle troponin-C and their tryptic fragments.

Buschmeier, B., Meyer, H. E. & Mayr, G. (1987) Journal of Biological Chemistry **262**, 9454-62. Characterization of the calmodulin binding sites of rabbit muscle phosphofructokinase and comparison with known calmodulin binding domains.

Cachia, P.J., Gariepy, J. & Hodges, R.S. (1985) Structural studies on calmodulin and troponin-C. In "Calmodulin antagonists and cellular physiology" edited by H, Hidaka & D.J. Hartstone, 63-68. New York Academic.

Campbell, A. P. & Sykes, B. D. (1991) Journal of Molecular Biology **222**, 405-21. Interaction of troponin I and troponin C.

Campbell, A. P., Van Eyk, J. E., Hodges, R. S. & Sykes, B. D. (1992) Biochimica et Biophysica acta **1160**, 35-54. Interaction of troponin I and troponin C.

Cantor, C. R. & Schimmel, P. (1980) Biophysical Chemistry: Part II, Techniques for the Study of Biological Structure and Function, WH Freeman and Company, San Francisco.

Carafoli, E. (1995) Journal of hypertension **12**, 10s47-56. The signaling function of calcium and its regulation.

Carvalo-Alves, P. C., Freire, M. M., Barrabin, H. & Scofano, H. M. (1994) European Journal of Biochemistry **220**, 1029-36. Regulation of the erythrocyte Ca2+-ATPase at high pH.

Cave, A., Pages, M., Morin, P. & Dobson, C. (1979) Biochimie **61**, 607-13. Conformational studies on muscular parvalbumins cooperative binding of calcium (II) to parvalbumins.

Chakrabartty, A., Kortemme, T., Padmanabhan, S. & Baldwin, R. L. (1993) Biochemistry **32**, 5560-5. Aromatic side-chain contribution to far-ultraviolet circular dichroism of helical peptides and its effect on measurement of helix propensities.

Chapman, E. R., Au, D., Alexander, K. A., Nicolson, T. A. & Storm, D. R. (1991) Journal of Biological Chemistry **266**, 1207-13. Characterization of the calmodulin binding domain of neuromodulin.

Chattopadhyaya, R., Meador, W. E., Means, A. R. & Quiocho, F. A. (1992) Journal of Molecular Biology **228**, 1177-92. Calmodulin structure refined at 1.7A resolution.

Chazin, W. J. (1995) Nature structural biology **2**, 9707-10. Releasing the calcium trigger.

Chen-Zion, M., Lilling, G. & Beitner, R. (1993) Biochemical medicine and metabolic biology **49**, 173-81. The dual effects of calcium on binding of the glycolytic enzymes PFK and aldolase to muscle cytoskeleton.

Chou, P. Y. & Fasman, G. D. (1978) Advances in enzymology **47**. Prediction of the

secondary structure of proteins from their amino acid sequence.

Clark, D. J., Hill, C. S., Martin, S. R. & Thomas, J. O. (1988) Embo **7**, 69-75. a-Helix in the carboxy-terminal domains of histones H1 and H5.

Clore, G. M., Bax, Ikura, M. & Gronenborn, A. M. (1993) Current opinion in structural biology **3**, 838-45. Structure of calmodulin-target peptide complexes.

Conti, M. A. & Aldstein, R. S. (1981) Journal of Biological Chemistry **256**, 73178-81. The relationship between calmodulin binding and phosphorylation of smooth muscle myosin kinase by the catalytic subunit of 3':5' cAMP-dependent protein kinase.

Cook, W. J., Walter, L. J. & Walter, M. R. (1994) Biochemistry **33**, 15259-65. Drug binding by calmodulin: Crystal structure of a calmodulin-trifluoroperazine complex.

Cornellussen, B., Holm, M., Waltersson, Y., Onions, J., Hallberg, B., Thornell, A. & Grundstrom, T. (1994) **Nature**, 760-4. Calcium/Calmodulin inhibition of basic helix-loop-helix transcription factor domains.

Craig, T. A., Watterson, D. M., Prendergast, F. G., Haiech, J. & Roberts, D. M. (1987) Journal of Biological Chemistry **262**, 3278-84. Site specific Mutagenesis of the a-helices of Calmodulin.

Creamer, T. P. & Rose, G. D. (1994) Proteins: Structure, Function and Genetics **19**, 85-97. Alpha-helix propensities in peptides and proteins.

Crivici, A. & Ikura, M. (1995) Annual Review of Biophys and Biomol Struc **24**, 85-116. Molecular and Structural Basis of Target Recognition by Calmodulin.

Crosbie, R. H., Chalovich, J. M. & Reisler, E. (1995) Journal of muscle research and cell motility **16**, 509-18. Flexation of caldesmon: effect of conformation on the properties of caldesmon.

Crouch, T.H. & Klee, C.B. (1980) Biochemistry **19**, 3692-98. Positive cooperativity of calcium binding to bovine brain calmodulin.

Cruzalegui, F. H., Kapiloff, M. S., Morfin, J. P., Kemp, B. E., Rosenfeld, M. G. & Means, A. R. (1992) Proc Natl Acad Sci **89**, 12127-31. Regulation of intrasteric

inhibition of the multifunctional calcium/calmodulin-dependent protein kinase.

Dalgarno, D.C., Klevit, R.E., Levine, B.A., Scott, G.M.M., Williams, R.J.P., Gergely, J., Grabarek, Z., Leavis, P.L., Grand, R.J.A. & Drabikowski, W. (1984) Biochim Biophys Acta **791**, 164-172. The nature of trifluoroperazine binding sites on calmodulin and troponin-C.

Dasgupta, M., Honeycutt, T. & Blumenthal, D.K. (1989) Journal of Biological Chemistry **264**, 17156-62. The gamma subunit of skeletal muscle myosin light chain kinase contains two non-contiguous domains that act in concert to bind calmodulin.

Davis, T. (1992) Cell **71**, 557-64. What's new with Calcium?

Degrado, W. F. (1988) Advances in Protein Chemistry **39**, 51-125. Design of peptides and proteins.

Degrado, W. F., Erikson-Viitanen, S., Wolfe, H. R. & O'Neill, K. T. (1987) Proteins: Structure, Function and Genetics **2**, 20-33. Predicted Calmodulin-Binding Sequence in the z Subunit of Phosphorylase b Kinase.

Drabikowski, W., Kuznicki, J. & Grabarek, Z. (1977) Biochim Biophys Acta **485**, 124-133. Tryptic fragments of calmodulin.

Ehrhardt, M. R., Urbauer, J. L. & Wand, A. J. (1995) Biochemistry **34**, 92731-8. The energetics and dynamics of molecular recognition by calmodulin.

Eisenberg, D., Schwartz, E., Kamarny, M. & Wall, R. (1984) J. Mol. Biol **179**, 125-42.

Evans, P. R., Farrants, G. W. & Hudson, P. J. (1981) Phil Trans R Soc Lond B **293**, 53-62. Phosphofructokinase: structure and control.

Evans, P. R. & Hudson, P. J. (1979) Nature **279**, 500-5. Structure and control of PFK from *Bacillus starothermophilus*.

Farah, C. S., Miyamoto, C. A., Ramos, C. H. I., Da Silva, A. C., Quaggio, R. B., Fujimori, K., Smillie, L. B. & Reinach, F. C. (1994) Journal of Biological Chemistry **269**, 75230-40. Structural and regulatory functions of the NH2- and COOH- terminal

regions of skeletal muscle troponin I.

Farrar, Y. J. K., Lukas, T. J., Craig, T. A., Watterson, D. M. & Carlson, G. M. (1993) Journal of Biological Chemistry **268**, 64120-5. Features of calmodulin that are important in the activation of the catalytic subunit of phosphorylase kinase.

Findlay, W. A., Martin, S. R., Beckingham, K. & Bayley, P. M. (1995) Biochemistry **34**, 2087-94. Recovery of Native Structure by Calcium Binding Site Mutants of Calmodulin upon Binding of sk-MLCK Target Peptides.

Findlay, W. A., Shaw, G. S. & Sykes, B. D. (1992) Current opinion in structural biology **2**, 57-60. Metal ion binding by proteins.

Findlay, W. A. & Sykes, B. D. (1993) Biochemistry **32**, 3461-7. 1H-NMR Resonance assignments, Secondary Structure, and Global Fold of the TR1C fragment of Turkey Skeletal Troponin-C in the Calcium-Free State.

Finn, B.E., Evenas, J., Drakenberg, T., Waltho., J.P, et al. (1993) FEBS Letts, **336**, 368-74. The structure of apo-calmodulin. A ^{1}H NMR examination of the carboxy-terminal domain.

Finn, B. E., Evenas, J., Draknberg, T., Waltho, J. P., Thulin, E. & Forsen, S. (1995) Nature structural biology **2**, 777-83. Calcium-induced structural changes and domain autonomy in calmodulin.

Fisher, P. J., Prendergast, F. G., Erhardt, M. R., Urbauer, J. L., Wand, A. J., Sedarous, S. S., McCormick, D. J. & Buckley, P. J. (1994) Nature **368**, 651-3. Calmodulin interacts with amphiphilic peptides composed of all D-amino acids.

Foe, L. G., Latshaw, S. P. & Kemp, R. (1983) Biochemistry **22**, 4601-6. Binding of Hexose bisphosphates to muscle phosphofructokinase.

Forsen, S., Vogel, H.J. & Drakenberg, T. (1986) Biophysical studies of calmodulin. in "Calcium and Cell Function" (R.H. Wasserman and C.S. Fullmer, eds.) 6, 113-57. Academic press, New York.

Foster, C. J., Johnston, S. A., Sunday, B. & Gaeta, F. C. A. (1984) . Potent peptide inhibitors of smooth muscle myosin light chain kinase: Mapping of the pseudosubstrate

and calmodulin binding domains.

Gagne, S. M., Tsuda, S., Li, M. X., Chandra, M., Smillie, L. B. & Sykes, B. D. (1994) Protein science **3**, 1961-74. Quantification of the calcium-induced secondary structural changes in the regulatory domain of troponin-C.

Gagne, S. M., Tsuda, S., Li, M. X., Smillie, L. B. & Sykes, B. D. (1995) Nature structural biology **2**, 9784-9. Structures of the troponin-C regulatory domains in the apo- and calcium-saturated states.

Gangola, P. & Pant, H. C. (1983) Biophysical and Biochemical Research Communications **111**, 1301-5. Temperature dependent conformational changes in calmodulin.

Gao, Z. H., Krebs, J., VanBerkum, M. F. A., Tang, W. J., Maune, J. F., Means, A. R., Stull, J. T. & Beckingham, K. (1993) Journal of Biological Chemistry **268**, 2720096-104. Activation of four enzymes by two series of calmodulin mutants with point mutations in individual calcium binding sites.

Garone, L. & Steiner, R. F. (1990) Archives of Biochemistry and Biophysics **276**, 112-8. The interaction of calmodulin with the C-terminal M5 peptide of MLCK.

Geiser, J. R., van Tuinen, D., Brockerhoff, S. E., Neff, M. M. & Davis, T. N. (1991) Cell **65**, 949-59. Can calmodulin function without binding calcium?.

George, S. E., Su, Z., Fan, D. & Means, A. R. (1993) Journal of Biological Chemistry **268**, 33. Calmodulin-cardiac troponin-C chimeras.

Gerendasy, D. D., Herron, S. R., Jennings, P. A. & Sutcliffe, J. G. (1995) Journal of Biological Chemistry **270**, 126741-50. Calmodulin stabilizes an amphiphilic alpha-helix within RC3/Neurogranin and GAP-43/Neuromodulin only when Ca2+ is absent.

Gill, S. C. & von Hippel, P. H. (1989) Anal Biochemistry **182**, 319-26. Calculation of protein extinction coefficients from amino-acid sequence data.

Goold, R. & Baines, A.J. (1994) European Journal of Biochemistry **224**, 229-40. Evidence that two non-contiguous non-overlapping high affinity calmodulin binding sites are present in the head region of synapsin I.

Grabarek, Z., Grabarek, J., Leavis, P.C. & Gergely, J. (1983) Journal of Biological Chemistry **258**, 14098-102. Cooperative binding to the calcium-specific sites of troponin-C in regulated actin and actomyosin.

Graff, J.M., Rajan, R.R., Randall, R.R., Nairn, A.C. & Blackshear, P.J. (1991) Journal of Biological Chemistry **266**, 14390-97. Protein kinase C substrate and inhibitor characteristics of peptides derived from the myristoylated alanine-rich C kinase substrate (MARCKS) protein phosphorylation site domain.

Gregori, L., Gillevet, P.M., Doon, P. & Chau, V. (1985) Curr Top Cell Regul **27**, 447-454. Mechanisms of enzyme regulation by calmodulin and calcium.

Guimard, L., Afshar, M., Haiech, J. & Calas, B. (1994) Analytical Biochemistry **221**, 118-26. A protein/peptide assay using peptide-resin adduct: Application to the calmodulin/RS20 complex.

Haiech, J., Klee, C. B. & Demaille, J. G. (1981) Biochemistry **20**, 3890-7. Effects of Cations on Affinity of Calmodulin for Calcium: Ordered Binding of Calcium Ions Allows the Specific Activation of Calmodulin -Stimulated Enzymes.

Haiech, J., Kilhoffer, M.-C., Lukas, T. H., Craig, T. A., Roberts, D. M. & Watterson, D. M. (1987) Journal of Biological Chemistry **262**, 3278-84. Site specific mutagenesis of the ∝-helices of calmodulin.

Haiech, J., Kilhoffer, M.-C., Lukas, T. H., Craig, T. A., Roberts, D. M. & Watterson, D. M. (1991) Journal of Biological Chemistry **266**, 3427-31.

Heidorn, D.B. & Trewhella, J. (1988) Biochemistry **27**, 909-15. Comparison of the crystal structures of calmodulin and troponin-C.

Heidorn, D.B., Seeger, P.A., Rokop, S.E., Blumenthal, D.K., Means, A.R., Crepsi, H. & Trewhella, J. (1989) Biochemistry **28**, 6757-64. Changes in the structure of calmodulin induced by a peptide based on the calmodulin-binding domain of myosin light chain kinase.

Heidorn, D. B. & Trewhella, J. (1992) Mol Cell Biol **6**, 329-59. Low-resolution structural studies of proteins in solution.

Heilmeyer, L. M. G., Gerschinski, A. M., Meyer, H. E. & Jennissen, H. P. (1993) Molecular and Cellular Biochemistry **127; 128**, 19-30. Interaction sites on phosphorylase kinase for calmodulin.

Hidaka, H. & Ishikawa, T. (1992) Cell calcium **13**, 465-72. Molecular pharmacology of calmodulin pathways in the cell functions.

Hincke, M. T., McCubbin, W. D. & Kay, C. M. (1978) Eur J Biochem **56**, 384-95. Calcium-binding properties of cardiac and skeletal troponin-C as determined by circular dichroism and ultraviolet difference spectroscopy.

Houdusse, A. & Cohen, C. (1995) Proc Natl Acad Sci **92**, 10644-7. Target sequence recognition by the calmodulin superfamily: Implications from light chain binding to the regulatory domain of scallop myosin.

Huang, C. Y. F., Yuan, C. J., Blumenthal, D. K. & Graves, D. J. (1995) Journal of Biological Chemistry **270**, 7183-8. Identification of the substrate and pseudosubstrate binding sites of phosphorylase kinase gamma subunit.

Hulme, E. C. & Tipton, K. F. (1971) FEBS Letters **12**, 197-200. The dependence of PFK kinetics upon protein concentration.

Ikura, M., Hiraoki, T., Hikichi, K., Mikuni, T., Yasawa, M. & Yagi, K. (1983) Biochemistry **22**, 2568-2572. Nuclear Magnetic Resonance assignments of calmodulin in the calcium free state.

Ikura, M., Clore, G. M., Gronenborn, A. M., Zhu, G., Klee, C. B. & Bax, A. (1992) Science **256**, 632-8. Solution structure of a calmodulin target peptide complex by multidimensional nmr MLCK.

Ikura, M. (1996) Tibs **21**, 14-7. Calcium binding and conformational response in EF-hand proteins.

Jagannatha, G. S., Cook, P. F. & Harris, B. G. (1991) Journal of Biological Chemistry **266**, 148884-90. Effector induced conformational transitions in *Ascaris suum* phosphofructokinase.

James, P., Vorherr, T. & Carafoli, E. (1995) Tibs **20**, 38-42. Calmodulin-binding

domains: just two faced or multi faceted?.

Jasanoff, A. & Fersht, A. R. (1994) Biochemistry **33**, 2129-35. Quantitative determination of helical propensities from trifluoroethanol titration curves.

Johansson, C., Ullner, M. & Drakenberg, T. (1993) Biochemistry **32**, 8429-38. The solution structures of mutant calbindin D9K's as determined by NMR, show that the calcium-binding site can adopt different folds.

Johnson, J.D., & Snyder, C. (1993) Abstracts 11th IUPAB Congress, Budapest, B1.28, pp101.

Johnson, J. L. & Reinhart, G. D. (1994) Biochemistry **33**, 2635-43. Influence of MgADP on phosphofructokinase from Escherichia Coli, elucidation of coupling interactions with both substrates.

Johnson, J. D., Snyder C., Walsh, M. & Flynn M. (1996) JBC **271**, 761-67. Effects of myosin light chain kinase and peptides on Ca^{2+} exchange with the N- and C-terminal Ca^{2+} binding sites of calmodulin.

Juminaga, D., Albaugh, S. A. & Steiner, R. F. (1994) Journal of Biological Chemistry **269**, 31660-7. The interaction of calmodulin with regulatory peptides of phosphorylase kinase.

Kakalis, L. T., Kennedy, M., Sikkink, R., Rusnak, F. & Armitage, I. M. (1995) FEBS Letters **362**, 55-8. Characterization of the calcium-binding sites of calcineurin B.

Kao, M. C., French, B. A., Chang, S. H. & Ho, C. (1990) Proc Natl Sci Counc B ROC **14**, 269-74. The rabbit muscle phosphofructokinase gene: cDNA cloning and sequencing.

Kasturi, R., Vasulka, C. & Johnson, J. D. (1993) Journal of Biological Chemistry **268**, 117958-64. Ca2+, caldesmon, and myosin light chain kinase exchange with calmodulin.

Kataoka, M., Head, J.F., Vorherr, T., Krebs J, & Carafoli, E. (1991) Biochemistry **30**, 7247-51. Small angle X-ray scattering study of calmodulin bound to two peptides corresponding to parts of the calmodulin binding domain of the plasma membrane Ca^{2+} pump.

Kawasaki, H. & Kretsinger, R. H. (1994) Protein Profile **1** (4). Calcium-binding proteins 1: EF-Hands.

Keller, C.H., Olwin, B.D., Laporte, D.C. & Storm, D.R. (1982) Biochemistry **21**, 156-162. Determination of the free energy coupling for binding of calcium ions and troponin-I to calmodulin.

Kemp, B. E., Pearson, R. B., Guerriero, V., Bagchi, I. C. & Means, A. R. (1987) Journal of Biological Chemistry **262**, 62542-8. The calmodulin binding domain of chicken smooth muscle myosin light chain kinase contains a pseudosubstrate sequence.

Kemp, B. E. & Pearson, R. B. (1991) Biochimica et Biophysica acta **1094**, 67-76. Intrasteric regulation of protein kinases and phosphatases.

Kennelly, P. J., Starovasnik, M. A., Edelman, A. M. & Krebs, E. G. (1990) Journal of Biological Chemistry **265**, 3. Modulation of the stability of rabbit skeletal muscle myosin light chain kinase through the calmodulin binding domain.

Kholodenko, B. N. & Westerhoff, H. V. (1995) **Tibs**, 2052-4. The macroworld versus the microworld of biochemical regulation and control.

Kilhoffer, M.-C., Demaille, J. G. & Gerard, D. (1981) Biochemistry **20**, 4407-14. Tyrosine fluorescence of ram testis and octopus calmodulins. Effects of calcium, magnesium, and ionic strength.

Kilhoffer, M.-C., Kubina, M., Travers, F. & Haiech, J. (1992) Biochemistry **31**, 8098-106. Use of engineered proteins with internal tryptophan reporter groups and perturbation techniques to probe the mechanism of ligand-protein interactions: investigation of the mechanism of calcium binding to calmodulin.

Kilhoffer, M.-C., Roberts, D. M., Adibi, A. O., Watterson, D. M. & Haiech, J. (1988) Journal of Biological Chemistry **263**, 17021-9. Investigation of the mechanism of calcium binding to calmodulin.

Kilhoffer, M.-C., Roberts, D. M., Adibi, A. O., Watterson, D. M. & Haiech, J. (1989) Biochemistry **28**, 6086-92. Fluorescence characterisation of VU-9 calmodulin, and engineered calmodulin with one Trp in calcium binding domain III.

Kitajima, S., Sakakibrara, R. & Uyeda, K. (1984) Journal of Biological Chemistry **258**, 13292-8. Significance of phosphorylation of PFK.

Klee, C.B. (1977) Biochemistry **16**, 5. Conformational transition accompanying the binding of calcium to the protein activator of 3',5'-cyclic adenosine monophosphate phosphodiesterase.

Klee, C.B. & Vanaman, T.C. (1982) Adv Prot Chem **35**, 213-321. Calmodulin.

Klee, C.B. (1988) Mol Asp Cell Regul **5**, 35-56. Interaction of calmodulin with Ca^{2+} and target proteins.

Klevit, R.E., Dalgarno, D.C., Levine, B.A. & Williams, R.J.P. (1984) Eur J Biochem, **139**, 109-114.

Klevit, R. E., Blumenthal, D. K., Wemmer, D. E. & Krebs, E. G. (1985) Biochemistry **24**, 8152-7. Interaction of calmodulin and a calmodulin-binding peptide from myosin light chain kinase: Major spectral changes in both occur as the result of complex formation.

Kretsinger, R.H. & Nockolds, C.E.J. (1973) Journal of Biological Chemistry **248**, 3313-26. Carp muscle calcium binding protein.

Kretsinger, R. H. (1992) Science **258**, 50-1. Calmodulin and myosin light chain kinase: How helices are bent.

Kretsinger, R. H. (1992) Cell calcium **13**, 363-78. The linker of calmodulin: to helix or not to helix.

Kretsinger, R. H. (1996) Nature structural biology **3**, 112-5. EF-hands reach out.

Kretsinger, R. H., Rudnick, S. E. & Weissman, L. J. (1986) J Inorg Chem **28**, 289-302. Crystal structure of calmodulin.

Kuboniwa, H., Tjandra, N., Grzeski, S., Ren, H., Klee, C. B. & Bax, A. (1995) Nature structural biology **2**, 768-76. Solution structure of calcium-free calmodulin.

Kundrot, C. E. & Evans, P. R. (1991) Biochemistry **30**, 1478-84. Designing an allosterically locked PFK.

Lackowicz, J. R., Gryczynski, I., Laczko, G., Wiczk & Johnson, M. L. (1994) Protein science **3**, 628-737. Distribution of distances between the tryptophan and the N-terminal residue of melittin in its complex with calmodulin, troponin-C, and phospholipids.

Lad, P. M., Hill, D. E. & Hammes, G. G. (1973) Biochemistry **12**, 4303-9. Influence of allosteric ligands on the activity and aggregation of rabbit muscle phosphofructokinase.

Lan, J. & Steiner, R. F. (1991) Biochemical Journal **274**, 445-51. The interaction of troponin-C with phosphofructokinase.

Lanciotti, R. A. & Bender, P. K. (1995) European Journal of Biochemistry **230**, 139-45. The gamma subunit of phosphorylase kinase contains a pseudosubstrate sequence.

Li, M. X., Chandra, M., Pearlstone, J. R., Racher, K. L., Trigo-Gonzales, G., Borgford, T., Kay, C. M. & Smillie, L. B. (1994) Biochemistry **33**, 917-25. Properties of isolated recombinant N and C domains of chicken troponin-C.

Ling, K. H., Paetkau, V., Marcus, F. & Lardy, H. A. (1988) Carbohydrate metabolism Vol IX Academic press New, York. Phosphofructokinase.

Linse, S., Drakenberg, T. & Forsen, S. (1986) FEBS Letters **199**, 28-33. Mastoparan binding induces a structural change affecting both the N-terminal and C-terminal domains of calmodulin.

Linse, S., Brodin, P., Drakenberg, T., Thulin, E., Sellers, P., Elmden, K., Grunstrom, T. & Forsen, S. (1987) Biochemistry **26**, 6723-35. Structure-function relationships in EF-hand Ca2+-binding proteins. Protein engineering and biophysical studies of calbindin D9K.

Linse, S., Brodin, P., Johaasson C., Thulin E., Grundstorm T. & Forsen S. (1988) Nature **335**, 651-52. The role of protein surface charges in ion binding.

Linse, S., Helmersson, A., & Forsen S. (1991) JBC **266**, 8050-54. Calcium binding to calmodulin and its globular domains.

Linse, S., Bylsma, N. R., Drakenberg, T., Sellers, P., Forsen, S. & Thulin, E. (1994) Biochemistry **33**, 12478-86. A calbindin D9K mutant with reduced calcium affinity and enhanced cooperativity. Metal ion binding, stability, and structural studies.

Livnat, T., Chen-Zion, M. & Beitner, R. (1993) Biochemical medicine and metabolic biology **50**, 24-34. Stimulatory effect of epidermal growth factor on binding of glycolytic enzymes to muscle cytoskeleton and the antagonistic action of calmodulin inhibitors.

Lowenstein, C.J. & Snyder, S.H. (1992) Cell **70**, 705-08. Nitric oxide, a novel biologic messenger.

Luby-Phelps, K., Hori, M., Phelps, J.M. & Won, D. (1995) Journal of Biological Chemistry **270**, 21532-38. Calcium regulated dynamic compartmentalization of calmodulin in living smooth muscle cells.

Lukas, T. J., Burgess, W. H., Prendergast, F. G., Lau, W. & Watterson, D. M. (1986) Biochemistry **25**, 1458-64. Calmodulin binding domains: Characterization of a phosphorylation and calmodulin binding site from myosin light chain kinase.

Luther, M. A., Hesterberg, L. K. & Lee, J. C. (1985) Biochemistry **24**, 2463-70.

Malencik, D.A. & Anderson, S.R. (1982) Biochemistry **21**, 3481-89. Binding of simple peptides, hormones, and neurotransmitters by calmodulin.

Malencik, D. A. & Anderson, S. R. (1983) BBRC **114**, 150-6. High affinity binding of the mastoparans by calmodulin.

Malencik, D. A. & Anderson, S. R. (1995) BBRC, 149, 50. Binding of hormones and neuropeptides by calmodulin.

Malencik, D. A., Ausio, J., Byles, C. E., Modrell, B. & Anderson, S. R. (1989) Biochemistry **28**, 8227-33. Turkey gizzard caldesmon: Molecular weight determination and calmodulin binding studies.

Manalan, A.S., & Klee, C.B. (1987) Biochemistry **26**, 1382-1390.

Marston, S. B., Fraser, I. D. C., Huber, P. A. J., Pritchard, K., Gusev & Torok, K. (1994) Journal of Biological Chemistry **269**, 8134-9. Location of two contact sites between human smooth muscle caldesmon and Ca2+-calmodulin.

Martin, S. R., Andersson, A. A., Bayley, P. M., Drakenberg, T. & Forsen, S. (1985) European Journal of Biochemistry **151**, 543-50. Kinetics of calcium dissociation from

calmodulin and its tryptic fragments.

Martin, S. R. & Bayley, P. M. (1986) Biochem J. **238**, 485-90. The Effects of Ca2+ and Cd2+ on the secondary and tertiary structure of Bovine Testis Calmodulin.

Martin, S. R., Linse, S., Johansson, C., Bayley, P. M. & Forsen, S. (1990) Biochemistry **29**, 4188-93. Protein surface charges and Ca2+ binding to individual sites in calbindin D9K: Stopped-flow studies.

Martin, S. R., Maune, J. F., Beckingham, K. & Bayley, P. M. (1992) European Journal of Biochemistry **205**, 1107-14. Stopped-flow studies of calcium dissociation from calcium binding site mutants of *Drosophila melanogaster* calmodulin.

Martin, S.R., Bayley, P.M., Brown, S.E., Porumb, T., Zhang, M. & Ikura, M. (1996) Biochemistry **35**, 3508-17. Spectroscopic characterization of a high affinity calmodulin-target peptide hybrid molecule.

Matsushima, S., Huang, Y.-P., Dudas, C. V., Guerriero, V., Jr. & Hartshorne, D. J. (1994) bbrc **202**, 329-1336. Mutants of Smooth Muscle Myosin Light Chain Kinase at Tryptophan 800.

Maune, J. F., Klee, C. B. & Beckingham, K. (1992a) Journal of Biological Chemistry **267**, 5286-95. Ca2+ Binding and conformational Change in Two series of Point Mutations of the Individual Ca2+-binding sites of Calmodulin.

Maune, J. F., Beckingham, K., Martin, S. R. & Bayley, P. M. (1992b) Biochemistry **31**, 7779-86. Circular Dichroism Studies on Calcium Binding to Two Series of Ca^{2+} Binding Site Mutants of Drosophila melanogaster Calmodulin.

Mayr, G. W. (1984a) European Journal of Biochemistry **143**, 513-20. Interaction of calmodulin with muscle phosphofructokinase. Changes in the aggregation state, conformation and catalytic activity of the enzyme.

Mayr, G. W. (1984b) European Journal of Biochemistry **143**, 521-9. Interaction of calmodulin with muscle phosphofructokinase interplay with metabolic effectors of the enzyme under physiological conditions.

Mayr, G. W. (1987) Methods in Enzymology **139**, 745-63. Interaction of calmodulin

with phosphofructokinase:binding//studies and evaluation of enzymatic and physicochemical changes.

Mayr, G. W. & Heilmeyer, L. G. (1983) Biochemistry **22**, 4316-26. Shape and substructure of skeletal muscle myosin light chain.

Mayr, G. W. & Heilmeyer, L. G. (1983) FEBS Letters **159**, 51-7. Phosphofructokinase is a calmodulin binding protein.

McDowell, L., Sanyal, G. & Prendergast, F. G. (1985) Biochemistry **24**, 2979-84. Probable role of amphiphilicity in the binding of mastoparan to calmodulin.

McPherson, A. (1982) Preparation and analysis of protein crystals. **Chapter 4.** Crystallization

Meador, W. E., George, S. E., Means, A. R. & Quicho, F. A. (1995) Nature structural biology **2**, 943-5. X-ray analysis reveals conformational adaptation of the linker in functional calmodulin mutants.

Meador, W. E., Means, A. R. & Quicho, F. A. (1992) Science **257**, 1251-5. Target enzyme recognition by calmodulin : 2.4 A structure of a calmodulin peptide complex : MLCK.

Meador, W. E., Means, A. R. & Quiocho, F. A. (1993) Science **262**, 1718-21. Modulation of calmodulin plasticity in molecular recognition on the basis of X-ray structures.

Means, A. R. (1994) FEBS Letters **347**, 1-4. Calcium, calmodulin and cell cycle regulation

Means, A. R., Bagchi, I. C., VanBerkum, M. F. A. & Kemp, B. E. (1991) in Regulation of smooth muscle contraction, Plenum Press, New York.

Means, A. R., VanBerkum, M. F. A., Bagchi, I. C., Ping-Lu, K. & Rasmussen, C. D. (1991) Pharmac Ther **50**, 255-70. Regulatory functions of calmodulin.

Medvedeva, M. V., Bushueva, T. L., Shirinsky, V. P., Lukas, T. J., Watterson, D. M. & Gusev, N. B. (1995) FEBS Letters **360**, 89-92. Interaction of smooth muscle

caldesmon with calmodulin mutants.

Menegazzi, P., Yreves, S., Guerrini, R., et al. (1994) Biochemistry **33**, 9078-84. Identification and characterization of three calmodulin binding sites of the skeletal muscle ryanodine receptor.

Michelson, S. & Schulman, H. (1994) Journal of theoretical biology **171**, 281-90. CaM Kinase: A model for its activation and dynamics.

Milos, M., Schaer, J.-J., Comte, M. & Cox, J. A. (1986) Biochemistry **25**, 6279-87. Calcium-proton and calcium-magnesium antagonism in calmodulin: Microcalorimetric and potentiometric analyses.

Minowa, O. & Yagi, K. (1984) J. Biochem, (Tokyo) 96 1175-1182. Calcium binding to tryptic fragments of calmodulin.

Molnar, A., Liliom, K., Orosz, F., Vertessy, B. G. & Ovadi, J. (1995) European Journal of Pharmacology **291**, 73-82. Anti-calmodulin potency of indol alkaloids in *in-vitro* systems.

Mukherjea, P. & Beckingham, K. (1993) Biochemistry and molecular biology international **29**, 3555-63. Calcium binding site mutants of calmodulin adopt abnormal conformations in complexes with model target peptides.

Najib, M. A., Harkins, P. C., Fox, R. O., Anderson, K. & Patton, C. (1995) Proteins: Structure, Function and Genetics **21**, 354-7. Crystallization and preliminary X-ray investigation of the recombinant *Trypsanoma brucei* rhodesiense calmodulin.

Novack, J.P., Charbonneau, H., Bentley, J.K., Walsh, K.A. & Beavo, J.A. (1991) Biochemistry **30**, 7940-51. Sequence comparison of the 63-, 61-, and 59-kDa calmodulin-dependent cyclic nucleotide phosphodiesterases.

Ohki, S-Y., Yazawa, M, Yagi K. & Hikichi K. (1991) J Biochem (Tokyo) **110**, 737-42. Mastoparan binding induces Ca^{2+} transfer between two globular domains of calmodulin. A ^{1}H NMR study.

Ohki, S., Iwamoto, U., Aimoto, S., Yazawa, M. & Hikichi, K. (1993) Journal of Biological Chemistry **268**, 1712388-92. Magnesium inhibits formation of 4Ca2+-

calmodulin-enzyme complex at lower Ca2+ concentration.

Oldenburg, D. J., Gross, M. K., Wong, C. S. & Storm, D. R. (1992) Biochemistry **31**, 8884. High affinity calmodulin binding is required for the rapid entry of Bordetella pertussis adenylyl cyclase into neuroblastoma cells.

Olwin, B.R. & Storm, D.T. (1985) Biochemistry **24**, 8081-8086. Calcium binding to complexes of calmodulin and calmodulin binding proteins.

O'Neill, K. T. & Degrado, W. F. (1990) Tibs **15**, 59-64. How calmodulin binds its targets: sequence dependent recognition of basic amphipathic alpha-helices.

O'Neill, K. T., Wolfe, H. R., Erickson-Viitanen, S. & Degrado, W. F. (1987) Fluorescence properties of calmodulin binding peptides reflect alpha-helical periodicity.

Orosz, F., Christova, T. Y. & Ovadi, J. (1988) Biochimica et Biophysica acta **957**, 293-300. Modulation of PFK action by macromolecular interactions, quantitative analysis of the PFK-aldolase-calmodulin system.

Orosz, F., Telegdi, M., Liliom, K., Solti, D., Korbonits, D. & Ovadi, J. (1990) Molecular pharmacology **38**, 910-6. Dissimilar mechanism of action of anticalmodulin drugs: Quantitative analysis.

Ovadi, J. (1988) Tibs **13 (Dec)**. Old pathway-new concept: control of glycolyisis by metabolite-modulated dynamic enzyme associations.

Ovadi, J. (1992) Current Topics in Cell Regulation **33**, 105-? Calmodulin and dynamics of interaction of cytosolic enzymes.

Ovadi, J. & Orosz, F. (1993) Current topics in cellular regulation **33**, 105-26. Calmodulin and dynamics of interactions of cytosolic enzymes.

Parmeggiani, A., et al. (1966) JBC **241**, 4625-47. Crystallization and properties of rabbit skeletal muscle phosphofructokinase.

Pavelich, M.J. & Hammes, G,G. (1973) Biochemistry, **12**, 1408-19.

Payne, M.E., Fong, Y.L., Ono, T., Colbran, R.J. & Kemp, B.E. (1988) Journal of

Biological Chemistry **263**, 7190-98. Calcium/calmodulin-dependent protein kinase II.

Pearlstone, J.R., Borgford, T., Chandra, M., Oikawa, K., Kay, C.M., Herzberg, O., Moult, J., Herklotz, A., Reinach, F.C. & Smillie, L.B. (1992) **31**, 6545-53. Construction and characterization of a spectral probe mutant of troponin-C: application to analyses of mutants with increased calcium affinity.

Pedigo, S. & Shea, M. A. (1995) Biochemistry **34**, 10676-89. Discontinuous equilibrium titrations of cooperative calcium binding to calmodulin monitored by 1-D 1H-Nuclear Magnetic Resonance Spectroscopy.

Perrino, B. A., Ng, L. Y. & Sorderling, T. R. (1991) . Calcium regulation of calcineurin phosphatase activity by its B subunit, calmodulin.

Persechini, A. & Kretsinger, R.H. (1988) Journal of Biological Chemistry **263**, 12175-78. The central helix of calmodulin functions as a flexible tether.

Persechini, A., McMillan, K. & Leakey, P. (1994) Journal of Biological Chemistry **269**, 16148-54. Activation of Myosin Light Chain Kinase, Nitric Oxide Synthase Activities by Calmodulin Fragments.

Persechini, A., White, H. D. & Gansz, K. J. (1996) Journal of Biological Chemistry **271**, 162-7. Different mechanisms for Ca2+ dissociation from complexes of calmodulin with nitric oxide synthase or myosin light chain kinase.

Poorman, R. A., Randolph, A., Kemp, R. G. & Heinrikson, R. L. (1984) Nature **309**, 467-9. Evolution of phosphfructokinase - gene duplication and creation of new effector sites.

Popescu, A. I. & Craescu, C. T. (1993) Romanian J. Biophys **3**, 295-16. Secondary structure prediction of the calmodulin binding domains pertaining to target proteins.

Racker, E. (1947) JBC **167**, 843-49. Spectrophotometric measurement of hexokinase and phosphohexokinase activity.

Raghunathan, S., Chandross, R. J., Cheng, B. P., Persechini, A., Sobottka, S. E. & Kretsinger, R. H. (1993) Proc.Natl.Acad.Sci USA **90**, 6869-73. The linker of des-Glu84 calmodulin is bent.

Rao, S.T., Wu, S., Satyshur, K.A., Ling, K.Y, Kung, C. & Sundaralingam, M. (1993) Protein Science **2**, 436-47. Structure of *Paramecium tetraurelia* calmodulin at 1.8A resolution.

Rayment, I., Holden, H. M., Whittaker, M., Yohn, C. B., Lorenz, M., Holmes, K. C. & Milligan, R. A. (1993) Science **261**, 58-65. Structure of the actin-myosin complex and its implications for muscle contraction.

Rayment, I., Rypniewski, W. R., Scmidt-Base, K., Smith, R., Tomchick, D. R., Benning, M. M., Winkelman, D. A., Wesenberg, G. & Holden, H. M. (1993) Science **261**, 50-7. Three-Dimensional structure of myosin subfragment-1: A molecular motor.

Reid, R. E. & Procyshyn, R. M. (1995) Archives of Biochemistry and Biophysics **323**, 1115-9. Engineering magnesium selectivity in the helix loop helix calcium binding motif.

Roberts, D. & Kellett, G. L. (1979) Biochem J. **183**, 349-60. The kinetics of effector binding to PFK: The allosteric conformational transition induced by 1,Ne6-ethenoadenosine triphosphate.

Sacks, D. B. (1994) Biochimica et Biophysica acta **1206**, 120-8. Alteration of calmodulin-protein interactions by a monoclonal antibody to calmodulin.

Sacks, D. B., Mazus, B. & Joyal, J. L. (1995) Biochem J. **312**, 197-204. The activity of calmodulin is altered by phosphorylation: modulation of calmodulin function by the site of phosphate incorporation.

Schirmer, T. & Evans, P. R. (1990) Nature **343**. Structural basis of the allosteric behaviour of PFK.

Schmidt, H. H. H. W., Pollock, J. S., Nakane, M., Forstermann, U. & Murad, F. (1992) Cell calcium **13**, 427-34. Ca2+/Calmodulin-regulated nitric oxide synthases.

Scholtz, J. M. & Baldwin, R. L. (1992) Annu Rev Biophys. Biomol. Struct **21**, 95-118. The mechanism of alpha-helix formation by peptides.

Scholtz, J. M., Quian, H., Robbins, V. H., Stewart, J. M. & Baldwin, R. L. (1993) Biochemistry **32**, 9668-76. The energetics of ion pair and hydrogen-bonding interactions in a helical peptide.

Scholtz, J. M., Quian, H., York, E. J., Stewart, J. M. & Baldwin, R. L. (1991) Biopolymers **31**, 1463-70. Parameters of helix-coil transition theory for alanine-based peptides of varying chain length in water.

Schulman, H., Hanson, P. I. & Meyer, T. (1992) Cell calcium **13**, 401-11. Decoding calcium signals by multifunctional CaM Kinase.

Schulman, H. & Lou, L. L. (1989) Tibs **14**, 62-6. Multifunctional Ca2+/calmodulin - dependent protein kinase: domain structure and regulation.

Shearwin, K. & Masters, C. (1990) Biochemistry Int **22**, 735-40. The Binding of Glycolytic Enzymes to the Cytoskeleton: Influence of pH.

Sjolin, L. (1993) Drug design and discovery **9**, 261-76. 3D-structural elucidation of biologically important macromolecules.

Skelton, N. J., Kordel, J., Akke, M., Forsen, S. & Chazin, W. J. (1994) Nature structural biology **1**, 239-45. Signal transduction versus buffering activity in calcium binding proteins.

Slupsky, C. M., Shaw, G. S., Campbell, A. P. & Sykes, B. D. (1992) Protein science **1**, 1595-603. A 1H NMR study of a ternary peptide complex that mimics the interaction between troponin C and troponin I.

Smith, M. K., Colbran, R. J., Brickley, D. A. & Soderling, T. R. (1992) Journal of Biological Chemistry **267**, 1761-8. Functional Detrminants in the Autoinhibitory Domain of Calcium/Calmodulin-dependent Protein Kinase II: Role of His 282 and Multiple Basic Residues.

Sobieszek, A. (1992) Regulation of myosin light chain kinase: kinetic mechanism, autophosphorylation, and cooperative activation by Ca2+ and calmodulin.

Somlyo, A. P. & Somlyo, A. V. (1994) Nature **372**, 231-6. Signal transduction and regulation in smooth muscle.

Sorderling, T. R. (1990) Journal of Biological Chemistry **265**, 41823-6. Protein kinases: Regulation by autoinhibitory domains.

Sorderling, T. R. (1993) Molecular and Cellular Biochemistry **127; 128**, 93-101. Calcium/Calmodulin-dependent protein kinase II: role in learning and memory.

Sparrow, J. C. (1995) Nature **374**, 592. Flight and phosphorylation.

Starovasnik, M.A., Su, D-R, Beckingham, K. & Klevit, R.E. (1992) Prot Sci **1**, 245-253. A series of point mutations in calcium binding sites of calmodulin.

Stanfield, R. L. & Wilson, I. A. (1991) Current Biology, 103-13. Protein-peptide interactions.

Steiner, R. F., Albaugh, S. & Kilhoffer, M.-C. (1993) J Fluor **1**, 15-22. Distribution of separations between groups in an engineered calmodulin.

Stemmer, P. M. & Klee, C. B. (1994) Biochemistry **33**, 6859-66. Dual calcium ion regulation of calcineurin by calmodulin and calcineurin B.

Storrs, R. W., Truckses, D. & Wemmer, D. E. (1992) Biopolymers **32**, 1695-702. Helix propagation in trifluoroethanol solutions.

Strydnaka, N. C. J. & James, M. N. G. (1990) Proteins: Structure, Function and Genetics **7**, 234-48. Model for the interaction of amphiphilic helices with troponin-C and calmodulin.

Strydnaka, N. C. J. & James, M. N. G. (1991) Current opinion in structural biology **1**, 905-14. Towards an understanding of the effects of calcium on protein structure and function.

Su, Z., Fan, D. & George, S. E. (1994) Journal of Biological Chemistry **269**, 2416761-5. Role of domain 3 of calmodulin in activation of calmodulin stimulated phosphodiesterase and smooth muscle myosin light chain kinase.

Tanaka, T., Ames, J. B., Harvey, T. S., Stryer, L. & Ikura, M. (1996) Nature (in press). Sequestration of the membrane-targeting myristoyl group of recoverin in the calcium free state.

Tansey, M. G., Luby-Phelps, K., Kamm, K. E. & Stull, J. T. (1994) Journal of Biological Chemistry **269**, 13. Ca2+-dependent phosphorylation of myosin light chain

kinase decreases the Ca2+//sensitivity of light chain phosphorylation within smooth muscle cells.

Taylor, D.A., Sack, J.S., Maune J.F., Beckingham, K. & Quiocho, F.A. (1991) Journal of Biological Chemistry **266**, 21375-80. Structure of recombinant calmodulin from *Drosophila melanogaster* refined at 2.2 A resolution.

Teleman, O., Drakenberg, T., Forsen, S. & Thulin, E. (1983) Eur J Biochem **134**, 453-57. Calcium and cadmium binding to troponin-C. Evidence for cooperativity.

Thulin, E., Andersson, A., Drakenberg, T., Forsen, S. & Vogel, H.J. (1984) Biochemistry **23**, 1862-70. Metal ion and drug binding to proteolytic fragments of calmodulin: proteolytic, cadmium-113, and proton nuclear magnetic resonance studies.

Torok, K., Lane, A. N., Martin, S. R., Janot, J.-M. & Bayley, P. M. (1992) Biochemistry **31**, 3452-62. Effects of Calcium Binding on the Internal Dynamic properties of Bovine Brain Calmodulin, Studied by NMR and Optical Spectroscopy.

Torok, K. & Trentham, D. R. (1994) Biochemistry **33**, 12807-20. Mechanism of 2-chloro-(epsilo-amino-Lys75)-[6-[4-(N,N-diethylamino)phenyl]-1,3,5-triazin-4-yl] calmodulin interactions with smooth muscle myosin light chain kinase and derived peptides.

Torok, K. & Whitaker, M. (1994) Bioessays **16**, 4221-4. Taking a long hard look at calmodulin's warm embrace.

Trave, G., Lacombe, P. J., Pfuhl, M., Saraste, M. & Pastore, A. (1995) Embo **14**, 204922-31. Molecular mechanism of the calcium induced conformational change in the spectrin EF-hands.

Trewhella, J. (1992) Cell calcium **13**, 377-90. The solution structures of calmodulin and its complexes with synthetic peptides based on target enzyme binding domains.

Tsalkova, T. N. & Privalov, P. L. (1985) Journal of Molecular Biology **181**, 533-44. Thermodynamic study of domain organization in troponin-c and calmodulin.

Tsuji, T. & Kaiser, E. T. (1991) Proteins: Structure, Function and Genetics **9**, 12-22. Design and synthesis of the pseudo-EF hand in calbindin D9K: Effect of amino acid

substitutions in the alpha-helical regions.

Tsuruta, H. & Sano, T. (1990) Biophysical Chemistry **35**, 75-84. A fluorescence temperature-jump study on calcium-induced conformational changes in calmodulin.

Urbauer, J. U., Short, J. H., Dow, L. K. & Wand, A. J. (1995) Biochemistry **34**, 8099-109. Structural analysis of a novel interaction by calmodulin: High affinity binding of a peptide in the absence of calcium.

Uyeda, K. (1979) Adv Enzymol. **48**, 193-244.

Uyeda, T. Q. P. & Spudich, J. A. (1993) Science **262**, 1867-70. A functional recombinant myosin II lacking a regulatory light chain binding site.

Valatis, A. P., Foe, L. G., Kwiatkowska, D., Latshaw, S. P. & Kemp, R. G. (1989) Biochimica et Biophysica acta **995**, 187-94. The sites of phosphorylation of rabbit brain phosphofructokinase by cyclic AMP-dependent protein kinase.

Vandonselaar, M., Hickie, R. A., Quail, J. W. & Delbaere, L. T. J. (1994) Structural biology **1**, 11795-801. Trifluoroperazine-induced conformational change in Ca2+-Calmodulin.

Vorherr, T., James, P., Krebs, J., Enyedi, A., McCormick, D. J., Penniston, J. T. & Carafoli, E. (1990) Biochemistry **29**, 355-65. Interaction of calmodulin with the calmodulin binding domain of the plasma membrane Ca2+ pump.

Vorherr, T., Knopfel, L., Hofmann, F., Mollner, S., Pfeuffer, T. & Carafoli, E. (1993) Biochemistry **32**, 6081-89. The calmodulin binding domain of nitric oxide synthase and adenylyl cyclase.

Wang, C.-L. A. (1989) Biochemistry **28**, 4816-20. pH-Dependent Conformational Changes of Wheat Germ Calmodulin.

Weber, P. C., Lukas, T. J., Graig, T. A., Wilson, E., King, M. M., Kwiatkowski, A. P. & Watterson, D. M. (1989) Proteins: Structure, Function and Genetics **6**, 70-85. Computational and site-specific mutagenesis analyses of the asymmetric charge distribution on calmodulin.

Weggerhoff, J. & Wagner, G. (1992) Journal of crystal growth **122**, 351-4. Crystal growth of plant calmodulin.

Wendt, B., Hofmann, T., Martin, S. R., Bayley, P. M., Brodin, P., Grunstrom, T., Thulin, E., Linse, S. & Forsen, S. (1988) European Journal of Biochemistry **175**, 439-45. Effect of amino-acid substitutions and deletions on the thermal stability, the pH stability and unfolding by urea of bovine calbindin D9K.

Williamson, M. P. (1994) Biochemical Journal **297**, 249-60. The structure and function of proline-rich regions in proteins.

Wills, F. L., McCubbin, W. D., Gimona, M., Strasser, P. & Kay, C. M. (1994) Protein science **3**, 2311-21. Two domains of interaction with calcium binding proteins can be mapped using fragments of calponin.

Xu, J., Oshima, T. & Yoshida, M. (1990) Journal of Molecular Biology **215**, 597-606. Tetramer-Dimer conversion of PFK from Thermus thermophilus induced by its allosteric effectors.

Yagi, K., Yazawa, M., Ikura, M., & Hikichi, K. (1989) in Calcium Protein Signalling (Hidaka, H., Carafoli, E., Means, A.R., & Tanaka, T., Eds.) 147-154, Plenum Publishing Co., New York.

Yamanska, M.K., Saugstad, J.A., Hanson-Painton, O., McCarthy, B.J., & Tobin, S.L. (1987) Nucleic Acid Res **15**, 3335-48.

Yazawa, M., Ikura, M., Hikichi, K., Ying, L. and Yagi, K. (1987) Journal of Biological Chemistry **262**, 10951-54. Communications between two globular domains of calmodulin in the presence of mastoparan or caldesmon fragment. Ca^{2+} binding and ^{1}H NMR.

Yazawa, M., Vorherr, T., James, P., Carafoli, E. & Yagi, K. (1992) Biochemistry **31**, 3171-76. Binding of calcium by calmodulin: Influence of the calmodulin binding domain of the plasma membrane calcium pump.

Yuan, T., Mietzner, T. A., Montelaro, R. C. & Vogel, H. J. (1995) Biochemistry **34**, 10690-6. Characterization of the calmodulin binding domain of SIV transmembrane glycoprotein by NMR and CD spectroscopy.

Zhang, M., Tanaka, T. & Ikura, M. (1995) Nature structural biology **2**, 758-67. Calcium induced conformational transition revealed by the solution structure of apo calmodulin.

Zhang, M. & Vogel, H. J. (1993) Protein science **2**, 1931-7. A peptide analog of the calmodulin binding domain of myosin light chain kinase adopts an alpha helical structure in aqueous trifluoroethanol.

Zhang, M. & Vogel, H. J. (1994) Biochemistry **33**, 1163-71. The calmodulin binding domain of caldesmon binds to calmodulin in an alpha helical conformation.

Zhao, Z., Malencik, D. A. & Anderson, S. R. (1991) Biochemistry **30**, 2204-16. Protein-induced inactivation of phosphorylation of rabbit muscle PFK.

Zhong, L. & Johnson, C. (1992) Proc Natl Acad Sci **89**, 4462-5. Environment affects amino acid preference for secondary structure.

Zhou, N. E., Kay, C. M., Sykes, B. D. & Hodges, R. S. (1993) Biochemistry **32**, 6190-7. A single stranded amphipathic alpha-helix in aqueous solution: Design, structural characterization, and its application for determining alpha-helical propensities of amino-acids.

Zhu, X., Byrnes, M., Nelson, J. W. & Chang, S. H. (1995) Biochemistry **34**, 2560-5. Role of glycine 212 in the allosteric behaviour of PFK from *Bacillus stearothermophilus*.

Literature Added:

Andreasen, T. J., Leutje, C. W., Heideman, W. & Storm, D. R. (1983) Biochemistry **22**, 4615-18. Purification of a novel calmodulin binding protein from bovine cerebral cortex membranes.

Brown, S. E., Martin, S. R. & Bayley, P. M. (1996) Kinetics of calcium dissociation from calmodulin binding peptides. accepted for publication by JBC, September 1996.

Browne, J. P., Martin, S. R. & Bayley, P. M. (1997) The role of β-sheet interactions in domain stability and target recognition reactions of calmodulin. In preparation.

Wishart, D. S., Boyko, R. F., Willard, L. & Sykes, B.D. (1994) CABIOS, **2**, 121-32. SEQSEE: a comprehensive program suite for protein sequence analysis.

APPENDICES

Appendix 1

Equilibrium studies: Methods for the determination of dissociation constants.

Characterizing the molecular interaction of calmodulin with target sequences of phosphofructokinase requires the determination of the stoichiometry of the interaction and the associated binding constants. In these studies fluorescence spectroscopy was used to investigate the binding of calmodulin to phosphofructokinase target peptides.

Considerations in analyses of stoichiometry and equilibria

Figure A1 shows the theoretical binding curves for the reaction between protein P and Ligand L at a protein concentration of 10μM. The data are plotted as degree of saturation, ([PL]/[P_{TOT}]) against the ratio ([L_{TOT}]/[P_{TOT}]). Note:

When the affinity of the complex is low relative to the experimentally accesible concentration range the end-point is difficult to establish, consequently determination of the stoichiometry and association constant are difficult.

When the affinity of the complex is high relative to the experimentally accesible concentration range the end-point is well defined and stoichiometry is clearly established. However figure A1.1a indicates that above a limiting value of $\sim 5 \times 10^7$ for the association constant, all curves look the same within the experimental error and only a lower limit can be reported for the association constant.

Figure A1.1

(a) Theoretical binding curves for the reaction P + L ⇌ PL at 10μM concentration for reactions with affinity K_a 1 x 10^4 to 1 x 10^8.

(b) Titration of TR2C to P9-21 at 5μM. The ■ symbols represent experimental data, the solid curve is the non-linear least squares fit to the data and the two straight lines are assymptotes superimposed to display the titration if the binding was extremely tight, $K_a = 10^{12}M^{-1}$.

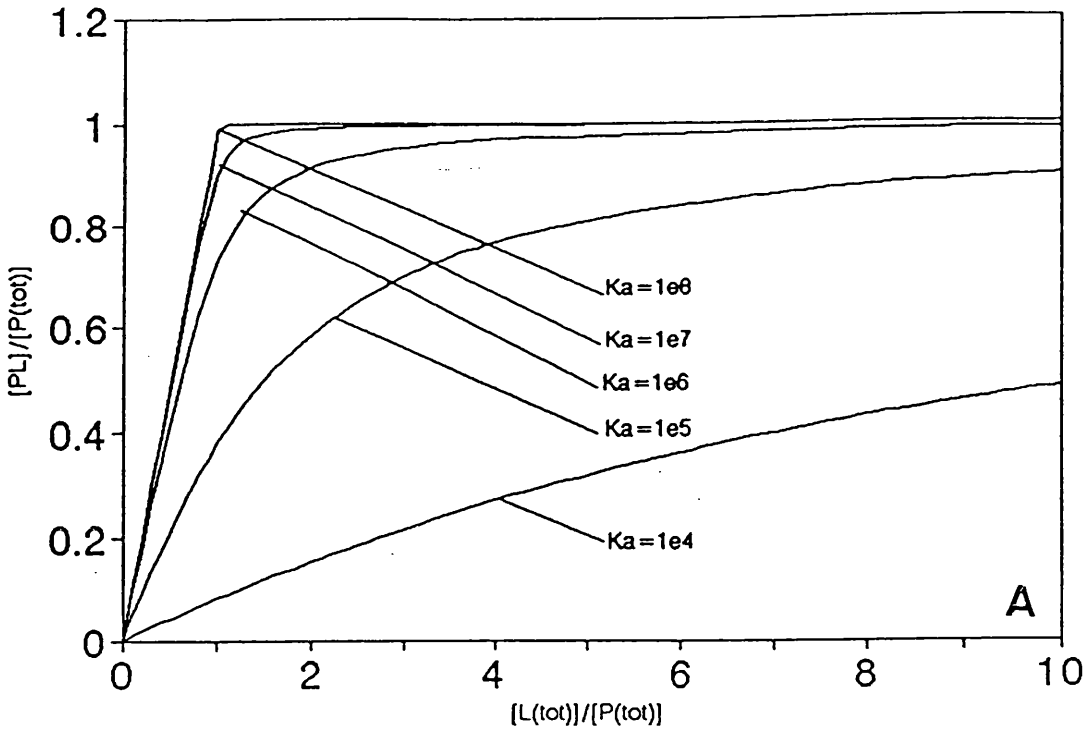
1.2
1
0.8
0.6
0.4
0.2
0
[PL]/[P(tot)]
Ka=1e8
Ka=1e7
Ka=1e6
Ka=1e5
Ka=1e4
A
0
2
4
6
8
10
[L(tot)]/[P(tot)]

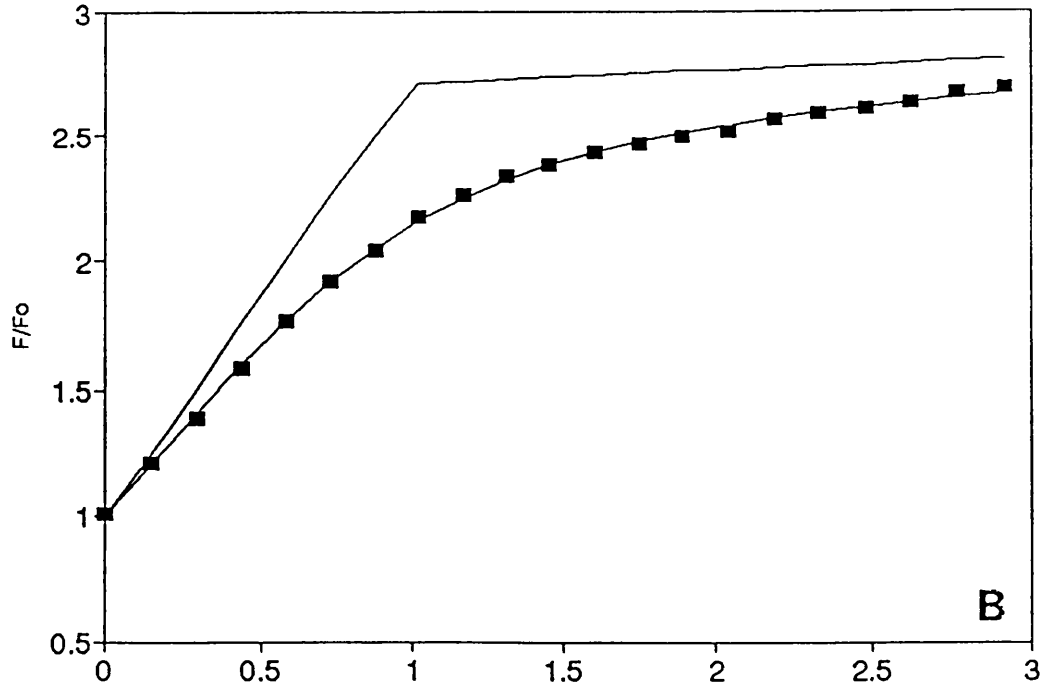
3
2.5
2
1.5
1
0.5
F/Fo
B
0
0.5
1
1.5
2
2.5
3
[TR2C]/[P9-21]

The concentration range accesible using tryptophan fluorescence spectroscopy is typically in the range 0.1-20μM. This range allowed accurate determination of stoichiometry and association constants for most of the peptides studied in this work. For complexes with very high affinity (K_d < nM) a simple competition method was used (see section A1.2). A typical titration of TR2C to P9-21 is shown in figure A1.1b, the points represent the experimental data, the solid curve is the fit to the data and the two straight lines are assymptotes superimposed to display the titration if the binding was very tight ($K_a = 10^{12}M^{-1}$.

A1.1 Determination of dissociation constants by direct methods.

The experiment involves titration of calmodulin into a solution of tryptophan containing peptide. The increase in fluorescence emission intensity (typically at 330nm) is a measure of the concentration of bound peptide (see section 3.2). At each titration point the total protein and peptide concentrations, and associated fluorescence signal are known. A probable error of 0.5-1.0% is placed on the signal and the data is fitted to a single dissociation constant using the non-linear least squares method described by Marquardt, (1963). The interaction of CaM with peptide P is described by the equation CaM + P ⇌ CaM:P. The dissociation constant in this reaction is given by:

$$K_d = [CaM][P]/[CaM:P]$$

The total concentrations of calmodulin and peptide are known and are given by:

$$[CaM_{TOT}] = [CaM] + [CaM:P]$$

$$[P_{TOT}] = [P] + [CaM:P]$$

Therefore K_d can also be defined as:

$$K_d = ([CaM_{TOT}] - [CaM:P]).([P_{TOT}] - [CaM:P])/[CaM:P]$$

Which may be expanded to give:

$$\mathbf{[CaM:P]^2 - [CaM:P].([CaM_{TOT}]+[P_{TOT}]+K_d) + [CaM_{TOT}].[P_{TOT}] = 0}$$

[CaM:P] is then obtained as the solution of the quadratic $ax^2 + bx + c = 0$, where $a = 1$, $b = ([CaM_{TOT}]+[P_{TOT}]+K_d)$, and $c = [CaM_{TOT}].[P_{TOT}]$.

There are 6 parameters in the fitting procedure; the dissociation constant, the specific fluorescence of the protein, peptide and protein:peptide complex, and factors to correct for errors in determination of concentrations of protein and peptide. χ^2 minimization is used to determine the best fit. χ^2 is defined as the weighted average of the individual variances of the fit (s^2) divided by the weighted average of the individual variances of the data (σ^2). Each parameter contributing to the fit is varied in turn and χ^2 is minimized with respect to each parameter independently. If the fitting function is a good approximation then the estimated variance (s^2) should agree well with the variance (σ^2) of the data and the value of χ^2 should be approximately 1. To illustrate how χ^2 varies with dissociation constant the Figure 4.1.1b illustrates the location of χ^2 minimum by allowing the parameters other than the K_d to vary.
This assumes no errors have been made in determination of these parameters. χ^2 is minimal over a very narrow range which is the dissociation constant.

A1.2 Determination of dissociation constants by competition methods.

As noted above, it is not possible to determine the K_d for high affinity interactions using a direct fluorimetric titration. Therefore a competition assay was used to study the interaction between CaM and those PFK target peptides which showed very high affinity binding. The method involves competition of two peptides, W and S, for calmodulin. Peptide W is a tryptophan containing PFK target peptide and peptide S is a spectroscopically silent peptide with known affinity. The spectroscopically silent peptide has no tyrosine or tryptophan residues and therefore contributes no fluorescence signal. The experiment involves titration of the spectroscopically silent peptide (S) to a complex of calmodulin and the tryptophan containing target (W). One can determine the unknown K_d for the Trp containing peptide providing that the K_d for the silent peptide is known and the concentration of the complex between CaM and Tryptophan containing peptide can be measured.

For two ligands W and S competing for the same site on CaM (C) one can write:

$$C + S \rightleftharpoons CS \qquad K_d(S) = [C][S]/[CS]$$

$$C + W \rightleftharpoons CW \qquad K_d(W) = [C][W]/[CW]$$

The ratio of the dissociation constants of peptides W and S for CaM given by:

$$K_d(W)/K_d(S) = ([W][CS]/([CW][S])$$

The experiment is performed under conditions where there is **no free calmodulin**

(ie: $W_T > C_T$). Therefore if X is the fraction of calmodulin with peptide W bound one can write:

$$[CW] = X.C_T$$

$$[CS] = C_T - X.C_T$$

$$[W] = W_T - X.C_T$$

$$[S] = S_T - C_T + X.C_T$$

Subscript T represents the total concentration of the species. For ease of representation the ratio of the dissociation constants ($K_d(W)/K_d(S)$) shall be described subsequently as R.

Therefore R is given by:

$$\mathbf{R = \{(W_T - X.C_T)(C_T - X.C_T)\}/\{(X.C_T)(S_T - C_T + X.C_T)\}}$$

X is given by the solution of a quadratic:

$$X = (-b + (b^2 - 4.a.c)^{1/2}/(2.a)$$

where $a = R.C_T - C_T$, $b = R.S_T - R.C_T + W_T + C_T$, $c = W_T$

The measured fluorescence is then fitted to the equation:

$$\mathbf{F_{\lambda em330nm} = X(F_o - F_{inf}) + F_{inf}}$$

F_o and F_{inf} are the fluorescence intensities observed at [S] = 0 and as [S] tends to

infinity. F_o, F_{inf} and R are treated as variable parameters in the fitting of data. χ^2 minimization is again used as a determination of best fit, see section A1.1.

Appendix 2

Determination of the stoichiometric calcium binding constants for calmodulin.

The calcium binding experiment is described in section 3.3. Briefly, the experiment involves competition between calmodulin and the chromophoric chelator BAPTA for calcium. The spectroscopic properties of BAPTA are altered when it binds calcium and this provides the signal which permits determination of binding constants.

The equilibria involved are described by the following equations. The symbols P, Ca, and B have been used to represent protein (or protein:peptide complex), calcium, and the chromophoric calcium chelator BAPTA respectively.

$P + Ca \rightleftharpoons PCa \qquad K_1 = [PCa]/([P].[Ca])$

$PCa + Ca \rightleftharpoons PCa_2 \qquad K_2 = [PCa_2]/([PCa].[Ca])$

$PCa_2 + Ca \rightleftharpoons PCa_3 \qquad K_3 = [PCa_3]/([PCa_2].[Ca])$

$PCa_3 + Ca \rightleftharpoons PCa_4 \qquad K_4 = [PCa_4]/([PCa_3].[Ca])$

$B + Ca \rightleftharpoons CaB \qquad K_{CaB} = [CaB]/([Ca].[B])$

The subscripts refer to the **number of sites filled**, without identifying the actual sites occupied. Thus $[PCa_3]$ is the sum of the concentrations of all calmodulin species with 3 sites occupied. These sites could be 1,2,3; 1,2,4; 1,3,4 or 2,3,4.

Total calcium $[Ca_{TOT}]$ is given by equation A2.2:

Equation A2.2: $[Ca_{TOT}] = [Ca] + [CaB] + [PCa] + 2[PCa_2] + 3[PCa_3] + 4[PCa_4]$

The method of analysis requires an expression from which free [Ca] can be obtained. This involves substitution for [CaB], [PCa] etc in equation A2.2.

$$K_{CaB} = [CaB]/([Ca].[B])$$

$$= [CaB]/\{[Ca].([B_{TOT}]-[CaB])\}$$

$$= [CaB]/([Ca].[B_{TOT}]-[Ca].[CaB])$$

$$[CaB] = K_{CaB}([Ca].[B_{TOT}]-[Ca].[CaB])$$

$$[CaB].(1 + K_{CaB}.[Ca]) = K_{CaB}[Ca].[B_{TOT}]$$

Hence:

Equation A2.3: $[CaB] = K_{CaB}.[Ca].[B_{TOT}]/(1 + K_{CaB}.[Ca])$

The ratio of {[Ca bound to CaM]/[Total CaM] can be described in terms of the concentration of free calcium, using the Adair equation, equation A2.4.

Equation A2.4:

[Ca bound to CaM]/[Total CaM] =

$$\{K_1.[Ca] + 2.K_1.K_2.[Ca]^2 + 3.K_1.K_2.K_3.[Ca]^3 + 4.K_1.K_2.K_3.K_4.[Ca]^4\} / \{1 + K_1.[Ca] + K_1.K_2.[Ca]^2 + K_1.K_2.K_3.[Ca]^3 + K_1.K_2.K_3.K_4.[Ca]^4\}$$

It can be seen from equation A2.2 that [Protein bound to calcium] = $[PCa] + 2[PCa_2]$

+ $3[PCa_3]$ + $4[PCa_4]$. Therefore one can write:

Equation A2.5:

$$([PCa] + 2[PCa_2] + 3[PCa_3] + 4[PCa_4]) = [P_{TOT}] .\{\{K_1.[Ca] + 2.K_1.K_2.[Ca]^2 + 3.K_1.K_2.K_3.[Ca]^3 + 4.K_1.K_2.K_3.K_4.[Ca]^4\} / \{ 1 + K_1.[Ca] + K_1.K_2.[Ca]^2 + K_1.K_2.K_3.[Ca]^3 + K_1.K_2.K_3.K_4.[Ca]^4\}\}$$

Substituting equation A2.5 and A2.3 in equation A2.2 gives:

Equation A2.6:

$$[Ca_{TOT}]-[Ca] - K_{CaB}.[Ca].[B_{TOT}]/(1 + K_{CaB}.[Ca]) - [P_{TOT}].\{K_1.[Ca] + 2.K_1.K_2.[Ca]^2 + 3.K_1.K_2.K_3.[Ca]^3 + 4.K_1.K_2.K_3.K_4.[Ca]^4\} / \{ 1 + K_1.[Ca] + K_1.K_2.[Ca]^2 + K_1.K_2.K_3.[Ca]^3 + K_1.K_2.K_3.K_4.[Ca]^4\} = 0.$$

This equation can be solved for [Ca] using a standard Newton-Raphson method.

Variation of absorbance with free calcium concentration

The absorbance A at any wavelength is given by:

$$A = \epsilon_{CaB}.[CaB] + \epsilon_B.[B] + A_{PROT}$$

where A_{PROT} is the absorbance from the protein, which is assumed not to change as the free calcium concentration changes.

$$A = \epsilon_{CaB}.[CaB] + \epsilon_{B}.([B_{TOT}] - [CaB]) + A_{PROT}$$

Substitute from equation A2.3:

$$A = \epsilon_{CaB}.\{K_{CaB}.[Ca].[B_{TOT}] / (1 + K_{CaB}.[Ca])\} + \epsilon_{B}.[B_{TOT}] - \epsilon_{B}.\{K_{CaB}.[Ca].[B_{TOT}] / (1 + K_{CaB}.[Ca])\} + A_{PROT}$$

$$= \epsilon_{B}.[B_{TOT}] + \{\epsilon_{CaB}.[B_{TOT}] - \epsilon_{B}.[B_{TOT}]\}.\{K_{CaB}.[Ca] / (1 + K_{CaB}.[Ca])\} + A_{PROT}$$

As [Ca] → infinity then $A \rightarrow \epsilon_{CaB}.[B_{TOT}] + A_{PROT}$ (= A_{PLUS}, the absorbance in the presence of saturating calcium).

As [Ca] → zero then $A \rightarrow \epsilon_{B}.[B_{TOT}] + A_{PROT}$ (= A_{MINUS}, the absorbance in the complete absence of calcium).

$$\epsilon_{CaB}.[B_{TOT}] - \epsilon_{B}.[B_{TOT}] = A_{PLUS} - A_{MINUS}$$

Then

$$A = A_{MINUS} + \{A_{PLUS} - A_{MINUS}\}.\{K_{CaB}.[Ca]/(1 + K_{CaB}.[Ca]$$

The experimental data are fit directly to this equation. The variables are A_{PLUS} and A_{MINUS} and the stoichiometric constants K1-K4 used in the calculation of the free [Ca] are determined using equation A2.6.

Appendix 3

Stopped-flow spectrophotometry: Data analyses

Stopped-flow spectrophotometric techniques were used to determine the rates of calcium and peptide dissociation from calmodulin and calmodulin:target peptide complexes as described in section 4.4. For each reaction studied at least nine individual stopped-flow traces were collected and averaged. The average of the nine traces was then fitted using a commercially available (Hi-Tech SF-61) non-linear least squares procedure based on the Marquardt method, (Marquardt, 1963). A single exponential was considered acceptable unless a significantly better χ^2 and distribution of residuals were obtained for a double exponential fit. Each experiment was repeated at least three times and the average rate constant with standard deviation was reported.

Appendix 4

Relationship between intrinsic and stoichiometric association constants

The relationship between the stoichiometric association constants and intrinsic (site) constants are described by the following equations:

$$K_1 = k_1 + k_2 + k_3 + k_4$$

$$K_2 = (k_1k_2 + k_1k_3 + k_1k_4 + k_2k_3 + k_2k_4 + k_3k_4) / (k_1 + k_2 + k_3 + k_4)$$

$$K_3 = (k_1k_2k_3 + k_1k_3k_4 + k_1k_2k_4 + k_2k_3k_4) / (k_1k_2 + k_1k_3 + k_1k_4 + k_2k_3 + k_2k_4 + k_3k_4)$$

$$K_4 = k_1k_2k_3k_4/(k_1k_2k_3 + k_1k_3k_4 + k_1k_2k_4 + k_2k_3k_4)$$

Summary of Selected Experimental Findings

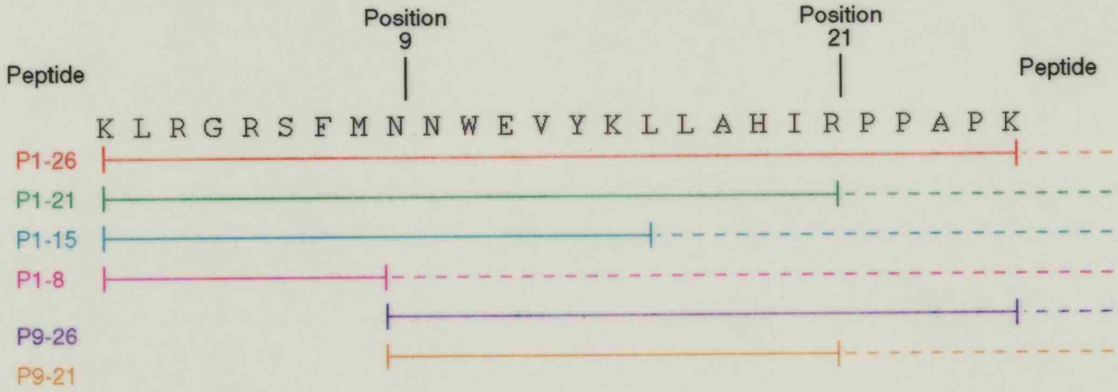

	K_d (CaM) M, pH7.0 Note 2	K_d(TR2C) M, pH7.0 Note 2	K_{SV} M^{-1} Note 3	# HEL Residues Note 4	CaM:Peptide Calcium Dissociation Rates (Q2) Note 5	CaM:Peptide Calcium Dissociation Rates (EGTA) Note 5
P1-26	2.8×10^{-10}	4.0×10^{-7}	1.14	6.7(8.6)	11(1.2)	13(1.6)
P1-21	1.0×10^{-9}	-	-	7.4(8.1)	-	-
P1-15	1.0×10^{-6}	-	3.44	-	-	-
P1-8	1.0×10^{-5}	-	-	-	-	-
P9-26	1.2×10^{-8}	1.0×10^{-7}	0.96	7.5(7.8)	18(2.4)	14(2.2)
P9-21	3.2×10^{-8}	1.0×10^{-7}	0.96	5.0(4.8)	16(2.6)	17(2.5)

Notes

1. Peptide length, name and biophysical parameters highlighted in specific colour.
2. K_d's calculated in section 4.1
3. K_{SV}'s calculated in section 4.1
4. Number of peptide helical residues are calculated for difference spectra as ([CaM : PFK peptide complex])-[CaM] value in brackets is for peptide in 50% TFE, see section 4.2 for calculations of α-Helicity
5. For quin-2 (Q2) and EGTA induced calcium dissociation two rates are given.The slower rate (k_s) is in brackets. NB: k_f and k_s for calcium dissociation from CaM are $\simeq$700 and 6.9s^{-1} respectively, see section 4.4.